Druckfreigabe/approval for printing

Without corrections/ ohne Korrekturen ☐

After corrections/ nach Ausführung der Korrekturen ☐

Date/Datum: .....

Signature/Zeichen: .....

6
Extraterrestrial Drilling and Excavation

Kris Zacny, Yoseph Bar-Cohen, Kiel Davis, Pierre Coste, Gale Paulsen, Stewart Sherrit, Jeffrey George, Brian Derkowski, Steve Gorevan, Dale Boucher, Jose Guerrero, Takashi Kubota, Bradley J. Thomson, Scott Stanley, Peter Thomas, Nicholas Lan, Christopher McKay, Tullis C. Onstot, Carol Stoker, Brian Glass, Sachiko Wakabayashi, Lyle Whyte, Gianfranco Visentin, Edoardo Re, Lutz Richter, Mircea Badescu, Xiaoqi Bao, Roger Fincher, Takeshi Hoshino, Piergiovanni Magnani, and Carlo Menon

6.1
Why Subsurface Exploration?

The 4 October, 1957 launch of Sputnik 1 by the Soviet Union that was followed by the 31 January 1958 launch of Explorer 1 by the United States marked the beginning of space exploration. Initially, the objectives were limited to exploration using orbital spacecraft, but very soon the scope expanded to *in situ* investigations. The first landing on an extraterrestrial body was marked in July 1964 with the US Ranger 7 crashing on to the Moon while sending pictures to Earth. This milestone was followed on 3 February 1966, by the first soft landing on the Moon by the Russian Luna 9. The United States followed this success with the Surveyor 1 soft landing on the Moon in June 1966. Mankind's natural desire to explore physically other planets was realized soon after with the landing of astronauts on the Moon on 20 July 1969. Apollo 11, which was launched on 16 July, 1969, was the fifth human spaceflight of the Apollo program and the third human voyage to the Moon. Much of the scientific return achieved by the six successful Apollo missions (Apollo 11, 12, 14, 15, 16, and 17) was derived from the analysis of rocks and drill cores collected and returned to Earth by the astronauts. The last human mission to the Moon took place in December 1972. The two Apollo 17 astronauts, Eugene Cernan, Apollo 17 Commander, and Harrison ("Jack") Schmitt, Lunar Module Pilot and also a geologist, left the lunar surface on 14 December 1972 and, since then, no human has set foot on the surface of the Moon. The three remaining missions, namely Apollo 18, 19, and 20, were canceled due to budget cuts and the ~~two~~ Saturn V rockets destined to launch astronauts to the Moon were placed on displays at the Johnson Space Center ~~and~~ the Kennedy Space Center.

Drilling in Extreme Environments. Edited by Yoseph Bar-Cohen and Kris Zacny
Copyright © 2009 WILEY-VCH Verlag GmbH & Co. KGaA, Weinheim
ISBN: 978-3-527-40852-8

Meeting the objectives of planetary exploration missions increasingly involves *in situ* sampling and analysis and this involves acquiring subsurface samples. Because of harsh planetary and lunar environments that include extremely low temperatures and vacuum, the challenges of drilling on these bodies are significantly more complex than drilling on Earth (Briggs and Gross, 2002; Zacny *et al.*, 2008b). Extraterrestrial drilling dates back to the 1970s, when Apollo 15 astronauts drilled a hole on the Moon to a depth of approximately 2.4 m and recovered a continuous core sample. The drill, called the Apollo Lunar Surface Drill (ALSD) was a ~500 W rotary-percussive drill with a coring bit capable of acquiring a continuous 2 cm diameter core; it had an auger for moving cuttings to the surface.

Today, one of the major goals of planetary drilling is to facilitate the detection of habitable zones in addition to signs of past or present life. This involves *in situ* analysis of acquired samples and, eventually, analysis of samples returned back to Earth. More generally, by examining the stratigraphy of acquired samples, scientists seek to learn the geological history of planets since the time of their formation. Looking further ahead, information obtained from such studies can support future human exploration of the Moon and Mars by locating resources that could allow astronauts to exploit for habitation and generate rocket fuel for their return journeys.

6.1.1
Search for Evidence of Existing or Extinct Life

One of the major goals of space exploration is the study of the subsurface of Mars and some of the outer planets moons in search of evidence of extant or extinct life. Some of this exploration can be carried out *in situ* or by studying samples from future sample return missions. In the case of Mars, the prospect of eventual human exploration necessitates understanding the biological potential in order to deal with planetary protection issues – both forward and back contamination (see Chapter 9). Forward contamination refers to organic material brought from Earth and introduced into a planetary body, whereas back contamination refers to an organic material brought back to Earth from an extraterrestrial body. The required capabilities are addressed in the documentation of the National Aeronautics and Space Administration (NASA) Strategic Objectives and the Scientific Goals of NASA's Astrobiology Program Roadmap. Subsurface access is identified as an essential element of future missions. To this end, there is a critical need for effective samplers that can operate robustly and, at the same time, require minimal resources of power, mass and volume. The sampling tools need to be able to acquire volatiles, powdered cuttings and cores while in some cases maintaining the stratigraphy of the sample and preserving the original form of volatiles.

"Life as we know it" requires carbon, liquid water and an energy source. Therefore, detecting water is critical to the search for extraterrestrial life and, as a practical matter, to support eventual human habitation. Consequently, one of the guiding principles of the NASA Mars program has been to "follow the water." We have known since the Viking missions that there is plenty of frozen water on the surface of Mars;

lander missions such as Phoenix have been planned to assess whether today's frozen water may have been in the liquid phase in the recent past.

In planning the subsurface exploration of Mars, an important consideration involves the depth of penetration required to address key questions. The continuing exposure of the surface to galactic cosmic rays and solar energetic particles over geological time has most likely damaged any biomarkers in the top surface layer (the oxidized zone is estimated to extend at least 2 m, whereas the sterilized zone can potentially extend down to 2–10 m depending on the formation). Therefore, the search for evidence of past or present life on Mars and on other planetary bodies requires techniques to reach below the disruptive influence of surface oxidants and cosmic radiation to sample underground ice, permafrost and rocks. When sampling in search of life it is essential to assure the aseptic cleanliness of the acquisition tools and prevent potential contamination. These topics are covered extensively in Chapter 9 and other publications (see, for example, Juck *et al.*, 2005; Sherrit, 2005).

6.1.2
Science Rationale for Drilling on Mars

Ground ice is an important target for astrobiologists for two reasons. First, ice can provide a source of liquid water if the pressure and temperature conditions are suitable. Second, ice can encase and preserve biological evidence of past life.

Generally, the permafrost environment is considered extreme because indigenous microorganisms must survive prolonged exposure to subzero temperatures. Also, these organisms need to survive background radiation for geological time scales in a habitat with low water activity and extremely low rates of nutrient and metabolite transfer. On Earth, there are considerable numbers and biodiversity of bacteria that exist in permafrost, some of which may be among the most ancient viable life that was discovered (Steven *et al.*, 2006).

There are two broad science strategies for sampling ground ice on Mars. In the northern polar regions of Mars, shallow ground ice (4–10 m depth) may record recent (~5 million years) evidence of liquid water conditions at the surface. In such relatively young ice we might find organics and, conceivably, preserved organisms.

For liquid water to form from ice, two conditions must be satisfied: (1) temperatures must rise above the melting point and (2) the ambient pressure must be at or above the vapor pressure of the liquid at that temperature. Because the melting point and the boiling point are equal at the triple point, the production of liquid water from ice is often expressed as the requirement that the pressure and temperature exceed their triple point values of 0 °C and 6.1 mbar.

6.1.2.1 **Shallow Ice in the North of Mars**

The *average* surface pressure on Mars is 6.1 mbar – at the triple point pressure of water. Thus regions in the northern lowlands have pressures that exceed this value whereas regions in the southern highlands have pressures that are below this value. In the 1970s, the two Viking landers, at 22°N and 44°N on Mars, both recorded pressures that were always above the triple point of water. In addition at the Viking

Page proof WILEY-VCH

sites, temperatures occasionally exceed 0 °C. However no liquid water was available at either site because there was no ice to melt when conditions were thermodynamically favorable (Lobitz *et al.*, 2001; Haberle *et al.*, 2001).

In the northern lowlands of Mars, the potential occurrence of liquid water is limited by the distribution of ice in locations where temperatures and pressures rise above the required thresholds. This does not occur in the present era, but ∼ 5 Myr ago the Martian obliquity is modeled to have reached values of up to 45°, much larger than the present value of 25° (Laskar, Levrard and Mustard, 2002). Under such conditions, the polar regions would have received twice the amount of daily sunlight at summer solstice than they do today. It is plausible that under these conditions, the surface temperature reached values high enough for liquid water to form at the surface of ice-rich regolith.

The ice at the Phoenix landing site (68.2°N, 234°E) on Mars exchanges with the environment by vapor transport only. This is very different from most ground ice on Earth, which experiences a melt period each summer during which the upper layers of the ice-cemented ground melt to form liquid water. This sort of liquid water-active zone is found everywhere in the Arctic and in the low elevations of the dry valleys of Antarctica. Only high in the mountains (over 1500 m elevation) in the dry valleys of Antarctic has there been dry permafrost with ice-cemented ground below it. This is Mars-like permafrost. The reference location in question is in University Valley (77°51.891, 163°45.062′, elevation 1693 m). The top of the ice-cemented ground is ∼30 cm below the surface and the maximum temperature of the ice is −10 °C. There is an extensive zone of dry permafrost above the ice. The top of this ice never melts – it exchanges only as vapor. This area at high elevations in the dry valleys of Antarctica is evidently the best analog on Earth to ice conditions on Mars at the Phoenix site.

Studies of microbes in ice show that metabolism can occur down to −15 °C and perhaps as low as −20 °C (e.g., Rivkina *et al.*, 2000). Presumably the solute content of the microorganism is high enough to maintain internal liquid at these low temperatures.

The ice below the surface at the Phoenix site almost certainly does not warm to −20 °C at the present time, but 5 Myr ago it might have. Hence even if large-scale surface melt did not occur, warm ice temperatures could have provided a microscale habitable zone for life.

The main astrobiological objective for missions that follow up on Phoenix will be to sample the ice record of the past 5 Myr to search for evidence that the ice did indeed support liquid water and, if so, to search that refrozen ice for biosignatures. The depth required to reach back 5 Myr is probably of order 4–10 m.

6.1.2.2 **Deep Ice in the South**

The science rationale for drilling into ice in the southern highlands of Mars is very different to that for the north. Because of the high elevation of the southern polar regions, the atmospheric pressure is well below the triple point and there is no prospect for recent liquid water even at high obliquity. However, as pointed out by Smith and McKay (2005), the southern plains are the most likely place to find ancient frozen ice-rich ground that dates back to the early period of Martian history. Data from the Mars Odyssey spacecraft have confirmed the expectation that the polar regions of Mars are rich in ground ice (Feldman *et al.*, 2002). The high southern

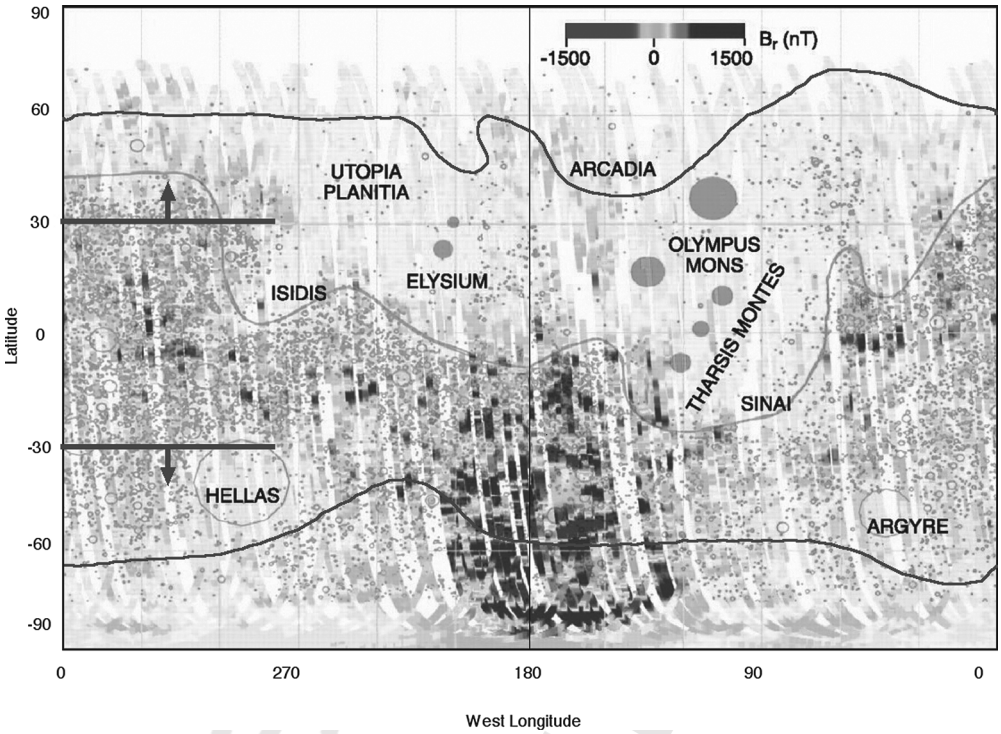

Figure 6.1 Crustal magnetism, crater distribution and ground ice on Mars. Each green dot represents a crater with diameter greater than 15 km. The boundary between the smooth northern plains and the cratered southern highlands is shown with a green line. The crustal magnetism is shown as red for positive and blue for negative. Full scale is 1500 nT. The typical strength of the Earth's magnetic field at the surface is 50 000 nT. The solid blue lines show the extent of near surface ground ice as determined by the Odyssey mission. Ground ice is present near the surface poleward of these lines. Crater morphology indicates deep ground ice poleward of 30° (Squyres, Wilhelms and Moosman, 1987), shown here by dark blue lines and arrows. The region between 60 and 80°S at 180°W is heavily cratered, preserves crustal magnetism, and has ground ice present. This is a possible target site for deep drilling to meet astrobiology goals. Adapted from Smith and McKay (2005). (Please find a color version of this figure on the color plates).

latitudes are of particular interest because ancient cratered terrain in this region evidently dates back to the end of the heavy bombardment, 3.8 Gyr ago. The actual polar cap deposits are much younger. One region of particular interest, centered on 80°S, 180°S, is shown in Figure 6.1 from Smith and McKay (2005). Here the terrain is heavily cratered, there is ground ice present, and, furthermore, there is strong crustal magnetism in the surface materials. The presence of such magnetism confirms the antiquity of these terrains and suggests that they have been relatively unaltered since their initial deposition. This location may represent the site of the oldest, coldest, undisturbed permafrost on Mars. Martian microorganisms may be trapped and preserved in this permafrost (Smith and McKay, 2005).

The astrobiology goal at this site would be to access materials from 3 to 4 Gyr old that may contain a frozen ice-protected record of early life on Mars. The depth to such material may be hundreds of meters or more.

6.1.2.3 Second Genesis

If we find biomarkers (and especially preserved organisms) from a polar habitable zone in the north polar ice or ancient microbes in the southern ice, we will have made great progress in answering fundamental questions in astrobiology, namely, whether life has existed on Mars and whether such life represents a second genesis (McKay, 2001, 2004).

6.1.3 Search for Resources and *In Situ* Resource Utilization to Support Human Exploration

Other major objectives of space missions are the development of the foundations and infrastructure that will be required to support human visitation and presence. In addition to the Moon, Mars is the primary target for such missions. These objectives focus on the availability of *in situ* resources and the means for their effective utilization. A secondary consideration is the possible risk that Martian dust may pose ~~for~~ astronauts. Specifically, the 2008 Strategic Sub-goal 3C looks to "Advance scientific knowledge of the origin and history of the solar system, the potential for life elsewhere and the hazards and resources present as humans explore space."

Sampling methodology must be developed for the extraction of Martian near-surface materials. ~~Also,~~ there is a need to develop and demonstrate technologies capable of reliably returning sampled materials back to Earth – with utmost attention to any potential contamination of either Mars or Earth (see Chapter 9). Also, there is a need for new instrumentation for *in situ* sample analysis that is low in mass, power, and volume (see Chapter 8).

6.2 Methods for Subsurface Access on Extraterrestrial Bodies

As described in Chapter 1, drills have been developed and used as penetration tools in nearly all the civilizations for which we have recorded history. For a drill to be useful under extraterrestrial conditions, it needs to overcome the challenges that are involved with operation at such remote locations and that, in most cases, involves an extreme environment. Some of the problems and limitations include:

1. While drilling, the cuttings need to be removed from the hole~~; their extraction requires an escape route while the drill bit is operating. Because the cutting edges at the tip of the drill bit are connected to a relatively flexible tool, the geometric accuracy of the drilled hole may be compromised.~~
2. During the initiation of a hole, the drill may experience "drill walk" as a result of drill bit bending and instability of the mount or drilled object. The result may

page proof @WILEY-VCH

produce positioning error and an inclined hole. Furthermore, excessive bending may cause failure of the bit.

3. Undesirable heating resulting from the ~~friction between the drilled bit and the drilled medium. This heat is in addition to that produced by the formation of cuttings.~~ Such heat can damage or melt samples taken from the drilled medium.

4. A drill bit's torsional stiffness can be relatively low, resulting in natural vibration frequencies that may be excited during a drilling operation. These may cause chatter between the drill bit and the drilled medium, which in extreme cases can cause bit failure.

Most of the drills that have been used in previous ~~US and Russian~~ missions or that have been considered for future use are ~~based on mechanical mechanisms and mostly driven in rotation.~~ Increasingly there is recognition that incorporating percussive action has significant benefits. The drill that was developed to be used on the ~~2009~~ Mars Science Laboratory (MSL) mission is a percussive–rotary drill that requires two independent actuators to produce impact and rotation together with a specialized control system to synchronize these two forms of motion. Such synchronization results in the most effective penetration rates and highest efficiency. It has become possible to avoid the need to use the two independent actuators and their synchronization through the use of self-excitation systems that combine the driving and synchronization of the striker from the rotation (Batako, Babitsky and Halliwell, 2003). The system not only introduces favorable impulsive events into the drilling process but also reduces uncontrolled stick–slip events in the entire drill string that can cause damage to both the cutting bit and, in extreme cases, the entire drill string. Further, the drilling system is self-regulating, and intensifies its impulsive action when resistance is encountered. Such drills are most effective when drilling media that are hard and brittle; they are superior to conventional drills both in increased penetration rate and in reduced preload (Batako, Babitsky and Halliwell, 2004).

Application of drills under planetary conditions necessitates addressing the drilling related issues that were mentioned above. Various alternative drilling and rock handling mechanisms have been developed and some of the leading approaches are described and discussed later in this chapter. Note that additional information concerning the principles of drilling and constraints on drilling in extraterrestrial environments can be found in a recent paper by Zacny *et al.* (2008b).

Automated sample acquisition and handling are of obvious importance for future robotic exploration missions to Mars, the Moon, Venus, and other planetary bodies. Identified missions include the Mars Astrobiology Field Laboratory, Mars Sample Return, and the mid-sized Mars rovers. For these mission concepts, consolidated or unconsolidated core samples (as opposed to scooped regolith or collected drill cuttings) are of special interest for a number of reasons. ~~Thus, from~~ a science standpoint, a core provides much more information than drill cuttings, including:

- The stratigraphy of the target formation can be delivered intact to the analysis suite.

- A core can be photographed or imaged microscopically to determine the morphology of the sample and search for fossilized evidence of life. Layers of interest can then be sub-sampled by a fine sample acquisition device and analyzed without being diluted by the bulk sample.
- A consolidated core can be split to reveal an uncontaminated surface.
- A thin section for petrographic analysis can be made from a consolidated core more easily than from drill cuttings.
- The elemental composition of specific regions of a core can be obtained from the core surface using X-ray fluorescence, laser-induced breakdown spectroscopy, or other techniques.
- A core may be crushed to a desired particle size allowing for powder mineralogical analysis.
- Volatiles that escape from cuttings during the drilling process may remain well preserved at the center of a consolidated core. These can be evolved and analyzed in a controlled manner later in the sample processing chain.

Core drilling also offers advantages from an engineering standpoint. A coring bit cuts an annular space in the formation, as opposed to drilling out the entire volume of a hole, reducing the required power, torque, and weight on bit (WOB) (i.e., thrust applied on the bit). However, from the perspective of robust mechanical design, obtaining a core is significantly more complex than drilling a non-cored hole. Given limited spacecraft resources, harsh environmental conditions, and the need to preserve sample fidelity, core handling is a technically challenging problem. Critical properties to retain for scientific investigation include geology, geochemistry, and geophysics.

In addition to these issues, there is the programmatic reality that requirements for extraterrestrial sampling tools are in a constant state of flux. For example, there are four possible mission site scenarios outlined in the final report of the AFL Science Steering Group (Steele and Beaty, 2006), each one suggesting a radically different set of sampling tool requirements. Proceeding down a design path targeted specifically towards consolidated sedimentary rock could result in a system inadequate for icy soil. Future development must consider a variety of materials. Honeybee Robotics has defined the three "tall-pole" targets as: strong basalt, icy soil, and loose regolith.

Several previous coring tool development efforts have resulted in complete systems designed around general technology goals and NASA-directed contractual requirements. Examples include the Honeybee MARTE (Mars Astrobiology Research and Technology Experiment) drill and Mars Technology Program Coring and Abrading Tool (CAT), the ATK Space (formerly Swales Aerospace) deep drill systems, and the Johnson Space Center (JSC)/Baker-Hughes Mars/Arctic Deep Drill.

The system evaluations presented here are intended to aid future mission planners in identifying the maturity of specific aspects of sampling system designs across a broad range of performance metrics. Decisions to mature and characterize a set of key subsystems can then be ~~rapidly and with some confidence~~ selected to satisfy a desired set of mission requirements.

page proof

6.3
Grinders and Rock Abrasion Tools

Sometimes the science requirements may include analysis of surface rocks. This has been, for example, one of the science goals of the Mars Exploration Rover (MER) mission. However, surfaces of rocks tend to be chemically and physically altered and covered with dust. Therefore, in order to reach the rock's pristine interior, the outer layer (which can be only a few millimeters thick) needs to be removed. Tools that can do the job are called surface grinders, abrasion tools and brushers. Once the clean surfaces is exposed, instruments such as a Mössbauer spectrometer or a microscopic camera can then be brought in to perform measurements and take photographs.

The Mars Science Laboratory Rover mission will not have any rock abrasion tools or surface grinders due to mass and cost constraints on the mission. However, it will have a high-speed brush, called the dust removal tool (DRT), which is being developed by Honeybee Robotics.

6.3.1
Rock Abrasion Tool (RAT)

In 2003, the MERs Spirit and Opportunity were launched on a journey to Mars. Since arriving on the Red Planet, the two rovers have been performing a number of experiments [at the time of this writing (~~October 2008~~), the MERs were still operational], and collecting data that have greatly expanded our knowledge about Mars. One of the science instruments onboard the MERs is the rock abrasion tool (RAT) (shown on a turret at the end of the MER robotic arm in Figure 6.2). This instrument was designed and developed by Honeybee Robotics (Gorevan *et al.*, 2003). It is roughly the size of a soda can and operates with about 10 W of power. The RAT produces a hole approximately 45 mm in diameter and can grind to a depth of roughly 5 mm with less than 10 N of down-force on most targets. The main purpose of the RAT was to remove the weathered and thus altered outer surface of rocks and to reveal

Figure 6.2 Rock abrasion tool (a) and abraded surface (b). Courtesy NASA/JPL.

virgin rock structure for analysis. The requirements for both RATs were to grind at least three holes. So far, the combined number of successful grinds performed on Mars is over 40 (Zacny *et al.*, 2008b). In addition to grinding rocks, the RAT can use its brushers to brush off the outer dust layer. This has been proven very valuable for initial interrogation of rocks.

6.3.2
The Beagle 2 Rock Corer Grinder

The rock corer grinder (RCG) of the Beagle 2 lander (see Figure 6.3) had to prepare a flat surface on the rocks to be analyzed by an X-ray spectrometer (XRS) (for age dating of rocks) and a Mössbauer spectrometer (for rock mineralogy and petrology). It also had to take samples for analysis by the gas analysis package in the lander. Unfortunately, Beagle 2 was lost in December 2003. The rock core would have been acquired with a short drill made of two halves, which ~~were closed to break the base~~ (Figure 6.3b). It was mounted on the Beagle 2 ~~PAW~~ next to the sampling mole PLUTO (Planetary Underground Tool) (Figure 6.3a). This RCG was designed and constructed by a team from Hong Kong Polytechnic University (HKPU) (Ng *et al.*, ~~2008~~; Richter *et al.*, 2002). Q1

6.3.3
Ultrasonic Rock Abrasion Tool (URAT)

Abrasion of the surface of a rock using low axial force and limited average power is needed to remove weathered layers from rock surfaces and expose pristine sections. Conventional rotating mechanisms require high axial loads and ~~they are involved with~~ contamination sources such as lubricants ~~and filings from their~~ motor gearbox. To address the need for an abrasion tool, an ultrasonic rock abrasion tool (URAT) was developed. For this purpose, an abrasion bit was configured similar to the hammering surface of a meat tenderizer. Teeth were machined on to the bottom of the disk

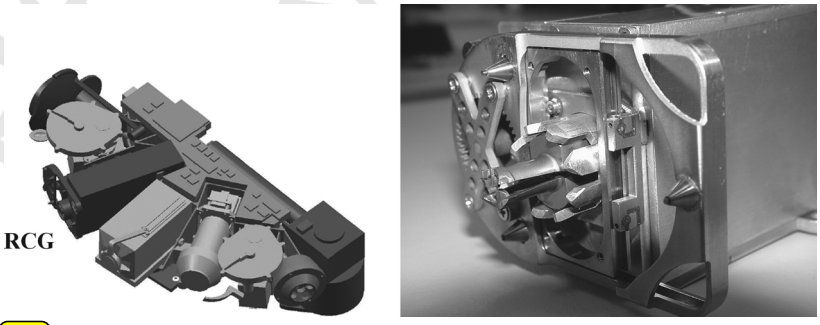

Figure 6.3 Rock corer grinder (RCG). (a) RCG in ~~Paw~~ on Beagle 2 arm; (b) RCG mechanism, showing coring halves. Courtesy HKPU and Beagle 2 team. (Please find a color version of this figure on the color plates).

page proof WILEY-VCH

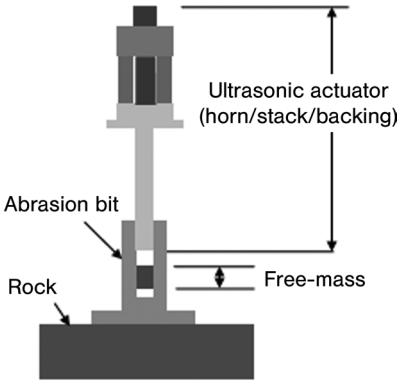

Figure 6.4 Schematics of the ultrasonic rock abrasion Tool (URAT). Courtesy NASA/JPL.

that is part of the abrasion bit. These teeth amplify the drilling pressure and enhance the action of the URAT. A schematic cross-section drawing is shown in Figure 6.4, illustrating the components and the compact structure of the URAT. A view of abraded basalt is shown in Figure 6.5 (Dolgin *et al.*, 2001b).

The developed abrasion tool was made with a 40 mm (1.6 in) diameter disk that is attached to a shank that fits around the horn. A free mass is placed inside a shank between the horn and the bottom of the hole along the inner part of the bit. On the bottom of the disk teeth were machined in the form of pyramidal pins that stick out of the disk. Tests have shown that in order to maintain effective abrasion operation over depths greater than the length of the pins, it is essential to rotate the bit and avoid

Figure 6.5 Photographic view of basalt that was abraded by the URAT. The circular footprint of the abrasion bit can be seen on the surface. Courtesy NASA/JPL.

WILEY-VCH Proof

embedding the pins in the powdered cuttings and the formed indentations. Pins of various shapes were made and it was observed that the use of an asymmetric shape introduces rotation without the need for a dedicated motor.

6.4 Scoops

Whenever surface regolith is required, scoops are the tools of choice. Because of their inherent simplicity, they also tend to be very robust. The greatest drawback of this method of sample acquisition is that scoops have difficulty in penetrating highly compacted soils, and when soil contains ice, the scoop will not be able to penetrate it.

6.4.1 Surveyor Scoop

Designed by the Hughes Aircraft Company, the Soil Mechanics Surface Sampler (SMSS), shown in Figure 6.6, was flown on the Surveyor 3 and 7 lunar landers from 1966 to 1968. The SMSS was used to collect information about the lunar surface in preparation for the manned Apollo missions ~~to come~~ (Scott and Roberson, 1968, 1969). The Surveyor landers were the first lunar landed missions to have a sampling device.

The SMSS, shown in Figure 6.7, consisted of a scoop attached to the end of a three degrees of freedom (DOF) (azimuth, elevation, and retraction) extension–retraction mechanism that had a 1.5 m lateral and 112° angular reach capability. The scoop was 120 mm long and 50 mm wide and could positively retain up to 100 cm^3 of regolith or up to a 32 mm diameter rock via an actuated door. The scoop could theoretically reach to a depth of 306 mm below the lunar surface via the 3-DOF arm.

The SMSS has four primary functions, bearing, trenching, picking, and lifting. Bearing and trenching operations provided information regarding soil strength, and

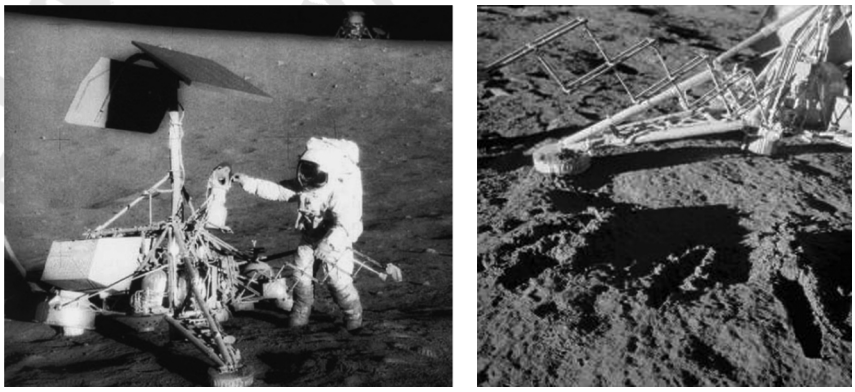

Figure 6.6 (a) Apollo 12 astronaut shown with left hand on Surveyor 3 SMSS arm; (b) trenches created by Surveyor 3 scoop Images: NASA.

page proof WILEY-VCH

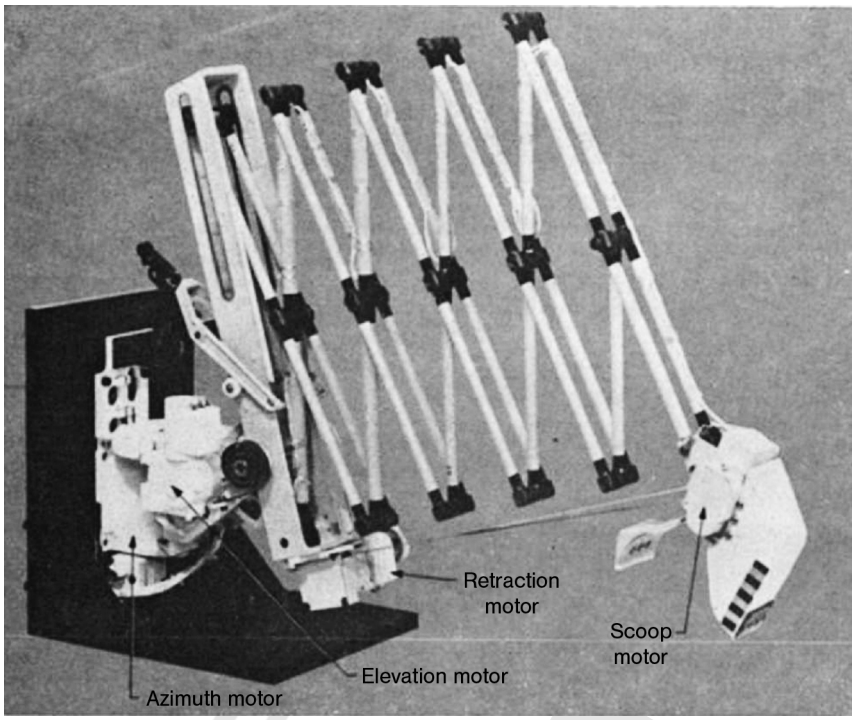

Figure 6.7 SMSS prototype shown on test stand with lid opened (Scott and Roberson, 1969).

also strength variation with depth. Picking operations involved striking a surface with the SMSS via a force created by a combination of a torsion spring and gravity. Position and torque telemetry ~~was~~ not available on Surveyor 3, so operation was not closed loop or fully autonomous. Motor current data were available on Surveyor 7 and were used to analyze soil physical properties.

Operations for the Surveyor 3 SMSS on the lunar surface included 25 bearing and impact tests, and four trenching operations totaling 6 m and up to 180 mm deep. Surveyor 3 SMSS performed operations over the course of one lunar day (11 Earth days) totaling 18 h and 22 min of activity. Operations for the Surveyor 7 SMSS included 36 h and 21 min of activity over the course of one lunar day (12 Earth days). Operational temperatures ranging from −167 to +180 °F (−111 to +82 °C) were seen via temperature sensors attached to the motors. Successful operations included picking up rocks, bearing tests, trenching, and impact tests.

6.4.2
Viking Lander Surface Sampler Acquisition Assembly

With surface operations running from 1975 to 1982, the Viking mission was the first to sample the Martian surface (Holmberg, Faust and Holt, 1980). It included

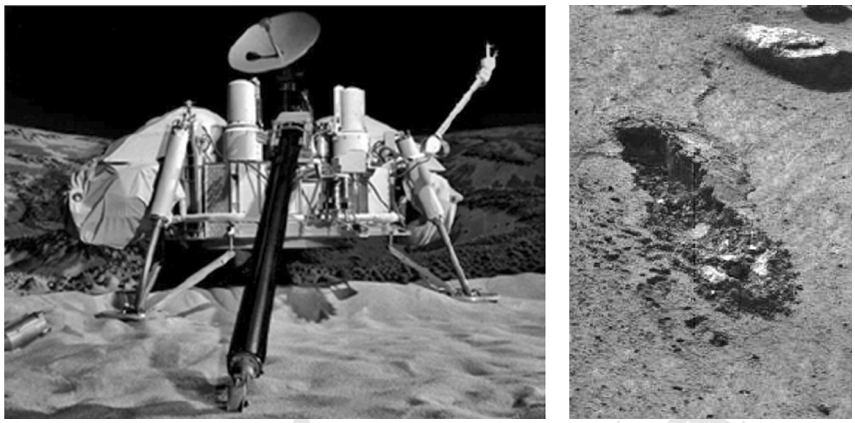

Figure 6.8 ~~Viking lander model shown with SSAA fully extended and image of trench created during mission operations Images: NASA.~~

two identical landers, Viking 1 and Viking 2 (Figure 6.8a), and was intended to gather information relating to biological, chemical, and environmental characteristics that may support life. The surface sampler acquisition assembly (SSAA) was comprised of a 3 m, 3-DOF furlable boom with a collector head assembly at its end. The boom enabled the SSAA to reach an area of 12.1 m^2 in front of the lander. The collector head assembly was meant to acquire soil and rock samples to hand-off to on-board analysis instruments (chemical and biological), and also to infer soil physical characteristics via telemetry information (position and motor current) during trenching operations, as was done on the Surveyor mission. The SSAA power usage was 30 W maximum and the specific sampling energy was 4.3–8.6 kJ cm^{-3} (conservative estimate). The total mass of the SSAA was 11.3 kg and the overall dimension of the system when retracted were $614.8 \times 233.7 \times 342.9$ mm. Sampling typically took 24–28 min and the maximum allowable sampling forces were 20 N shear, 133 N digging, and 88 N scraping.

The SSAA collector head, shown in Figure 6.9, consisted of a scoop with lid, a 2 mm sieve screen, a vibrator, and a backhoe attachment with integral magnet array and brush. The scoop was 4.8 cm wide and the lid provided positive retention of captured sample. To capture a soil sample, the lid was opened and the boom was extended into and along the surface. The lid was then closed to capture the sample positively. After being positioned over a drop-off location, the arm was rotated 180° to dump the captured sample on to the sieve screen. The solenoid-actuated vibrator was turned on to sieve the sample into inlets that were integral to analysis instruments. A gas chromatograph–mass spectrometer (GC/MS) and biology instruments had their own integral sieves to control particle size and the SSAA could deliver raw, unsieved, samples to them. The backhoe attachment was used to perform trenching operations (Figure 6.8b), acquire magnetic surface materials, and brush target surfaces to provide an unobstructed look at the natural surface.

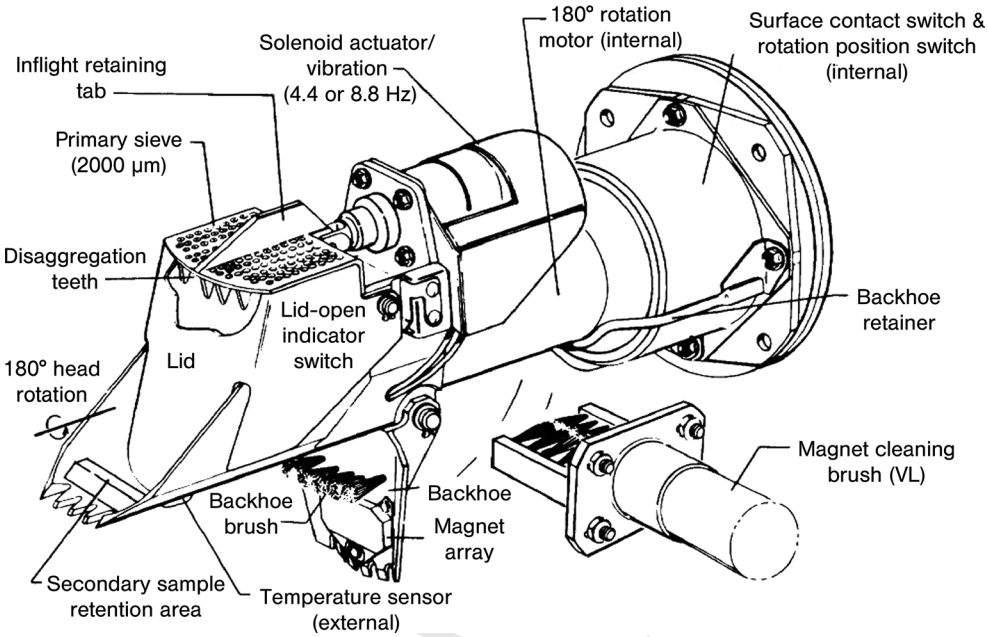

Figure 6.9 Viking ~~SSAA~~ collector head (Holmberg *et al.*, 1980).

In addition to the sample collection capabilities of the SSAA, the GC/MS processing and distribution assembly (PDA) and biology PDA had sample processing capabilities including comminuting course material, sieving, and metering controlled volumes of sample. In some respects, these subsystems could be viewed as part of the sample acquisition chain. ~~Details of the GC/MS PDA and biology PDA are shown in Figures 6.10 and 6.11~~. The GC/MS PDA received a 2000 μm sample from the SCAA, comminuted the sample down to a maximum particle size of 600 μm, sieved the sample via a 300 μm sieve; and finally metered a 1 cm^3 sample for subsequent analysis. The biology PDA received a 2000 μm sample from the SCAA, sieved the sample via a 1500 μm sieve, and finally metered a 7 cm^3 sample for subsequent analysis. During surface operations, the temperature at the landing sites ranged from 155 to 275 K, and the pressure ranged from 4 to 7.5 mbar. Q27

6.4.3
Phoenix 2007 Scoop

Scoops are a useful tool for collecting and presenting loose top soils to other science instruments. NASA has flown two missions to the Martian poles to investigate signs of water ice on the Martian North Pole. The first mission was the 1998 Mars Polar Lander. This lander included a scoop on the end of a robotic arm that would collect material for analysis. Unfortunately, communication was lost while this lander was attempting to touch down on Mars, which ended in a failed mission. The second

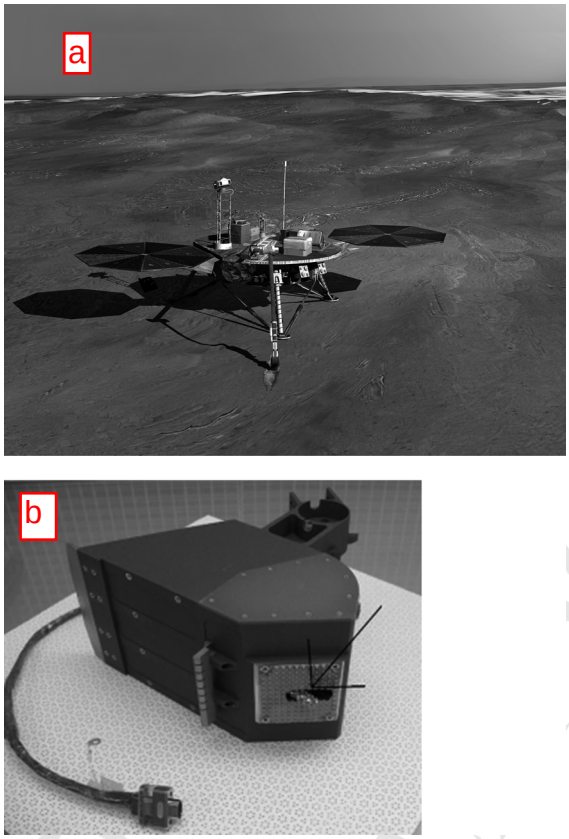

Figure 6.10 (a) Phoenix Icy Soil Acquisition Device (ISAD), mounted on the Phoenix lander's robotic arm. Photograph courtesy NASA/JPL. (b) The ISAD consists of a scoop and a small drill called the RASP at the back of the scoop. Courtesy Honeybee Robotics.

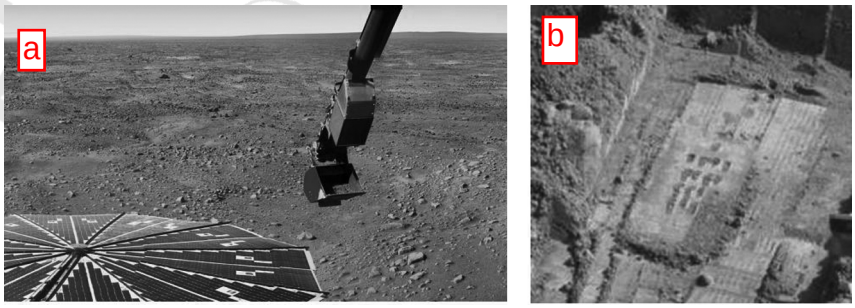

Figure 6.11 Captured images from Phoenix surface operations: (a) ISAD shown after first scooping operation with regolith inside, (b) ~~rasp~~ holes in Martian permafrost Images: NASA.

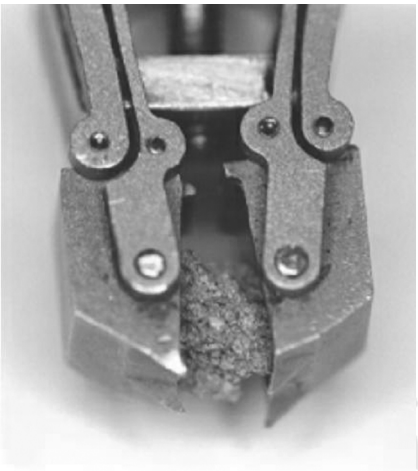

Figure 6.12 SSA/DT tools: Micro End-Effector No.1 (MEE-I). Detail: two jaws handling a mini-rock. Courtesy HKPU and ESA.

6.10 and 6.11

mission was the Phoenix Lander mission, which was launched in 2007. It was a rebirth of the Mars Polar Lander and therefore contained many of the same or similar instruments. Phoenix landed successfully at the Martian North Pole in May 2008 and ~~is currently performing scientific studies of the Martian soil. It is doing so with the help of a revised scoop.~~

The scoop on the Phoenix Lander, known as the Icy Soil Acquisition Device (ISAD), ~~is~~ a combined scoop and ~~rasping~~ unit (Figures ~~6.12 and 6.13~~). It was designed and built by Honeybee Robotics with the main goal of penetrating and collecting a sample from the very hard permafrost layer just below the top

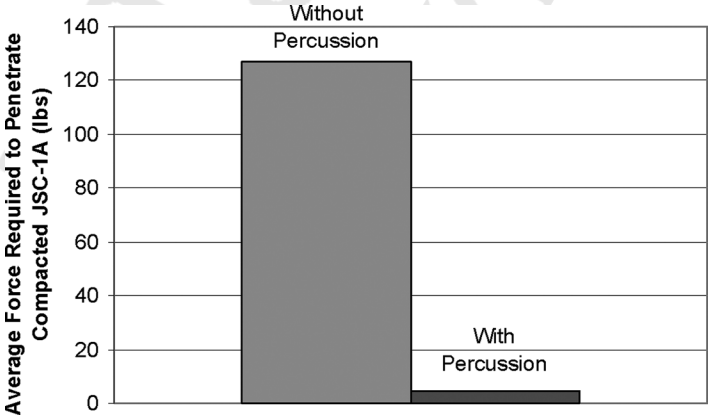

Figure 6.13 Honeybee Robotics percussive scoop tests showed that percussion dramatically reduces the reaction loads necessary to penetrate compacted lunar regolith simulant, JSC-1a.

soil (Chu *et al.*, 2008). The idea of collecting cuttings using a ~~rasp~~-like device was proposed and test proven by G.H. Peters at the NASA Jet Propulsion Laboratory (JPL) (Peters *et al.*, 2007).

Given the mass restrictions on spacecraft, it was not feasible to design a scoop or robotic arm that could penetrate the very hard frozen layer with the sole use of blades or scrapers. Therefore, a motor and rasp bit were packaged into the scoop. The motor operates with less than 30 W of power and cuts a hole that is roughly 6.3 mm (0.25 in) in diameter. The rasp is set out of the rear end of the scoop and is preloaded on to the surface with a torsional spring. Preloading of the rasp is complete when the base of the scoop contacts and sits flush on the Martian surface. Once activated, the rasp kicks material up into a rear chamber on the ISAD. This material is then transferred through a labyrinth to the front of the scoop, where it can be delivered to other science instruments.

The ISAD is 85.8 × 157.3 × 169.5 mm, has a total mass of 688.3 g, ~~and an average power consumption of approximately 38 W.~~

The ISAD can be used in either a scoop mode or rasp mode. During scoop mode, the robotic arm is used to scrape the target surface to obtain sample material in the front chamber of the ISAD. A blade attached to the front of the ISAD aids in breaking up weak soil. A tungsten carbide blade attached to the bottom of the ISAD can be used to break up tougher materials. The scoop operations are limited to 1170 N of digging force. Up to 310 cm^3 of sample may be collected ~~in this chamber.~~

During rasp mode, the rasp is spun at 5500 rpm while preloaded to the surface with 6 N (the Phoenix robotic arm provides a 40 N minimum reaction preload). Prior to preloading to the surface, the ISAD blades are used to prepare, or flatten, the target surface. As it penetrates over the course of 30–60 s, cuttings are thrown into the ISAD's rear sampling chamber. A series of robotic arm wrist articulations, combin 6.10b with vibration from a cam-impact feature on the ISAD, transfers the powdered cuttings from the rear sampling chamber to the front open chamber, where they can be imaged by a camera and transferred to science instruments. The carbide rasp protrudes at an angle through a slotted load plate in the scoop floor (Figure 6.12b) and pivots about a spring-loaded hinge so that the preload applied at the bit is dictated by the spring.

The ISAD sample acquisition performance was tested using frozen soil mixtures having an unconfined compressive strength (UCS) of 45 MPa. With a new bit, four 15 -s rasp operations will produce 1–4 cm^3 of powdered cuttings depending on the surface conditions. One parameter that greatly affects the amount of sample acquired is the gap between the ISAD's slotted load plate and the surface. Ideally, no gap would exist if the surface was perfectly prepared and there was no robotic arm positioning error. However, there will most certainly always be some measurable gap. ~~While the exact sensitivity is still being studied, gaps of 1–2 mm have been shown to cause at least a 50% drop in the volume of material acquired.~~ Also, rasping with the current ISAD rasp bit design has been shown to remove a significant fraction of water in permafrost samples (Peters *et al.*, 2007). It is hypothesized that a different cutting bit design would likely mitigate water loss.

page proof WILEY-VCH

6.4.4
Micro End-Effector (MEE)

In contrast to the basic Small Sample Acquisition and Distribution Tools (SSA/DTs), which were rugged and simple, the Micro End-Effector (MEE) tool (Figure 6.14) was fairly complex, but also extremely innovative. Its inventor, T.C. Ng, with a team at the HKPU, had previously presented their research to the European Space Agency (ESA): it was related to large sampling tools, such as planetary rock pickers. This team undertook (freely for ESA) the challenge of miniaturizing their concepts, made of articulated parts and screw joints (Ng *et al.*, 2002; Yung *et al.*, 1997).

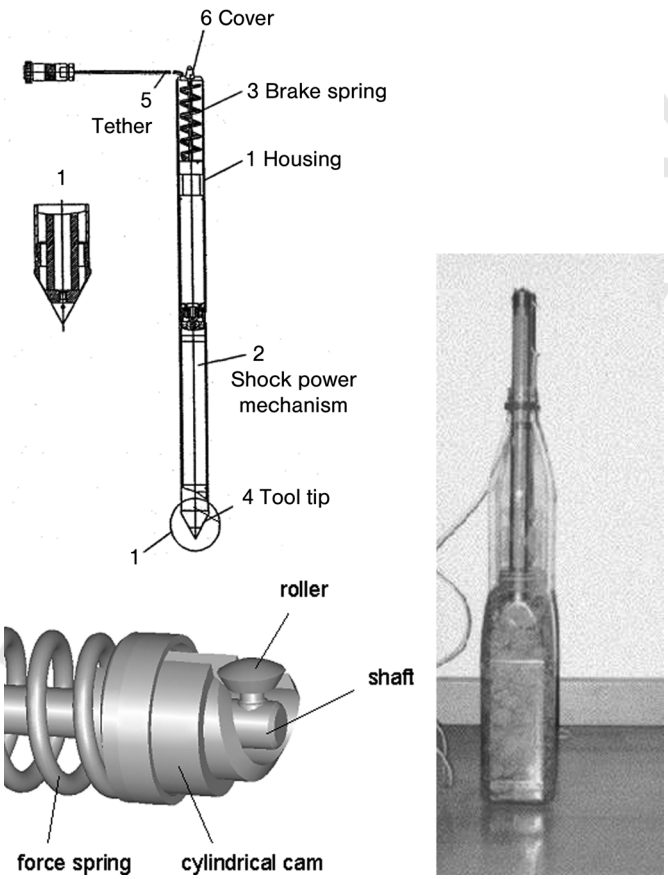

Figure 6.14 (a) Mobile penetrometer or "mole"; (b) roller-cam detail; (c) mole prototype desk-top test: penetration in pebbles. Courtesy DLR, VNII Transmash and ESA.

The MEE tool is articulated like pliers, which may rotate along the main axis around a threaded support; when pushed on a soil surface and rotated, the friction torque, transmitted via a linkage, allows opening or closing.

One MEE tool was ~~kindly~~ delivered to ESA free of charge (1996–1997); it ~~could be~~ used for ambient testing with SSA/DT. A number of prototypes were later built, tested on soils under ambient conditions, and further improved.

~~The MEE has shown that, in principle, complex miniature tools may be designed.~~ To survive the ~~oven~~ environment, a number of considerations in the tribology ~~of the joints should be designed in further detail, in particular the materials and lubricants.~~

6.4.5 Percussive Scoop

The extraction of top surface and also of highly compacted material on the lunar surface is critical to the success of long-term utilization of resources for the production of oxygen, water, and other consumables needed for propulsion and life support systems and also for other "civil" engineering applications such as building berms, roads, trenches, and so on.

Terrestrial earth-moving machines, such as bulldozers and bucket wheel excavators, rely on shear force to break up and excavate the soil and softer rocks. They use a hydraulic system which has inherent advantages (over electromechanical systems) that include the ability to generate larger forces, small size, simplicity, and robustness. Another advantage that terrestrial earth-moving machines have is their large weight, reaching hundreds of tons and more. This will not be possible on the Moon, which with its lower gravity of one-sixth that of the Earth, would require similarly capable excavation systems to be six times heavier. The solution to this problem is to use the percussive approach. A scoop with a percussive actuator can dig deeper and faster with force that is at least 25 times lower than that for a corresponding non-percussive scoop. This directly translates into a 25 times lighter excavator and in turn money saved by not launching heavier systems. Apart from much higher efficiencies, percussive and vibratory system will enhance particle discharge into the bin (the scoop can be vibrated during the regolith discharge cycle to speed up the discharge of particles). Other applications include vibrating blades and plows. Vibrating surfaces reduce sliding friction between the particles and soil and in turn forces and power required in moving the regolith.

Honeybee has developed a percussive shovel for use on the military's Man-Transportable Robotic Systems such as iRobot's PackBot and Foster Miller Talon. Due to their light weight, these robots can provide only limited reaction force for digging and hence lessons learned from using these platforms can be directly applicable to the Moon, where lunar gravity leads to a reduction of the system weight to one-sixth compared with that on Earth.

A number of tests conducted in a compacted lunar regolith simulant, JSC-1a, have shown that the force reduction allowable by turning a percussive actuator on is of the order of 15–25-fold. This means that the mass of the required mobile platform would

page proof WILEY-VCH

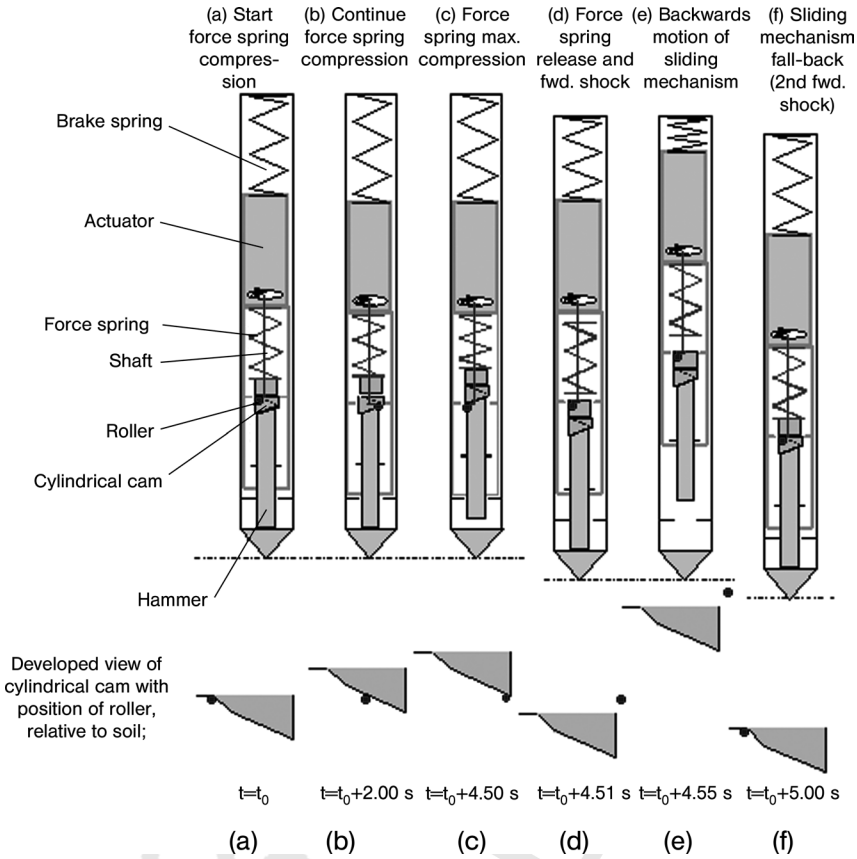

Figure 6.15 Mole shock cycle: note penetrations on first shock (d) and second shock (f) after rebound. Courtesy DLR and ESA.

also be reduced 15–25-fold (Figure 6.15). Thus, instead of using a vehicle that weighs 150 kg, now the vehicle needs to weigh only 10 kg to provide the same necessary traction. This translates directly into launch savings or allows the launching of 15 times more vehicles with percussive scoops.

Note that percussive scoops could potentially be used to dig into icy soils on Mars; however, the percussive power would have to be much higher than when digging into dry, compacted soil.

6.5 Moles

The mobile penetrometer or "Mole" is a mobility concept invented by VNII Transmash (Russian Mobile Vehicle Engineering Institute, St Petersburg, Russia), experienced in lunar rovers – they contributed to Lunokhod's instrumentation for measuring the

lunar soil mechanical properties – and in soil sampling devices (Gromov *et al.*, 1997). The Mole uses an internal mechanism to propel itself into loose planetary regolith. Although the progress tends to be slower than using conventional subsurface access methods such as drills or scoops, the Mole offers simplicity and robustness. The original prototype Mole was on the order of 1 m long and 10 cm in diameter.

6.5.1
The European Space Agency Mobile Penetrometer

The original prototype Mole has been miniaturized approximately fivefold in length and made space-worthy within a development performed with the German Aerospace Center, Deutsches Zentrum für Luft und Raumfahrt (DLR), and managed by the ESA in the period 1996–1997.

The Mole carries an internal hammering mechanism, sliding to reduce recoils; it is initially slightly compressed by the brake spring (Figure 6.16). Details of the shock cycle are illustrated in Figure 6.17: a roller following a helical cam compresses a spring and releases it: a hammer hits the tip and rebounds, falling back for a second hit and a new shock cycle. The repeated shocks drive it through the soil. It penetrates preferably into loose and unconsolidated soils, typically regolith, and also harder soils such as permafrost. The mechanism is powered via a tethered cable.

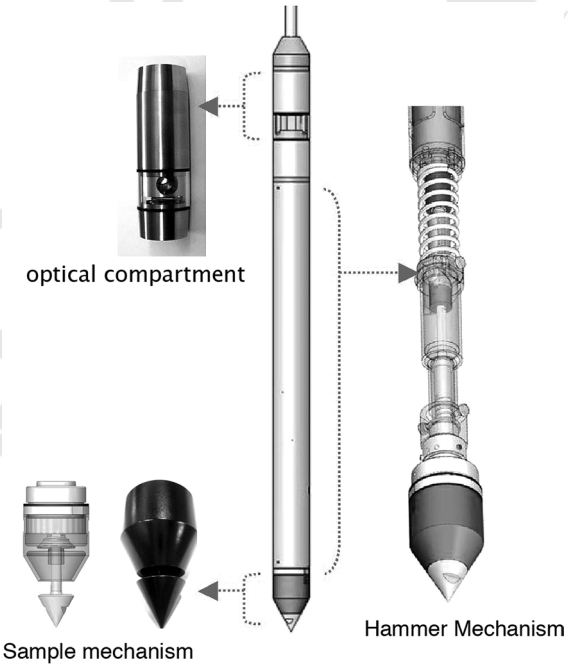

Figure 6.16 The MMUM penetrator elements are illustrated. Courtesy NASA Ames Research Center.

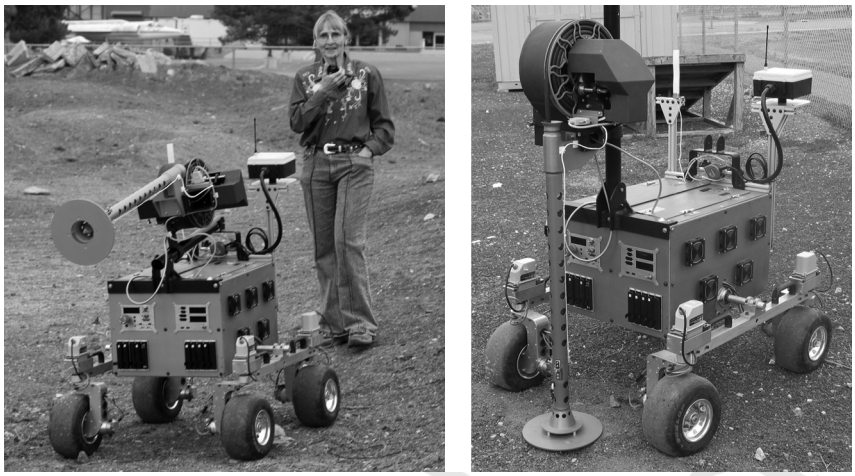

Figure 6.17 The MMUM including deployment and retrieval system shown mounted on the NASA Ames Research Center K10 rover. (a) The MMUM system retracted for driving; (b) the MMUM deployed for penetration. Courtesy NASA Ames Research Center.

The Mole is a pointed cylinder, with a length of 33 cm and a diameter 2 cm; its mass is 0.4 kg; its small motor, 5 W maximum, imparts 12 impacts per minute with only 2 W, providing useful shock energy of 0.1 W. The advance is typically 1 cm min^{-1} in sand and 1 mm min^{-1} in medium-hard regolith. Tests have demonstrated the mobility of the miniaturized Mole in ambient and thermal vacuum conditions. Ground tests have shown its capabilities of penetration in heaps of large pebbles (Coste, 1998). The depth capability is estimated to be 5 m. Retrieval tests by means of tether pull showed that the extraction force was greatly reduced when the shock mechanism was still operating. This prototype demonstrated the interest in the Mole as means of sub-soil penetration with low energy and power ~~– a basis for its further developments.~~ The Sampling Mole is an improved Mole design, with capabilities of sampling and backwards shock, developed for flight.

6.5.2
The Moon/Mars Underground Mole (MMUM)

The Moon/Mars Underground Mole (MMUM) (Stoker, Gonzales and Zavaleta, 2007; Stoker, 2008) is a device designed to burrow subsurface into soil. The MMUM was developed with support from the NASAs Mars Instrument Development Program to provide an alternative to drilling for planetary subsurface sampling and *in situ* sensing applications targeted to future Mars and/or lunar missions. The MMUM design derives from the PLUTO (Richter *et al.*, 2001, 2002; Coste *et al.*, 2001) that was built for the unsuccessful ESA Beagle 2 Lander, part of the Mars Express mission.

Table 6.1 Moon/Mars underground mole characteristics.

Parameter	Value
Mole mass (actual mass)	1900 g
Mass deploy/retrieve system (estimated flight mass)	5000 g
Mole diameter	4 cm
Mole length	62 cm
Peak power draw	10 W
Maximum penetration depth	2 m
Volume of sample collected	5 cm^3
Operation time to reach maximum depth	20 h (depends on soil properties)
Retraction mechanism	Surface winch
Retraction force capability	2500 N
TRL level	Mole = 5, deploy/retrieve system = 4
Science payload	Raman spectrometer, temperature sensor
Science data returned	Soil mineralogy, organic content, soil density, porosity, compressive strength, temperature, thermal conductivity, planetary heat flow

6.16

Table 6.1 shows the characteristics of the MMUM, which was designed to be larger than the tiny PLUTO so that it could accommodate carrying instruments to perform *in situ* analysis of the soil.

Figure 6.18 shows external and internal views of the MMUM penetrometer, a pointed slender cylinder that advances into the soil by way of an internal sliding hammer mass. Part of the energy released by the spring-loaded hammer is transferred to the mole casing with each impact and from there to the regolith, generating displacement. Using a single motor, the penetrator can hammer forward or in reverse, and can collect a sample. Additional support c[illegible]s remain on the surface and include a launch tube for ground insertion, a tether, a reel to pay out and retrieve the tether, power and control electronics, and operations software. The complete system mounted on a prototype surface rover is shown in Figure 6.19.

6.16

6.17

The mole hammering mechanism (Figure 6.18) consists of a stainless-steel housing structure, an encoded motor/gearhead system, a compression spring connecting the motor gearhead to a striking mass, and a recoil absorption spring. The hammering mechanism operates as a result of the motor and gearhead system turning a shaft that drives the spring and compresses it as the mechanism follows a guide path to the release point. Upon reaching the release point – a mechanical feature in the trajectory of the hammer mass travel – the striking mass is released by the compressed force of the spring. The hammer slides forward and impacts the front tip section of the mole. This cycle repeats every few gearhead shaft turns and produces a downward impact force at a rate of about 12 impacts per minute. Each hammer strike results in a forward penetration increment in soil; the actual penetration amount per shock cycle depends on the soil physical properties, ~~primarily the compressive strength of the soil.~~

page proof © WILEY-VCH

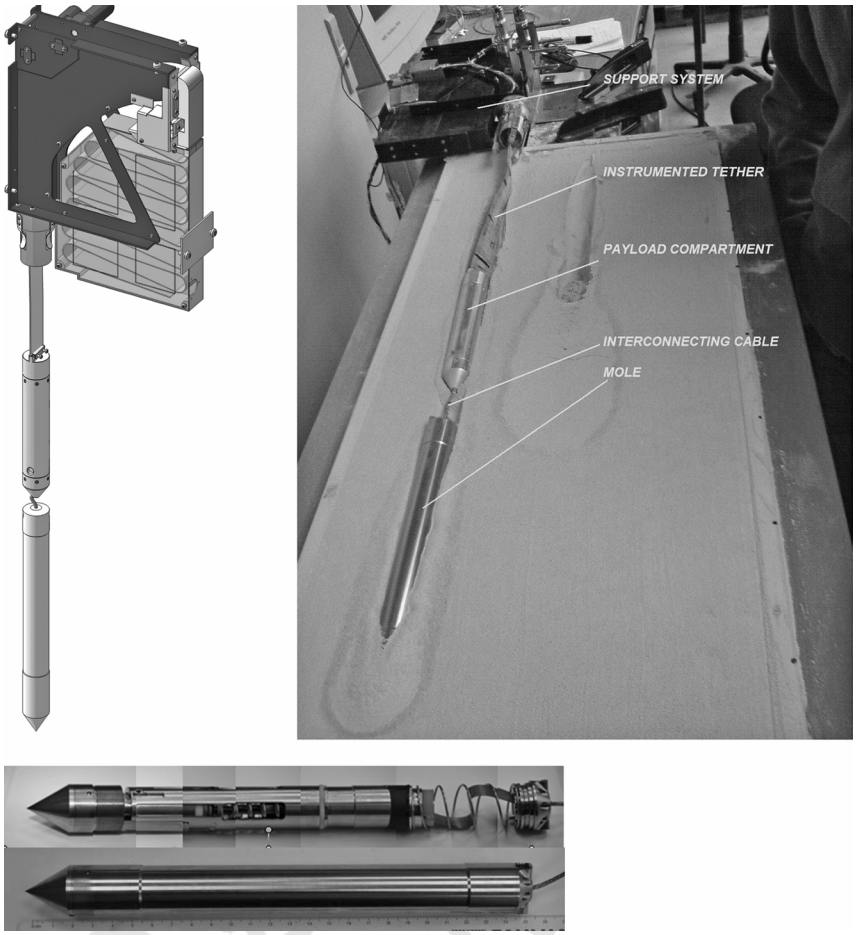

Figure 6.18 (a) Instrumented mole system with tractor mole and payload compartment fully released from the support system; (b) tractor mole and internal shock mechanism. Courtesy ESA, Galileo Avionica and DLR.

The sample collection mechanism is located on the tip end of the mole and can collect a volume of 5 cm^3 of soil. The sample collection mechanism is operated by the same motor as the hammering mechanism. To open the sample mechanism, the mole motor is operated in reverse mode activating a ball-lock mechanism that turns the front-tip guide screw open, thus pulling the nose cone open. Normally, while in forward penetration mode, the front tip is held ~~together~~ closed by a tension spring; however, when opening, the screw located in the front forces the spring open exposing the collection chamber. Then forward hammering is performed to drive the mole downwards and the collected sample is pushed into the collection chamber where it is trapped. After a few hammering operations cycles, the mechanism is closed by the screw, releasing the additional tension force on the spring and

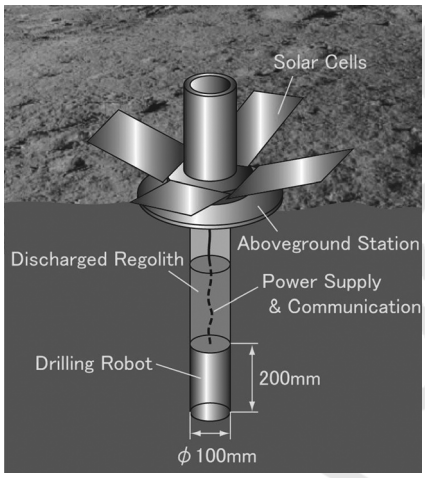

Figure 6.19 Concept of drilling robot system. Courtesy JAXA. (Please find a color version of this figure on the color plates).

continued hammering closes it. Once the operation is complete, the mole is retrieved to the surface and the sample is extracted from the collection chamber by again opening it. Forward hammering knocks any material out of the chamber.

The MMUM is connected to the surface via a tether containing electrical power and signal wires and also fiber-optic lines that carry light to/from optics housed in a compartment in the penetrator body. The tether is covered by a woven Kevlar jacket that carries the load required to pull the MMUM out of the ground after insertion. The required retraction force can be reduced by running the hammer mechanism during retrieval, which disturbs the soil and lowers the friction force of soil particles against the penetrator shaft. The tether is wound around a reel with a mandrel diameter of 21.6 cm requiring only three wraps around the reel to accommodate a tip depth on the mole of 2 m. The MMUM avoids the use of slip rings by using extra winds of tether inside a drum adjacent to the mandrel that contracts to a smaller diameter curvature as the reel pays out tether.

The MMUM incorporates a Raman spectrometer to analyze the subsurface composition *in situ*. The wall of an optical compartment section in the rear of the penetrator (~~Figure 6.19~~) is made of sapphire and light collection optics, focused just beyond the wall, and it is supported on shock mounts in this section. Fiber-optics located in the tether transmit light from a surface-mounted 785 nm, 300 mW diode laser to these optics to illuminate the soil, and light collected from the resulting stimulated emission is transmitted back to the surface where an InPhotonics InPhotote spectrometer (EIC Laboratories) is used to collect Raman spectra. A variety of minerals and compounds of interest to Mars exploration can be identified in these spectra, including sulfates, carbonates, and organic compounds.

Using the tether, MMUM can be repeatedly deployed and retrieved from a fixed lander or mobile rover. ~~moles~~ have advantages over drills for rover application

because once a small fraction of the mole body is underground there are no surface reaction forces, and there are never any torques exerted on the deployment platform. In the MMUM design, deployment and retrieval forces are reacted only on the support system (launch tube) and not on the rover body. Moles can be of much lower mass than a drill of comparable depth capability and so can be a single payload element on a rover. For example, the Beagle PLUTO with a tip depth of 1 m weighed less than 0.5 kg.

While MMUM was built to the parameters specified in Table 6.1, power, mass, volume, penetration depth, instrument payload, and operating speed are all variables that can be modified in a mole designed for a particular mission application. For example, in certain applications, such as the case where the mole and its deployment station may be operating in a permanently shadowed region of the Moon and solar power is not available, higher speed or reduced system mass may be necessary to minimize resource requirements, and other payload elements such as a water sensor may be desirable alternatives to the Raman spectrometer.

6.5.3
Instrumented Mole System (IMS)

Future planetary surface exploration will undertake several physical and chemical measurements. Some require subsurface penetration to bring the sensors underground: for example, for thermal flux investigations, or to search for water films on soil grains. An instrumented mole system (IMS) – a system able to insert (without retrieval) a mobile penetrometer carrying a payload of sensors for subsurface measurements down to 5 m depth – was developed for ESA and tested while being technologically partly based on the PLUTO mole developed for the Beagle 2 Mars lander (Section ~~1.11.6~~). This IMS, intended to be mounted on a planetary lan 6.18 could potentially be used on future planetary missions.

The IMS consists of a double-body mole system, composed of a tractor mole (which houses the hammering section) and a trailed mole (which houses the scientific experiment section) connected by a short cable (Figure 6.20). This allows the accommodation of the moles disposed at 90° to each other in a compact lightweight

Figure 6.20 Initial experimental testing of prototype robot. Courtesy JAXA.

structure, ~~so~~ minimizing the storage volume. The lightweight carbon fiber-reinforced polymerCFRP structure also has a storage compartment for a long, flat cable (3–5 m) which is used to provide the moles with electrical power and data transfer for their operation.

Two mechanisms of the pin-puller type are used to keep the moles constrained for launch and landing. No active deployment mechanism was necessary since deployment is achieved by the reaction to the hammering shocks provided by sets of springs included in the guiding tube. The tractor mole is 25 cm long, 2.6 cm in diameter and has a mass of 0.43 kg. It delivers to the soil a useful shock energy of 0.19 J every 4 s, with an average power of less than 4 W. The IMS ~~FM~~ mass is 1.4 kg.

A breadboard of the IMS has been manufactured including, amongst others, a structure (made of carbon fiber) and the mechanisms to secure the moles at launch and landing.

The breadboard has been extensively tested in its main constituent part individually and in integrated mode. Integrated deep soil penetration tests, simulated reduced gravity tests, thermal vacuum/climatic chamber tests, and vibration tests have been performed with good results (Gelmi *et al.*, 2007).

The industrial team of this study, completed in 2006, was led by Galileo Avionica (Italy) with DLR Cologne (Germany), responsible for the development of the tractor, University of Münster (Germany), for the scientific payload assessment with the preliminary definition of the HP3 instrument package intended for the ExoMars Surface Platform, University of Leicester (UK), for the X-ray fluorescence spectrometer preliminary definition, Kayser-Threde (Germany), for the Raman spectrometer, and Space-X (Switzerland), for the camera. Since the completion of the study, the IMS has been serving as the basis for the development of the HP3 instrumented mole for flight on the surface platform of ExoMars.

6.5.4
Mole-Type Excavation Robot for Subsurface Exploration

The Japan Aerospace Exploration Agency (JAXA) is promoting lunar and planetary exploration missions, Hayabusa mission and Kaguya mission. Lunar lander-rover missions (Hashimoto *et al.*, 2008) are also under study to follow the SELENE mission. For these missions, it is necessary to perform sampling in order to conduct the *in situ* analysis of geological samples and to deploy vario[illegible]es for measurement and observation.

JAXA is studying and developing a mole-like robot which is maneuverable in the regolith (Watanabe *et al.*, 2003). Figure 6.21 shows the concept of the proposed robot system, which consists of a drilling robot and above-ground avionics. The whole body of the drilling robot is to be buried. The above-ground section is connected with the drilling robot by a wire in order to supply electric power and communications. The above-surface avionics has power generation (solar cells, ~~etc.~~), and also a communication system between the robot and the lander or the mother rover in order to relay commands and telemetry data between the drilling robot and the lander or the rover.

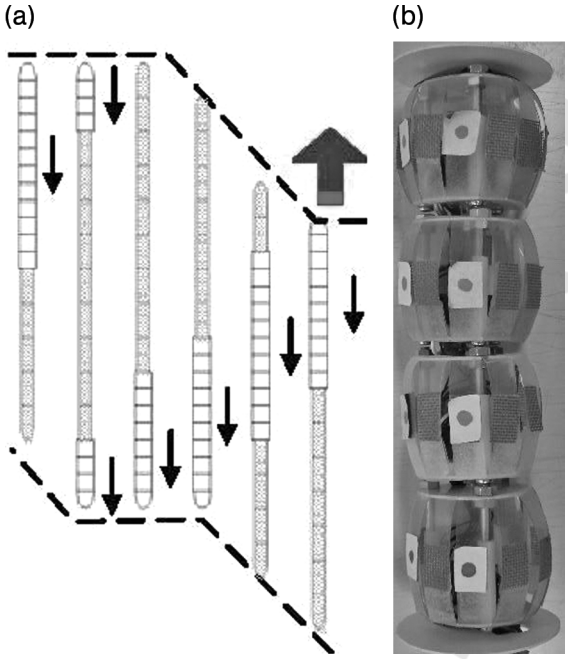

Figure 6.21 Locomotion pattern and peristaltic crawling mechanism of earthworm. Courtesy JAXA.

Regarding the excavating mechanism, the robot subsurface exploration can be divided into the following three phases:

- Phase 1. Moving to the drilling point and deploying.
- Phase 2. Starting to drill (half-b[illegible]).
- Phase 3. Moving in the soil (ful[illegible]).

6.19

In phase 1, the robot can move under the guidance of the mother rover. That means that the mother rover can carry the robot to the drilling exploration point. ~~Therefore, the drilling robot need not move across the surface by itself.~~ In phase 2, the above-ground station, as shown in Figure 6.21, can control the robot to initiate drilling. Phase 3 is more complicated and is described in the following ~~detailed discussion~~. In order to move forward in the soil, the following two mechanisms are required:

1. clearing the space in front of the robot
2. moving into that space once it is available.

With regard to the first function, the robot has to carry the excavated regolith backwards and discharge it, because the filling factor of regolith on the Moon is known to be very high. In addition, the second function is complicated by the fact that gravity on the lunar surface is only one-sixth of Earth's surface gravity. Therefore, it is difficult for the robot to keep moving downwards by gravitation alone. Hence a mechanism that propels the robot downwards is required. Overall, the following

Page proof WILEY-VCH

functions are needed for the subsurface exploration robots of this type: excavation, carrying, discharging, forward movement, and direction control. JAXA is ~~proposing and~~ developing a novel forward-movement method that makes use of reactive force caused by pushing the discharged regolith above the robot. In the proposed method, first the robot excavates the regolith and channels it into its body. Second, the robot carries the excavated regolith upwards through the body and discharges it from the top (the rear of the robot). Finally, by pushing against the discharged regolith, the robot moves forward.

A discharging mechanism is required to force the regolith that is channeled or carried internally through the body out while preventing external regolith from re-entering the robot body. A novel discharging mechanism was developed which has two rollers. One roller rotates clockwise and the other rotates counterclockwise. The concept testbed consisted of two parallel rollers, whose length is 100 mm and diameter is 20 mm. The rollers rotate at 2.5 rpm. The ~~interval~~ between ~~them~~ can be fixed arbitrarily ~~while being kept parallel.~~ In addition, it is possible to apply tension between the rollers ~~by~~ using springs. In these simple experiments, it was confirmed that the regolith can be discharged using this ~~mechanism~~.

A carrying mechanism is required to move the drilled regolith through the robot body to its upper part to facilitate forward movement. A variety of carrying mechanisms have recently been developed. One is the bucket elevator method (Yoshida *et al.*, 2002) ~~to use the~~ principle of a belt conveyer. Another approach is a vibration-based transportation method (Yokoyama and Higuchi, 2002). The mechanism based on the bucket elevator was found to be complex and to require many parts and a large volume. The vibration-based transportation approach was modified to carry regolith. By applying vibration to the plate trough, particles with an upper velocity along the trough can be produced with the net effect of particle flow upwards. To confirm the effectiveness of this carrying mechanism, an experimental model was developed.

The feasibility of the proposed mechanism was confirmed through analyses and some experiments on each component part, including a forward movement mechanism, a discharging mechanism, and a carrying mechanism (Kubota *et al.*, 2005). The integrated prototype robot was developed and tested as shown in Figure 6.22. The prototype robot was found to penetrate to a depth of half its length.

~~1. *Moving mechanism:*~~ To move forward efficiently, a novel mechanism based on biomimetics is currently under study. An earthworm moves by a locomotion mechanism called peristaltic crawling. This locomotion requires less space than other approaches and allows for movement across irregular ground and inside narrow pipes. Therefore, it was desirable to apply this locomotion mechanism to subsurface exploration robots. ~~A crawling mechanism based on earthworm locomotion was studied and developed.~~ The inner wall of the body is composed of a two-layer muscle: the outside layer is called the circular muscle while the inside layer has a muscle that acts in the longitudinal direction. When the circular muscle is contracted in a radial direction, the segment is thinner, and is extended in the axial direction. When the longitudinal muscle is contracted in the axial

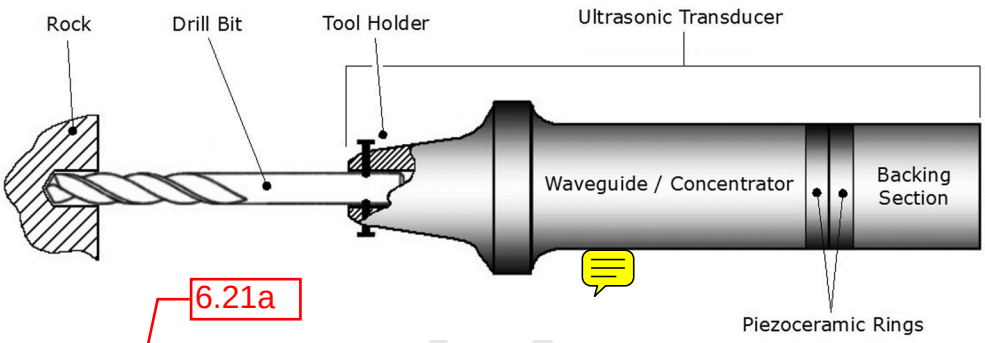

Figure 6.22 Typical ultrasonically assisted drilling arrangement.

6.21a

direction, the segment becomes thicker and shorter (Nakamura *et al.*, 2006). Figure 6.23a shows the locomotion pattern of an earthworm with peristaltic crawling. The earthworm propagates a longitudinal wave from the front to the back of its body by contracting the muscles in each consecutive segment.

The locomotion pattern can be illustrated as follows: the segments of the earthworm head are contracted by the longitudinal muscle. In this case, because the thicker segments contact the moving surface for locomotion, the friction between the segments and the ground is increased. Hence the segments remain on the contacting surface.

2. ~~The contracted segments propagate to the back continuously. This movement pulls the more rearward segments in the direction of the movement.~~

3. ~~The segments of the earthworm head are extended in the axial direction by the circular muscle. In this case, since the friction between the segments and the moving surface is decreased, thinner segments can be smoothly moved. Furthermore, because the more rear segments remain in contact with the surface, the thinner segments can be moved forward.~~

4. ~~The extended segments propagate to the back continuously. The more forward segments are pushed out in the direction of the movement.~~

The peristaltic crawling robot is composed of several contraction–extension (CE) units and a PIC microcontroller. Figure 6.23b shows the configuration of the

6.21b

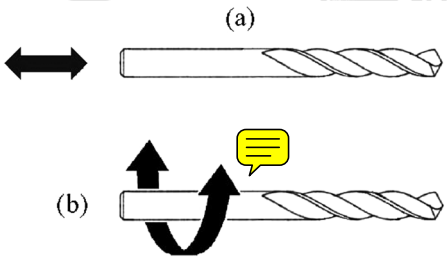

Figure 6.23 UAD excitation.

developed peristaltic crawling robot. The CE unit is flexibly connected in the axial direction. Since peristaltic crawling requires at least three contraction segments, the robot also needs at least three contraction units.

A new mole-type robot for lunar subsurface exploration is under development by integrating the proposed discharging, carrying and earthworm movement mechanism. Subsequent demonstrations of the proposed methods ~~by drilling experiments have been~~ planned.

6.6 Ultrasonic and Percussive Actuated Drills

6.6.1 Ultrasonically Assisted Drilling

6.22

Ultrasonically assisted drilling (UAD) takes place when high-frequency (ultrasonic) oscillations are superimposed on the cutting motion of a conventional twist drill (Thomas and Babitsky, 2007). A typical arrangement for UAD is to mount a conventional drill bit into an ultrasonic transducer (Figure 6.24). The ultrasonic transducer consists of two piezoceramic rings, a backing section, a waveguide/concentrator, and a tool holder. The concentrator serves to amplify the vibration (with respect to displacement amplitude) generated by the piezoceramic rings and, with the employment of the tool holder, applies it to the drill bit. The complete ultrasonic system including the drill bit must be tuned in order that it resonates at a suitable frequency (usually within the range 20–40 kHz) and generates a high displacement amplitude at the working end of the drill bit. Either the whole assembly is rotated or the workpiece is rotated. Drilling is then conducted in a manner similar to

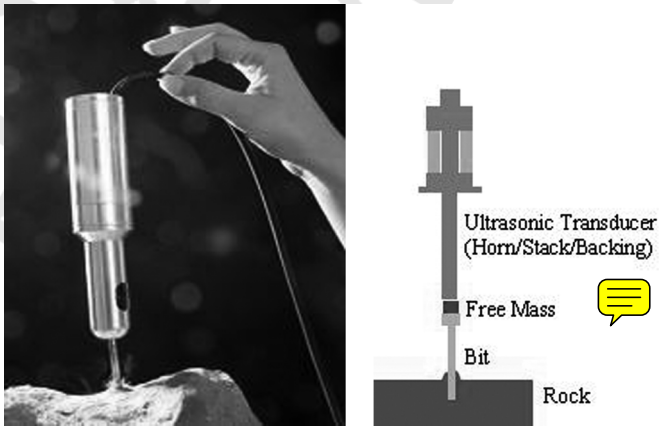

Figure 6.24 (a) A photographic view of the USDC showing its ability to core with minimum axial force; (b) a schematic cross-section view. Courtesy NASA/JPL.

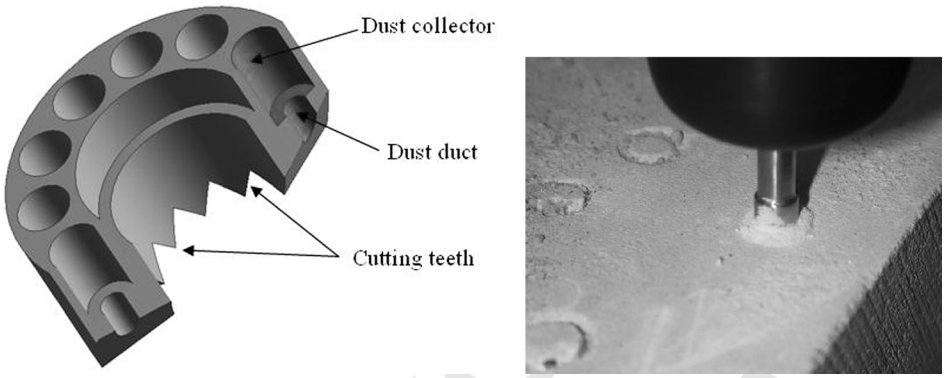

Figure 6.25 (a) A cross-section of the bit of the powdered-cuttings sampler; (b) a photograph of the sampler in action drilling a limestone and accumulating cuttings inside the bit. Courtesy NASA/JPL.

6.23a

6.23b

conventional twist drilling. The typical direction in which ultrasonic vibration is applied to a drill bit is in the longitudinal (or axial) direction (Figure 6.25a), although it may be excited torsionally (Figure 6.25b).

Alternative names for UAD are ultrasonic vibration drilling (UVD) (Zhang *et al.*, 1994), ultrasonic-assisted (UA) drilling (Chang and Bone, 2005), drilling with ultrasonic support (Neugebauer and Stoll, 2004), and ultrasonic twist drilling (Graff, 1975; Devine, 1985). UAD has previously been employed predominantly in the drilling of metals (Thomas, 2008), although metal matrix composites (MMCs) such as aluminum–silicon carbide (Liu *et al.*, 2005), glass fiber-reinforced plastics (GFRPs) (Takeyama and Kato, 1991; Aoki and Nishimura, 2004; Zhang *et al.*, 1994; Babitsky *et al.*, 2007), and glass/engineering ceramics (Egashira *et al.*, 2002; Babitsky *et al.*, 2007) have shown positive results when drilled with UAD. Recently, efforts at Magna Parva led to the development of the ultrasonic drill tool (UDT) that uses sonic vibrations that are excited by a nonlinear vibro-impact mechanism (Babitsky, 1998; Astashev and Babitsky, 2007).

A device that oscillates in a purely ultrasonic manner (at frequencies of about 20 kHz and above) can be employed to drill/core holes in rock and other hard and brittle materials. High stresses must be generated in order to cause compressive rock fracture (especially when drilling harder rocks), hence the mode in which purely ultrasonic drill tools are presumed to cut is that of erosion; forcing small particles of rock against the consolidated rock's surface, causing more particles to break off and perpetuate the drilling/coring process. The rock and particles are usually composed of a similar material, so unless the cuttings are removed a large proportion of the energy in the system is expended in reducing the size of the loose particles. Smaller particles cause a lower material removal rate, meaning that this process is relatively inefficient. The manner in which purely ultrasonic rock drilling tools operate is similar to traditional ultrasonic machining techniques which employ either an abrasive slurry or particle-impregnated MMC abrasion tools. The abrasive particles

contained in abrasive slurry are harder than the material that is being drilled. Ultrasonic drills employing a drilling fluid/slurry have also been used to drill rocks (Maurer, 1968), where the rock was abraded by the hard and sharp particles suspended in the drilling fluid. The fluid was continually circulated to feed the tool with fresh abrasive particles and remove rock particles. Cavitation was also assumed to play a role in the drilling process, but primarily ~~cavities~~ agitate the particles. The use of drilling fluid makes this specific approach unsuitable for most extraterrestrial applications.

Drilling with a full face bit makes such drills inefficient compared with other rock drilling techniques (Maurer, 1968); however, employing a coring bit substantially improves the efficiency by reducing the area that requires breakage. An evolution of the purely ultrasonic rock drilling is the use of sonic frequency oscillations that are excited by the ultrasonic actuation. This method was first developed by scientists at the JPL jointly with Cybersonics, Inc., and the drill is called the Ultrasonic/Sonic Driller/Corer (USDC) (Bar-Cohen *et al.*, 2001). As described in this chapter, numerous modifications were made following its development in 1999 towards making this drilling method applicable to as many possible future planetary missions as possible.

6.6.2
Ultrasonic/Sonic Driller/Corer (USDC)

Rotary drilling techniques are limited by the need for high force on the bit, and by an inability to duty cycle efficiently. To address these limitations, the JPL's Advanced Technologies Group and engineers from Cybersonics, Inc. jointly developed the USDC (Bar-Cohen *et al.*, 2001, 2007; Bao *et al.*, 2003; http://ndeaa.jpl.nasa.gov/nasa-nde/usdc/usdc.htm). The USDC is a penetration mechanism that is driven by a low-frequency hammering action resulting from conversion of high-frequency vibration (see Figure 6.26). It was developed to support the NASA search for existing or past life in the Universe, allowing probing and sampling of rocks, ice, and soil. This

6.24

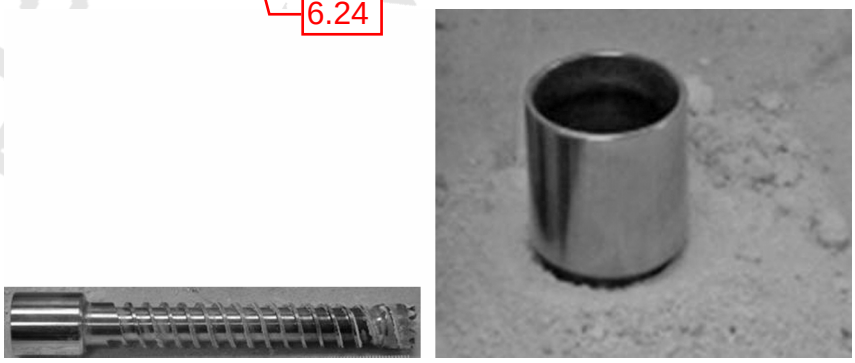

Figure 6.26 Photographs of (a) the drill bit with the flutes and (b) the bit in the formed borehole and the extracted powdered cuttings. Courtesy NASA/JPL.

mechanism is driven by an ultrasonic piezoelectric actuator that impacts a bit at sonic frequencies through the use of an intermediate free mass. The USDC was designed to produce both core and powdered cuttings, operate as a sounder to emit elastic waves and serve as a platform for sensors. The USDC requires low axial force, thereby overcoming one of the major limitations of planetary sampling using conventional drills in low gravity environments. This capability offers the advantage of being able to perform rough tasks of drilling and coring in hard rocks, ice, and packed soil using relatively small force and relatively lightweight hardware. Also, the requirement for a low axial load allows operation from lightweight robots and rovers.

The USDC consists of three key components: actuator, free mass, and bit (Figure 6.26) (Bao *et al.*, 2003). The actuator operates as an ultrasonic vibration mechanism that imparts energy to the free mass and the free mass in turn impacts the bit, producing a stress impulse. This impulse fractures rock when its ultimate strain is exceeded at the rock/bit interface. The actuator consists of a piezoelectric stack with a backing layer for forward power delivery and a horn for amplification of the induced displacement. The actuator is driven in resonance and is held in compression by a stress bolt that prevents its fracture during operation. In the basic design, the piezoelectric stack has a resonance frequency of about 20 kHz. The drive electronics are designed to maintain tuning of the actuator either in software or hardware and thus ensure maximum electric current input. This tuning is required since there are several factors that affect the resonance frequency, including the action of the drilled medium reducing the Q of the resonator and slightly shifting the frequency. In addition to the need for tuning that is common to ultrasonic actuated mechanisms, the USDC requires attention to the impacts that cause time variations in the current signal. This effect is minimized using various control algorithms, including hill climbing and extremum seeking (Aldrich *et al.*, 2006). Unlike typical ultrasonic drills where the bit is acoustically coupled to the horn, in the USDC the actuator drives a free mass that converts ultrasonic impacts to hammering at sonic frequencies.

Following the development of the mechanism that drives the USDC, a series of novel designs were conceived and disclosed in NASA New Technology Reports and patents (e.g., Aldrich *et al.*, 2006; Badescu *et al.*, 2006; Bao *et al.*, 2004; Bar-Cohen *et al.*, 2001, 2002, 2005; Bar-Cohen, Sherrit, and Herz, 2003; Bar-Cohen and Sherrit, 2003; Chang *et al.*, 2004; Dolgin *et al.*, 2001a; Dolgin *et al.*, 2001b; Sherrit *et al.*, 2001, 2002, 2003. Some of the devices that were developed include the ultrasonic/sonic rock abrasion tool (URAT), ultrasonic/sonic gopher for deep ice drilling, the lab-on-a-drill, and many others. The USDC was demonstrated to drill ice and various rocks including granite, diorite, basalt, and limestone.

The development of the USDC is being pursued on various fronts, ranging from analytical modeling to field testing and the implementation of improvements in support of a wide range of potential applications. While developing the analytical capability to predict and optimize its performance, efforts are being made to enhance its ability to drill at higher power and high speed. Taking advantage of the fact that the bit does not require rotation, sensors (e.g., thermocouple and fiber-optics) were integrated into the bit to examine the borehole during drilling.

6.6.2.1 Operation in Extreme Environments

NASA's strategic goals and science objectives are increasingly requiring future missions to be involved with robotic exploration of planets where the environment poses greater challenges to existing technologies. These extreme environments include very high temperatures as on Venus (460 °C) and very low temperatures as on Europa and Titan (−180 °C). In addition, potential missions may require sampling at very low gravity as is found on asteroids and comets and also in high-pressure environments such as on Venus (90 bar). These conditions pose challenges to the technologies that can be used for *in situ* exploration tasks and are requiring new capabilities. Although there have been significant advances in capability for low-temperature applications, the technologies for high-temperature applications are still limited. For the low-temperature range, the USDC was demonstrated to drill at temperatures as low as −180 °C. Further, under an on-going NASA Planetary Instrument Definition and Development Program (PIDDP)-funded task, a USDC-based high-temperature sampler is being developed for operation at the ambient temperatures of Venus. For this purpose, piezoelectric materials with a Curie temperature that is higher than 500 °C are being developed jointly with Penn State University (Shrout *et al.*, 2004). Some of the potential candidates that are being investigated include; $LiNbO_3$ and modifications of bismuth titanate, ~~BSTpe3,~~ and Bi $(MgTi)O_3$–$PbTiO_3$ (Eitel *et al.*, 2002).

Q3

6.6.2.2 USDC as Powdered Cuttings Sampler

As part of the sampling process, the USDC generates fine powdered cuttings (Sherrit *et al.*, 2001, 2003). Tests of the powder that was produced by the USDC have shown that their size allows for high-quality X-ray diffraction spectra (Blake *et al.*, 2003; Chipera *et al.*, 2003). The XRD patterns obtained from the USDC generated powder are essentially indistinguishable from powders that were obtained using a laboratory Retsch mill. Also, the particle size distributions are comparable to those obtained from standard laboratory Retsch mills.

6.25a

In an effort to produce a sampling mechanism for cuttings that is compact and lightweight, a USDC bit was configured with trapping cavities. These cavities acquire the upward-traveling powder that enter a hollow inner section of the bit (see Figure 6.27a) and retain the particles until they need to be delivered to an instrument or disposed of (Sherrit *et al.*, 2006). Using finite element design models, JPL developed a compact horn configuration (Chang *et al.*, 2004) that allowed for the development of a 265 g device. The bit was made hollow with an end-effector section that is brazed on the bit and has teeth to enhance the cutting performance.

6.6.2.3 USDC with Integrated Sensors

Studies of the operation of the USDC have shown the capability to sample, probe, and sense while drilling and the developed system was called lab-on-a-drill. Two types of sensors have been successfully integrated and demonstrated to date: thermocouple and fiber-optic. A thermocouple was used to measure the rate and maximum rise of temperature and these values were found to correlate with the hardness of the rock being drilled. Even though these thermal variables are dependent on the heat

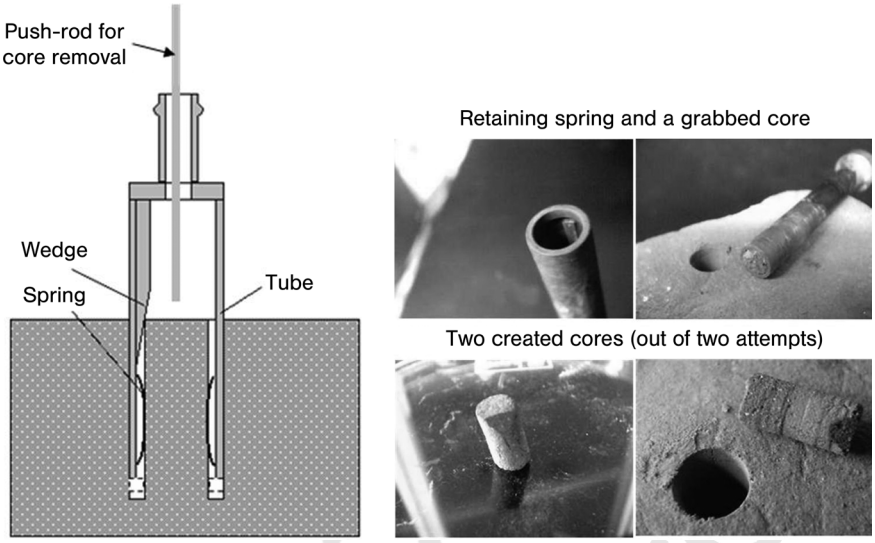

Figure 6.27 (a) A cross-sectional illustration of the all-in-one bit; (b) the bit and some formed cores. Courtesy NASA/JPL.

conductivity and capacity of the drilled object, most rocks have thermal properties within a comparatively narrow range. Compiling temperature rise rate and maxima as a function of time for a variety of drilled materials has demonstrated the feasibility of using a thermocouple-on-the-bit as a means of assessing the drilled medium hardness (but this could lead to errors if the rock contains water or ice that could be evaporated and generate cooling). Also, using an optical fiber provided a sensing capability where a fiber with approximately 160 μm diameter probe head was imbedded into a 10 mm diameter coring bit with a 1 mm wall thickness. Reflection data in the wavelength range 400–1200 nm were recorded. The use of fiber-optics with UV light of wavelength in the region of 200 nm has the potential for identifying biological markers using biofluorescence.

6.6.2.4 Various USDC Configurations and Designs

A variety of novel designs of the bit, horn, and the other components of the USDC were developed to deal with the various challenges and requirements of autonomous sampling in extreme environments. In many cases, the design of a complete system to meet the various potential mission configurations was developed. The various configurations that were developed are partially covered in this section, while the designs that were made to address the need to drill 1 m and deeper are covered later in this chapter.

6.6.2.5 USDC-Based Rotary Hammer for Rapid Drilling

Lessons learned from the field test of the ultrasonic/sonic gopher in Antarctica have shown that powdered cuttings removal is a significantly limiting factor in achieving rapid drilling to great depths (Badescu *et al.*, 2006). To improve the cuttings removal

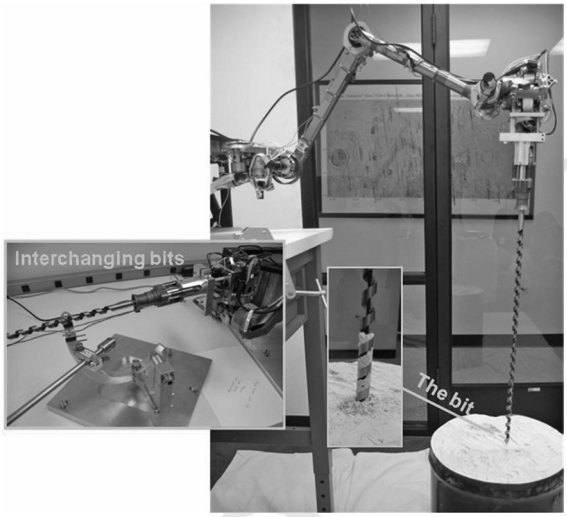

Figure 6.28 The MIDAS system with an interchangeable bit mechanism for the USDC. Photographed at Alliance Spacesystems by Lori Shiraishi, JPL/Caltech/NASA, and published with her permission.

and the drilling speed effectively, a rotation capability was introduced in the form of a rotary hammer (Badescu *et al.*, 2007). The hammering and rotation actuations were decoupled, providing a drilling redundancy in case of failure of one of these two mechanisms.

At shallow depths of less than 2–2.5 cm, the powdered cuttings travel along the shaft partially as a result of the air pressure from the vibrating bit and partially due to the induced vibration. To permit greater depth of penetration, pressurized gas was introduced from the center of the bit. Using this technique, a basalt core approximately 10 cm long was produced. To increase the rate of penetration further and avoid the use of pressurized gas, the rotary hammer capability was developed. The bit was designed with flutes allowing the cuttings to be augered up the outer shaft of the core. These helical flutes help the cuttings to travel upwards along the side of the bit to the surface of the penetrated medium. Photographs of the bit, the drilled hole and the powdered cuttings are shown in Figure 6.28. For the demonstration of the capability of the developed rotary hammer drill, a 14 mm diameter bit was used to penetrate a limestone. The USDC was operated with ~100 W continuous power and ~29 N (6.5 lb) WOB and it reached a depth of approximately 8.5 cm in a total continuous drilling time of 5 min.

6.26

6.6.2.6 USDC with All-in-One Bit

Exchanging bits is a necessity for replacing a worn-out bit or allowing other capabilities and it requires a manipulation system. For this purpose, an all-in-one bit was developed and demonstrated (Bar-Cohen *et al.*, 2002). The bit consists of a tube with a wedge at the top of the inner surface, a set of springs near the tip and a

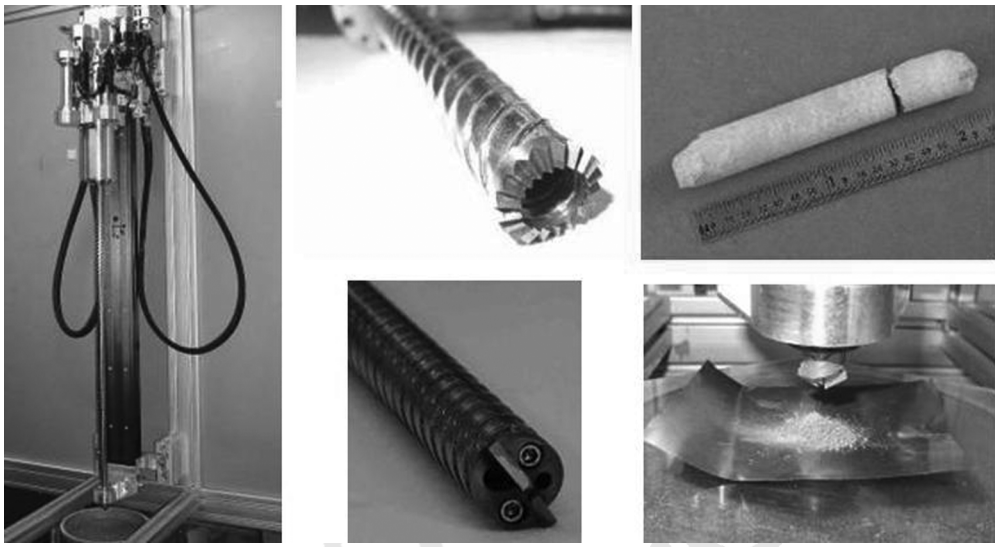

Figure 6.29 Subsurface sampler. Clockwise from left: full assembly; coring drill string; core sample; regolith sample; regolith sampling drill string. Courtesy Honeybee Robotics.

push rod that is inserted through a center hole (see Figure 6.29). Once a core is produced at a length of the inner section of the bit, the wedge introduces transverse forces at the top of the core to cause maximum stress near the base of the core and shear fracture. The side springs hold the core segment for removal from the borehole. The core is extracted from the bit using the push rod by overcoming the frictional retaining force of the spring. In Figure 6.29, photographs of the coring bit and the cores produced are shown.

Using the ability to exchange bits of the USDC, the JPL team worked jointly with Alliance Spacesystems (Alliance) to employ their robotic arm with a USDC unit. A bit interchange mechanism and a tool caddy of bits were developed and the system was called Mars Integrated Drilling and Sampling (MIDAS) (see further description later in this chapter). A composite photograph of the developed system that includes the robotic arm, the USDC, and a tool caddy of bits is shown in Figure 6.30.

6.6.2.7 The 0.5 m USDC

To reach a depth of 0.5 m in regolith, Honeybee Robotics and JPL jointly developed a sampler that combines a USDC mechanism and bit rotation. The objective of making this sampler was to produce an all-in-one type of bit with the capability to produce, retain, and transfer samples. A photograph of the drill is shown in Figure 6.31.

Both coring and powder/regolith sampling drilling mechanisms were created. The coring drill is capable of creating 9 mm diameter cores that are up to 51 mm long. The regolith sampling drill has a sample chamber allowing the capture of 0.25 cm^3 of material. Both drill configurations create a borehole that is 14.5 mm in diameter. The

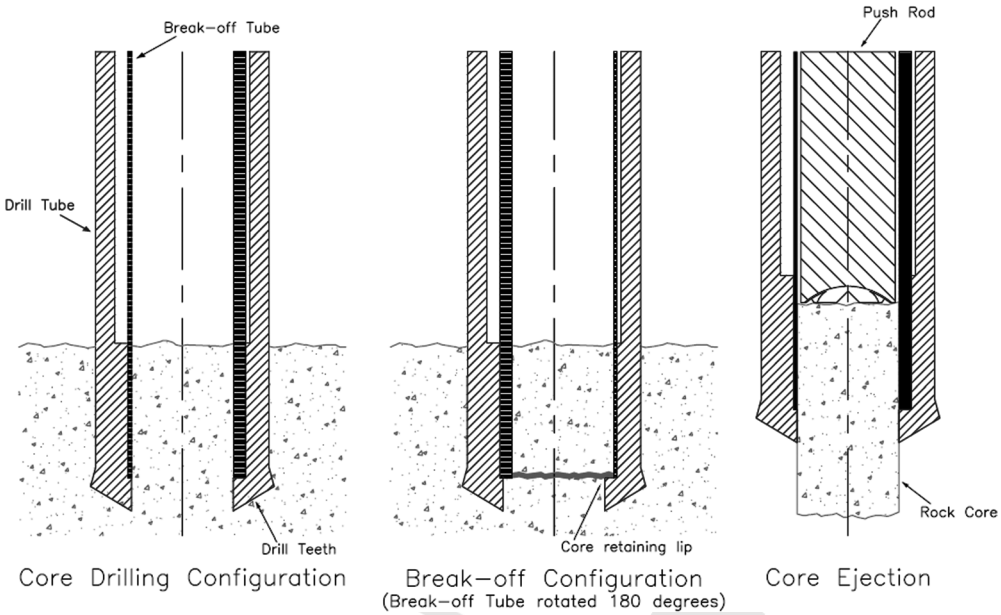

Figure 6.30 Subsurface sampler core break-off and ejection. Courtesy Honeybee Robotics.

system has an integrated load cell to sense preload and provides closed-loop control of feed rate and WOB.

The coring drill configuration contains an additional core break-off tube, inside the primary drill tube, that can separate the core from the base material via a rotary shea[illegible]n. Taking place at the lower end of the core near [illegible] of the drill bit, the shearing force is created by the relative rotation o[illegible]centric components. These components also act to retain a consolidated core in the break-off configuration (Figure 6.32b). During core drilling and core ejection operations, the center bore axes of these two components are aligned (Figure 6.32a, c).

Similarly to the coring drill, the regolith sampling drill has internal cavities for capturing either regolith or powder cuttings. The regolith sampling drill can penetrate both consolidated and unconsolidated material. The delivered sample is in the form of sand or fine powder, depending on the material being sampled. The

Figure 6.31 The MIDAS USDC and bit interchange mechanism assembly. Courtesy NASA/JPL and Alliance Spacesystems.

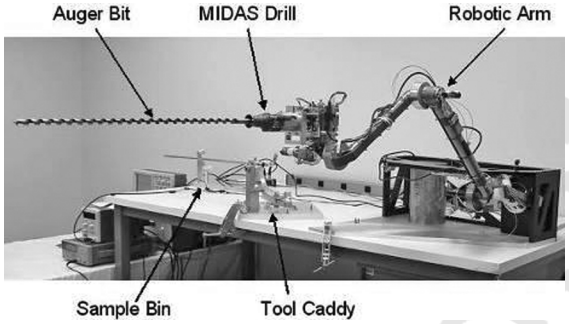

Figure 6.32 The MIDAS system with the tool caddy. Courtesy NASA/JPL and Alliance Spacesystems.

system can selectively sample from a desired depth via a "door" that blocks the pathway to the internal cavities during nominal drilling operations, and opens the pathway to acquire the sample. The "door" also acts to retain the sample once captured. Once the sample has been acquired and brought to the surface, the mechanism has the capability to push out the fine collected sample inside the sample cavities. Twin push rods translate up and down inside their respective sample cavities when handing over the sample to an external cache.

Testing included capturing both consolidated cores and powder samples in laboratory ambient and Mars-relevant environments. Coring in ambient conditions showed that a 2 in limestone core could be created and captured in 3.7 h using a 20% duty cycle on the piezoelectric stack. Drilling into Mojave Mars Simulant (MMS) in ambient conditions showed a capture of 696 mg of MMS in 3 h at a depth up to 4.5 in using a 20% duty cycle. Drilling into stacked layers of colored plaster verified the systems capability to selectively sample from a given depth and retain stratigraphy. Environmental testing was done in a vacuum chamber at 3 Torr CO_2 at $-20\,^{\circ}$C and showed the capability to core to a depth of 0.465 in in 4 h. No core was captured since the breadboard could not autonomously perform the capture operation at the time the testing was performed. It should be noted that decreased, but satisfactory, performance was observed compared with ambient performance. It was concluded that this was due to a shift in the natural frequency of the USDC piezoelectric stack due to the cold temperatures. This frequency shift has been shown to affect drilling performance drastically.

6.6.2.8 The 1m USDC-Based Penetrator

The ability to penetrate packed soils using low axial load was demonstrated in a USDC-based penetrator that is capable of reaching a depth of about 1 m using a 3.18–4.76 mm diameter bit. Inserting the bit into this soil by a pushing force alone requires several hundred pounds, which could easily result in bit buckling. Using the ultrasonic/sonic impacting mechanism a penetrator was developed and demonstrated to reduce the required push force greatly. In the demonstration of the penetrator capability, it was shown that the required push force to penetrate highly packed soil down to about 1 m was reduced from 200 to 7 lb (from 890 to 31 N) (Bao *et al.*, 2004). This effort involved modal and harmonic actuator analysis and system impact

analysis that allowed for the effective design of the penetrator. The modal analysis was used in the actuator design and the harmonic analysis to predict the actuator performance. The actuator design parameters were determined such that the mounting location coincides with the actuator neutral plane. The impact analysis, which determines the interaction between the free mass, the ultrasonic horn, and the bit, was used to derive an optimal weight of the free mass.

6.6.3 Mars Integrated Drilling and Sampling (MIDAS) System

The MIDAS system for low-mass, mobile, robotic platforms is a lightweight system developed by Alliance that permits the automated retrieval of multiple samples from regolith up to a depth of 0.5 m. MIDAS combines a 5-DOF robotic arm (derived from the MER) and a USDC (Bar-Cohen *et al.*, 2001) developed by JPL. MIDAS has an interchangeable bit mechanism and bits tool caddy capable of retrieving samples from 0.5 m and depositing them into an in 6.31 t for further analysis or a storage container for return to Earth. The complete system is approximately 1 m in length and weighs less than 6 kg. The MIDAS USDC and bit interchange mechanism assembly is shown in Figure 6.33.

The MIDAS system (Figure 6.34) was designed to acquire, handle, and deliver samples for storage or analysis. Its 5-DOF robotic arm is based on the Instrument 6.32

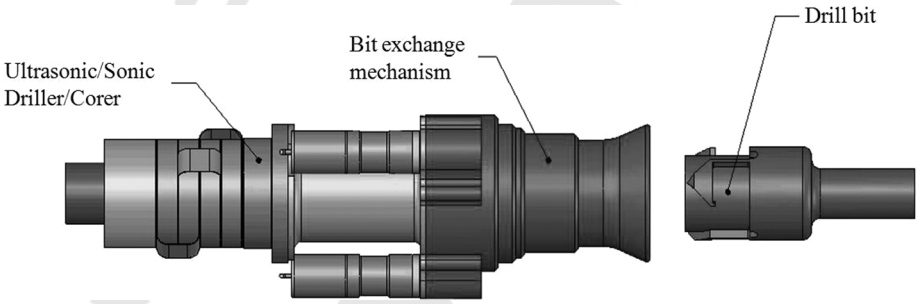

Figure 6.33 The interfacing of the bit and the drill via snap-on design. Courtesy NASA/JPL and Alliance Spacesystems.

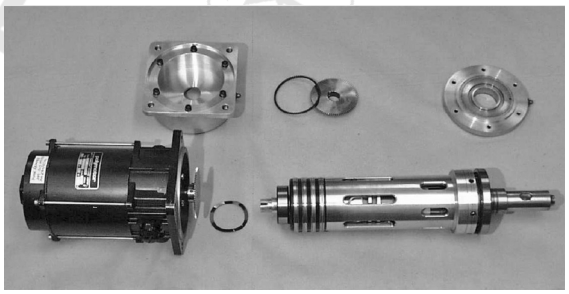

Figure 6.34 Ultrasonic drilling module for terrestrial applications. Courtesy University of Aberdeen.

Deployment Device (IDD) developed by Alliance for the MERs launched in June 2003 and still functioning on Mars as of May 2008. This low-mass robotic arm provides very precise positioning and feedback, allowing MIDAS to:

- control the rate of progress and WOB
- sense the depth of drilling
- automate the acquisition of multiple samples.

The major benefits of utilizing the USDC are:

- low force requirements that allow operation from flexible, low-mass platforms
- power-effective and mass-efficient drilling
- relatively simple bits that are reliable, do not need sharpening, and reduce contamination
- simple mechanical bit interface making possible the use of multiple specific-function bits to accomplish a wide variety of tasks.

The interchangeable bit mechanism and a tool caddy enable the system to:

- perform change-out of multiple bits, potentially to perform a variety of tasks
- replace damaged or worn-out bits
- return repeatedly to the worksite with different bits or to collect multiple samples
- place different tools and instruments on the target.

The USDC approach combined with the dexterity of the robotic arm make multiple, interchangeable tool bits a practical means of accomplishing a wide variety of tasks and provide a very powerful tool for exploring the Martian subsurface. Utilizing different tool bits is an efficient way to perform many tasks, but has traditionally required an overly complicated mechanism. MIDAS solves this problem by providing a simple interface for transferring the mechanical energy of the USDC to the bit. Rotation of the bit is introduced to provide a fresh work surface to the bit and aid in debris transfer, minimizing the need to transfer high torque or have complicated couplings. The interface is essentially a spring-loaded detent that allows the bit to be attached and detached with ease then locked in place to provide sufficient holding force for all operations.

MIDAS utilizes encoders at each joint for position feedback and in a flight configuration would implement a force sensor to measure the applied drilling force and sense contact with a target. Motor and sensor electronics are commercial off-the-shelf (COTS) for the current stage of development. Standard interfaces were used in producing the MIDAS so that it can be driven and controlled by any future flight or testbed platform.

Such a control system will allow MIDAS to control the rate of progress, WOB, and drill depth during regolith drilling and with further development additional operations such as rock abrading and coring. MIDAS has capabilities very similar to those of the IDD (positioning within ± 4 mm and 10°). This allows MIDAS consistently to retrieve and release bits in the tool caddy and return to the target with sufficient accuracy to guarantee alignment with a previously drilled hole. This accuracy allows the retrieval of multiple samples and access to the target by multiple instruments. It also allows the sample to be delivered to a storage container or instrument very precisely.

Page proof © WILEY-VCH

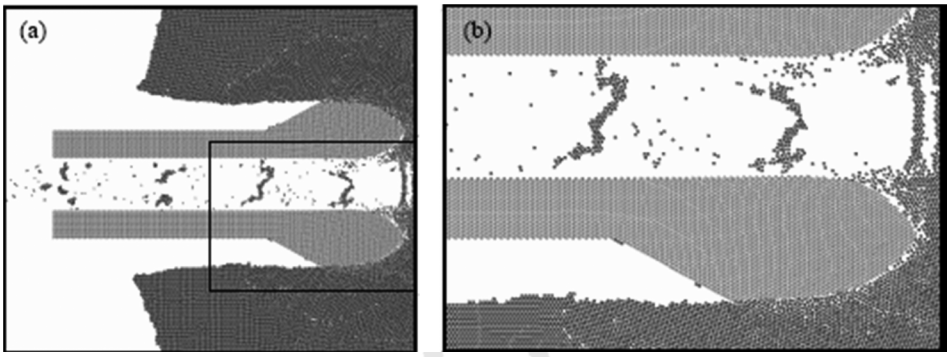

Figure 6.35 Particle simulation of down-hole percussive drilling. (a) Propagation of the drill bit; (b) detail of (a). Courtesy Universities of A 6.33 and Leicester.

One of the most promising benefits of the USDC is the simple bit interface (see Figure 6.35). The use of multiple bits is essential for multi-functional sampling as it is simply not practical to accomplish the multitude of tasks envisioned for future missions with a reasonable probability of success with a single tool. These tasks can, however, be accomplished by a single actuator that utilizes multiple bits for drilling, coring, surface preparation, and sampling. The USDC and bit interchange mechanism makes multiple bits and the exchange of those bits very practical. Many of the bits 6.33 ple as a tube of a single material joined to the standard bit interchange mechanism interface. The bits typically do not require sharpening, but if a bit were damaged or jammed it could be readily disengaged and replaced. The latching mechanism that allows the attachment and release of bits to the USDCs horn is shown in Figure 6.35. The interface is not required to transmit high torque, nor is it required to have power or communications connections. The interface must simply keep the bit straight and free in the axial direction and allow a very light axial force to be applied to the bit by the USDC.

Bits are carried in a tool caddy installed on the support platform in a location accessible to the arm. The bits would be restrained by simple mechanized latches and be restrained during launch, landing and platform positioning. The USDC engages the bits via three spring-loaded features that lock the bits axially but allow them to "float" in any direction laterally (over a limited distance) with a minimum of force. The caddy has built-in compliance and arrays the bits in a radial pattern. This allows the robotic arm with the USDC to couple with the bit even though the USDC may not be perfectly aligned with the bit on its approach path, a likely scenario due to robotic arm joint inaccuracies. The final prototype design is a simplified version capable of holding two bits. Table 6.2 gives MIDAS system specifications.

Extended development testing was performed on the first MIDAS prototype system and it eventually successfully acquired samples from 0.5 m in a simulated Martian regolith. A performance summary is given in Table 6.2. With a more powerful actuator and further development, the system could potentially perform the additional tasks of rock drilling, coring, and abrading.

Table 6.2 MIDAS system specifications.

Parameter	Units	Value	Comments
Mass	g	496	Actual (drill only)
Length	mm	148	Actual (drill only)
Diameter	mm	48	Actual (drill only)
Bit diameter	mm	11.5	Actual
Drill depth	mm	500	In regolith
Power (peak)	W	250	Actual
Power (average)	W	30	Actual
Penetration rate	$cm\,h^{-1}$	140	In regolith
Hold down force	N	13–31	Actual
Operational temperature range	°C	−70 to +45	Projected
Survival temperature range	°C	−120 to +110	Projected
Pressure range	torr	0–760	Projected
Life	Samples	75	Projected

6.6.4
ESA Ultrasonic Rock Corer

6.34

An ESA study for the design of an ultrasonic rock corer for use in planetary missions has been performed by a team with members from the Universities of Leicester and Aberdeen (Sims *et al.*, 2002). Leicester was deeply involved in Beagle 2 activities and Aberdeen houses experienced developers of ultrasonic tools for terrestrial applications (Figure 6.36).

The concept and technique of ultrasonic drilling have been examined and it is seen to offer potential advantages in terms of faster cutting rates with consequent

1. lower energy to cut to a given depth
2. lower preloads than are normally associated with rotary drilling.

An ultrasonic tool transforms low-amplitude oscillations in a transducer into higher amplitude vibrations at the tip, which allow cutting effectively into rocky

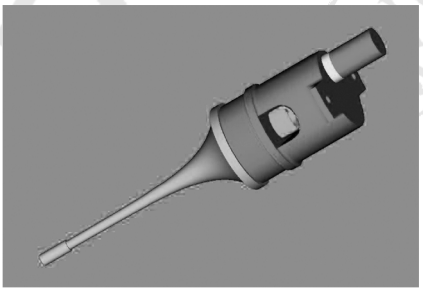

Figure 6.36 Concept of an ultrasonic drill for planetary applications. Courtesy ESA and Universities of Aberdeen and Leicester.

page proof © WILEY-VCH

materials – solid or unconsolidated. The lessons learned from previous work, in particular at JPL and NASA (see discussion related to the USDC in this chapter), have been reviewed.

It is accepted that the main mechanism in ultrasonic drilling is dynamic fracture. The dynamic fracture propagation under percussive loading has been used to analyze dynamic interactions between the drill and the drilled formation. The particle dynamics method is used to simulate material fracture during the drilling process. The drilled material is modeled by set of particles representing grains. Advanced laws of interparticle interactions allow simulation a wide range of the material properties. A r 6.35 program at the University of Aberdeen into the application of novel nonlinear dynamics methods for percussive drilling of hard rock formations has led to the development of particle dynamics simulation methods (Figure 6.37).

An ultrasonic corer tool with a tip diameter of 3 mm could operate at around 28 kHz with an amplitude of 10 μm, with a power of less than 20 W and a mass of less than 0.5 kg, and reach a depth of 30 mm. A novel drive electronics design has been identified based on a bidirectional switching amplifier controlled by control logic (perhaps using a digital signal processor) allowing waveform synthesis to be performed if required. This design overcomes the lower efficiency inherent in other potential designs. The concept of sample collection and retention has been briefly investigated with the option of a separate collection mechanism being identified as a less risky development option. The use of a manipulator similar to the Beagle 2 instrument arm would appear adequate for these tasks. The proposed outline design for such an ultrasonic rock corer is depicted in Figure 6.38.

6.36

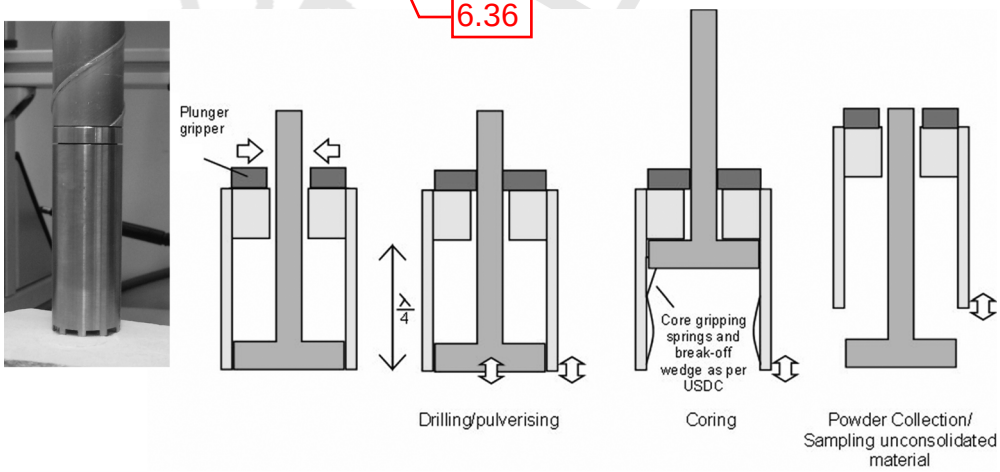

Figure 6.37 Ultrasonic drill tool. (a) View of coring test. Sketches of plunger positions in corer: (b) ungripped for displacement; (c) flush for drilling; (d) retracted for coring; (e) down to sample regolith or extract core. Courtesy ESA and Magna Parva.

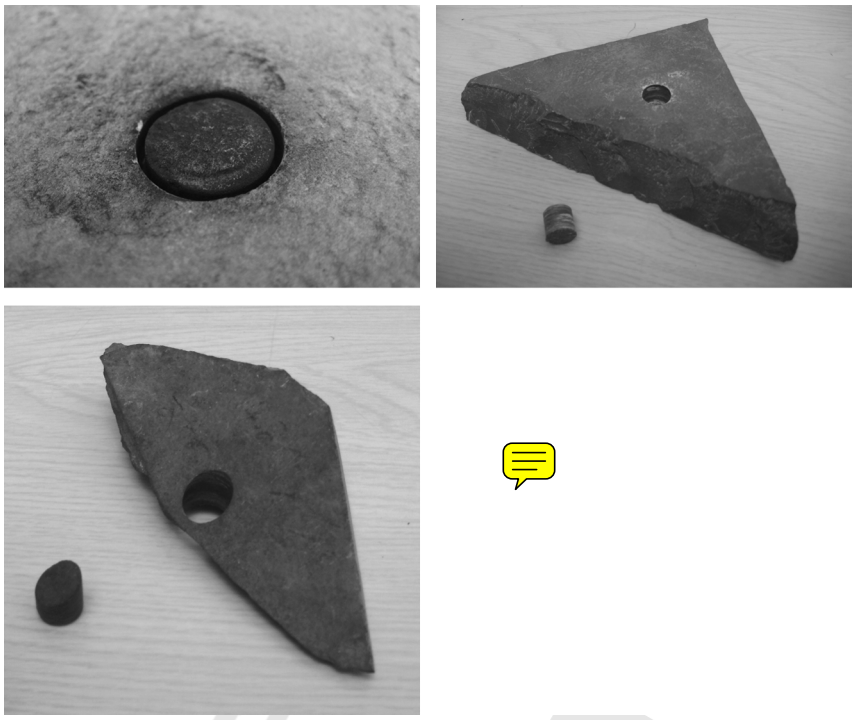

Figure 6.38 Ultrasonic drill tool coring test results in (a) sandstone; (b) limestone; (c) slate, inclined. Courtesy ESA and Magna Parva.

6.6.5
ESA Ultrasonic Drill Tool (UDT)

The UDT is a current ESA-funded project, to develop a device for ultrasonically assisted drilling and sampling of planetary rocks and regolith. The tool transforms low-displacement, high-frequency oscillations in a transducer into higher displacement vibration at the tip, which effectively cuts into material. The operation concept is illustrated in Figure 6.39.

In addition to creating the tuned mechanical design, Magna Parva have developed a proprietary "auto-resonant" control system that keeps the resonance of the UDT in tune and working at optimum efficiency, independent of the loading condition. December 2007, the tool has been tested in a variety of materials, and the results of these tests are being used to make improvements to the design. Typical results of using the breadboard to drill various rocks are shown in Figure 6.40. For this purpose, the drill required a thrust force of 8–10 N, the corer diameter was 12 mm and it cored slate to 12 mm deep in ~70 min while consuming less than 40 W power.

Drill rotation speed:	25-250 rpm
Drill motor nominal power:	50 W
Drill rotation speed measure:	Encoder
Linear translation speed:	0-55 mm/minute
Linear stroke:	1 meter
Linear stroke measure:	linear potentiometer
Electrical slip ring:	12 tracks
Load cell for thrust measure (implemented at the base of TE):	0-2400 N
End stops:	Micro switches

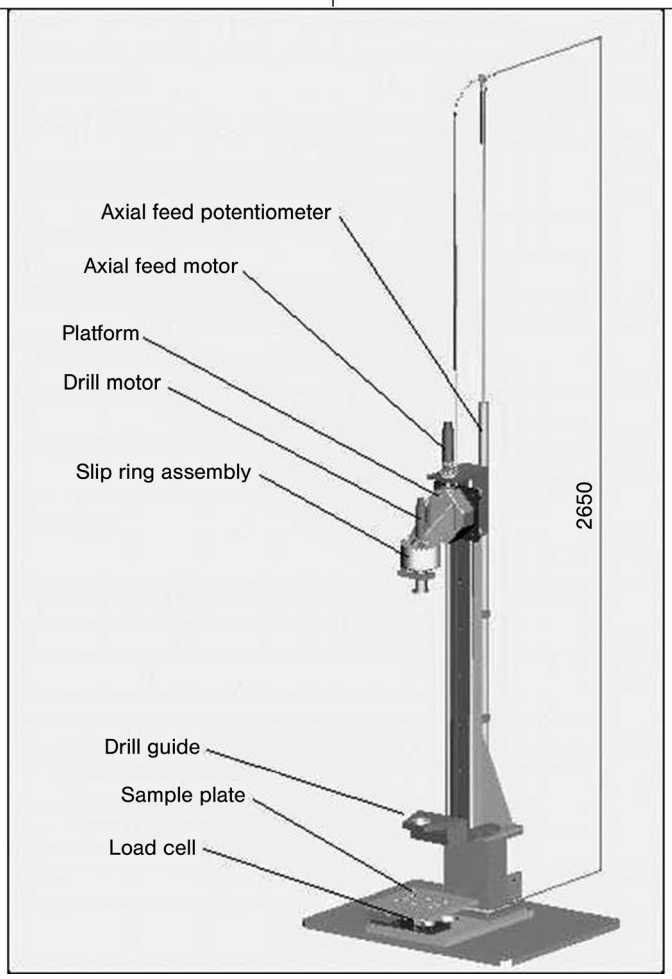

Figure 6.39 Schematics of TE at Galileo Avionica. Courtesy ESA and Galileo Avionica.

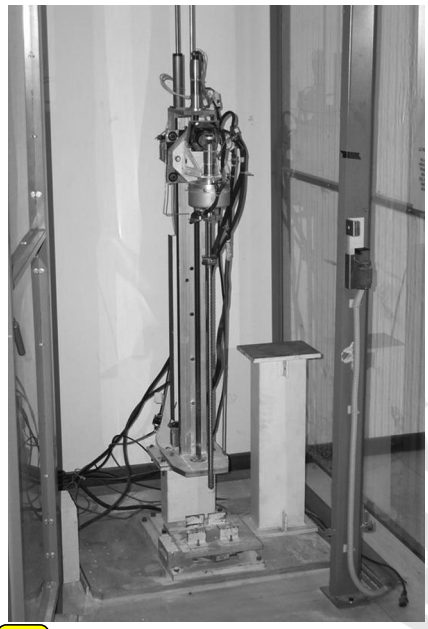

Figure 6.40 Test equipment with integrated drill/corer tool that is 70 cm long. Courtesy ESA and Galileo Avionica.

6.6.6
Drill with Hammering Mechanism (DHM)

Ongoing ESA studies consider the implementation of hammering/impacting mechanisms in rotary drills, to increase their efficiency when drilling hard rock. The ExoMars drill is considered as the reference drill on which such a device would be mounted. Galileo Avionica in Milan teamed with Helsinki University of Technology for this study, which was completed in 2008.

Among the candidate systems, spring-loaded impacters released by a cam have been considered on ~~the~~ one hand, and various resonant systems on the other. Preliminary testing was done on hardware representative of both concepts to facilitate the selection of a concept for full prototyping ~~(Table 6.3)~~.

The results of the trade suggest continuation of the work with the development of a cam-hammer mechanism, which uses the sudden release of a compressed spring, previously loaded by a cam, to produce 1 J of impact energy at a nominal frequency of 1 Hz. The challenge of the mechanism design and its realization lies in the very limited room available for its implementation, mainly the reduced diameter (24 mm maximum available for the accommodation of the mechanism).

- *Mechanism description:* The cam-hammer is based on a rotary cam that moves up and down, driven by an electric motor. The cam works against a compression spring that provides the hammering energy when the cam is released. The cam extends with a striker that hits a coupling interface holding the drilling tool

Page Proof WILEY-VCH

Table 6.3 Main characteristics of TE available at Galileo Avionica.

Drill rotation speed	25–250 rpm
Drill motor nominal power	50 W
Drill rotation speed measure	Encoder
Linear translation speed	0–55 mm min^{-1}
Linear stroke	1 m
Linear stroke measure	Linear potentiometer
Electrical slip ring	12 tracks
Load cell for thrust measure (implemented at the base of TE)	0–2400 N
End stops	Microswitches

mounted to the hammering mechanism. presents a cross-section of a drill with hammering mechanism (DHM). The length of the threaded outer tube (part no. 23) is 480 mm, the effective length of the rod (excluding male coupling thread is) is 505 mm and the total length is 515 mm. The drill tube inner diameter is 24 mm and the outer diameter is 27 mm without auger and 29 mm with auger. A Maxon EC22 motor (55 W) and a gearbox, 22 mm in diameter, are used in the prototype.

The prototype was manufactured and extensively tested in different types of hard materials and in different operating conditions. Dedicated drill test equipment and a set of mock-up drill tools, both commercial and specifically designed and built (Figures 6.41–6.44), were used for the tests. The DHM prototype has

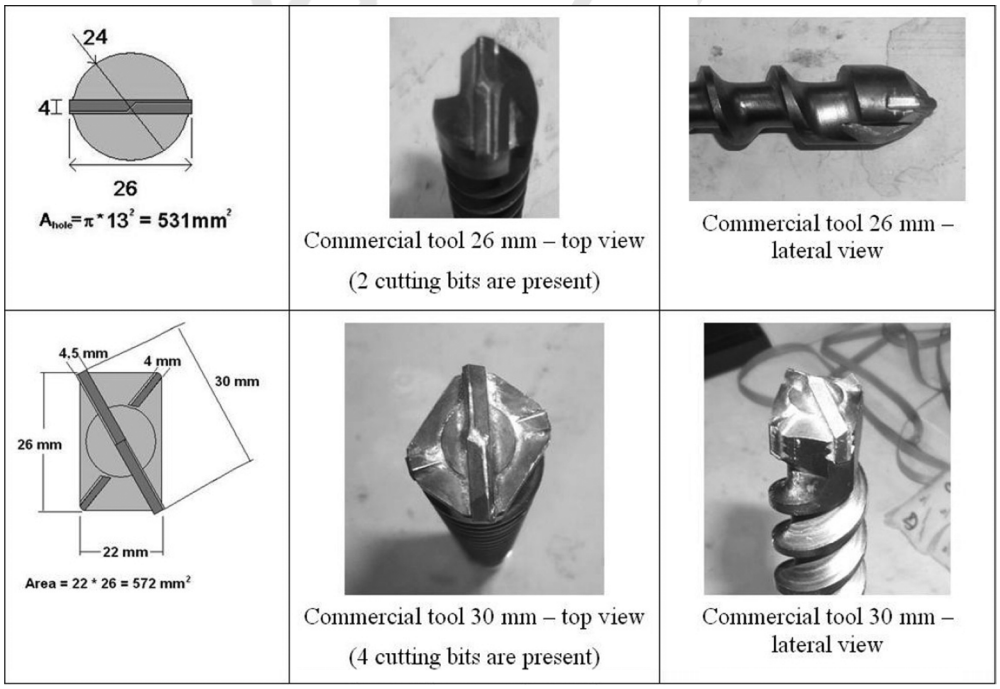

Figure 6.41 Schematics and pictures of commercial drill tools. Courtesy ESA and Galileo Avionica.

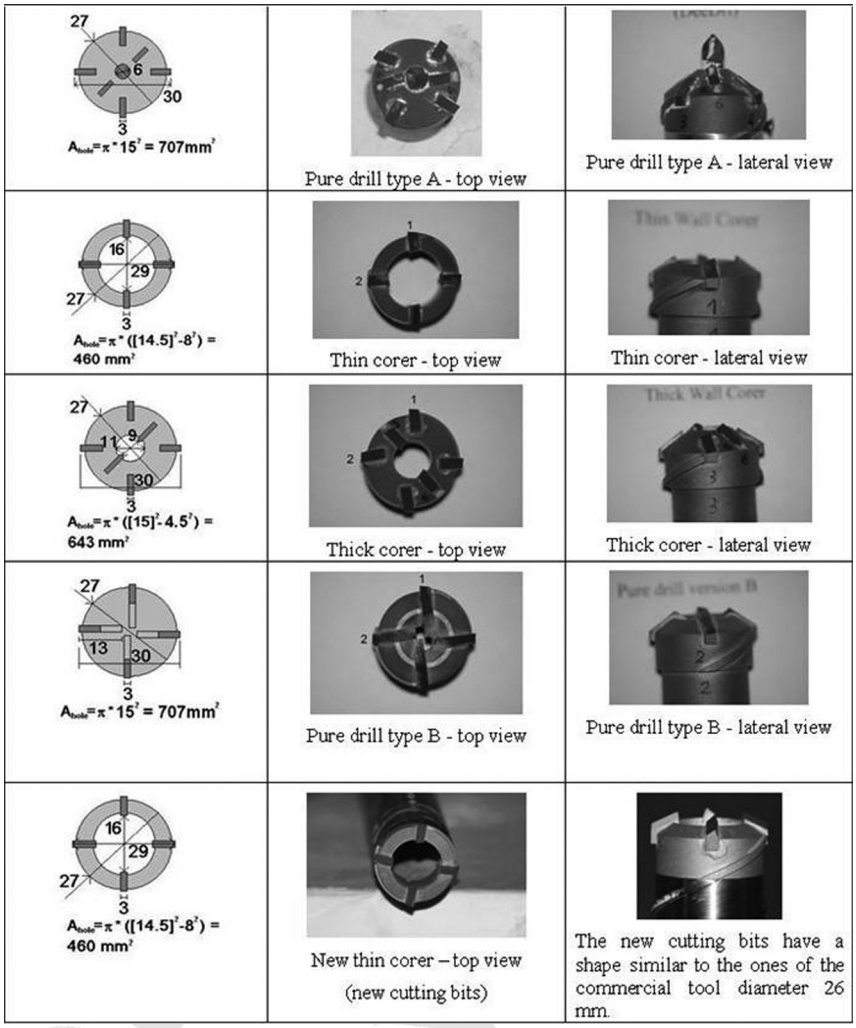

Figure 6.42 The drill tools used during the DHM test campaign. Courtesy ESA and Galileo Avionica.

proven its effectiveness by drilling into granite (compressive strength 160 MPa), and acquiring samples, with low thrust applied (e.g., 100 N) and with very low power consumption (e.g., 5–10 W) at penetration speeds of about 0.02 mm min^{-1}.

- *Prototype test results:* As an example the results of the test performed with the tool named "new thin corer" are reported below for marble and granite cases (Figure 6.45).

- *Drilling marble:* The tool was tested at 98 N thrust with a rotational speed of 6 rpm. The first part of the test was performed with a frequency of the DHM of 1 Hz. In the second part of the test, the frequency was doubled (2 Hz). The power consumption ranges from 5.5 to 7.5 W depending on the DHM frequency. In this test, it was possible to take a sample fragmented into three parts.

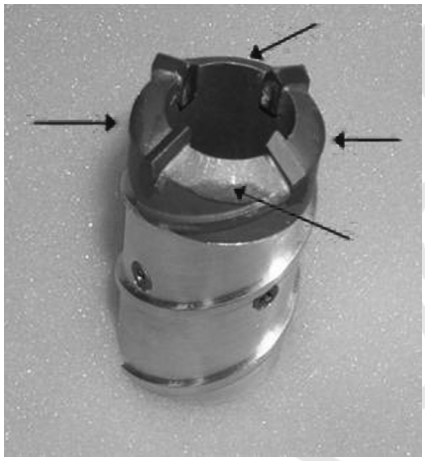

Figure 6.43 New thin corer after test in granite. Arrows indicate the points where the external part of the tool were hitting the material. Courtesy ESA and Galileo Avionica.

- *Drilling granite:* ~~During this test, the estimated indexing rotational speed was achieved. A slow rotation speed of 0.26 rpm was imposed by the test equipment. The other fundamental parameters were not changed through the whole test. In this case also, a sample could be taken from the material (right). The strange shape of the core sample and of the hole (pentagonal shape) is visible. Another effect of this imperfect drilling action is seen in the visible marks of the tip produced by the direct contact of the area of the tool between the cutting bits with the granite, as shown in. This can be explained by the imperfect fitting between the tool and the guiding bush. This problem does not appear in the second test into granite presented hereafter, where an adaptation was introduced to fit the drill tool and the guiding bush better.~~

Q4

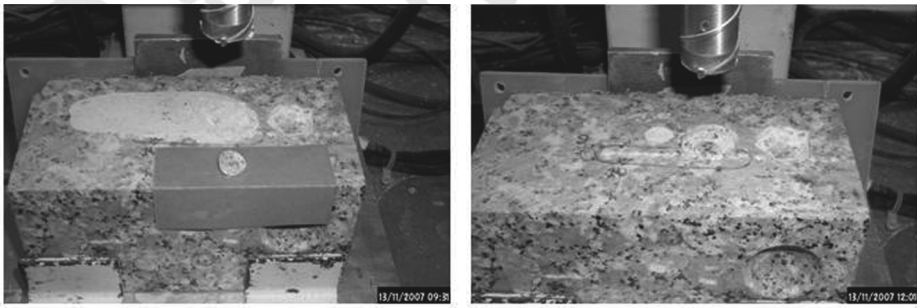

Granite hole with powder. The sample was removed and placed on the blue sheet

Granite hole with core and powder removed

Figure 6.44 Test No. 2 into granite: hole and sample. (a) Granite hole with powder. The sample was removed and placed on the blue sheet. (b) Granite hole with powder removed. Courtesy ESA and Galileo Avionica. (Please find a color version of this figure on the color plates).

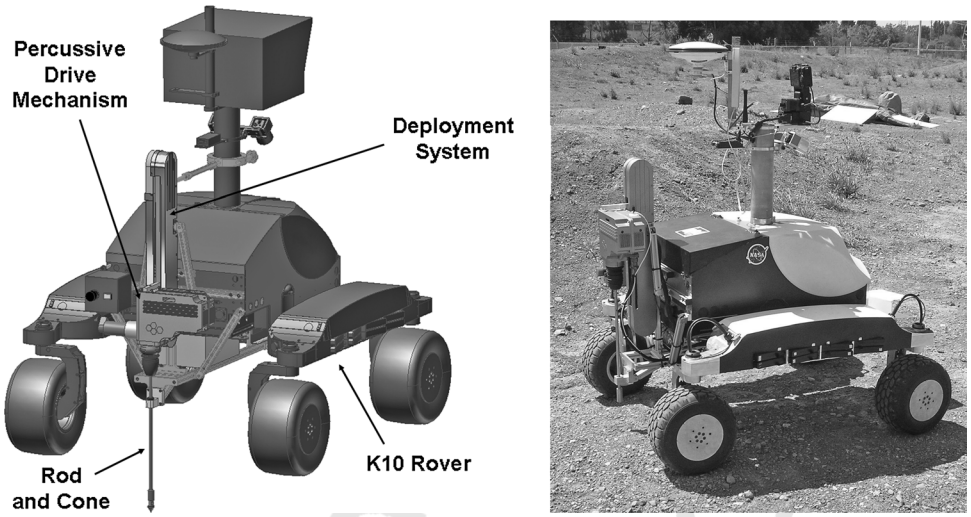

Figure 6.45 (a) A schematic diagram of the percussive cone penetrometer developed by Honeybee Robotics. (b) Actual percussive penetrometer mounted on 80 kg NASA Ames rover. Courtesy Honeybee Robotics and NASA Ames Research Center.

A following test confirmed the importance of driving the rotation of the tool with a proper indexing speed instead of a "random" speed relative to the position of the cutting bits when the shock is transmitted by the tool to the material. With the proper indexing rotational speed, the shock is transmitted in a synchronized way to the material. In this test, a well-shaped, circular sample was obtained (Figure 6.46). With

6.44

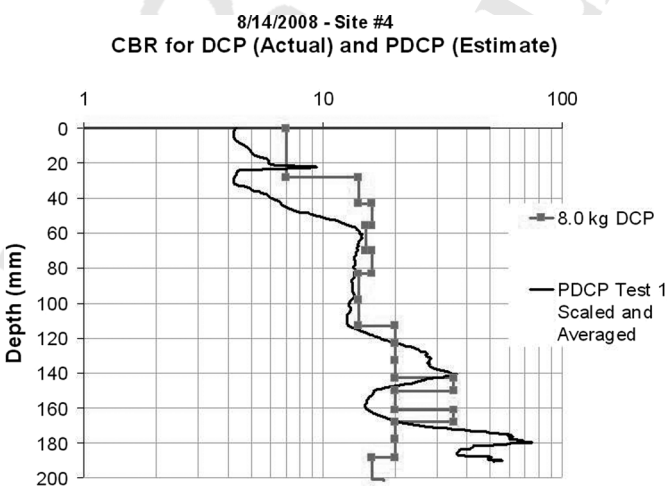

Figure 6.46 Field tests using a percussive dynamic cone penetrometer on NASA Ames 80 kg K-10 rover. The data show close correlations to ~~California bearing ratio~~ and in turn other soil geotechnical properties such as bearing strength.

respect to the thrust effect during this test, it can be noted that, with DHM action, a high thrust is not beneficial to the rate of penetration. It seems that the best results are achieved with a thrust of 100 N.

The testing was interrupted by a DHM motor failure. After dismantling the system, the failure was judged to result from damage of the gearbox due to an overload of the item. It was noted that the DHM system was designed to operate at 1 Hz, but during the test it worked for a considerable time at 2 Hz, with a gear input shaft speed of 25% more than recommended by the manufacturer.

6.6.7 Percussive Regolith Penetrometer

Many subsurface access applications require penetrating dry granular material. This is the case, for example, when deploying heat flow probes in lunar regolith. Although the rotary–percussive approach to penetrating lunar regolith was proven effective during the Apollo experiments, it is believed that a pure percussive approach will make the probe deployment simpler not only for Astronaut deployment but also for autonomous landers. The percussive penetrometer uses high-frequency and low-energy impacts to penetrate the regolith. When a rod is inserted into regolith, the resistance to insertion comes from two sources: regolith being displaced/crushed ahead of the probe and regolith sliding against the rod as it is being inserted (the latter is referred to as sleeve friction). The combination of high-frequency and low-energy percussive impacting reduces ~~the~~ resistance forces. The regolith ahead of the pointed tip of a penetrometer becomes displaced, packed, and crushed due to the vibration; this allows the cone to penetrate deeper. Simultaneously, the regolith rubbing against the penetrometer surface continuously vibrates and reduces the sleeve friction; this makes insertion of the penetrometer relatively easy. ~~In addition,~~ the penetrometer head can be made lig 6.45 ~~a its~~ counterpart for an auger system, because no rotation is required.

Honeybee Robotics has developed a percussive penetrometer system, referred to as a percussive dynamic cone penetrometer, for the NASA Ames 80 kg K-10 roving platform (Figure 6.47). Preliminary laboratory and field tests of the percussive penetrometer were conducted in manual operation modes. Several different designs were built for an initial laboratory ~~test at the Honeybee Robotics facilities.~~ Each design consisted of three parts: the percussive actuator for creating the hammering penetrating force, the detachable cone that was hammered into the lunar regolith simulant, and the connecting rod that held the detachable cone to the percussive hammer. The connecting rod held the detachable cones loosely by using rubber O-rings squeezed between the rod/cone interfaces. Initial tests were carried out by penetrating into columns of compacted (1.9 g cm^{-3}) lunar regolith simulant, JSC-1A to a depth of 0.9 m. Compaction was achieved using a vibrating table. The regolith was introduced in small batches and a dead load applied to ensure high relative density ~~and prevent the Brazilian "nut effect" (larger nuts in a jar being displaced by smaller ones and eventually moving to the surface).~~ All penetrometer designs were able to reach the bottom, although with different speeds. The fastest one reached the bottom in a few tens of seconds whereas the slowest took 3 min.

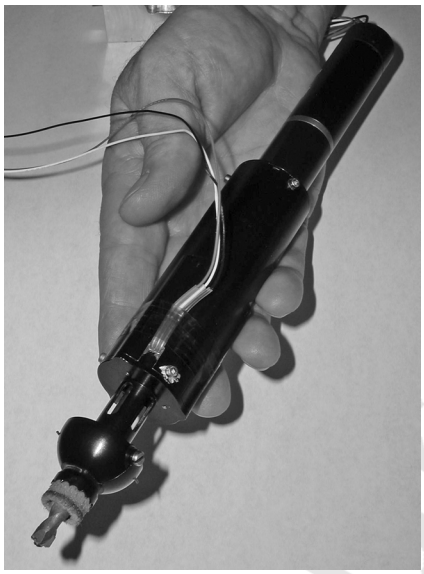

Figure 6.47 The LSAS. Courtesy ASI.

The ~~above~~ tests show that it is indeed possible to penetrate the highly compacted regolith simulant using the percussive method. Penetrating real lunar regolith may in fact be easier. This is because, in spite of a very high relative density approaching 90% and more, the porosity of lunar regolith is in the range ~~40–50%~~ (Carrier, 2005). Thus, almost ~~50~~% of the lunar regolith is actually empty space which can be filled with additional material. The high porosity is due to a broad particle size distribution and very irregular particle shapes (especially agglutinate, which makes up a large fraction of the regolith). About 25% of the regolith porosity is attributed to intragranular porosity, that is, porosity of individual particles. These particles are very fragile, and therefore can break up easily, especially when in contact with the percussive penetrometer. Lunar soil in contact with the tip of the percussive penetrometer cone will no doubt be crushed and, because of the high porosity, the crushed material will be pushed into the soil's open skeleton.

~~Astronauts on Apollo 14 used a simple penetrometer and on Apollo 15 and 16 they used a more sophisticated soil penetrometer, called a self-recording penetrometer (SRP), to determine soil properties to around 70 cm depth. The SRP consisted of a 30° cone, with a diameter of either 1.28 or 2.03 cm. The penetration resistance for the SRP varied from 500 to 1700 kPa. Probably the maximum force that astronauts could apply, given the lunar gravity of one-sixth of that on Earth, is on the order of 300 N (~67 lb) or less.~~

~~In order to determine how a percussive dynamic cone penetrometer (PDCP) will perform on the Moon, it is imperative to prepare a lunar regolith simulant such that the performance of a static cone penetrometer is similar to that on the Moon. Since terrestrial gravity is six times higher than lunar gravity, the penetration resistance should in turn also be around six times higher (this is true because lunar regolith is a~~

Proof WILEY-VCH

~~frictional soil). If the simulant is less resistant than that, then the simulant has not been compacted enough. If the simulant is more resistant than that, the regolith was compacted too much.~~

Initially a number of tests were conducted with a 1 cm diameter cone in compacted to 1.9 g cm^{-3} lunar regolith simulant, JSC-1a. The soil container was 10 cm in diameter and 1 m high. The cone would not penetrate the regolith with a force of 860 N (the weight of a person), which is equivalent to a penetration resistance of 12 000 kPa or just over six times the resistance measured by Apollo astronauts. Therefore, it seems that a JSC-1a soil simulant compacted to 1.9 g cm^{-3} is more resistant to penetration than lunar soil on the Moon. Probably this higher penetration resistance is attributable (in addition to simulant density) to the small-diameter pipe and the proximity of the rigid walls (Carrier, W.D., personal communication, 10 November 2008).

Although it was impossible to push the cone with a weight of an average person, when the percussive actuator ~~of the PDCP~~ was used to drive the cone into the soil, the cone reached a depth of around 70 cm in less than 10 s. Since the soil simulant had a higher penetration resistance than lunar soil on the Moon, the PDCP on the Moon with a 1 cm diameter cone would be able to reach a depth of 70 cm in much less than 10 s, saving a lot of time (and frustration) for astronauts.

~~Note also that the Apollo astronauts had a problem driving core tubes (for acquiring undisturbed cores of lunar soil) into the lunar regolith (Carrier, Olhoeft and Mendell, 1991). This was attributed to two issues. First, as the core tubes were being driven deeper into the regolith, the sleeve friction would drastically increase. Second, the astronauts used hammer blows in driving the tube into the regolith. In dealing with the first, drill rods should be slightly thinner than the penetrometer cone (22 vs 25 mm) and hence reduce the sleeve friction. The second issue can be solved by using lower energy but higher frequency impacts (~35 blows per second) instead of a few, "powerful" hammer blows. The high-frequency vibration reduces the force required for pushing a rod into regolith by almost two orders of magnitude (Zacny *et al.*, 2008c; Nathan *et al.*, 1992) This does not occur with hammer blows, even very powerful ones.~~

In penetrating lunar regolith, the tool may also run into a rock. According to Carrier, the probability of running into a rock with a diameter two or more times greater than that of the penetrometer cone (~~in our case~~ ~2.5 cm or less) in 5–10 m depth is only 1–2% (Carrier, 2005). ~~The same study also predicted that smaller rocks can be pushed aside by the drill/penetrometer because of the high regolith porosity.~~

An added advantage of using a percussive penetrometer is that the penetration rate can be used to assess geotechnical soil properties. The Honeybee Robotics percussive tool is based on the PDCP, an instrument used to assess ~~soil~~ geotechnical soil properties in terms of the California bearing ratio (*CBR*). The *CBR* can also be correlated with the soil's bearing capacity and dynamic modulus (Huekelom and Klomp, 1962) as shown in Table 6.4. The bearing capacity, *q*, is a parameter used in the design of shallow foundations, dynamic modulus (*E*) or resilient modulus (~~*k*~~) provides a means of characterizing surface soil under a variety of temperatures and Q5

Table 6.4 Correlations between CBR and other geomechanical soil properties.

q (kPa) $= 26.16CBR^{0.664}$
E (MPa) $= 10.34CBR$
~~E (MPa) $= 17.58CBR^{0.64}$~~
~~k (M m^{-3}) $= -65.91 - 1.49CBR + 35.23CBR^{0.5}$ for $CBR < 20$~~
~~k (M m^{-3}) $= -3.05 - 0.59CBR + 16.34CBR^{0.5}$ for $CBR > 20$~~

stress states that simulate the conditions in a soil subjected to moving wheel loads. Therefore, from the penetration rate of the percussive actuator we can additionally assess the lunar regolith properties in terms of many geotechnical properties of the soil, and from these also estimate of the soil density. Honeybee Robotics recently built a fully autonomous percussive penetrometer system for the NASA Ames K-10 rover (Figure 6.48). The system was able to penetrate soils of high CBR and determine soil strength in real time.

6.46

6.7 Surface Drills

Surface drills can be defined as drills designed to penetrate into surface rocks and boulders or into regolith to a limited depth. These drills can be deployed from robotic arms and thus can drill at any angle into surface rocks. Surface drills also do not require assembly/disassembly of drill rods. The ~~flowing~~ sections present a number of different surface drills developed by various government agencies and aerospace companies for extraterrestrial applications.

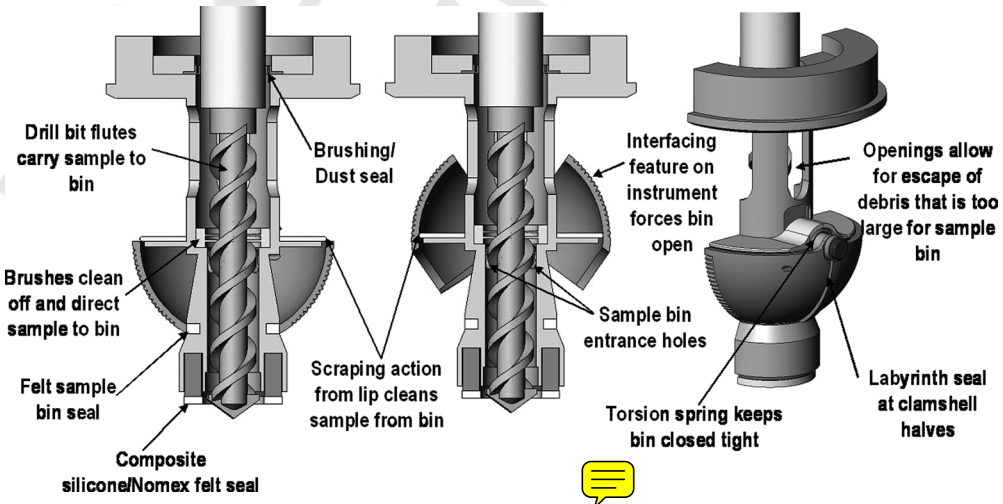

Figure 6.48 Details of operation of the LSAS. Courtesy ASI.

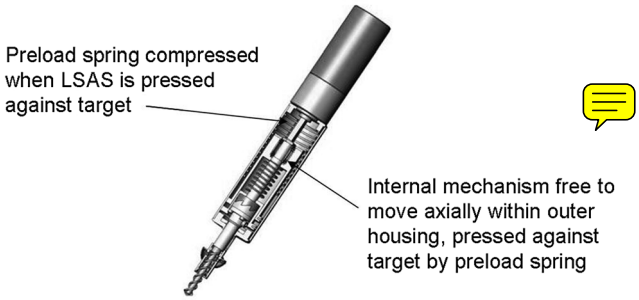

Figure 6.49 The sequence of operations of the LSAS. Courtesy ASI.

6.7.1
Low-Force Sample Acquisition System (LSAS)

6.47

The Low Force Sample Acquisition System (LSAS) (Figure 6.49) is a percussive drill with integral sample acquisition capability developed by Alliance. Intended to drill into a wide variety of rocks and frozen soils while being supported by lightweight platforms, the primary design goals were to minimize force, mass, volume, envelope, and power (Stanley, Dougherty and Laramee, 2007). This simple and elegant mechanism uses a single motor to acquire samples by drilling into the surface of a target material. The drill bit, which is made of very specific materials to ensure life and minimize contamination issues, is driven by a space-qualified brushless DC motor. The drilling action is hammer driven, which allows the mechanism to acquire a sample with a minimum amount of force. The hammer is actuated by a spring/free mass system driven by the motor and a cam follower. As material is removed from the target surface or hole, it is fed into the mechanism by the bit flutes which deposit the sample in a storage bin via holes for later delivery to the support platform's instruments. Further details of the mechanism operation are shown in Figure 6.50.

LSAS operation is straightforward and readily made autonomous (Figure 6.51). First, the sampling tool is placed against a target. Preload is set and maintained by

6.48

6.49

Figure 6.50 The LSAS mounted on the robotic arm of the Rocky 8 rover. Courtesy ASI.

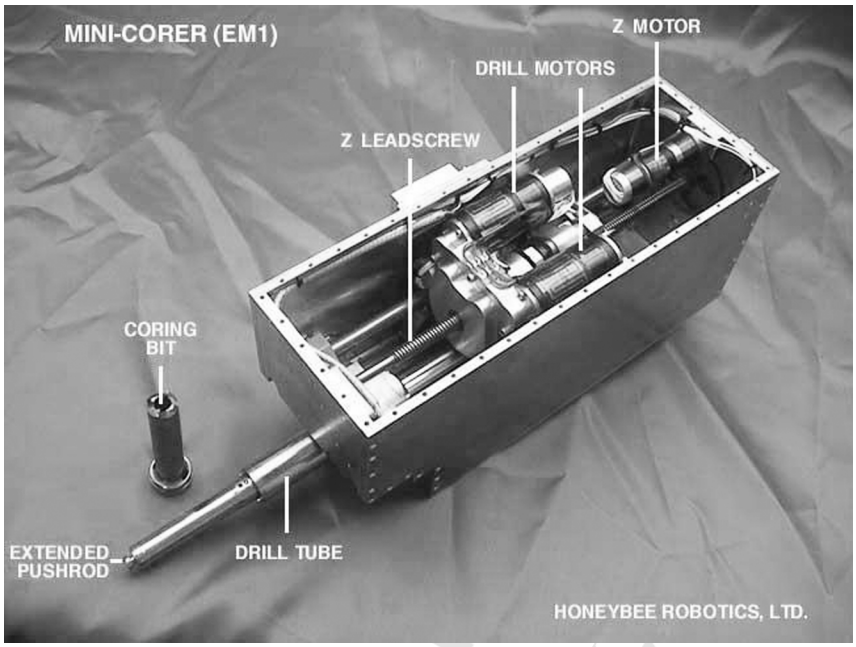

Figure 6.51 Athena Mini-Corer Engineering Model developed by Honeybee Robotics. Courtesy Honeybee Robotics.

compressing an internal spring that supports the hammer drill system. Redundant contact sensors indicate that the bit has been depressed to the correct position, automatically resulting in the tool being placed against the target with the correct amount of force. Once in position, the motor spins the bit at approximately 800 rpm and the bit begins to drill into the surface of the target. Hammering action is the primary drilling effect and occurs three times per revolution. The hammering action is driven by the same motor that rotates the bit and is accomplished via the cam follower that forces the hammer up as it rotates, compressing a spring, and then releases the stored energy very quickly, driving the bit into the target. As material is removed it is carried into the mechanism by the fluted bit. Material travels up the flutes and is forced into the sample bin by brushes riding along the side of the gaps between the flutes. The sample bin gradually fills to the desired volume and any excess material simply travels past the bin and out of the mechanism.

Once the required amount of sample has been acquired, it can be delivered to instruments on the support platform. To allow for sample delivery, the LSAS incorporates a passive clamshell storage bin. Features on each instrument force the clamshell open as the tool comes into contact with the instrument. A simple scraper ensures that all material is removed from the bin as it is opened and actuating the hammer a few times helps to remove particularly cohesive material, minimizing cross-contamination between samples.

Extensive development testing was performed to evaluate the initial configuration, fine tune the design and optimize performance. Final performance characteristics

Table 6.5 Performance characteristic of LSAS.

Parameter	Units	LSAS (basic)[a]	LSAS (heavy)[a]
Mass	g	440	550
Length	mm	229	260
Diameter	mm	33	33
Drill diameter	mm	6.35	6.35
Drill depth	mm	19	19
Sample volume	cm^3	1.5	1.5
Core diameter	mm	NA	NA
Core length	mm	NA	NA
Power	W	15–20	40–50
Penetration rate	$cm\,h^{-1}$	2	5
Hold down force	N	35	148
Operational temperature range	°C	−120 to +35	−120 to +35
Survival temperature range	°C	−135 to +110	−135 to +110
Pressure range	Torr	0–760	0–760
Life	samples	75	75

[a]NA, not applicable.

are summarized in Table 6.5. A "Heavy" version was designed but not assembled due to concerns that the design might be inadequate for hard rock. However, the "Basic" version proved adequate even in basalt, the hardest rock expected on Mars.

After developmental testing, the final prototype was subjected to Mars temperatures and pressures in environmental chambers at the JPL. The LSAS unit successfully operated in these environments and also demonstrated the ability to drill into and acquire samples from frozen soil.

6.50

After environmental testing, the LSAS was integrated with the Rocky 8 rover at JPL and demonstrated its sample acquisition capability while mounted on this lightweight rover in JPL's Mars Yard. Figure 6.52 shows the LSAS mounted on the robotic arm of the Rocky 8 rover. An effort is currently under way to adapt the LSAS approach to coring applications. Using the same rotary percussive action, a scaled device is being developed under a Phase 2 Small Business Innovation Research (SBIR)

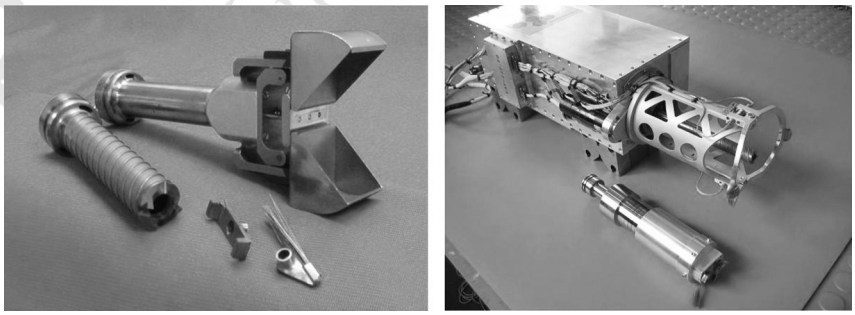

Figure 6.52 Honeybee Robotics Coring and Abrading Tool (b) and selection of tools that can be mounted on the main CAT shaft (a). Courtesy Honeybee Robotics.

page proof WILEY-VCH

contract to generate, extract, transport, and eject 1 cm diameter by 6 cm long cores in anticipated Martian target materials.

6.7.2 Mini-Corer

The Mini-Corer (MC) was originally designed and built by Honeybee Robotics 6.51 integrated with the 2003 Mars Sample Return (MSR) rover as part of the Athena Science Payload. The paragraphs below define the MC system, outline the system's high-level requirements and give a brief functional overview. Figure 6.53 shows the MC engineering model and points out some of the system's key components.

The MC system is defined as the complete set of hardware that would be integrated on a rover or lander. This includes the:

- MC drill mechanism with actuators and sensors such as a force sensor, motor encoders, limit switches, and temperature sensors (also equipped with motor heaters)
- MC drill bits
- MC drill bit storage module.

To meet the science goals of the MSR/Athena mission, the high-level functional requirements of the MC were as follows:

- core through Martian rocks
- break off cores from base rock

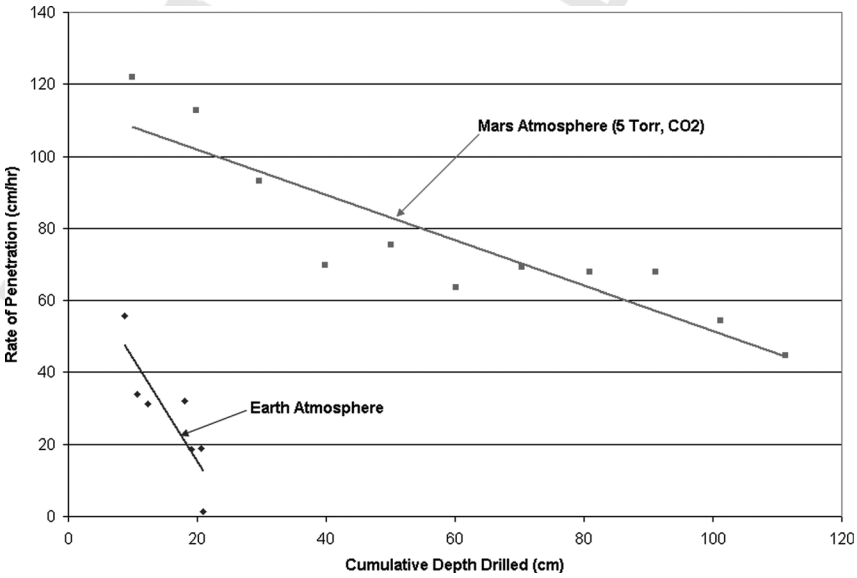

Figure 6.53 Coring bit life versus atmospheric pressures for drilling 100 MPa Keweenaw basalt at room temperature using 70 N WOB. ~~After Zacny *et al.* 2008b~~

Proof EY-VCH

- retain cores inside the MC core barrel
- allow cores to be viewed by other instruments such as the instrument arm's microscopic imager
- eject cores from inside MC core barrel into a sample storage site
- if desired, repeat the above steps one additional time per coring site
- return thrust, torque, and penetration rate data for rock and soil physical property investigations
- acquire and transfer samples of soil-like material
- change out coring bits when necessary
- obtain cores from rocks at angles up to 45°.

When collecting cores, the MC uses a hollow tube (drill bit) with custom-designed cutting teeth. Dual coring motors (drill motors) rotate the tube and a *z*-axis motor drives it into the rock using a standard lead screw design. A third motor (break-off motor) shears off the core from the base rock and engages the core retention lip. Finally, a fourth motor (pushrod motor) drives a linear pushrod mechanism that positively ejects the sample out of the coring tube into a sample storage site.

The MC is housed in an enclosure (or box) that acts as the mounting platform for the lead screw. This box is made up of six plates (top, bottom, and four side plates) and also serves to protect all MC mechanisms from dust. The drill tube extends and retracts through a wiper seal opening. The MC and its enclosure were to be fastened to the Rover by a two-axis motion base system referred to here as the pitch-translate (PT). The PT axes allowed the MC to access the sample container fully and also the exchangeable coring bits (drill bits) and a drill bit brush station. During rover traverses and for launch, the MC is pitched to the horizontal and translated to a "C" retention bracket to prevent back-driving.

Nominal coring and surface cup sampling operations are performed with the MC pointing straight down against the PT hard-stops. The MC nominally drills at thrust levels ranging from 90 to 110 N (20–25 lb) with rotational speed and torque ranging from 180 to 220 rpm and from 330 to 660 mN m (3–6 in-lb) at the drill bit, respectively. An integrated force sensor facilitates drilling force control and provides force feedback over a range of ±134 N (±30 lb). Energy allotted to the MC for nominal operations was not to exceed 50–60 W h (roughly 25–30 W continuously for 2 h). Off-nominal coring operations at attack angles of up to 45° were planned at reduced thrust levels.

To prevent excessive drill bit "walking, chattering, or tornadoing" during the initial bit-to-rock engagement, a number of software techniques were tested. One (or a combination) of these techniques was to be base-lined for mission operations. The preferred approach, at the completion of testing, was to use the pushrod to apply a force (via a spring-loaded tip) on the target rock to stabilize the drill tip and rock while the *z*-axis gradually translated the drill bit into the rock. This method required the *z*-axis and pushrod to move synchronously during the "engagement" so that the pushrod's position relative to the rock did not change. This method was successfully demonstrated in a variety of rocks, including basalt and limestone, during bench tests at Honeybee Robotics.

Unfortunately, the MSR mission was discontinued prior to delivery of a flight unit for the then scheduled 2003 launch date. However, a complete engineering model was designed, built, and tested in a controlled environment. This unit has a mass of 2.63 kg and its dimensions are 29.8 × 14.51 × 9.64 cm. The MC design integrates a bit change-out mechanism so additional bits can be carried at a mass cost of 33.1 g per bit and 84.7 g per bit holder. While drilling, the MC creates an 8 mm diameter by 25 mm long basalt core in less than 6 min at depths down to 50 mm. Currently, the technology readiness level (TRL) of the MC is 5.

~~6.7.3~~ Coring and Abrading Tool (CAT)

6.52

The CAT was designed and developed by Honeybee Robotics (Figure 6.54). Technology developed for the RAT and the MC drill were fused to form the CAT. This results in a versatile instrument capable of brushing, grinding, drilling, and collecting cores from rocks. The CAT utilizes five actuators to enable its versatility. These include a *z*-axis motor for providing drilling and grinding down-force; a drilling motor for rotating the bit and the grinding orbital feed; a break-off motor for capturing cores and enabling a quick change of bits or tools; a pushrod for core ejection, enabling quick change, and operating a sample scoop; and a grinding motor for rotating the grinding wheel at a high rotational speed. While operating, the CAT can provide up to 80 N of thrust, drill 100 mm long cores of 8 mm diameter, and grind or abrade a 35 mm diameter surface with using less than 80 W of power.

To date, a high-fidelity prototype, or brassboard, of the CAT has been developed. The coring mechanism of the CAT is based on the MC design. Also, fundamental

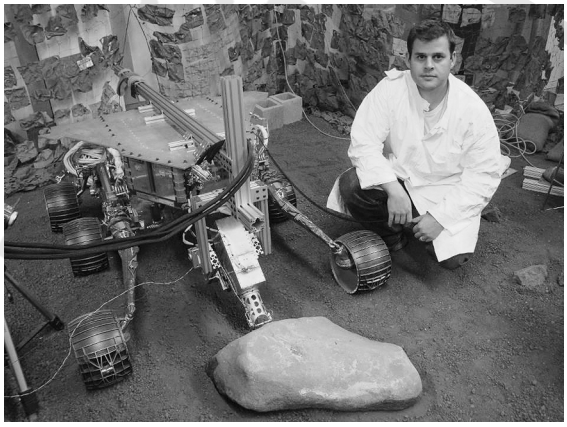

Figure 6.54 Kiel Davis of Honeybee Robotics inspects the Coring and Abrading Tool (CAT) mounted on the Mars Exploration Rover class rover at the JPL facilities. The CAT successfully acquired and delivered a 4.5 cm long core from a >130 MPa Saddleback basalt. The test was conducted on 25 September 2008. Courtesy Honeybee Robotics.

components, such as the drill transmission, the drill bit design, and the core break-off and transfer system, were verified during the MC development effort. Modified bits were designed and tested during the CAT development. Selected bits were life tested on Mars analog rocks in a 5 Torr CO_2 atmosphere. Specifically, Keweenaw basalt was chosen as the test material.

Washington University identified Keweenaw basalt as a valid Mars analog to be used for the 2003 Athena MC test program as one of the baseline performance rocks. Brad Joliff (Washington University) states that Keweenaw basalt is classified as a quartz tholeiite (~47–50% silica, quartz refers to "normative" quartz). This basalt contains little to no crystalline quartz and, having undergone moderate hydrothermal alteration it contains, in addition to primary silicates, softer alteration minerals including phyllosilicates and hematite. ~~Original samples (THB-106, THB-128) left over from a PhD study were sent to Honeybee in 1998 for coring bit development tests. For lack of a better candidate, Honeybee used this rock during CAT development testing and received direction from the JPL CTM to use this rock for CAT V&V testing.~~

Q6

Honeybee acquired new Keweenaw Basalt specimens for the CAT ~~V&V~~ program. All of the samples came from flows that are within about 25 miles north of Duluth, MN, along Highway 61 and North-shore Drive (approximately 47°00′N, 91°40′W). Specimens were gathered at four sites in this area along the shores of Lake Superior.

To confirm that the new specimens were the same as the original, the new specimens were analyzed for compressive strength and chemical composition. Small samples of each were parted off and sent to West Penn Test Laboratories for compressive strength tests per Q2700, ASTM C-170. Samples were also sent to Washington University for X-ray fluorescence analysis to determine chemical composition (Tables 6.6 and 6.7).

Although chemical analyses on the Keweenawan basalt specimens show little variability between specimens, the KB01 specimen was selected for testing, primarily because of its higher compressive strength. Since other parameters, such as drill bit type, atmospheric pressure, and atmospheric temperature, were variable, it was important to use the same specimen to evaluate the effects of changes in these parameters. Of the parameters that were variable, the one with the most interesting effects was atmospheric pressure.

All else being constant (same rock, coring bit, WOB, and speed), drilling in a low-pressure environment yielded a significantly different penetration rate and

Table 6.6 Unconfined compressive strength of Keweenaw basalt.

Sample	Site	Compressive strength (MPa)
Original KB	—	60–100
KB01	1 or 2	100.5
KB02	3	72.8
KB03	4	59.9
KB04	4	65.9

page proof WILEY-VCH

Table 6.7 Chemical composition of Keweenaw basalt.

Component	THB106	THB128	KB01	KB02	KB03	KB04
SiO_2	48.61	50.99	47.96	50.31	47.34	47.10
TiO_2	0.83	1.53	1.44	1.52	1.38	1.42
Al_2O_3	17.31	14.38	16.95	14.76	16.55	16.56
Fe_2O_3	9.83	13.32	12.26	13.74	12.64	12.96
MnO	0.13	0.17	0.18	0.21	0.13	0.16
MgO	8.43	5.83	6.99	6.00	7.23	7.31
CaO	11.03	7.49	10.67	9.49	10.72	10.29
Na_2O	2.01	3.43	2.42	2.24	2.30	2.46
K_2O	0.19	0.92	0.25	0.51	0.23	0.28
P_2O_5	0.07	0.15	0.15	0.18	0.12	0.13
LOI[a]	1.31	1.80	0.91	0.99	1.30	1.16
Total	99.66	99.9	100.2	99 6.53	99.9	99.8

[a]LOI, loss on ignition.

cumulative depth achieved, as shown in Figure 6.55. Coring bit tests at Earth STP yielded maximum penetration rates between 40 and 60 cm h^{-1} and a cumulative depth drilled of 20–25 cm before the penetration rate dropped below 5 cm/h^{-1}. When these tests were repeated in a 5 Torr CO_2 environment, maximum penetration rates above 120 cm h^{-1} were observed and a single coring bit achieved 117 cm before tests were stopped due to time constraints. Assuming a linear decline and excluding catastrophic failures, the bit might have achieved ~200 cm before the penetration rate dropped below 5 cm h^{-} marking the end-of-life.

This phenomenon is thought to result from trace amounts of water that remained trapped within the test basalt, despite efforts to remove it (prior to testing, the basalt specimens underwent a 110 °C bake-out, non-vacuum, for 2–4 days). As the trapped moisture was exposed by the coring process, it instantly transitioned to a gaseous phase. The resulting volumetric expansion contained enough energy to loft the fine

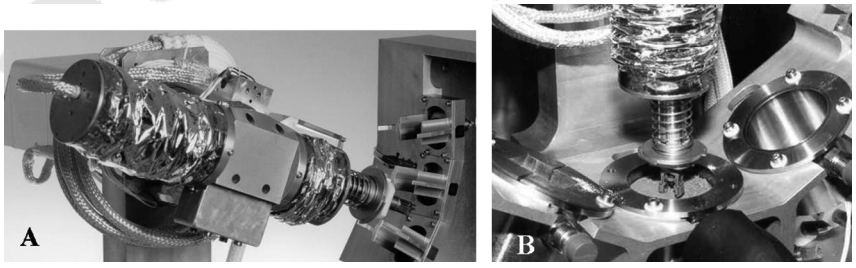

Figure 6.55 SSA/DT on its test stand (including, at bottom, three soil sample containers). (a) SSA/DT exchanging a tool in the rack; (b) SSA/DT during surface sample acquisition. The tool shown in operation is an MEE, tested with Mars stimulant. Courtesy ESA, Galileo Avionica, Tecnomare, SSS, VTT and HKPU.

Page proof WILEY-VCH

cuttings from the drill hole – in the relatively low atmosphere the fine particles experience less drag and therefore travel further. A constant plume of cuttings (~10–15 cm) was observed during all 11 trials at 5 Torr. With such efficient chip removal, the coring bit's cutting elements are free to exert all of their pressure on the rock, and the drilling process becomes much more efficient.

The results of these tests are encouraging insofar as they suggest the potential benefits of chip removal optimization. Previous bit development programs had focused predominantly on material selection and geometries designed to concentrate stress on the rock, while chip removal features went largely unexplored. If future improvements to coring bit design increase the efficiency of chip removal even incrementally, these tests show that the increase in penetration rate and life performance could be significant.

In September 2008, the CAT was mounted on the Mars Exploration Rover at the JPL facilities in Pasadena, CA (Figure 6.56). The purpose of these tests was to evaluate the operation of the drill for the potential MSR mission. The drill was mounted on the rover chassis by way of an arm-like structure which represented various characteristics (e.g., stiffness) of an envisioned low-DOF arm for positioning an MSR drill.

The CAT successfully acquired a number of rock cores from various rock types ranging from soft limestone to hard basalts. In particular, acquiring a 4.5 cm long core in Saddleback basalt (Mars simulant basal rock chosen by the Mars Science Laboratory team) took less than 60 min. The average power was less than 40 W and the maximum WOB was 180 N. Drilling and acquiring a core in a ~10 MPa

Figure 6.56 SSA/DT tool: "inverted cheese-scraper" (hollow drill cone). Courtesy ESA and Galileo Avionica.

kaolinite took approximately 10 min, with an average power of less than 4 W and a WOB of around 10 N.

6.7.4
Small Sample Acquisition and Distribution Tool (SSA/DT)

To prepare the ESA for the prospect of planetary missions, the development of a basic surface sampling tool, as simple as possible and quasi-minimalist in design, was undertaken as a technology study in 1995–1997. This concept would allow the collection of a soil sample and its distribution to payload instruments for *in situ* analyses (Re *et al.*, 1997).

The developed tool, the SSA/DT, is capable of sampling over a large range of surfaces properties, but can acquire only a few ~~soil grains (a few cubic millimeters)~~. The SSA/DT is small and compact: its essential requirements are a mass of 1.5 kg and a volume of 5 dm^3 ~~stowed~~. It can take and rotate any tool from a rack of three, extend it on its outreach radius from 100 to 150 mm and swing ±180°; it uses only a few watts of power. The SSA/DT could also carry more tool bits~~,~~ stored in a tool ~~rack, which could be exchanged~~.

The acquired sample is delivered to the analyzer oven within its tool bit which is used as a sample container. Sample and tool are left in the oven during sample heating and analysis. This chamber simulates the extreme cold temperatures foreseen from comets to Mars, ~~including~~ the Moon. ~~Mission application to this promising development remains to be found.~~ Figure 6.57 shows two views of the SSA/DT system.

The SSA/DT tools were purposely kept rugged and simple and were made with a single part (with brazed or welded assemblies). They could t 6.55 bed by their nicknames: the "inverted cheese-scraper" (Figure 6.58) and a "wire cage sampler."

6.56

Figure 6.57 Deimos touch-and-go sampling system, preliminary concept. Courtesy SENER.

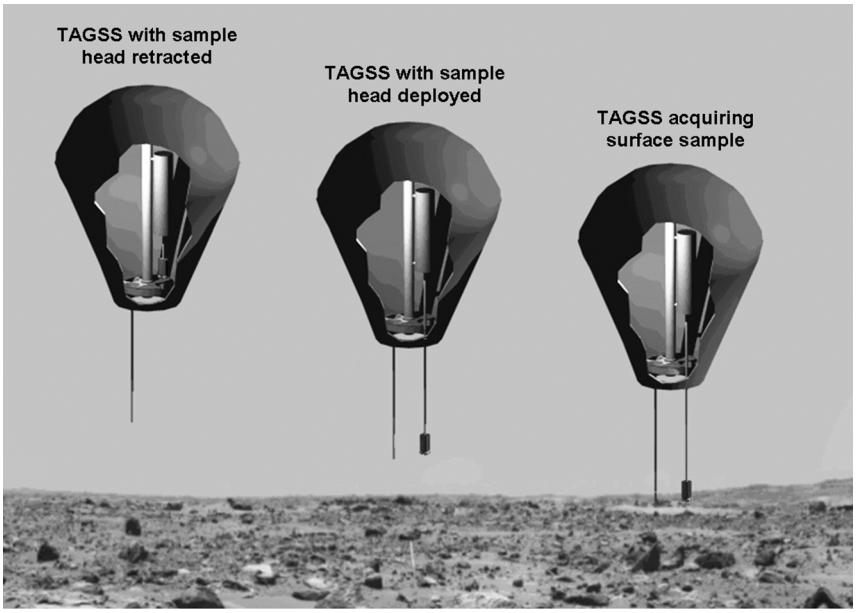

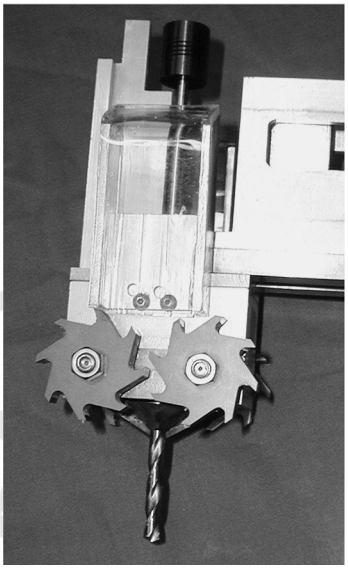

Figure 6.58 Honeybee Robotics touch-and-go surface sampler. (a) Operational sequence shown on balloon platform; (b) prototype that was tested in a zero-gravity environment on board the NASA KC-135 aircraft. Courtesy Honeybee Robotics.

6.7.5
SENER Touch-and-Go Sampler

Studies have been performed in order to return samples from the Martian moons Phobos and Deimos. In these scenarios, a spacecraft would perform a touch-and-go contact at about 0.5 m s^{-1}, without anchoring or use of additional thrust; sampling of dust, sand, gravel, pebbles, small rocks, and soil to collect 1 kg of materials would be performed solely with kinetic energy, with contacts and impulsive rebounds repeated up to four times.

A corresponding conceptual design was proposed in 2008 by the engineering company SENER (Las Arenas, Spain) and is illustrated in Figure 6.59. It is meant to collect and store granular regolith in a return container. Three feet damp the landing. The transport of granular sampled matter to the container is intended to be performed with a gaseous flow of helium.

6.57

6.7.6
Honeybee Robotics Touch-and-Go Sampler

Developed by Honeybee Robotics, the touch-and-go surface sampler (TAGSS) is designed to drill and acquire a sample of regolith (up to 50 cm^3) or weak consolidated materials (UCS < 10 MPa), providing stability while the cutters penetrate the surface to a depth of 1–4 cm. The system is reusable, with the possibility of storing sample containers for analysis by *in situ* instruments or sample return missions. The TAGSS is designed for balloon or orbiting spacecraft deployment (Figure 6.60a), avoiding the complexity and costs associated with a landed mission. It consists of a high-speed sampling head attached to the end of a flexible shaft (Figure 6.60b). The sampling

6.58a

6.58b

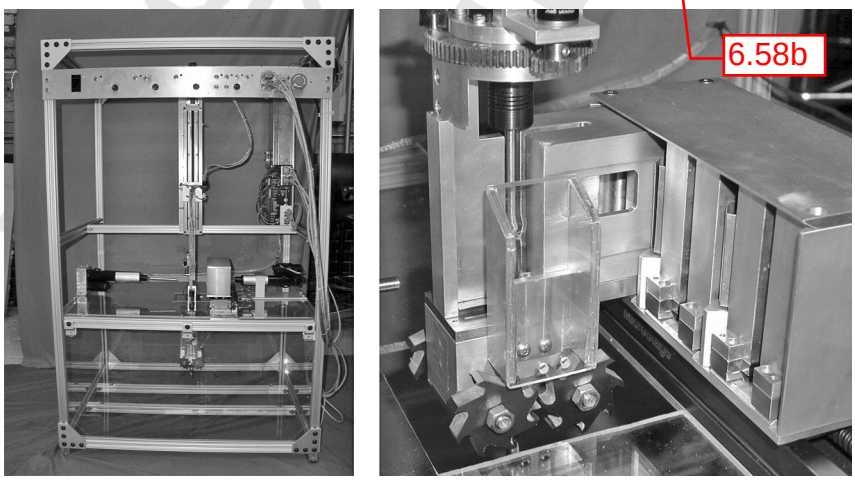

Figure 6.59 Honeybee Robotics touch-and-go surface sampler. (a) Prototype shown on test stand; (b) with sample chamber being loaded on to sample head. Courtesy Honeybee Robotics.

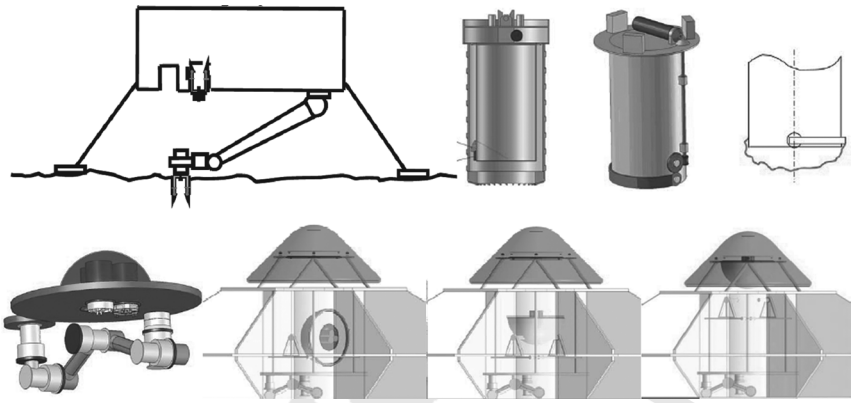

Figure 6.60 Near-Earth asteroid sampling system. (a) Sampling principle; (b) conceptual corer tool; (c) robotic arm; (d) sample transfer operations to the Earth re-entry capsule. Courtesy ESA and Galileo Avionica. (Please find a color version of this figure on the color plates).

head rotates its counter-rotating cutters at speeds of 5000–8000 rpm and consumes 20–30 W of power. The mass of the current prototype is 450 g, with a volumetric envelope of 50 × 75 × 150 mm (excluding the center drill bit); however, the design is scalable in size, mass, and sample volume to allow modification to fit a range of applications. ~~Deployment and sample containment mechanism designs are not yet completed; however, depending on the distance and stiffness required, the deployment mechanism's mass will likely be 500–1000 g. A mass estimate of the sample container and the sample container change-out system has not yet been determined. The TRL of the system is currently 4–5.~~

The TAGSS consists of three subsystems including: a deployment mechanism, a sampling head and a sample containment subsystem. The deployment mechanism deploys the sampling head by extending a boom or a shaft to reach the sampling site many meters below the spacecraft to obtain surface or subsurface samples. The sampling head contains a rotating/burrowing axis and three cutting axes. A total of five high-speed cutters are used and are driven by a single motor. These high-speed cutters throw up surface material on contact and two guides mounted above the cutters direct sample debris/chips into a removable sample chamber. The sample containment subsystem transfers and seals multiple samples. The sampling head has a removable sample chamber on top of the cutters. A prototype was developed and tested in a laboratory ambient environment on various target materials (Figure 6.61a).

The flexible shaft attached to the sampling head allows the sampler to conform to the comet or asteroid (or other planetary body) surface – an ideal method for sampling from unknown or high-risk surface regions. A hopping balloon or orbiting spacecraft will descend to a selected surface site in a 6.59a manner with a predetermined relative surface speed. At a given height above the surface, the TAGSS will be deployed. A leading contact sensor will give a positive indication of the sampling start

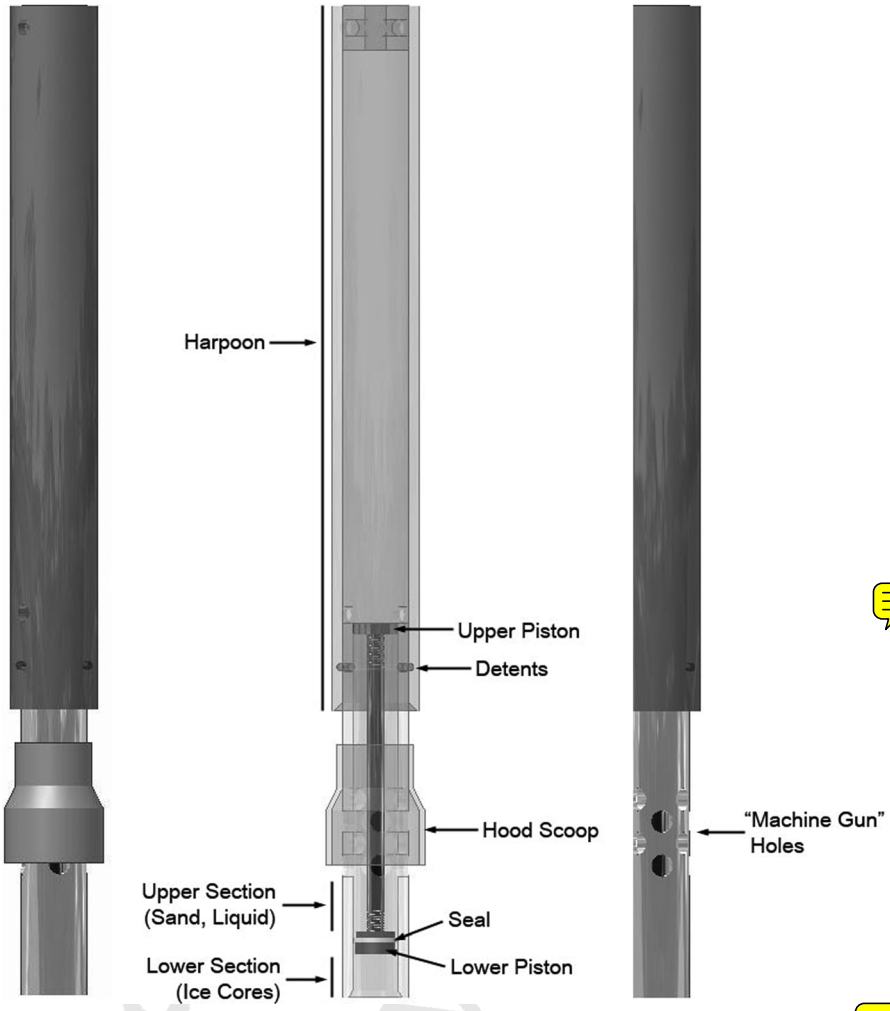

Figure 6.61 The design of the final sampling tip and harpoon sampler. Courtesy Honeybee Robotics.

time as the craft continues its slow descent. The flex shaft (1.5 m or longer) attached to the TAGSS, and also the inertia of the descending craft, will provide the required preload for sampling as the balloon/spacecraft continues its descent for an additional 1–2 s after the contact sensors have been triggered. The samples can either be collected and captured at the sampling head or be directly projected through the low-gravity atmosphere towards onboard sample analyzer apertures located at the bottom of the spacecraft instrument bay. The high-speed cutting bit ensures that the projected samples have enough momentum to reach the sample analyzers. In a controlled capture, multiple samples may be acquired and transferred to a storage cache. This is achieved by incorporating a removable sample container in the head of the TAGSS. The TAGSS is then reeled up to a sample container change-out station.

6.59b

The full sample container can then be replaced with a fresh container (Figure 6.61b) and placed in a storage bin. The sample container change-out system may be located either in the payload/instrument bay of the craft or in an intermediate location for transfer to the payload bay after all of the samples have been acquired. The system also allows for zero cross-contamination.

The TAGSS has demonstrated sampling regolith at a rate of 30 $cm^3 s^{-1}$ and consolidated chalk (10 MPa UCS) at a rate of 30 $cm^3 min^{-1}$. The sampling head was also tested in a zero-gravity environment on board the NASA KC-135 aircraft, which achieves zero gravity during parabolic flight paths. ~~Further refinement of the TAGSS design will be required, as issues related to misalignments and improper sealing were seen during testing.~~

6.7.7 Near-Earth Asteroid Sample Return

In the frame of "Cosmic Vision," current ESA studies are intended to focus on sampling and return on near-Earth objects such as near-Earth asteroids (NEA s), with a more modest requirement of 10 g of sample material (Agnolon, 2007). Samples would be acquired in one landing which might last for several minutes, preferably without anchoring. It is worth noting that no biological hazard is involved for NEAs, in contrast with Mars, hence no bio-containment is required.

In the preferred sampling scenario from a recent ESA study (Agnolon, 2007), a 2.3 ton spacecraft would carry a 700 kg-class composite; it would land on an NEA, preferably without anchoring, and stay several minutes to acquire core samples. In the preferred concept of the sampling system (Figure 6.62), three corers are stored in a half-sphere~~; after landing,~~ and a robotic arm takes each of them and cores the dusty soil surface ~~with rotation~~; a shutter closes the corer, which is ~~stored~~ back into the half-sphere. The half-sphere with full corers is transferred to the top of 6.60 ecraft and into the

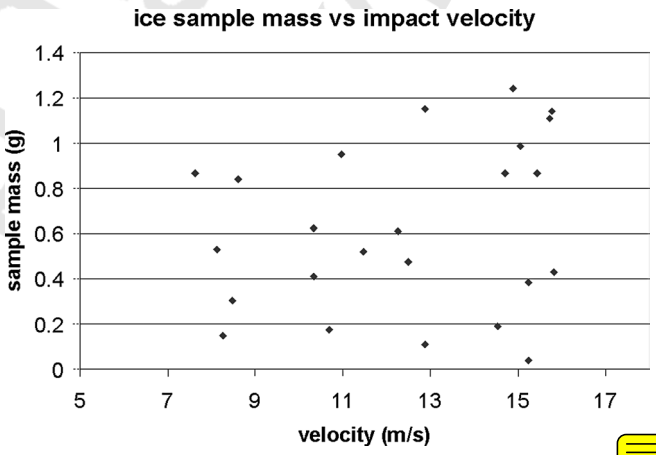

Figure 6.62 Mass of cryogenic ice samples acquired at various harpoon velocities. Courtesy Honeybee Robotics.

Earth re-entry capsule, where it is mated with another half-sphere. The spherical container is now ready for return within the Earth re-entry capsule. Galileo Avionica was the main contributor for sampling aspects of the study, ~~achieved~~ in early 2007.

6.7.8
Titan Harpoon Sampler

Scientific interest in Titan has intensified recently due to observations of the atmosphere and surface by Cassini and its Huygens probe. Remote sensing from Cassini is revealing Titan to be a complex world with active weathering and a wide range of surface materials. In addition to soils and ices, it is hypothesized that liquid hydrocarbons could be present on the surface. The geological interest in Titan is considerable due to its complex morphology and current activity. The significant atmosphere and complex chemistry draw attention in their own right and in their relationship to Earth and the other Earth-like planets. Also, most compellingly, the possible stability of liquids on the surface and the presence of hydrocarbons combine to create a plausible story for the existence of prebiotic and biotic activity. Cassini's remote sensing data and the fascinating but limited data provided by Huygens unequivocally state the case for a more capable surface mission to Titan to investigate these areas of interest that align so well with NASA's and the National Research Council's goals.

The thick atmosphere of Titan and its distance from Earth suggest that a balloon vehicle mission would serve well to make direct measurements and large area surveys. Being able to deliver surface samples to a highly capable scientific instrument payload would result in leaps in our understanding of the geochemistry of Titan.

Titan is one of Saturn's large moons with an atmosphere four times denser than that of Earth. The atmosphere is 95% nitrogen but it also contains hydrocarbons such as ethane, propane, and acetylene. The sunlight incident on the surface, due to the distance from the Sun and the thickness of the atmosphere, is one-thousandth of that on Earth, which is too low to use as a source of power for a spacecraft. The mean surface temperature of Titan is approximately 94 K, and the surface gravitational acceleration is 14% of that of Earth. Investigation has identified clouds of methane and other simple organics. It is proposed that there are methane rains, leading to methane lakes on the surface. Showing significant diversity, Titan's surface may be made up of cryogenic ice, hydrocarbon lakes, sand and other soils, and even possible tar-like tholin. These variations in the surface lead to difficulties in sampling because of the large variability of the sampled medium, varying from high-strength, solid ice to flowing sands and liquids.

Because the surface can take many forms, from a hard ice to a methane lake, the sampling device must be able to contend with the full range without advance knowledge. The science instruments require a sample of approximately 1.0–2.0 cm^3 of material (Table 6.8). Because the balloon mission may cover thousands of kilometers due to the blimp's mobility, it would be advantageous to build a sampling mechanism that would be able to take additional samples, even if they are not pristine, but with limited cross-contamination between sampling operations.

Table 6.8 Titan harpoon sampling requirements.

Sampling requirements	Value
Surface material to sample	Ices, wet and dry and icy soils, liquids
Sample size	1.0–2.0 cm^3
Sampling depth into surface	~3 cm
Number of first-use, pristine samples	10
Ability to reuse sampling hardware	Multiple reuses minimizing cross-contamination

6.7.8.1 Harpoon Design

A number of potential concepts for capturing and returning a sample to an airship were considered during the brainstorming phase. Concepts varied from using a passive harpoon dropped from the airship to lowering a mechanism that could fire a sampling tip into the surface using compressed air or stored mechanical energy.

It was also determined that many of the harpoon acceleration concepts could impart enough energy on the sampling tip to accomplish ice coring, so attention would be focused on the sampling tip design. Additional evaluation showed that a passively dropped harpoon concept was the least complex solution because it relied on gravity to impart energy, rather than a mechanism, and had the largest operatin 6.61 range.

The final tip design has a number of features which are specifically designed to collect, contain, and eject samples based on the previous testing (Figure 6.63). The lower section of the tip is used to collect an icy core or icy soil plug. The cross-section of the leading edge of the tip is sized to penetrate cryogenic ice at minimum energies while not buckling due to the imparted impact stresses. The diameter was selected based on tests on its ability to retain a core of cryogenic ice and the shape of the tip is such that the core is compressed as it enters the tip and is therefore retained as the tip is extracted from the ice. The piston inside the tip is used to eject the core from the tip.

The upper section of the tip is used to collect sand, both wet and dry, and also liquid. Note that the lower piston of the piston assembly forms a seal which creates a liquid and sand sampling chamber above the ice sampling chamber. The "machine gun" holes on the side of the harpoon allow the ingress of the sand or liquid into the sampling chamber above the lower piston. The "hood scoop" feature is required to force wet sand into the upper section during impact. Without it, very little wet sand is collected. Note that neither the sand nor the liquid are retained in the leading chamber of the harpoon. The two-part internal piston is translated forwards to eject a core if one is present and to eject sample from the upper section out of the tip also if any is present, delivering samples to a sample handling port.

The tip was placed in a harpoon that was also prototyped for testing purposes. The harpoon's mass was 460 g to ensure that it would provide adequate impact energy at velocity. The tip was designed to fit into the test rig described below and to test a prospective tip retention method. The tip slipped into a hole at the front of the harpoon and was retained via ball detents in the harpoon. The harpoon itself was

page proof

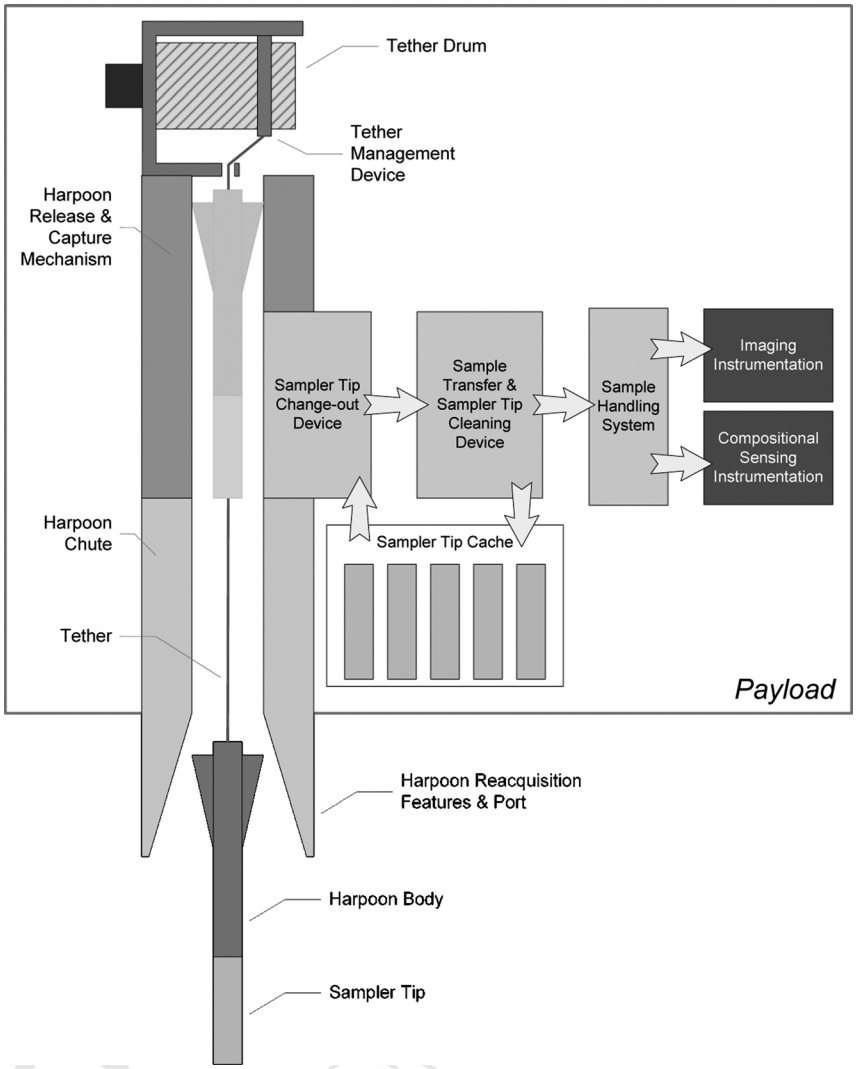

Figure 6.63 Block diagram of a flight system payload. Courtesy Honeybee Robotics.

approximately 10 in long to ensure that it exited from the test rig and flew straight into the ice or sand target. O-rings were mounted in the sides of the harpoon to provide some retention in the walls for the test rig barrel, and to ensure an air-tight fit. Overall, the harpoon performed fairly well in terms of providing a platform through which the tips could be tested.

6.7.8.2 Harpoon Testing

The harpoon was tested with cryogenic ice at approximately −150 °C. The tests were used to determine the ability of the tip to impact ice at a 45° and a 0° angle and still

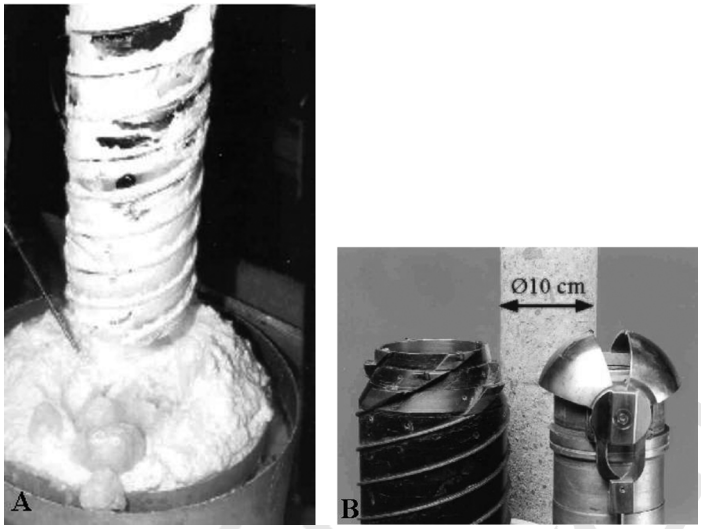

Figure 6.64 SAS-1m. (a) Coring tests of cometary analogue material in thermal vacuum. (b) Disassembled corer: from left to right, corer tube and drill bit; sample (tuff); and inner container tube with bottom shutter. Courtesy ESA and Galileo Avionica.

retain a sample. Each of the frozen buckets was placed at a 45° angle below the harpoon tip and perpendicular to the harpoon tip. Overall, the 6.62 show the harpoon is able to acquire 1.0 g samples in cryogenic ice at orientations up to 45° off of the direction of travel of the harpoon with reasonable consistency.

Additional tests were performed to determine if there was a minimum energy (or harpoon velocity) required to capture a sample. Figure 6.64 shows that although the reliability of the sample collection starts to drop off at around 8 m s^{-1}, as evidenced by the decrease in the maximum sample size, the tip still is occasionally able to capture a full-sized sample.

The harpoon was also tested in dry and wet sand. The results showed that the harpoon sampler can collect samples of dry or wet sand greater than 1.0 g. In addition, the harpoon was plunged into room temperature water to simulate liquid methane sampling. A layer of sand approximately 3 in deep was placed in the bottom of a 5 gallon bucket to absorb excess impact energy, and then water was poured into the bucket until the water depth was 10 in above the sand. Only two tests were performed and both of the samples that were taken showed that the device was able to retain more than 1 g of liquid.

6.63

6.7.8.3 System Level Design

The block diagram in Figure 6.65 shows the design concept, demarcating the subsystems and their interactions. The following is the operational time order: the harpoon is released from the holding mechanism and followed by tether which is paid out by the tether management system, the sampler tip impacts the ground collecting sample, the tether management system draws the harpoon back to the

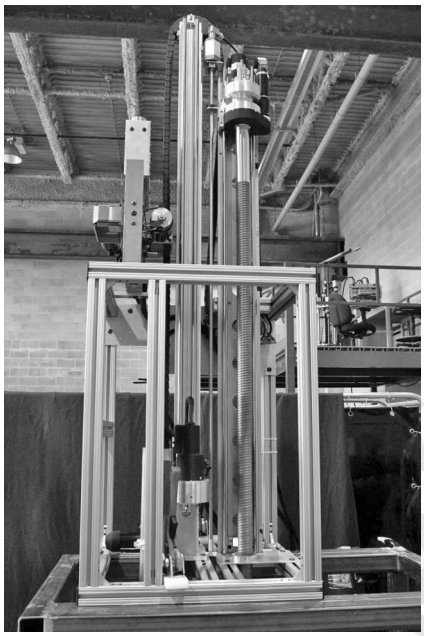

Figure 6.65 NASA RESOLVE TRL-4 Sample Acquisition and Processing System (EBRC). Courtesy NORCAT.

Aerobot, reeling in tether, the reacquisition features guide the harpoon into the payload section, the holding mechanism acquires the harpoon, the tip change-out device removes the sampler tip, and the sample transfer device ejects sample to the instruments for observation. To prepare for another sampling operation, the sampler tip is returned to the cache and a new tip is installed on the harpoon.

6.8 Shallow Drilling: One Meter Class Drills

One meter class drills are defined as drills that can penetrate from tens of centimeters into a surface and up to a few meters. This class of drill can be deployed from Mars Science Laboratory or ExoMars size rovers and are relatively compact and of low mass. Because these drills can penetrate deeper into the subsurface than surface drills, they can offer significantly greater scientific return. The sections that follow describe several drill developments efforts.

6.8.1 CNSR Sample Acquisition System for 1 m (SAS-1m) ~~(1990–1995)~~

The SAS-1m~~, like the SAS-3m studied earlier,~~ was an ESA ~~study~~ intended for a Comet Nucleus Sample Return mission~~; in~~ order to obtain a simpler, robust system, the

Page proof ©WILEY-VCH

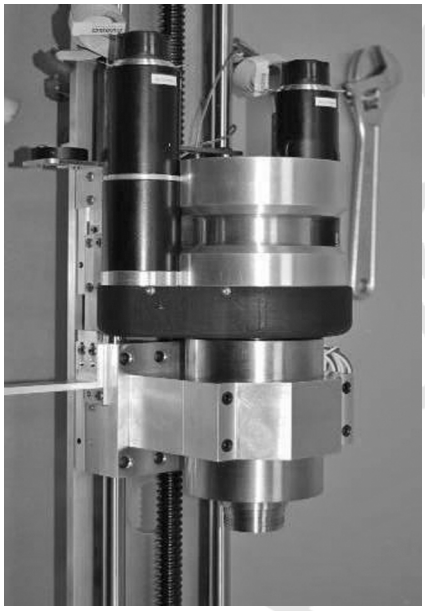

Figure 6.66 Standard drill head (deep drill version). Courtesy NORCAT.

6.64B

sampling depth requirement was ~~reconsidered, and its goal~~ reduced from 3 m to 1 m~~: 1 m was given as the very~~ minimum depth to find a meaningful volatile sample. Technically, cores ~~of~~ 1 m ~~in one piece~~ could be used. The diameter of the core sample was ~~still~~ equal to 10 cm (Fenzi, Pozzi and Coste, 1993). The sample was held in a container tube inside the corer~~; having reached~~ a depth of 1 m, a bottom shutter ~~closed~~ two hemispherical segments to cut the base (Figure 6.66B). The container tube holding the sample ~~was~~ extracted and segmented in two, using an external cutter~~; the~~ segments ~~were closed~~ with caps and stored in the Earth return container.

The SAS-1m industrial team included Galileo Avionica (formerly Tecnospazio) with Tecnomare and Rodio (Italy), DLR (Germany) and Rogalands (The Netherlands). An extensive testing program was performed. Rodio selected a coring drill bit with polycrystalline diamond ~~from~~ initial test results. The team extensively tested at DLR ~~a prototype of the SAS-1m:~~ Ettringer tuff (one of the reference materials) and solid ice were cored ~~in~~ liquid nitrogen. A cometary analog material (a frozen, dusty water emulsion) was cored in thermal vacuum in a large space simulation chamber ~~of~~ DLR (Figure 6.66a). These tests demonstrated that core sample acquisition could be achieved, ~~respecting~~ the requirements of low power (100 W at the bit), low axial force (100 N) and low torque (<50 N m) (Coste, Fenzi and Eiden, 1993). ~~Within~~ the same study, a surface sampler able to gather some 5 kg of loose soil ~~and~~ spacecraft anchors were developed and tested ~~propelled with~~ an air gun test rig.

6.64A

The SAS-1m was compliant with its requirement to core ~~at~~ 1 m depth. However, the intended NASA–ESA cooperation unfortunately did not materialize and the sample return plans were put on hold~~, and~~ the SAS-1m prototype was not developed ~~further~~.

6.8.2
Sample Acquisition and Preprocessing System (EBRC)

The Northern Centre for Advanced Technology (NORCAT) dry drilling technology is a core drilling and sampling system capable of drilling with low power, low reaction forces, and without the aid of lubricants or flushing fluids. The systems consists of a sample acquisition subsystem, a sample capture and transfer mechanism, and a sample preparation or prebeneficiation subsystem along with associated avionics, sensors, and embedded controller. The system is scalable from 50 cm to 5 m hole depth with the potential to scale deeper, given sufficient mass and power budgets. System scale, end-user requirements, and budgets will drive the final system configuration. The system configuration revolves about a central sample acquisition subsystem consisting of a dry drill head, drill bit, auger, sample capture subsystem, a cuttings management system, and an embedded controller. A good example is the 1 m class NASA-funded RESOLVE Sample Acquisition and Preprocessing System (EBRC), consisting of a 1 m class dry drill, 1 m sample capture system, sample transfer system and sample crusher (Figure 6.67). The scalability of the system relies upon a common or standardized drill head. Figure 6.68 shows the double rotation motor version for use on deep drills, such as the 20 m Class N drill.

Cartoons of the basic technology used in dry core drilling are shown in Figures 6.69 and 6.70. In this system, an annular drill bit is driven into a substrate via rotary and axial forces transmitted via the external pipe (drill string). Interior of the drill string is

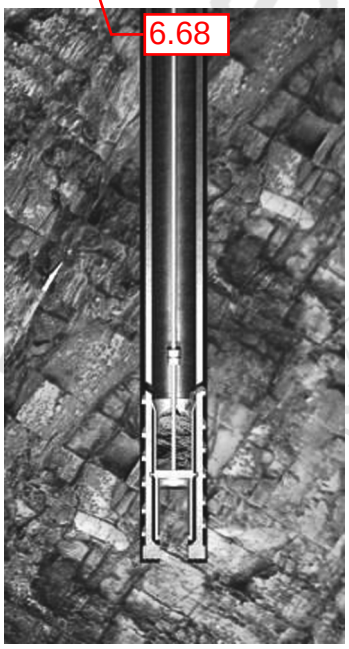

Figure 6.67 ERBC in drilling mode. Courtesy NORCAT. (Please find a color version of this figure on the color plates).

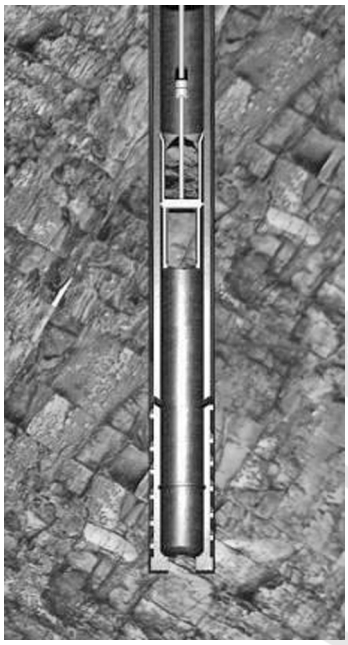

Figure 6.68 ERBC in sample retrieval mode. Courtesy NORCAT.

a core capture and retrieval system along with, in deeper drills, a cuttings removal system. The drilling action removes material from the drill bit face in an annular ring fashion, leaving behind a cylindrical sample in the center of the drill hole. The sample capture system is forced over this cylindrical sample as the drill progresses into the substrate. The sample retrieval system is activated and sample is captured when either the core capture device is deemed full or an external decision is made to retrieve a sample. The sample retrieval system is then removed from the drill string, leaving the drill string in the hole to stabilize the drill hole. The sample is removed to the surface and transferred to the next stage, likely a crusher or analytical package. The sample retrieval system is then re-inserted into the drill string and drilling resumes.

6.69

6.8.2.1 Drill Bit Design

Dry drill bit design for this technology relies on an understanding of some basic features of a drill bit. Figure 6.71 shows the anatomy of a drill bit and Table 6.9 gives the functionality matrix for various features of the bit. Field testing, testing in various lithologies, and testing in cryo-cooled substrates have led to a NORCAT patented dry drill bit design shown in Figure 6.72 that is capable of drilling at 80 K, and penetrating unconsolidated lunar simulant and also harder rocks such as basalt and anorthosites. The design of a dry drilling bit consists primarily of varying two key factors: the geometry of the drill bit and the materials of construction. The prime task of a dry drill bit is to comminute rock, creating cuttings, and leaving behind a cylindrical sample for capture and retrieval by other stages.

6.70

The bit design parameters (core diameter and kerf) were most readily varied by an early decision as to bit type. Some of the major factors influencing bit geometry were

page proof © WILEY-VCH

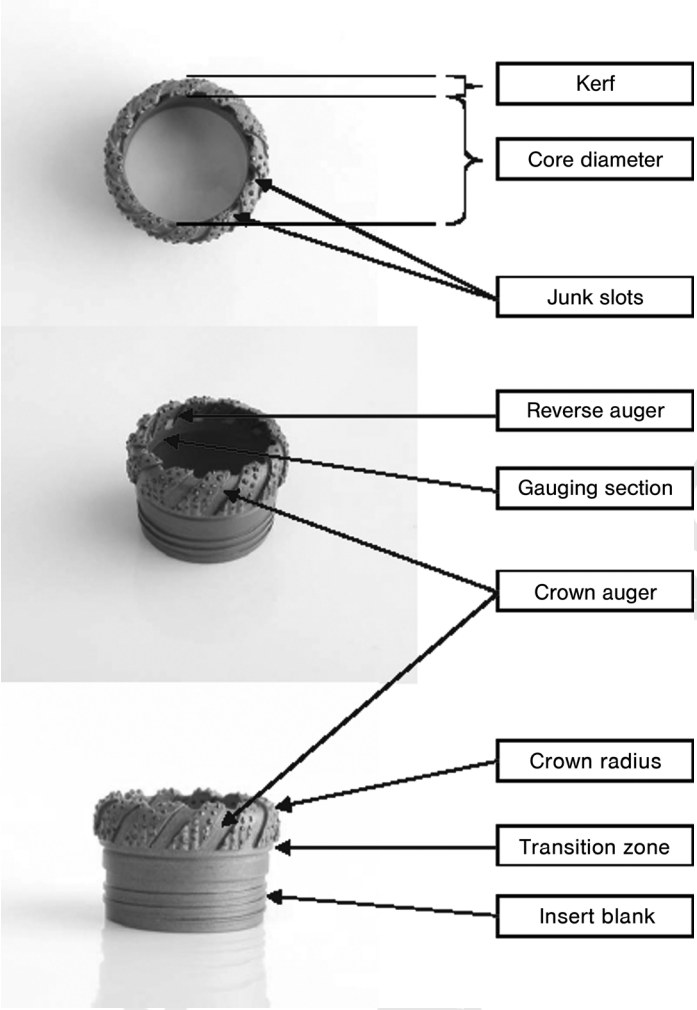

Figure 6.69 Anatomy of a dry drill bit and views of the bit cutting edge. Courtesy NORCAT.

set by this decision, including the core diameter, kerf, gauging section, reverse auger, junk slots, crown radius, crown auger, transition zone, and the insert blank. The primary factor influencing kerf size is the physical size of the core capture mechanisms housed in the drill bit/auger assembly. The simple guiding equation for estimating minimum kerf is

Q7

$$K = 0.5S + X + 2T + 2A - (0.5C)\cancel{2c} \tag{6.1}$$

where K = minimum kerf, S = sample capture mechanism OD, X = loose fit clearance (nominally 0.5–1 mm), T = depth of thread on insert blank, A = crown auger depth, and C = core sample OD.

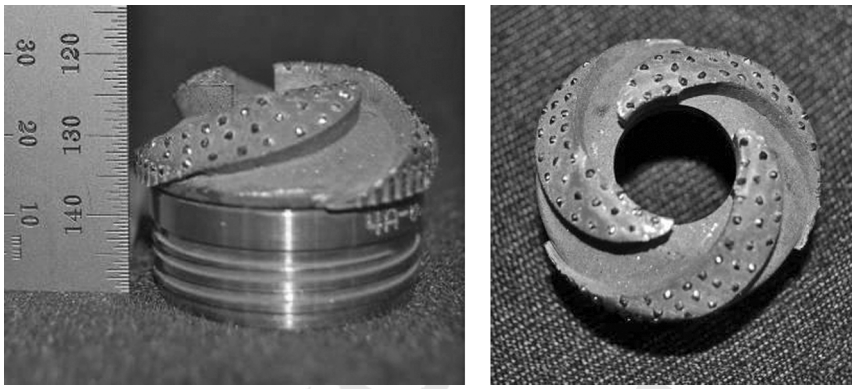

Figure 6.70 NORCAT dry drill bit (patented). Courtesy NORCAT.

The gauging sections are specially constructed using highly wear-resistant materials designed to reduce bit wear near the core. This ensures a relatively constant diameter ~~on~~ the core ~~developed.~~ The gauging section is also used to apply tension to the core sample to assist in separating it from the substrate. This is achieved passively

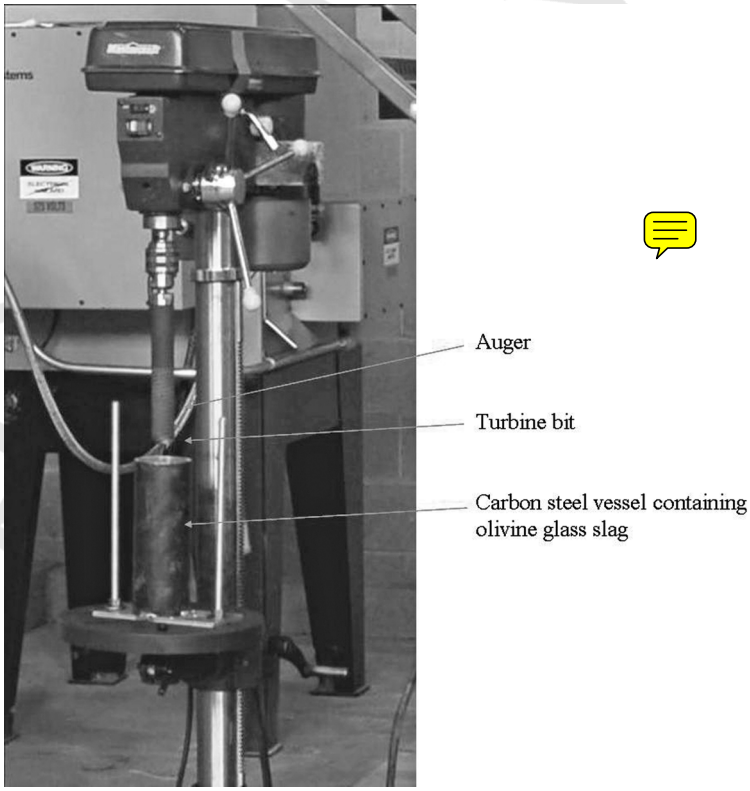

Figure 6.71 Drill press set-up for auger STP testing. Courtesy NORCAT.

Table 6.9 Functionality matrix for various features of the bit.

Parameter	Function	Influence
Core	The sample formed from the drilling action	Set by sampling needs. Drives ID and point loads
Kerf	Cutting zone. The difference between the inside and outside radii of the bit	Driven by core diameter and core capture mechanism. Drives point load and thrust
Gauging section	Wear resistant area inside diameter of bit used to ensure constant diameter of core	Can be used to assist in core capture. Home for reverse auger
Reverse auger	Unique to dry drilling. Used to remove cuttings from gauging section and prevent migration into capture zone	Impacts torque, core temperature, thrust. Prevents bit balling and capture packing
Junk slots	Forces cuttings from comminution zone into motion. Sweeps comminution zone	Rate of penetration. Efficiency in cuttings removal from comminution zone
Crown radius	Aids in centering drill during spudding (i.e., hole start) and longer hole drilling. Helps cuttings migrate up the drill (no right-angles)	Impact on cuttings transport and removal from face
Crown auger	Embedded auger section to move cuttings up the drill bit to the auger section	Impacts on torque thrust and temperatures at comminution zone
Transition zone	Facilitates cuttings transfer from bit to auger section. "Matches" multi-start augers	Impacts on ROP and transmitted forces. Bit balling, packing
Insert blank	Couples bit to drill string. Provides seat for core capture device	Core capture seat, cuttings infiltration and packing at capture device

Figure 6.72 (a) Proctor placement in cryo chamber; (b) the Auger and proctor vessel post-cryo test. Courtesy NORCAT.

page proof WILEY-VCH

in that a solid rock core tends to relieve or relax when formed and will relax into the gauging section forming a press-tight fit. This fit, along with the reverse augers, will grasp the core sample and allow the drill system to tension the core into failure at or near the bit face. The length of gauging section will affect the grab capability and wear rate of the bit.

A reverse auger section is specific to dry drilling. It is designed to start the cuttings moving down from the gauging section and to remove cuttings from the comminution zone (bit face) while mitigating packing in the core capture device.

In the bit junk slots are the primary zones in which cuttings are forced into motion. It is necessary to attempt to scrape the comminution zones clean of cuttings to prevent glassing and over-grinding, both of which consume energy and dramatically reduce the cutting efficiency. Cuttings left in place tend to act as a lubricant under low thrust. The junk slots are the scrapers and cuttings receptacles for the bit.

Crowns on bits can be profiled. The NORCAT bit was given a radius to ensure that very high point loads were achieved during hole start (spudding). This action returned the drill to stable drilling mode very quickly, since the drill hole became a rotary anchor point, thus effectively mechanically coupling the drill to the substrate. A secondary effect of encouraging the cuttings to exit the comminution zone more readily was achieved once the bit was buried. This is attributed to the curvature allowing the cuttings to get around the corner and start up the crown auger before having to be transported vertically.

A crown auger is carefully laid out to allow cuttings generated at the comminution zone to migrate up towards the drill auger section. The depth and profile of the auger grooves are driven by the volume of cuttings generated, and rpm at which the unit turns. Drill rpm is greatly influenced by the auger, since a higher auger rpm will tend to keep the auger flights more efficient and less full (unless the higher rpm generates more cuttings).

The prime task of an insert blank (also called a bit shank) is to provide a means of coupling the drill bit to the drill string. Secondary tasks relate to the provision of a seat for the core capture mechanism and an inner stiffener for the core capture crown. The metallic nature of the insert allows machining after the bit is manufactured to form the seat, adjust for loose fit clearance of the core capture mechanism, and so on.

6.8.2.1.1 **Design Influences and Rationale** Some of the key parameters listed above are dependent on the type of bit and material selection, that is, the selection of bit type will automatically set or eliminate one or more parameters. Other parameters are set and fixed by the dry drilling method itself, and still others are constrained by the manufacturing methodology. The net result is that there are very few parameter changes which may be introduced into the bit design. The core diameter is set by the science team and has been fixed at 10 mm. Core length is not relevant at this time. Further, kerf is fixed by the geometry of the core capture device and the core sample diameter. It should be minimized. The design of the gauging section of the bit is flexible where it can be eliminated entirely, shortened, or lengthened; the effect of such designs on the performance is given in Table 6.10. Also, the use of a reverse auger section can be eliminated or modified geometrically and it must have a gauging

Table 6.10 Effect of gauging section variations on performance.

Variation	Positive effects	Negative effects
Eliminated	• Very low thrust loss from this zone	• Premature bit wear-out • Inconsistent core diameter • Difficulty in capturing core
Short	• Reduction in thrust loss in this zone • Slow wear of bit	• Slow gauging section wear • Smaller grab surface for core fracture
Long	• Very slow bit wear • High consistency in core diameters • Larger grab surface for more positive fracture	• Increase in thrust loss • Larger "grab" surface for fracturing core making core difficult to extract from zone

section within which it is formed; the effect of such designs on the performance is given in Table 6.11.

As far as junk slots are concerned, they are a requirement of drilling and cannot be eliminated. The size, shape and positioning are related to manufacturing and to estimates of the cuttings volumes that must be removed during drilling. Also, the radius crown is required in surface set and impregnated matrix bits to build up slowly to full surface exposure when spudding a new hole. In addition, the radius tends to

Table 6.11 Effect of reverse auger on drilling performance.

Variation	Positive effects	Negative effects
Eliminated	• Simplified design and easier manufacture	• Cuttings will migrate up into the core capture device • Possible packing and jamming of capture mechanism • Possible bit stall
Angle of attack	• Higher angle improves cuttings transfer efficiency	• Too great a slope will halt cuttings transfer and cause bit balling and potential stall • Too low a slope will cause bit stall • Manufacture precludes low slopes
Depth of flight	• Increase in depth may increase cuttings transfer efficiency	• May affect kerf calculation if too deep • Too shallow may result in bit stall • Manufacturing methods preclude very shallow flights

page proof © WILEY-VCH

Table 6.12 Effect of angle of attack and size of auger flights on drilling performance.

Variation	Positive effects	Negative effects
Angle of attack	• Higher angle improves cuttings transfer efficiency • Low angle may improve transfer of cuttings	• Too great a slope will halt cuttings transfer and cause bit balling and potential stall • Too low a slope will cause bit stall • Manufacture precludes low slopes
Size of flight	• Increase in depth and/or width may increase cuttings transfer efficiency	• May affect kerf calculation if too deep • Too shallow may result in bit stall • Overly wide flights will cause bit balling and bit stall • Manufacturing methods preclude very shallow flights • Manufacturing methods preclude very thin flights, number of starts and overly wide flights

promote cuttings travel, as the cuttings are not required to turn a 90° angle to begin upward migration. It is not an absolute requirement. If incorporated in the bit, its geometry is dictated by manufacturing methods, sizing of the crown, and the size and set of surface set diamonds. Further, a crown auger must be incorporated for dry drilling. This is the only method by which cuttings may migrate up to the auger section. The only possible changes are in the angle of attack and the size of the auger flights, and their effect is described in Table 6.12. In a drill bit, a transition zone is required whenever two dissimilar auger sections are close coupled. The transition zone will allow a multi-flight crown auger to transfer cuttings effectively to a potentially non-matched auger section above. Also, an insert blank is a must for drill bits. The blank needs only to be large enough to accommodate the core capture mechanism and a coupling mechanism to the drill steel or auger section for the bit crown. The size and shape of the blank are set by the kerf, crown type, and coupling mechanism. Some opportunity exists to minimize the blank length, but this will have no impact on drill bit performance. Material selection of the blank is critical to the manufacture of the bit and also to performance under extreme temperatures, due primarily to thermal stressing and differences in coefficients of thermal expansion of the blank and matrix.

6.8.2.2 Drill String Auger Section

The purpose of the auger is to transfer mechanically cuttings developed by the drill bit away from the bit auger and transition zone to some vertically removed location for disposal. Augering of these cuttings can be accomplished either external or internal to the drill string, depending on application. Integration of the auger into the section of drill string closest to the drill bit also tasks the auger with transfer of

page proof

mechanical rotational and axial forces from the drill string and drill head to the drill bit. It has been shown in previous work that it may be energy efficient to auger direct to the surface on the outside of a drill string if the depth of augering does not exceed about 1.5 m. For greater depths, in excess of 2 m, an innovative approach to cuttings removal should be implemented. This innovative approach is to auger a short distance vertically (maximum 1.5 m) to a point on the drill string where the cuttings may be allowed to flow to the inside of the drill string via one or more controllable ports (auger ports). Inside the drill string is a receptacle (cuttings bucket) designed to capture and contain the cuttings entering through the auger ports. Once filled, this cuttings bucket can then be hoisted to the surface via the wireline mechanism used for retrieving the core sample. It is also possible to integrate the cuttings bucket with the sample capture device, thereby reducing the requirement for wireline "trips" during a drilling operation. This would require removal of the cuttings bucket at the same time as the sample via the sample capture device.

It is important to note that the cuttings bucket and core capture device, once integrated, are limited in length by the need to minimize the auger length. The maximum auger length is set for practical purposes at 1.5 m. Minimizing the auger length will also reduce the machine torque required to turn the auger during drilling operations. This is primarily due to friction between the borehole and the auger flights, which is compounded by drilling media characteristics, and auger plugging or choking. The auger design is based on two key factors: the materials of construction and the geometry of the auger flights.

6.8.2.2.1 **Materials of Construction** Auger materials become critical from the perspective of wear under "normal" drilling conditions [such as standard temperature and pressure (STP)] and also under those conditions expected to prevail at a lunar South Pole site, such as 40 K ground temperature and 10^{-12} Torr atmospheric pressure. NORCAT has performed extensive testing to select a low-wear and durable auger material that can survive temperature extremes without failure. Previous versions of the auger utilized carbon steel with a hard chrome plating to the auger flights. This plating had the effect of reducing friction between the borehole and the auger flights. It also reduced friction between the cuttings and the auger flights as the cuttings migrated up the auger. The hard chrome plating mitigated wear on the auger flights but, during various trials and testing of the dry drilling unit, it was noted that some galling of the flights occurred. It is possible that the galling was created by misalignments encountered during drilling of media transition zones (zones between two significantly different media, such as dolomite to basalt). NORCAT performed significant testing at both STP and under cryo-cooled conditions (90 K) of wear on various auger materials and coatings.

Augers were ~~to be~~ prepared from either 440C hardened stainless steel or titanium and then coated with one of two composite diamond coatings (CDCs) or a thermoplasma coating under the brand name Endura. Although the coatings manufacturer felt that the titanium augers could be coated with the CDCs, two attempts were made to apply the coatings, and both failed.

Figure 6.73 Inverted spring type passive sample capture device. Courtesy NORCAT.

6.71

The programmable variable-speed drive drill press and vessel used for testing the augers in olivine glass slag are shown in Figure 6.73. The drill press was operated at either 20 or 100 rpm, as per the test parameters. Olivine glass slag was added to the carbon steel vessel. NORCAT's turbine bit was added to the end of each auger in order to generate the flow of cuttings up the auger flights.

All measurements of major diameter, minor diameter, and flight thickness remained unchanged. The auger was evidently polished (a microscopically visible smoothing of high points undetectable by a digital vernier or micrometer) by exposure to the glass, but when viewed under a microscope the original machining marks were still evident. When subjected to the glass at 100 rpm, they still exhibited no wear after 48 h. The data for wear of auger coatings at STP are summarized in Table 6.13. The hardened 440C stainless-steel augers that were uncoated or coated with a CDC coating (either CDC nano or CDC 8), exhibited no wear during the STP testing, and therefore were selected to proceed to cryotesting.

For the cryo testing, a 6 in proctor vessel of 0% OB1 lunar simulant was pre 6.72
The simulant was oven-dried and then compacted into the vessel according to ASTM traceable procedures developed by NORCAT specifically for testing in lunar simulants. The vessel was then placed inside the cryo-chamber (Figure 6.74)

Each auger was tested in the cryo-chamber for wear in the 0, 5, and 10 wt% moisture OB1 (NORCAT's lunar simulant). Each of the three augers yielded similar results in 0% moisture OB1. There were no changes in measurements and no discernible wearing of the auger in the case of both the uncoated 440C and the coatings for the CDC nano or CDC 8. For the 5 and 10% moisture testing, the proctor vessels were prepared as per the procedure and then placed in a chest freezer to pre-freeze material and prevent loss of moisture between tests. Table 6.14 shows that 440C hardened steel was the most effective auger material, with the least complexity of manufacture.

The geometric design of the auger depends on a number of factors. Most notable at this time are cuttings volume and drill string performance. The volume of cuttings

page proof © WILEY-VCH

Table 6.13 Summary of auger coating wear at STP.

Base material	Coating	24 h at 20–25 rpm	48 h at 100 rpm	Advanced to cryotesting
440C hardened stainless steel		None	None	Yes
440C hardened stainless steel	CDC Nano	Glazing	None	Yes
440C hardened stainless steel	CDC 8	Glazing	None	Yes
440C hardened stainless steel	Endura 992	Chipping and flaking	Chipping and flaking	No
440C hardened stainless steel	Endura 993	Polishing	Polishing	No
Titanium	CDC Nano	Coating could not be applied		No
Titanium	CDC 8	Coating could not be applied		No
Titanium	Endura 992	Wear, polishing	Wear, polishing	No
Titanium	Endura 993	Polishing, smoothing	Polishing, smoothing	No

generated is directly related to the drill bit design. It is a function of the bit style, bit kerf, bit crown design, and drilling medium. Consolidated material will undergo a volumetric change during comminution that averages 3 : 1, but can be as high as 6 : 1 or as low as ~1 : 1. For the bit style and crown design that we selected, we expect to see a volumetric change in the 3 : 1 to 4 : 1 range. This volume of cuttings must be free to migrate up the auger flights by way of only rotary action of the auger flights against the stationary borehole side walls. Auger flights must be designed to accommodate the large volume of cuttings without forcing a packing condition to occur (i.e., a condition wherein the cuttings are so mechanically restricted that the rotary action forces the cuttings to pack up the auger flights, thereby causing a cessation of drilling).

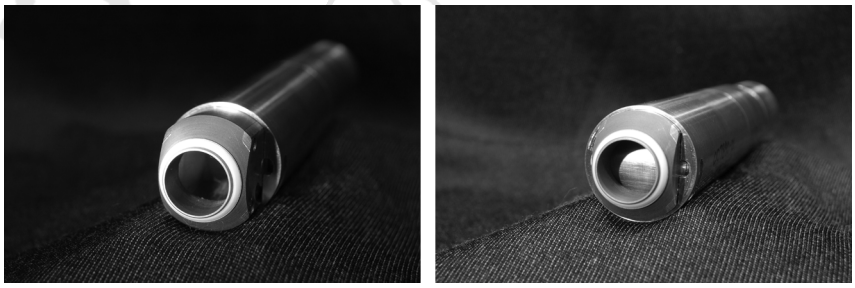

Figure 6.74 The SCaD nose (the end that contacts the drill bit and through which the sample is forced) in (a) an open or drilling condition and (b) a closed condition. Courtesy NORCAT.

page proof © WILEY-VCH

Table 6.14 Wear test results for auger coatings and materials.

Auger	Standard temperature and pressure		Cryotesting (% moisture in simulant by weight)		
	20 rpm	100 rpm	0%	5%	10%
440C	✓	✓	✓	✓	✓
440C CDC Nano	✓	✓	✓	✓[a]	✓
440C CDC 8	✓	✓	✓	✓	✓
440C Endura 992	✓	✓			
440C Endura 993	✓	✓			
Titanium, Endura 992	✓	✓			
Titanium, Endura 993	✓				
Titanium, failed CDC					
Titanium, failed CDC					

[a]This test was inconclusive.

Drill String Performance The performance of the drill string, for the purpose of auger design, relates to available rotary actions (i.e., available torque and rpm of the auger). A third parameter relates to the type of cuttings that we might expect the auger to handle. This parameter is most readily defined by the drilling action and can be set as either percussive or non-percussive. In the percussive mode, the drill string is essentially hammered during drilling. This causes rock chips to form, the size of which is based on rpm, "hits per revolution", and bit crown configuration. In the non-percussive mode, the bit is rotated against the drilling medium and the rock is fractured by a grinding type of action. This produces a smaller cutting than percussive drilling.

The torque and rpm interact on the auger design to drive the depth of auger flights, angle of the helix, number of flight starts and free space between flights (dictated in turn by the fill ratio).

Two models of helical screw conveyors, a volumetric performance model and a torque characteristic model, were developed by A.W. Roberts and colleagues at the University of Newcastle. Roberts developed vertical, inclined, and horizontal auger models, and published various technical papers and journal articles as the models evolved (Roberts and Willis, 1962; Roberts, 1999). Most of Roberts' work was aimed at grain handling technology as opposed to rock material handling and focused on the vortex motion that occurs in grain transport and its effect on volumetric efficiency. It is not clear that the vortex flow that develops in grain elevators also occurs in rock fragment transport where the interparticle friction is relatively high. Also, grain elevators and ore movers typically have a flight diameter to shaft diameter ratio that is greater than 2 : 1 and typically about 3 : 1. The auger geometry for a core bit with a

page proof WILEY-VCH

narrow kerf must have a ratio that is less than 1.1 : 1, and in the case of the present design, equal to 1.06 : 1. We have found no experimental results for an auger with such a low ratio, so the volumetric performance model is not likely to be accurate until it is modified to reflect this unusual auger geometry, and then calibrated and verified with experimental results. Despite these drawbacks, and lacking any better starting point, we used Roberts' model as a basis for our initial model and the analysis presented.

Yu and Arnold (1997) published a different approach to the torque calculation for a horizontal screw feeder and included data for cement and semolina. Kessler and Leitner (2000) described an auger sub-model that predicts the torque that occurs with milling and jamming in the clearance between the outside of the auger flight and the casing (bore wall). They also considered the lack of concentricity between the auger and the casing. They conducted experiments with fine ore, 2 mm grain size, and also crushed PVC and rapeseed. Various elements of these published models have been assembled to model the volumetric and torque performance of the auger above the bit.

Many of the properties that were used in the model were assumed, and if these properties are replaced by measured rock cuttings properties the validity of the model predictions increases. Various, potentially important, physical phenomena were not included in the model. The most important of these are likely to be the compaction of rock cuttings at maximum fullness factor and the reduction in particle size and resultant change in properties that occur with milling or regrinding of cuttings in the clearance gap. These factors may, in turn, lead to heating effects that are not modeled at this time.

6.8.2.3 Sample Capture Techniques

6.73

Sample capture techniques involve either active or passive devices. Passive devices include inverted springs, such as are used in hydrogeology studies or 6.74 ure of mud samples in overburden testing for civil work (Figure 6.75).

Active sample capture refers to a technique whereby a mechanized device at the hole bottom is used to close off and capture samples (Figure 6.76). This type of device requires an actuator for movement, either in the hole near the drill bit or at the surface. This technology is a requirement for the effective capture of unconsolidated material. The active capture technology is required for both deep and shallow drilling when science objectives require the examination of potential water-bearing, loosely consolidated, and unconsolidated material. Active capture may not be indicated when acquiring samples in hard rock formations, but may assist in the examination of hard rock anomalies such as gas pockets, mud slips, and fracture zones.

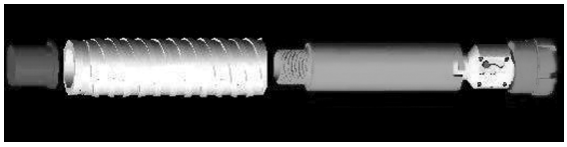

Figure 6.75 NORCAT active sample capture device (SCaD): schematic view and a photograph of the drill dumping loose material captured at depth of 1 m. Courtesy NORCAT.

Figure 6.76 NORCAT SCaD (patented) dumping loose material captured at depth of 1 m. Courtesy NORCAT.

In either case, the sample capture device is situated right behind (above) the drill bit and internal to the drill string. It is designed to allow the sample to enter (rather the device is pushed over the sample) the inner diameter with little or no impediment. In the case of passive devices, the sample must overcome stiction (a combination of stickiness and friction caused by press-fit tolerances and sample swelling inherent when relieving internal pressures during drilling) and perhaps spring tensions. In the case of active devices, the sample "hole" is wide open and presents an unimpeded route for the sample to enter the capture device.

Figure 6.77 depicts NORCAT's concept used in the NASA RESOLVE sample capture system (1 m sample) and also the working end of the CSA Class M (20 m) deep drill. Note that the sample capture device (SCaD) is internal to the auger section and is close coupled to the drill bit. The SCaD locks into place for the drilling mode, is actuated from the surface, and can be removed from the drill string auger and retrieved to the surface carrying a sample of unconsolidated or consolidated material.

The SCaD has been tested at cryo-temperatures and is used in the NASA RESOLVE drill and also the CSA deep drill. Figure 6.78 shows the manual removal of some NORCAT OB-1 lunar simulant from the SCaD after a drill and sample acquisition test.

When the SCaD is closed, the sample is trapped in the SCaD and the SCaD can be removed from the drill string without loss of material. The sample tube is a hollow cylinder sized to hold the sample evolved during drilling. The length of the tube is driven by operational considerations. For example, the NASA RESOLVE drill drills to 1 m depth and is required to acquire a continuous sample over the full meter. The 1 m sample tube is therefore attached to the SCaD to hold the sample. Since all drill cuttings are transferred by auger to the surface, there is no need to use drill string internals for cuttings transfer. In the case of the CSA deep drill, the sample tube is 10 cm long and a cuttings transfer bucket is attached above the SCaD to allow both sample and cuttings to be removed from the drill string at the same time. This results

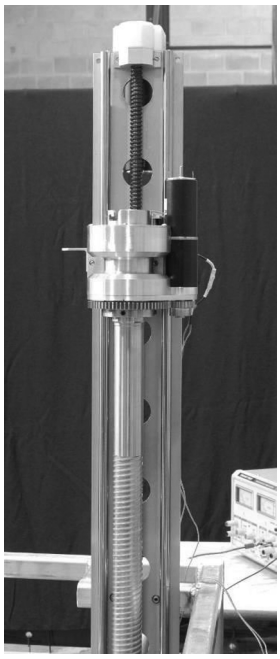

Figure 6.77 RESOLVE drill. Courtesy NORCAT.

Figure 6.78 RESOLVE transfer turret. Courtesy NORCAT.

proof WILEY-VCH

Figure 6.79 Sample transfer head. Courtesy NORCAT.

in a 50 cm long auger section, but allows the process to continue to depths of 20 m without significant changes to the internal structure or operational requirements.

The equipment required for dealing with sample removal and cuttings management is driven by end-user requirements. In shallow drills, simple SCaD and sample tube removal can be easily performed with a simple pick-and-place transfer mechanism. For deep drilling, a wireline system must be used.

6.8.3 NORCAT's SCaD 2 m Drill

6.77

The drill unit consists of the drill head which holds the drill string (auger, bit, and SCaD), and the mast, including the linear rails upon which the head rides in a vertical movement (Figure 6.79). The drill head also provides a bayonet mount to hold the SCaD in place while drilling and a means of removing the SCaD when necessary. The drill head includes a rotary motor. The drill's rotational motor provides a variable rpm. A thrust motor mounted on the drill mast drives a ball screw which imparts a vertical thrust to the drill head. A sensor provides information on the position of the drill head during the drilling operation.

6.78

6.79

The sample transfer turret (Figure 6.80) is comprised of the telescopic mast with a front-mounted linear rail system, turret head (Figure 6.81), and transfer arm. The telescopic mast and rail system can position the turret head and transfer arm at any vertical position at which the drill head may be in order to capture a sample. The transfer arm has the ability to close the SCaD gate, remove the SCaD from the drill bayonet mount and hold the SCaD for safe removal from the drill string. After removing the SCaD from the drill string and drill head, it is then transferred through a rotary motion of the turret head to a position above the next-stage device (likely a crusher). The turret transfer arm then opens the SCaD gate holding the SCaD in position to allow the core to be removed and processed. After the core has been completely removed, the sample acquisition system completes the cycle by replacing the SCaD back in to the drill head/string for the next drilling cycle.

6.80

6.8.3.1 Fully Integrated Unit

A fully integrated drill unit consists of a basic drill head and mast, sample retrieval and transfer system, a rod handler, and a wireline system (Figure 6.82). To address the

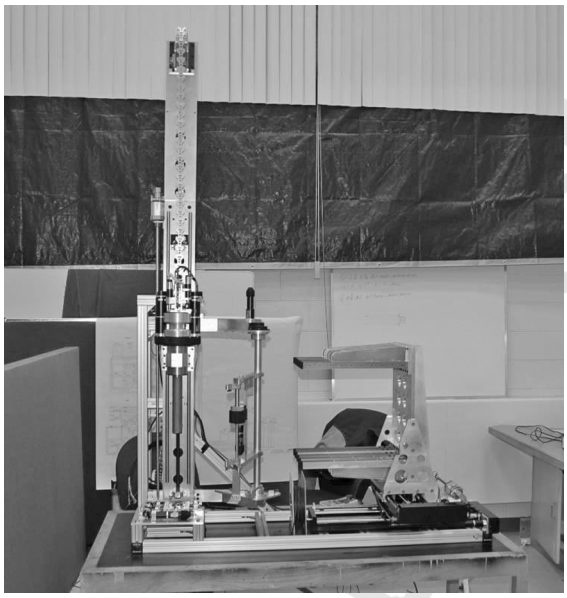

Figure 6.80 NORCAT's integrated deep drill. Courtesy NORCAT.

integration of these systems into a drill system efficiently, head clamping, foot clamping, fluidization, and superstructure are necessities.

Head clamping is required to transfer rotational and axial forces to the drill bit and auger from the drill drives. The head clamp also needs to allow free and unrestricted access to the drill string interior for the purpose of sample recovery.

Foot clamping is a requirement during rod handling. It stabilizes the drill string portion that is in the hole during the time that the drill head is disconnected from the

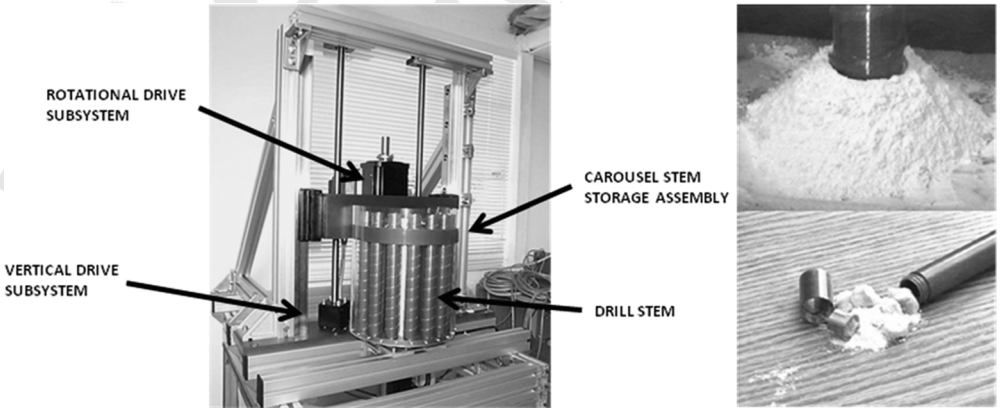

Figure 6.81 Images of ATK Space SCAD with subsystem and component callouts (a), SCAD rock drill test (b), and sample core capture container (c). Overall SCAD volume is about $90 \times 90 \times 100$ cm. Photographs courtesy of ATK Space.

Figure 6.82 Images of ATK subsurface access testing laboratory with SCAD 2 m drilling test configuration (a) and core samples from 2-meter test (b). Photographs courtesy of ATK Space.

drill string for rod handling. The foot clamp also holds the deadweight of the drill string when the drill rods are being removed from the hole and the string length is shorter than the hole depth; in other words, the drill string is suspended above hole bottom. Finally, the foot clamp is an integral part of the rod coupling sequence in that it ensures rod stability and zero rotation during coupling/decoupling actions.

The design utilizes a mechanical wrenching technique and associated flats on the drill rods to prevent rotation and to centralize and suspend the drill string. This technique is used in the mining industry on larger drills, such as blast hole drills and ITH-type drills. It is highly successful.

Fluidization utilizes a magnetic coil with integral hammering magnets. This resulted in a lower part count, reduced complexity, and improved life cycle. The fluidizer is installed on the drill below the drill head. Its prime function is to ensure cuttings fluidization in the auger flights and thereby prevent auger and bit packing.

6.8.4
ATK's Segmented Coring Auger Drill (SCAD)

The segmented coring auger drill (SCAD) was developed by ATK Space (formerly Swales Aerospace) in support of future Mars and comet missions. The results of the 1998 study provided the following three concepts:

1. The *tethered ultrasonic drill system* concept contains a drill head that vibrates at ultrasonic frequencies. Prior to operation, the drill head is held by a mechanical structure platform in a stowed position. During operation, the drill head is lowered by a cable tether. The tether contains the mechanical means to pull the drill up, transmission of electrical power, transmission of compressed gas for cuttings removal and a cuttings return line.

2. The *down-hole hammer drill system* concept contains a down-hole hammer drill bit assembly. This bit assembly is attached to a segmented extension stem to reach the target depth. The hammer drill uses a percussion motion combined with rotary motion to break up relatively hard rock formations. The cuttings removal was accomplished by means of a compressed gas subsystem.

3. the *segmented rotary drill system* concept contains a custom rotary bit assembly for dry drilling application. The bit assembly is lowered down the hole using a segmented stem joint technique. The cuttings and samples are retrieved using mechanical subsystems that provide a continuous sampling analysis option. The rotary and vertical subsystems provide the torque, cutting speed, and downward force to the bit assembly in order to break up the rock formation. No fluid medium (gas) is used to remove the cuttings. This concept uses auger and other mechanical features to remove cuttings and retrieve samples. The cuttings could be analyzed in real time to aid in locating areas of interest.

These three system concepts were evaluated to select one concept for a technology development plan and the results of the evaluation are given in Table 6.15.

The evaluation showed major differences in complexity of the design, cuttings removal method, expected performance and low development costs. Both the ultrasonic and hammer concepts were considered more complex than the segmented rotary concept due to the expected number of parts, subsystems, and programming effort. The cuttings removal method of using compressed gas was a concern because of the extraterrestrial low atmospheric condition, uncontrollable flow of cuttings, collapsing borehole, concerns about rapid dust flow jamming parts, and possible static charges during use that would cause jamming of the cuttings flow path. The engineering team believed that the compressed gas method would limit the ability to reach the target depth. This criterion also affected the expected performance rating score. The development costs were also an important criterion in selecting the final concept for the next phase of development due to the limited research funding that was available. Based on low complexity, rock destruction method, cuttings removal, expected performance, and development costs, the segmented rotary drill system concept received the best overall score and was selected and proposed for the next-phase development plan.

The detailed development of the SCAD breadboard began in 1999 with funding from the JPL's Robotic Sampling and Containerization Technology (RSCT) Program.

Table 6.15 Some of the evaluation criteria and results (score: 10 = best and 1 = worst).

System concepts	Low complexity	Rock destruction	Cuttings removal	Expected performance	Low development cost	Final score
Tethered ultrasonic	4	7	4	5	4	24
Down-hole hammer	5	9	4	6	6	30
Segmented rotary	8	8	8	9	9	42

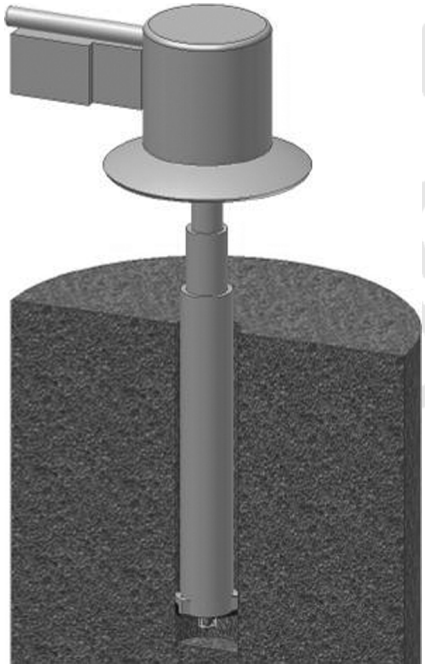

Figure 6.83 Telescopic pneumatic drill concept. A small internal combustion engine located at the top of the drill provides rotary motion. The exhaust may then be used to provide downward drill thrust and to extend the telescopic drill. Finally, as the gas exits the drill, it will blow cuttings out of the hole. The plate located above the drill will deflect the cuttings back to the ground. Courtesy Honeybee Robotics.

A careful evaluation of terrestrial technologies was conducted. Cuttings removal, axial preload, and borehole integrity maintenance problems limit dry drilling using terrestrial conventional fluted drill bits to depths of no more than 20–50 drill bit diameters. Deeper terrestrial drilling requires either drilling with mud or using compressed air for debris removal. In conventional dry drilling, a single drilling stem performs all the functions that ultimately limit the drilling depth. The cuttings accumulation consumes energy of the rotating drill bit, reduces the axial preload on the bit, and can cause jamming of the stem in the hole.

Once the SCAD breadboard unit was completed (in September 1999), initial rock drill tests were conducted in the ATK Space Subsurface Access Technology Laboratory. The SCAD system shown in Figure 6.83 identifies a few of the subsystems and assemblies. Additional assemblies and subsystems not shown were a custom diamond-impregnated bit assembly to provide the rock breakage function and an internal sample capture mechanism that collects core samples (solid and unconsolidated) while drilling occurs to obtain borehole stratigraphy. The SCAD uses a pure auger approach wherein the dry cuttings are removed and transferred from the

borehole to the surface using only the auger feature. Additional tests of SCAD consisted of a several drill tests into solid rocks that varied on Mohs' hardness scale from 1 (talc) to 6 (feldspar). Each of the rock tests varied in depth from 13 to 55 cm with a cumulative depth of 163 cm.

In 2001, the JPL RSCT program funded the development of a 2 m SCAD drill test. The initial successful tests provided justification for a continuous 2 m drill test in order to address the 20–50 drill bit diameter dry drilling depth limit. A new 2 m drill tower was completed to support this test (see Figure 6.84). After an 8 day laboratory

6.82

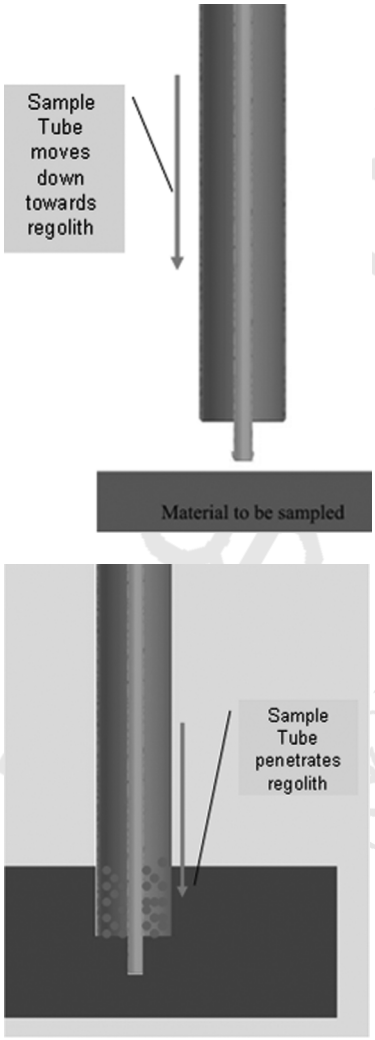

Figure 6.84 The steps in the plunge method of pneumatic lift/excavation Courtesy A. Ashley, Honeybee Robotics.

Proof WILEY-VCH

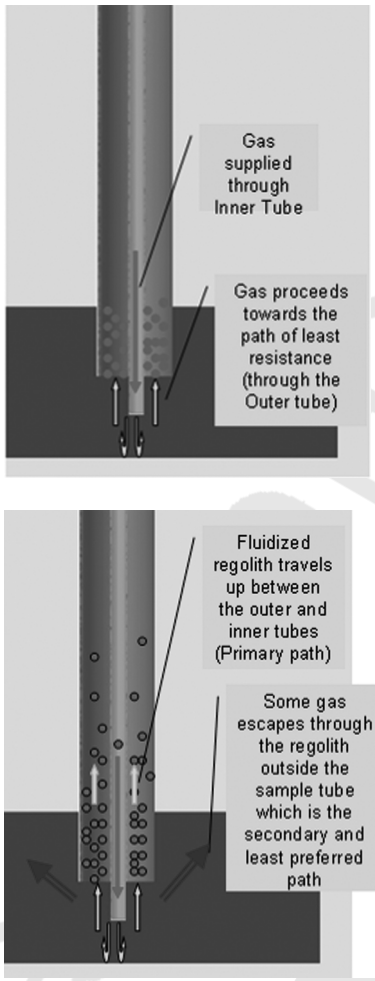

Figure 6.84 *(Continued)*

test, SCAD successfully drilled a total of 2.24 m through two solid rock layers, limestone (first 0.91 m) and Bishop tuff (last 1.32 m).

Although the SCAD drill was successful and mitigated the risk of going through ~~the 50 drill bit diameter limit,~~ laboratory test results showed a dramatic increase in drag friction at depths beyond 1 m due to auger and borehole wall friction. This increase in friction combined with high cuttings expansion would eventually lead to a limited depth and possible permanent jamming of the drill stem, causing the phenomenon called choking (Guerrero *et al.*, 2005).

Proof © WILEY-VCH

6.8.5
Pneumatic Drill and Excavation System

Any planetary landing system will have ~~small~~ residual portions of propellant typically budgeted for margin in lander operations in case it takes longer for the lander to reach the ground ~~than expected.~~ This propellant can be used to drive an internal combustion engine and in turn provide rotation and or percussion for the drill and the exhaust gases can be used to blow the chips out of the hole (Zacny *et al.*, ~~2002~~). This system is analogous to terrestrial high-power, hydraulic, and pneumatic drilling systems that use chemical fuel (i.e., gasoline) and fluids for cutting removal. Bi- or monopropellants (precombined fuel and oxidizer) have much higher energy storage density than, for example, batteries. For example, some monopropellants such as hydrazine have an energy density of more than 5000 W h kg^{-1}, that is, just 1 kg of fuel can provide 5000 W of power for 1 h. The internal combustion engine running on monopropellant has already been demonstrated by, for example, Firestar Engineering.

Figure 6.85 shows a concept of a pneumatic telescopic drill. There are a number of advantages of such a design. Since the drill does not require an auger, it can extend telescopically, making the drill system simpler, smaller, and lighter (there are no drill strings manipulation mechanisms, joints, and locking mechanisms, etc.). ~~In addition,~~ an auger accumulates cuttings at the rim of the hole, and once the drill is pulled out, these cuttings tend to fall back into the hole. With a pneumatic system, the cuttings will be ejected ~~to a~~ distance from the hole. However, to prevent dust from settling on the surface of the lander or rover, a deflection plate will have to be installed (shown just below the drill drive). Since cuttings removal will be achieved very effectively via gas flow, the rate of penetration (for the same power input) will be higher. Of course, having no auger will make the drilling process much more efficient, since an auger requires high torques to operate effectively. A pneumatic system can provide both rotation and drill thrust. In addition, the pneumatic drive can be designed to provide percussive motion in addition to rotation (this in turn

Figure 6.85 (a) Experimental set up inside vacuum chamber prior to lunar gravity flight. (b) The Honeybee Robotics team: from left to right, Kris Zacny, Phil Chu, and Jack Craft.

makes drilling more efficient). The greatest advantage of using a pneumatic drill is a faster penetration rate at reduced thrusts, which translates into less heat input into the formation. ~~In addition,~~ pneumatic ~~drills~~ have a more robust design and in turn are less susceptible to ~~fracture~~. Note also that, with an auger, a small deflection of the drill head off vertical can cause large torques, due to the rubbing of the auger against the side of the hole. The telescopic drill string, which will have a smaller diameter towards the top, will avoid this problem.

The pneumatic system can also be used as a stand-alone drilling system for excavating granular material. On Earth, one of the dredging methods (underwater excavation methods) that does not use moving parts is so-called "jet-lift dredging." Jet lift dredging uses the Venturi effect of a concentrated high-speed stream of water to draw adjacent material into a delivery pipe connected to a receiving container. The Venturi effect will work in an atmosphere or under water, but in [illegible] it will break down unless the system is sealed from vacuum. An alternative m[illegible]or a vacuum environment is a "modified jet-lift" that uses gas circulation inside a partially sealed system. The envisioned excavation tool, shown in Figure 6.86, consists of a central (or laterally placed) injector tube with a nozzle at the end and an outer collection tube for directing the return gas and mined regolith or soil into a storage container (Zacny *et al.*, 2008a). The excavation method relies on "injecting" gas into the top few centimeters of regolith and then guiding the gas as it escapes from regolith into the excavation tube. In essence, as the gas is injected into the regolith, it creates high-pressure gas pockets. As the gas escapes into the surrounding lower pressure atmosphere or vacuum, it exchanges its momentum with the regolith. This momentum exchange with the soil particles is instrumental to the excavation process. Note that some of this gas will no doubt escape into the surrounding vacuum or low-pressure atmosphere; however, the exact volume of gas lost will be a function of the permeability of regolith, the depth of the external tube buried inside the regolith and the depth of an injector nozzle inside the regolith. In tests conducted under low-pressure conditions, it was found that over 3000 g of granular material such as sand or lunar regolith simulant, JSC-1a, can be lifted using only 1 g of gas (Zacny *et al.*, 2007). This high excavation efficiency can be attributed to the fact that in the low-pressure atmosphere or vacuum, there is no back-pressure ~~against which the excavating gas has to work~~.

In September 2008, this pneumatic system was tested at lunar gravity. The tests were conducted at the NASA Johnson Space Center Reduced Gravity Office using a Zero Gravity Inc. airplane. The test fixture consisted of 10 individual cells with variable amount (50 or 100 g) of lunar regolith simulant JSC-1A (Figure 6.87). Preliminary data indicated that excavation efficiency is higher at lunar gravity; however, more tests will need to be performed to narrow down the data scatter. In these tests, it was also found that excavation efficiency at 1G was over 5500, that is, with only 0.018 g of nitrogen gas 100 g of soil were lifte[illegible]f the sampling tube.

There are numerous applications for such a pneumatic system. For example, a pneumatic excavation system can be the simplest system for returning regolith samples from a planet or a moon (Figure 6.88). The sample of soil can be acquired directly into an ascent vehicle (Zacny and Mungas, 2009). In the simplest scenario,

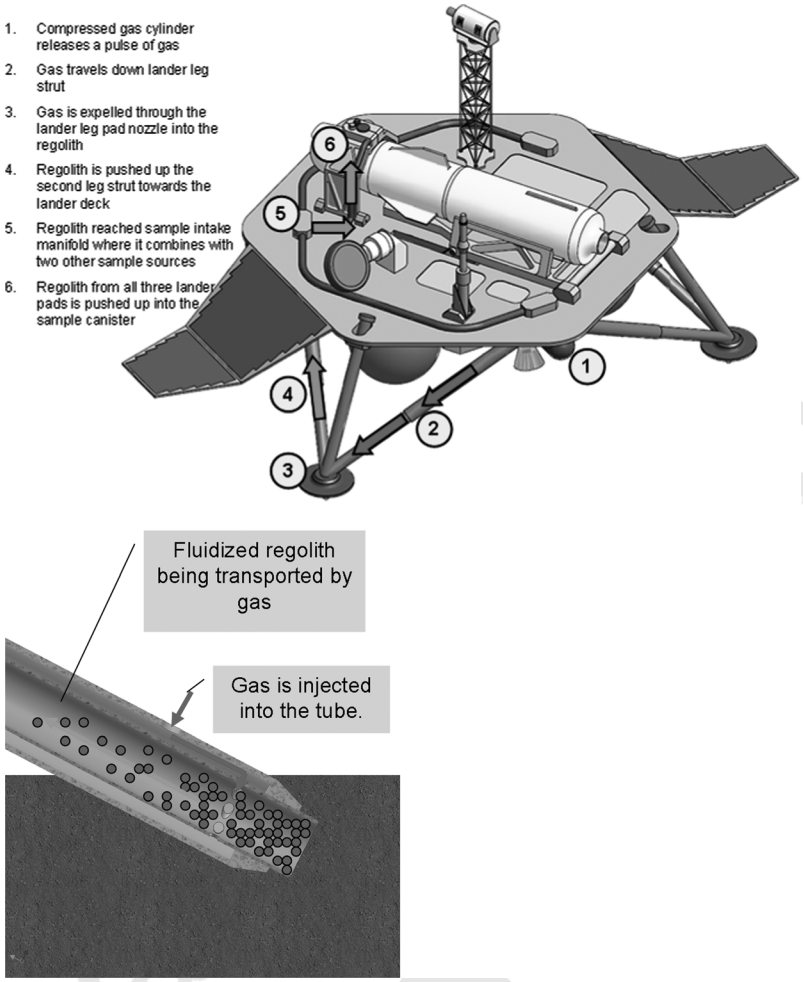

Figure 6.86 Pneumatic sample return: regolith pushed into the tubes embedded in three legs of the lander can be transferred into the ascent vehicle using a puff of gas (Zacny and Mungas, 2009).

three pneumatic tubes can be embedded inside the three legs of the lander. Upon landing, the legs will inevitably bury themselves into the regolith. The tubes within each of the legs will then fill up with regolith. With one puff of gas one can lift the soil enclosed within each tube to a sampling chamber onboard the ascent vehicle. At the same time, an additional chamber can be opened to acquire atmospheric gas and dust (in the case of Mars). The entire sample return will require (1) an actuator to open/close the sampling chamber and (2) a valve to open the gas cylinder. All mechanical systems for the proposed sampling acquisition system exist. Valves and gas canisters have been flown for the past 30 years and can be acquired in any size and from many

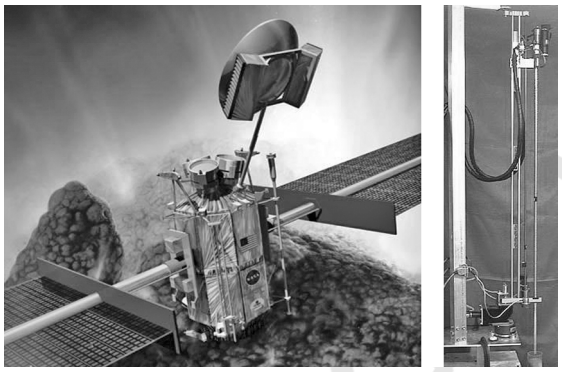

Figure 6.87 SATM system. (a) Artistic impression of SATM on Champollion spacecraft. Image: NASA. (b) Prototype system developed and tested by Honeybee Robotics.

vendors. There are many actuators that have been flight qualified and flown before (any system that has to be deployed ~~etc.~~ has a mechanical actuator).

The pneumatic sample acquisition does not necessarily have to be limited to a sample return mission. It can be used in place of a scoop to lift the regolith directly to an instrument. This is especially important if regolith contains water-ice. As was observed during the most recent Mars landed mission Phoenix, the water-ice in the regolith does not ~~stay~~ there for long but sublimes very quickly (or too fast before the sample can be delivered successfully to TEGA or MECA instruments). This will not be an issue with a pneumatic sample delivery. The pneumatic nozzle can be placed by a robotic arm into different parts of the regolith and "suck" regolith directly into the instrument. A few more puffs of gas can be used to clean the tube of any residue and in turn reduce cross-contamination between the two successive samples (in case of sampling in different locations). The pneumatic flow can also act as a natural size sorting mechanism. It was found by Zacny *et al.* 2008a that a pneumatic system can either be used to lift particles of certain sizes (i.e., initial sorting), or/and during the delivery the particles can be sorted based on how far they travel (i.e., the same principle as in a mass spectrometer). ~~Note that for sample~~ instruments such as an X-ray diffraction spectrometer ~~it is required that~~ particle sizes ~~are~~ smaller than 150 μm.

6.8.6
The Sample Acquisition and Transfer Mechanism (SATM) Drill

Developed by Honeybee Robotics Spacecraft Mechanisms Corporation (SMC), the Sample Acquisition and Transfer Mechanism (SATM) is a four-axis, highly instrumented drilling system that features sample preparation and handling ~~abilities~~ and also sample return containers. A prototype was developed and tested to validate the performance requirements for the NASA ST/4 Champollion mission (Figure 6.89a). The drill was designed to acquire subsurface samples from a comet at selectable

6.87a

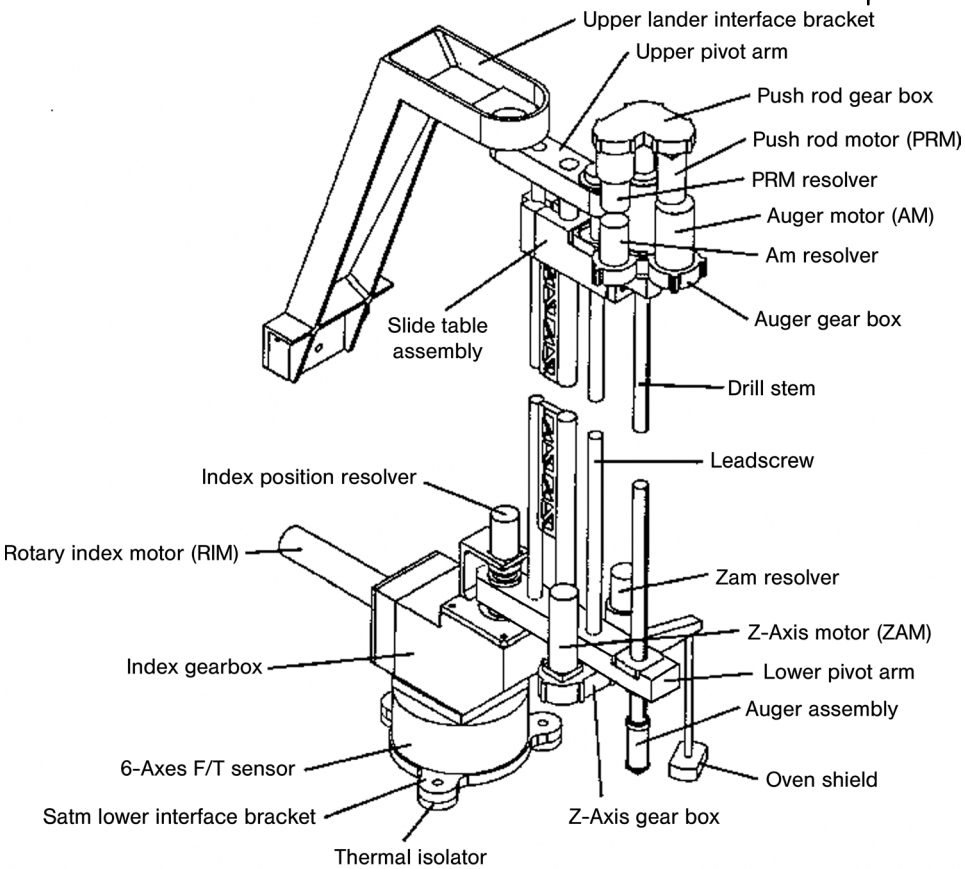

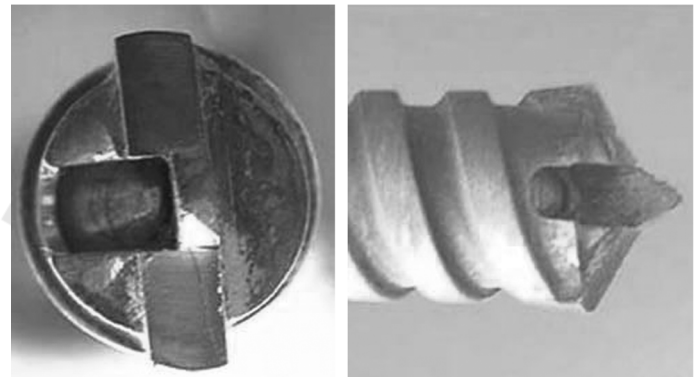

Figure 6.88 SATM system. (a) System components; (b) sample inlet feature. Courtesy Honeybee Robotics.

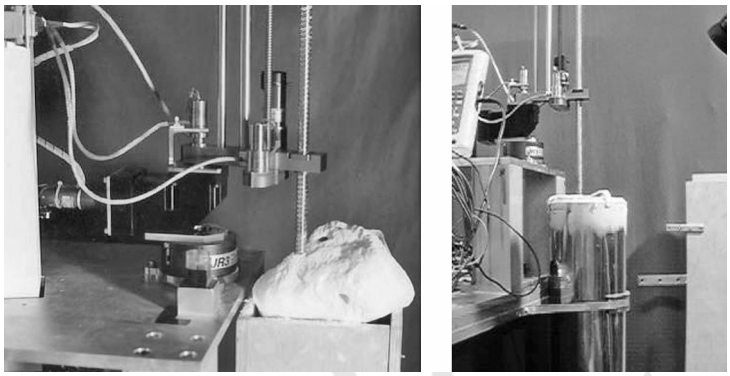

Figure 6.89 Prototype testing in laboratory with (a) limestone and (b) cryogenic regolith simulant. Courtesy Honeybee Robotics.

depths up to 1.2 m with little cross-contamination. The sample size is continuously adjustable between 0.1 and 1.0 cm^3 to cater for a variety of analytical instruments' requirements. The SATM creates a 13 mm diameter borehole. The mass of the prototype (Figure 6.89b) is 9 kg and its volume envelope is 60 × 60 × 138 cm. The TRL of the system is ~~currently~~ 4.

The "sniffer" drill concept 6.87b ct a sample at a selectable depth and heat it inside the sample chamber with a semipermeable ceramic heater until vapor is released. The vapor can then travel through a tube embedded in the non-rotating part of the drill to a mass spectrometer on the drill base. The SATM sample is always delivered as fine powder regardless of the material type sampled (i.e., consolidated or unconsolidated). Powder samples can be transported and transferred to instruments or vessels such as chemical analysis ovens, a microscope/IR spectrom 6.88 d a sample return container located at the base. To maintain the sample temperature to within 5 °C of its natural environment, the SATM drills at low speeds.

move this text

Major components of the SATM design are shown in Figure 6.90. The images on the right show the sample inlet feature of the drill tip. This door can be open at a desired depth to allow powder cuttings to flow into the sample chamber. The system also features a positive sample-eject mechanism within its sample chamber to ensure that samples are delivered to the *in situ* instruments. Samples can also be presented for analysis via a sapphire window located on the side of the drill stem. SATM can accommodate the bonding of a small cesium-137 source at the drill tip to permit density measurements. The drill tip can also be used as a tool to open and close the sample return container; eliminating the need for a separate actuator.

Specialized control algorithms were developed to allow autonomous adaptive operation in a low-gravity environment. The algorithms could also be adjusted for off-normal drill approach angles to minimize bit wandering. Laboratory tests were conducted in limestone, basalt, and a cryogenic regolith simulant (Figure 6.91). A total energy of 25 W h is required to sample limestone (40 MPa UCS) at a rate of 0.88 cm min^{-1} with an auger speed of 194 rpm, a WOB of 55.6 N, and a drilling torque of 325 mN m. 6.89

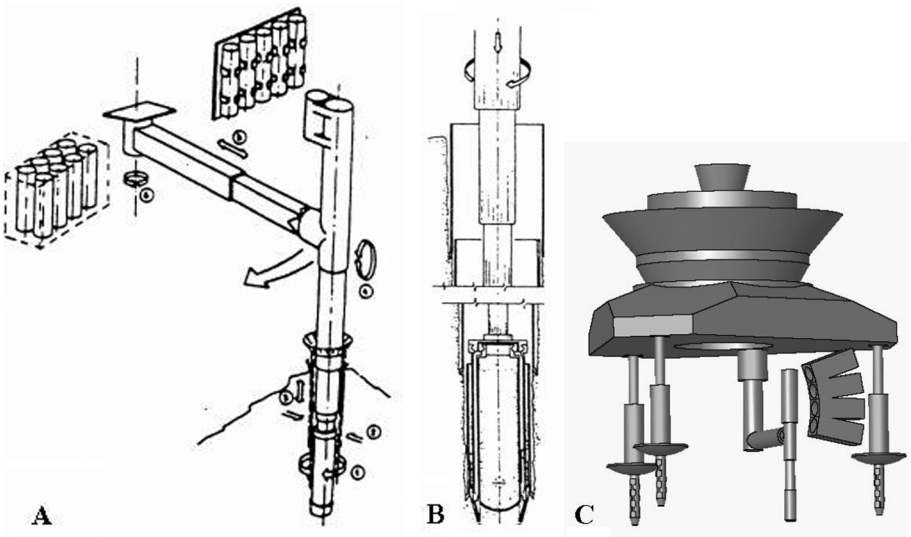

Figure 6.90 SAS-3m for CNSR/Comet Nucleus Sample Return. (a) Concept of SAS-3m; (b) detail of a telescopic corer drill; (c) schematics of installation on lander. Courtesy ESA, Galileo Avionica, and EADS/ASTRIUM.

6.8.7
CNSR Sample Acquisition System for 3 m (SAS-3m) ~~(1988–1990)~~

The ESA began preparing for comet and planet sampling in the mid-1980s, intending initially ~~a~~ comet nucleus sample return (CNSR) mission. In the CNSR scenario ~~of~~ the study performed by Galileo Avionica (Milan) and EADS/ASTRIUM for ESA (Atzei,

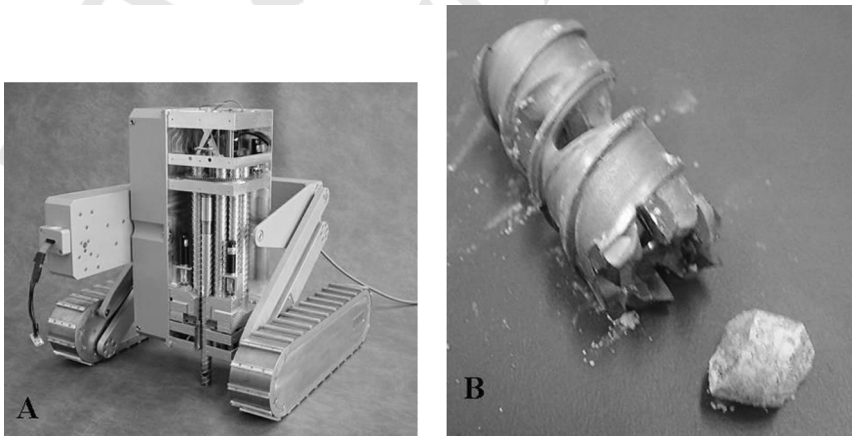

Figure 6.91 Rover-based deep drill "MicroRoSA." (a) Drill-rig on rover; (b) detail of corer. Courtesy ESA, VTT and HUT.

Hechler and Coste, 1989), the sample acquisition system (SAS) had to perform the following tasks:

- Anchoring the spacecraft ~~on~~ the comet (to counteract the drilling and other force/torque).
- Sampling of materials, to acquire:
  -a surface sample, that is, 1–5 kg
  -a core sample, down to a depth of 3 m
  -a volatile sample at the bottom (10–100 g).
- Manipulation and handling samples and tools: the core sample, of diameter ~~10 cm,~~ had to be cut into segments of 0.5 m long for storage in the Earth return container.

The requirement for sampling ~~down to 3 m led to~~ some complexity; a single corer was impractical, and a corer device 6.90a and b pic tube was selected. The total mass of the samples w 6.90c than 15 kg, and their volume about 25 L.

Several system studies were performed. Figure 6.92a and b depict the concept of the SAS-3m telescopic drill developed by Galileo Avionica, Milan (formerly Tecnospazio). Figure 6.92c shows the schematics of accommodation of the telescopic corer drill on a lander from a study by Astrium (formerly Matra Toulouse); coring elements are brought successively deeper by a telescopic tube carried by a manipulator arm. The companies NGI in Norway and Diamant Boart in Belgium performed parallel corer studies. ~~Finally,~~ the CNSR SAS-3m remained at the stage of a conceptual study (Eiden and Coste, 1991).

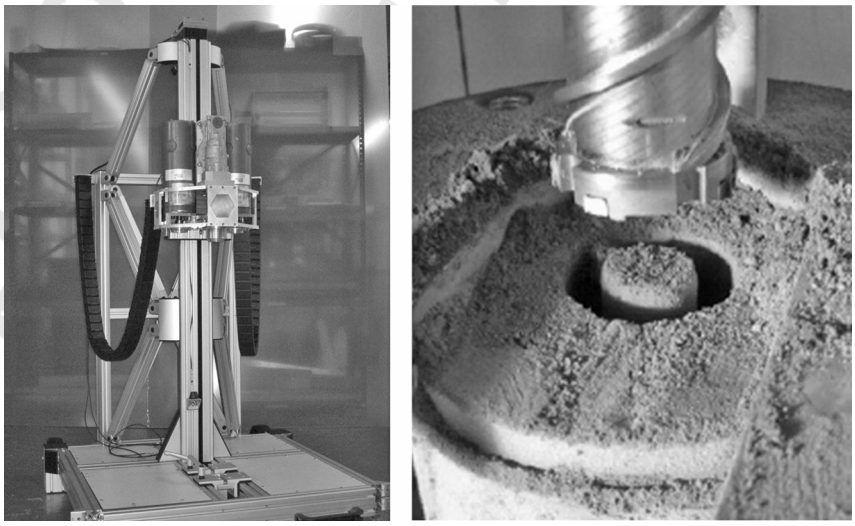

Figure 6.92 CRUX drill. (a) Prototype shown without drill string; (b) coring tests in lunar simulant at −85 °C and 4 Torr. Courtesy Honeybee Robotics.

page proof

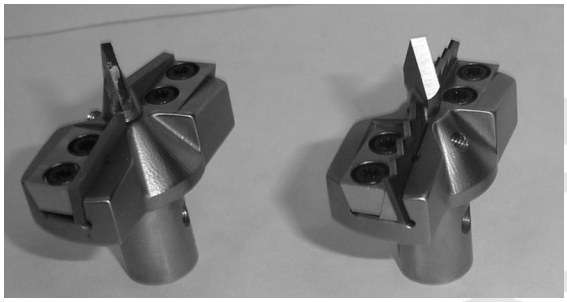

Figure 6.93 CRUX drilling bits including (a) full-faced tungsten carbide bit with $+5^\circ$ rake angle and (b) PCD bit with -15° rake angle. Courtesy Honeybee Robotics.

6.8.8
Rover-Based Deep Drill MicroRoSA

MicroRoSA is a compact and mobile automated drilling device, able to drill rock and to sample down to 2 m (Ylikorpi, Visentin and Suomela, 2001; Anttila, 2005). The drilling and sampling subsystem is enveloped in a box, 110 × 110 × 350 mm, of mass 5 kg. The extendable drill string is assembled from stems – 11 are stored in a carousel. The stem assembly is based on the truncated tetrahedron principle: three male faces coincide with three female faces, the fourth one being held by magnets; the drill string may transmit 6.91b mpression forces and torques, while also resisting moderate traction. The rock-sampling tool is a corer–drill bit with a core breaker ring; it acquires a core ~~of diameter 9 × 20 mm,~~ within a drill bit of diameter 17 mm, as in Figure 6.93b. A mobile drilling platform carries the drill – that is, a small tracked roving vehicle of dimensions 110 × 400 × 400 mm and with a mass of 12 kg (Figure 6.93a). It was provided by Helsinki University of Technology (HUT) in Finland. VTT (Finland) designed the MicroRoSA drill within an ESA study led by its Automati 6.91a botics Section. VTT was a member of the former SSA/DT team. MicroRoSA provided an initial baseline drill in the precursor ESA studies of a Mars Exobiology mission: its samples would feed the experiment package "Pasteur", when looking for signs of extinct or extant life on Mars.

6.8.9
Construction and Resource Utilization Explorer Drill

6.92a

Developed by Honeybee Robotics SMC for NASA, the Construction and Resource Utilization Explorer (CRUX) drill was developed as a test bed (Figure 6.94a) to allow the investigation of different penetration methods, different bit geometries, and different control algorithms in a variety of target surfaces and environmental conditions. The primary development was aimed at analyzing subsurface materials for *in situ* resource utilization (ISRU) prospecting, in particular to characterize the expected water-ice. Icy regolith is expected on the lunar surface with water content up to 10 wt%. Maintaining a low thermal impact on the sampled material and borehole is ~~therefore~~ critical.

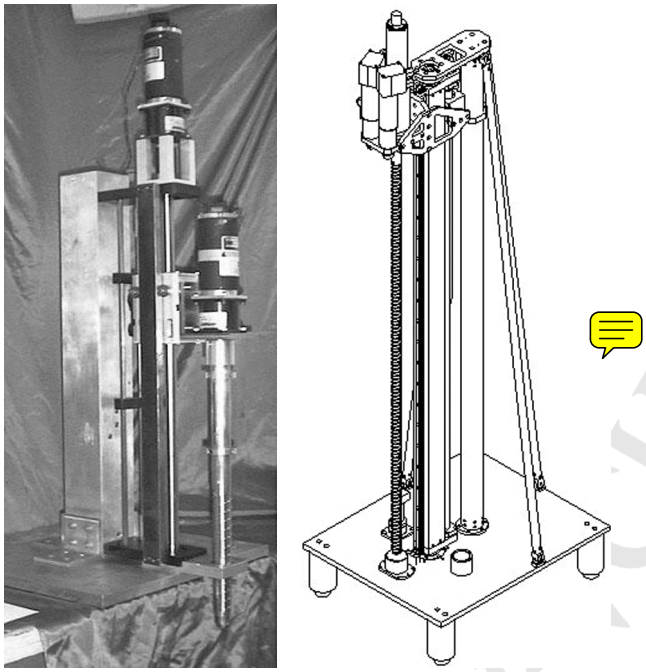

Figure 6.94 SCSS system prototype. (a) Breadboard tested during phase 1 of the development; (b) CAD model of full system developed during phase 2. Courtesy Honeybee Robotics.

The CRUX drill ~~is~~ designed to allow pure rotary, rotary–percussive, or percussive drilling to enable efficient drilling to be performed in a variety of target materials such as regolith, rock, or ice. The attainable sampling depth is at least 2 m. System capabilities include:

- maximum torque 45 N m
- rotational speed 200 rpm
- maximum WOB 1000 N
- percussive frequency 25 Hz (when turned on).

6.93

Both full-face and coring bits were developed for the CRUX drill. The full-face bits included tungsten carbide and polycrystalline diamond (PCD) bits (Figure 6.95). The rotary coring bit (not shown) had PCD cutters and a 38 mm OD. It created a core that was 25 mm in diameter. ~~No core break-off or retention mechanism was developed for the CRUX drill, making the overall drilling system incomplete.~~

Testing was carried out with lunar simulant (JSC-1 and FJS-1) refrigerated to −85 °C and at a pressure of 4 Torr ~~so no liquid water could exist. A study of pure rotary drilling was conducted on the various bits~~. Cores created by the coring bit were manually broken off and retrieved for analysis. Data logged during each test include specific energy, power, bit temperature, and core temperature, in addition to drilling telemetry [WOB, rate of penetration (ROP), etc.]. A study of water loss due to the

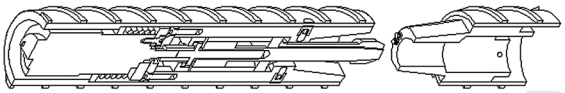

Figure 6.95 SCSS dust-tolerant drill string connection with two spring-loaded electrical contacts. Courtesy Honeybee Robotics.

sampling process showed that the core lost ~10 ~~wt~~% of its initial water whereas the augered cuttings lost ~20 ~~wt~~%. Cuttings were also lifted out of the borehole via the ~~sublimation of~~ ice. Those cuttings had lost 90% of their initial water. The development and testing of the CRUX drill were cut short due to funding cut-backs. The system is currently being revamped for integration into ~~a custom~~ environmental drilling chamber to allow for high-fidelity drilling tests.

6.8.10
Subsurface Corer Sampling System

Developed by Honeybee Robotics SMC ~~for NASA via SBIR funding,~~ the Subsurface Corer S[illegible] System (SCSS) is a multi-depth sample acquisition and handling tool that can be used for the exploration of planetary bodies, c[illegible] asteroids. It is a low-power, rotary coring drill capable of penetrating and sampling soft ~~or~~ hard rocks at cryogenic or elevated temperatures up to a depth of 1 m. The system (Figure 6.96b) has five axes including the auger axis, break-off axis, pushrod axis, *z*-axis, and rotate axis. The initially developed system (Figure 6.96a) had a core break-off and capture mechanism that could sample up to 50 cm^3 of consolidated (<40 MPa UCS) or unconsolidated material. The core break-off and retention mechanism was redesigned and currently an 8 mm diameter and 4 cm long core can be captured at any desired depth. The SCSS can provide up to 150 lb of WOB and has a maximum auger speed of 96 rpm. The mass [illegible] ototype system was 122 lb and the volumetric envelope was 56 × 46 × 173 cm. It should be noted that mass was not optimized for a flight-like design. The TRL of the system is currently 4.

The SCSS system (Figure 6.96b) consists of two drill strings coupled via a custom dust-tolerant connection (Figure 6.97). The connection is inherently dust tolerant due to its tapered design and also incorporates electrical connections to allow operation of the pushrod and break-off motors located [illegible] ead drill string. The pushrod is used to eject positively core samples for operation in a micro-gravitational environment. It can also double as a tool to open and manipulate *in situ* instruments and sample return containers during sample hand-off. A passive brush station is utilized f[illegible] internal (and external) chamber cleaning.

The initial prototype incorporated a core break-off and retention mechanism involving four shearing tips that radially cut the base of the core (Figure 6.98a). The drill approaches the rock with the shearing tips fully closed. The shearing tips are then retracted and the drill enters the rock. At a certain depth, the drill center is retracted, creating the sample cavity, and drilling continues. Once the sample cavity is filled with the target sample, extension is stopped and the shearing tips are extended; cutting through the core and completely closing while the auger is still rotating. The

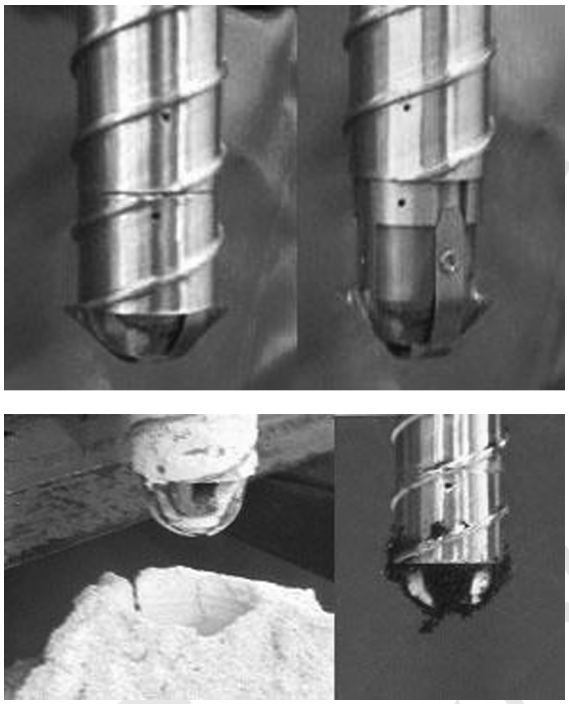

Figure 6.96 SCSS prototype. (a) Large-volume sampling head capable of retaining 50 cm^3 of material shown with removable fluted housing; (b) sampling loose chalk and soil regolith in a laboratory environment. Courtesy Honeybee Robotics.

6.96b

sample is contained and can be removed from the hole (Figure 6.98b). This design was tested successfully in materials with a UCS of up to 40 MPa in a laboratory environment.

As designed, the shearing tips rely on their flexibility and range of motion to cut through the core completely and close. In order for these shearing tips to cut through a harder rock (>40 MPa UCS), a harder material is required to reduce wear. By increasing the hardness of these tips, their stiffness is also increased; reducing their flexibility and thus reducing their useable elastic deflection. It was concluded that the shearing tip could not be designed to cut through a harder rock type completely and fully close. The SCSS ultimately used pivoting cutters, driven inwards by a set of cams, to accomplish the same purpose (Figure 6.99). It has a central, retractable, drill bit that allows a core to be captured at any desired depth. The drill bit, center bit, and core break-off cams all utilize carbide inserts as the cutting medium.

6.97

The SCSS system was tested in a laboratory environment in both limestone (UCS = 40 MPa) and basalt (UCS = 102 MPa). Testing in limestone showed a power consumption of between 40 and 50 W with an average penetration rate of 6.8 mm min^{-1} and a total drilling depth of 0.6 m. Two core samples were acquired during limestone tests at depths of 0.4 and 0.5 m and drilling operations lasted

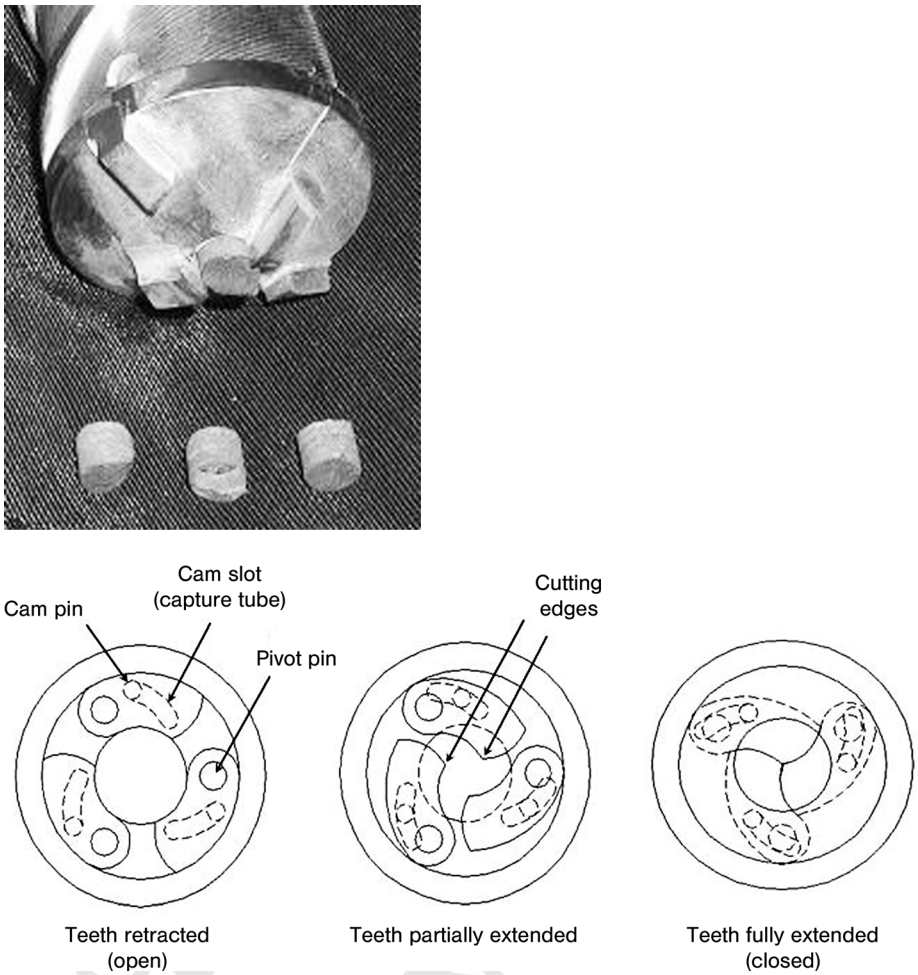

Figure 6.97 SCSS: left) drill bit with core samples; right) diagram showing how teeth close on the bottom of the core; cutting it off and capturing it in the tube. (Courtesy Honeybee Robotics).

approximately 90 min. Testing in basalt showed a power consumption of between 30 and 50 W with an average penetration rate of 3.6 mm min^{-1} and a total drilling depth of 5.49 cm. During coring, the power consumption increased to 60–70 Watts. A basalt core was captured during testing; however, the core was broken at its base due to forces imparted during drilling and not by the core break-off mechanism. A potential reason for this includes the packing of cuttings between the core and the core tube, which ~~causes~~ the core to shear due to twist during drilling operations.

Potential system improvements include:

- Optimized bit design and materials selection, since the carbide bits developed large wear flats when drilling into the basalt.

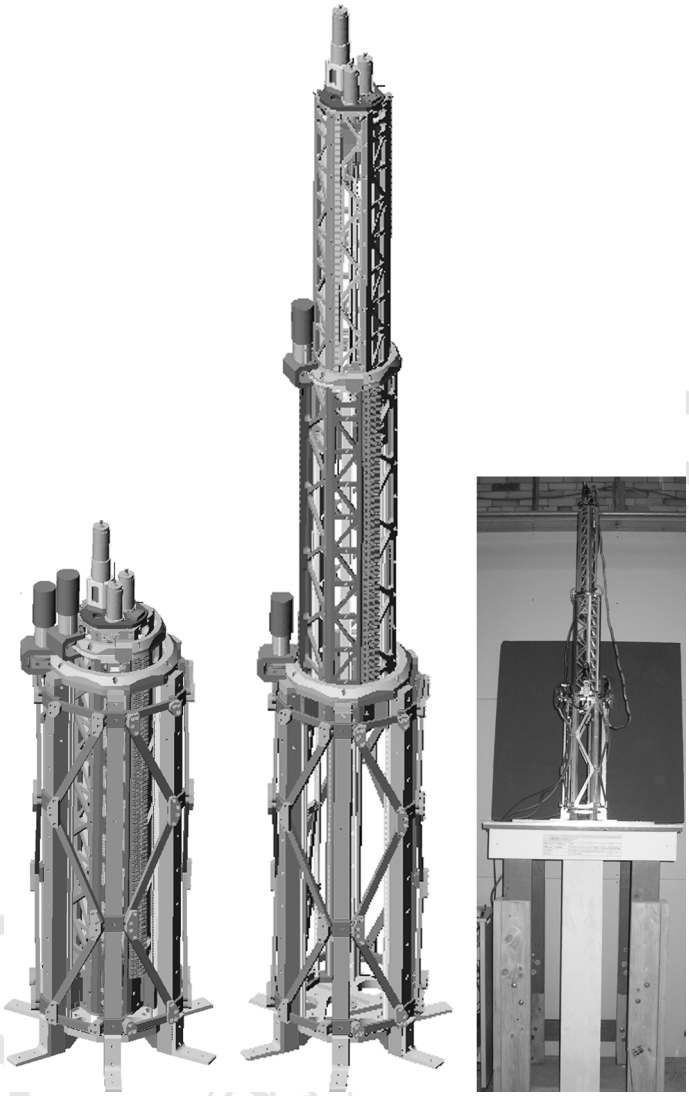

Figure 6.98 STSS prototype, shown (a) in the stowed position, (b) in the fully extended position, and (c) during testing in limestone in a laboratory environment. Courtesy Honeybee Robotics.

- Break-off tube modifications to increase clearance between the core and the tube walls, and also the integration of channels to allow cuttings to flow out of the break-off tube.

~~Future modifications and additions to the SCSS system include drill bit design, bit change-out mechanism, WOB sensor, vibration sensor, algorithm optimization, deployment system, and fault sensing and recovery algorithms.~~

Figure 6.99 High-temperature Venus drill inside a test oven. Photograph courtesy J. Ji, Honeybee Robotics.

6.8.11
Subsurface Telescoping Sampling System

Developed by Honeybee Robotics, the Subsurface Telescoping Sampling System (STSS) is a deployable that can stow itself into a small enough package so as to fit on an MER-class rover. The two-stage telescoping drill structure has a segmented auger with its individual drill strings stored within the inner volume of the assembly (Figure 6.100). This configuration would directly benefit an interplanetary mission by easing volume constraints on the spacecraft while continuing to meet deep drilling requirements. The final stowed-to-deployed length ratio is 48%, the stowed-to-maximum drilling depth ratio is 60%, and the maximum drilling depth-to-deployed ratio is 80%.

The main parts of the STSS assembly are two telescoping stages supported by the ground stage, the drill head, and three interconnecting drill strings. The upper assembly is called the second stage and has the capability of translating vertically inside the middle assembly, called the first stage. The drill head translates vertically inside the first stage and houses the two drill motors that provide the mechanical power for drilling operations. Two of the drill strings are stowed at the base of the drilling tower, in the existing clearance between the first stage and the ground stage; while the third

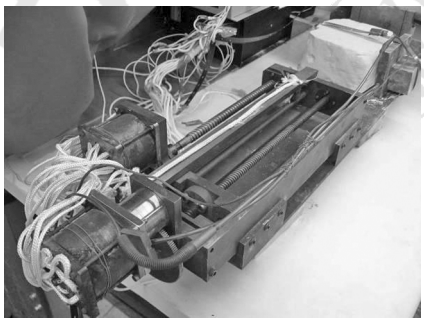

Figure 6.100 The high-temperature Venus drill after a test at 500 °C. Photograph courtesy N. Kumar, Honeybee Robotics.

Page proof WILEY-VCH

Table 6.16 STSS phase cycle time from laboratory testing.

Operational phase	Duration
1: Stage 1 extension	7 min 35 s
2: Mid drill connection	7 min 08 s
3: End drill connection	3 min 43 s
4: Stage 1 drilling	22 min 00 s
5: Stage 2 drilling	35 min 00 s
6: Drill head drilling	41 min 00 s
7: Drill head retraction	2 min 36 s
8: Stage 2 retraction	7 min 00 s
9: Stage 1 retraction	7 min 15 s

drill string is pre-attached to the drill head. This configuration utilizes efficiently the volume provided and yields the maximum packing coefficient for the stowed system.

The drilling operation has two distinct phases: connection of the drill strings followed by drilling. By design, the drill string connection mechanism forces the connection of all stored drill strings prior to drilling operations. The first and second stages translate vertically, connecting the drill strings as they go. Once the full auger is assembled, drilling begins. Although no sample collection mechanisms were employed in this system, methods such as those employed on previous Honeybee Robotics drills could easily be used.

Limited testing was done in a laboratory environment, mainly consisting of timed operations to characterize the cycle time (see Table 6.16).

Drilling operations were carried out in limestone at an auger rotational speed of 180 rpm and a rate of penetration between 0.3 and 1.0 cm min^{-1}.

6.8.12 Venus Drill

Off-the-shelf motors and actuators are not designed to survive in the harsh Venus environment with temperatures reaching 460 °C and pressures around 90 bar. Under these conditions the main atmospheric continuant, carbon dioxide gas, is supercritical.

The benefit of high-temperature motors is that they can drive a sampling drill or a grinder, robotic arm, or a deployment stage on the surface of Venus and thus allow for sample acquisition, transfer and analysis.

Note that high temperature is a much problematic issue to deal with than high pressure. High-temperature application either requires components to withstand this temperature or necessitates some kind of an active (or passive, depending on the time of exposure) cooling system. Active cooling system is very expensive and many proposed sample return missions from, for example, asteroids, which had to keep samples cool, could not fit within the mission cost cap. On the other hand, ~~high pressure requires a~~ pressure vessel, which is a passive system (does not require any power to work).

For the past few years, Honeybee Robotics, funded by NASA, has been developing two potential high-temperature motors: the switch reluctance motor and DC

Table 6.17 Motor characteristics comparison of existing Maxon RE-25 with current Honeybee Robotics high-temperature switch reluctance motor prototype.

Characteristics	Units	Maxon, RE-25: range at 25 °C	SRM, prototype: range at 460 °C
Applied voltage	V	4.5–48	20–48
Maximum speed	rpm	5500	7500
No-load speed	rpm	4790–5500	7000–7500
No-load current	mA	7–80	1000–1200
Stall torque	mN m	119–144	200–250

brushless motor. The motors essentially required selection of components that can withstand these high temperatures and at the same time that, when put together, can actually work. In addition, the components have to maintain certain electrical characteristics (e.g., relatively electrical low resistance even at high temperature).

The prototype SRM was tested and the motor parameters compared well with the Maxon RE-25 motor, as shown in Table 6.17. In particular, the stall torque for Maxon RE25 motor is around 130 mN m, which is almost 50% lower than that of the high-temperature SRM, at around 230 mN m. The Maxon RE-25 motor has been used to actuate various prototype and flight system drills, robotic arms, and other mechanism actuators by NASA and Honeybee Robotics. A flight version of the Maxon RE-25 is the largest motor used on the Mars Exploration Rover mission.

A drilling system actuated by two switch reluctance motors has been developed and was successfully tested under Venus conditions (temperature and CO_2 atmosphere) in a high-temperature chamber for 20 h (Figures ~~6.101 and 6.102~~). The current drill volume is $7 \times 4.5 \times 19$ in and the drill has a stroke of 10 in, allowing penetration to a depth of 10 in.

6.99 and 6.100

6.9 Ten-Meter Class Drills

6.9.1 Mars Astrobiology Research and Technology Experiment (MARTE)

In August 2005, a team consisting of members from NASA Ames Research Center, Honeybee Robotics, and Centro de Astrobiologia assembled the MARTE system near Rio Tinto, Spain, for a 6 week experiment (Paulsen *et al.*, 2006). The MARTE system design was led by NASA Ames and is a simulated lander that ~~includes~~ a 10 m class drill designed and developed by Honeybee Robotics. ~~This drill, shown in Figure 6.103,~~ is a rotary coring drill that has built-in functionality for autonomous core recovery and core delivery. To penetrate beyond depths of 1 m, the system would automatically add drill tubes to extend the length of the drill string.

page proof WILEY-VCH

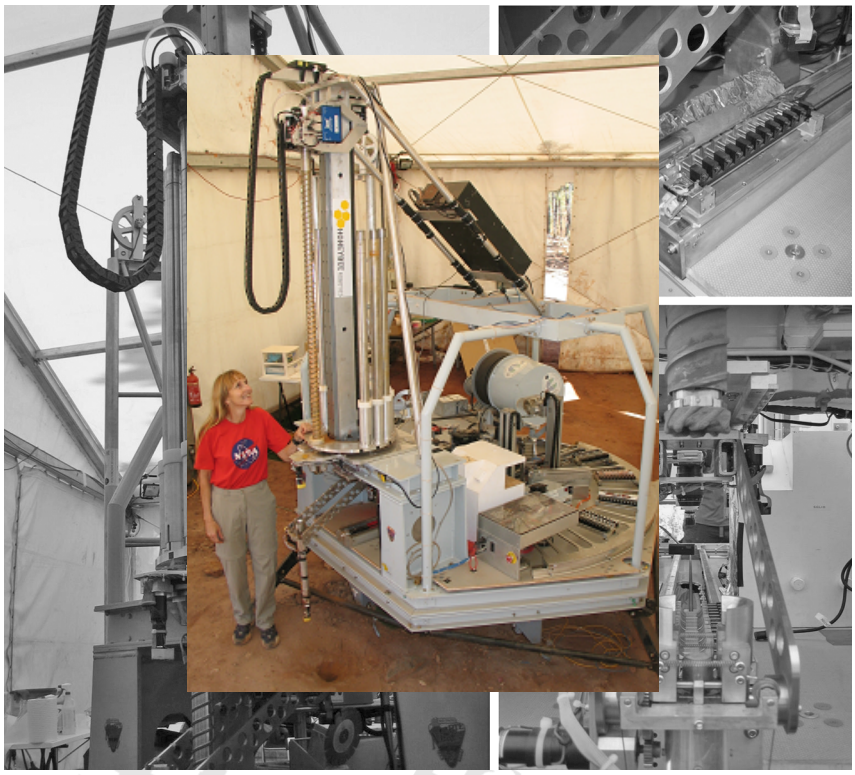

Figure 6.101 (a) Drill and (b) core handoff system on the MARTE simulated lander. Courtesy Honeybee Robotics and NASA Ames Research Center.

The drill for the MARTE system operates with less than 150 W of power (about what is used to power a single light bulb). It drills a hole with a diameter of roughly 48 mm (1.89 in) and can extract 200 mm (7.87 in) long cores. To enable the drill to reach 10 m, there are 10 drill tubes that are added in series to the leading drill string. These drill tubes are indexed on a carousel which rotates the drill tubes under the drill axis when additional length is needed or if the drill string needs to be disassembled.

Along with the hardware, Honeybee Robotics also developed the drill control software for the MARTE drill. This included some reactive-behavior-type control schemes to control WOB and minimize stalling of the drill axis. It also included controls for breaking, capturing, and delivering cores. In nominal drilling operations, there are 11 different control states in which the system can be operating. The nominal drilling operation and control scheme is illustrated in the schematic shown in Figure 6.104.

Under nominal conditions, the drill begins after receiving a high-level "drill" command. It then proceeds to locate the bottom of the hole (or the surface, if there is

6.102

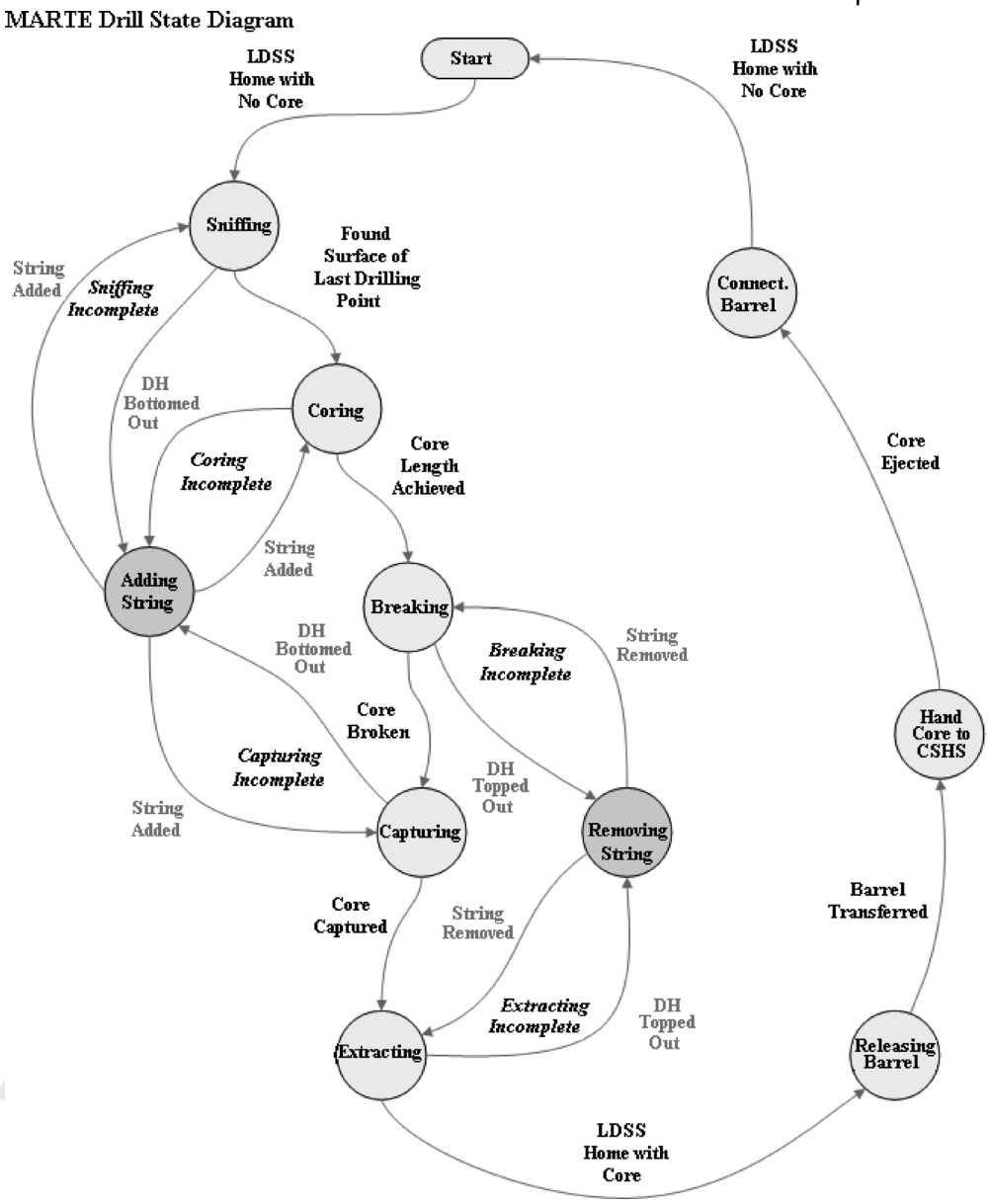

Figure 6.102 Schematic of MARTE operational states. Courtesy Honeybee Robotics.

no hole) through a mid-level "sniff" routine. If at some point during this routine, the drill head reaches the bottom of the drill column without detecting the bottom of the hole, an additional drill string is added, and the "sniff" routine continues. Once the bottom of the hole is detected, the drill begins "coring" or the physical process of

Figure 6.103 The DAME drill during a 2006 field test on Devon Island, Arctic. Courtesy Honeybee Robotics.

drilling. Again, drill strings are added as needed until the target drill depth is reached. Upon completion of the "coring" routine, the system begins "breaking" the core by ejecting the core barrel from the lead drill string until it can be cocked to break the core. Since the drill head must simultaneously retract during this process, it may be necessary to "remove" a drill string. After completing the "breaking" routine, the drill proceeds to capture the core by simultaneously retracting the core barrel while penetrating with the drill head. During this process, it may be necessary to add a drill string. Once captured, the drill extracts the new core from the hole. Drill strings are removed as necessary until the core is out of the ground and in position to be delivered to the core hand-off system. At this point, the core barrel is clamped into place and released by the drill system. The core is then ejected into a core sample handling system and the core barrel is reattached to the system. For this particular system, the reattachment of the core barrel was not automated.

Although the MARTE drill uses flutes to transport cuttings away from the drill bit, it only requires flutes on the lead drill string. This is because the lead drill string houses a cuttings volume that collects cuttings for transportation from the borehole to the surface. The purpose was to reduce the power required to drill to large depths. Studies have shown that power can increase linearly due to frictional effects between fluting and a borehole wall. Over a given depth, the amount of power required to overcome the frictional effects could prevent the drill from actually drilling. Instead, the lead drill string has a portion with slots cut above the fluting to allow cuttings to flow from the borehole, up the fluting, and into the cuttings chamber. This chamber was cleaned manually during every core extraction operation. However, conceptual mechanisms have been considered that allow the process to be automated.

Page Proof WILEY-VCH

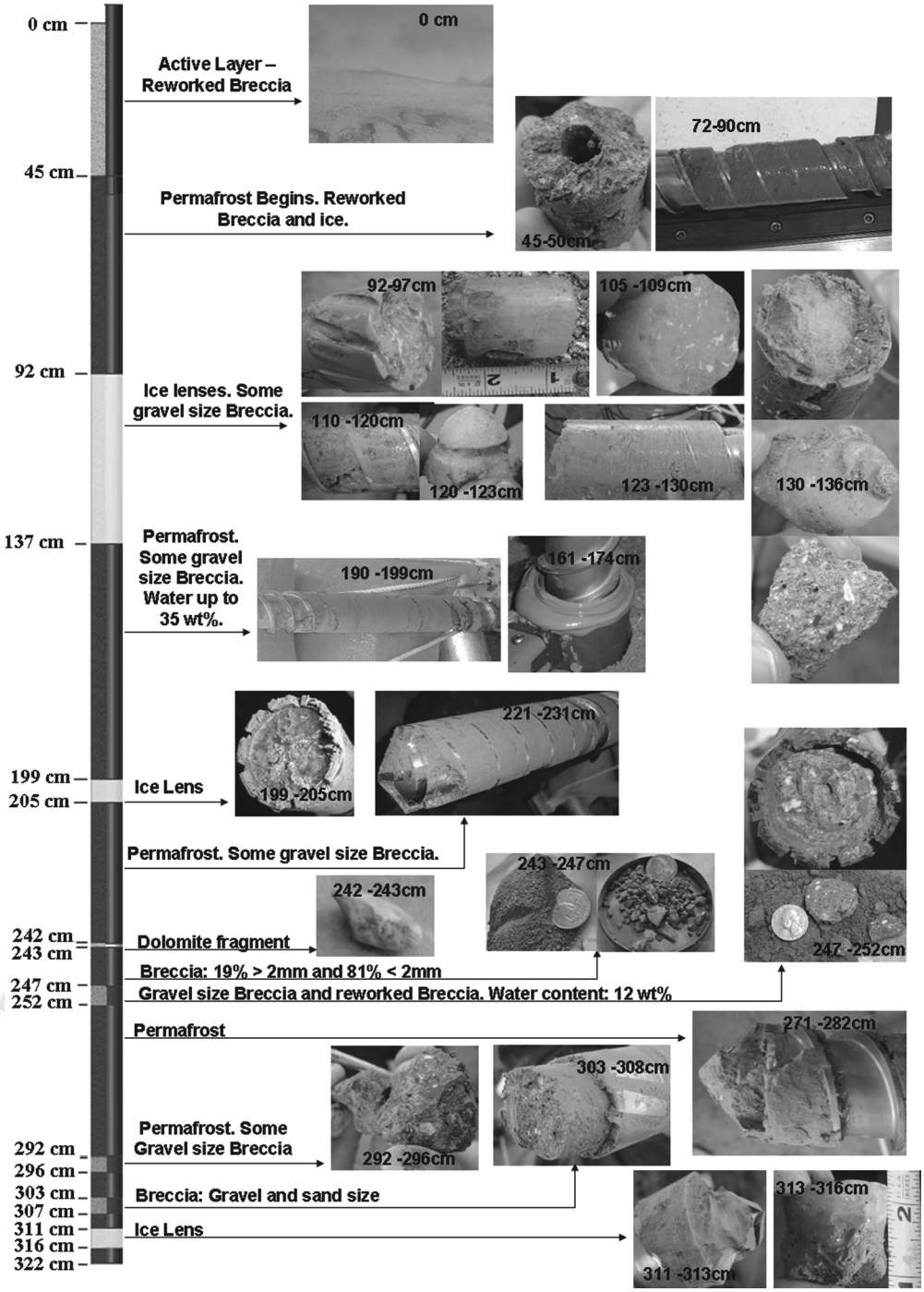

Figure 6.104 Subsurface stratigraphy inferred from coring and drilling using the DAME drill during the 2006 test in the Haughton Crater on Devon Island, Arctic. Courtesy Honeybee Robotics. (Please find a color version of this figure on the color plates).

6.9.2 Drilling Automation for Mars Exploration (DAME)

The Drilling Automation for Mars Exploration (DAME) project, like the MARTE project, was led by NASA Ames Research Center (Glass *et al.*, 2008). Honeybee Robotics designed and built the DAME drill as a sister drill to the MARTE 6.103 e Georgia Institute of Technology (Georgia Tech) provided additional sensor support in the form of laser vibrometers. This drill, shown in Figure 6.105, has similar mechanical dimensions to and consumes a similar amount of power as its sister drill, but is much more mobile. The DAME drill has endured four trips to the Canadian High Arctic to field test in the Haughton Crater (a Mars analog). It has also endured a number of trips across the United States that enabled testing at Honeybee Robotics in New York City, NASA Ames near San Jose, CA, NASA JPL in Pasadena, CA, and Georgia Tech in Atlanta, GA. To enable this mobility, many of the automation components present in the MARTE drill were stripped from the DAME drill. For

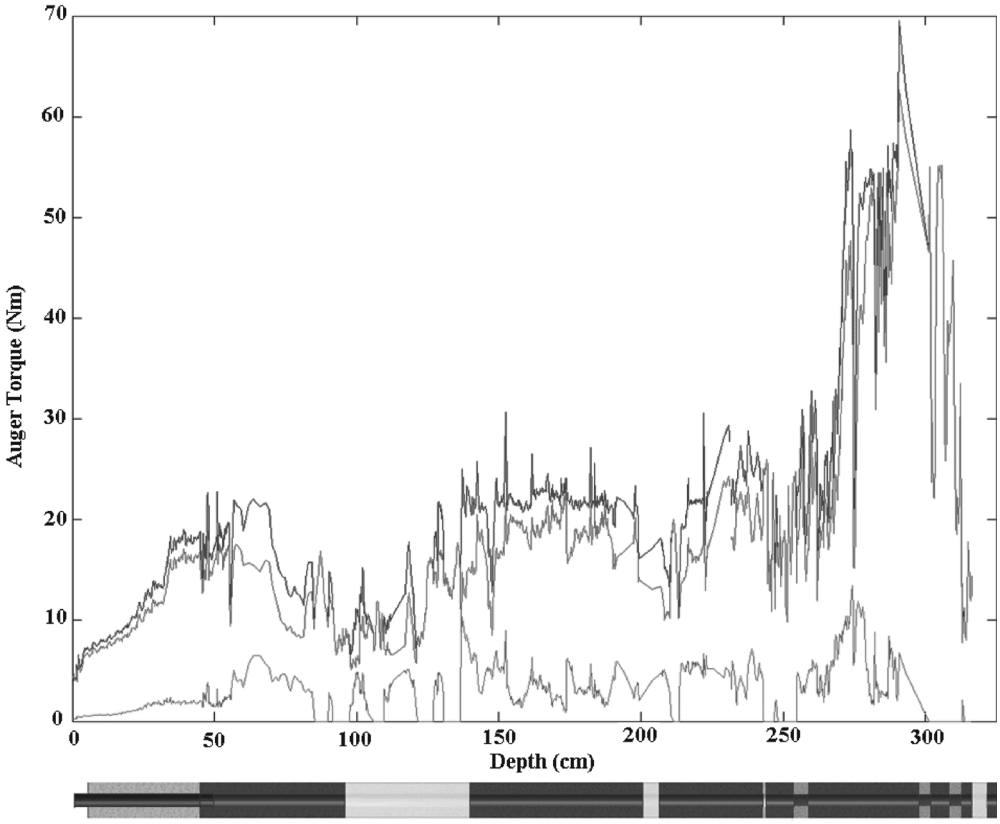

Figure 6.105 The DAME drill telemetry. Total torque, auger torque, and bit torque versus depth. (Please find a color version of this figure on the color plates).

instance, the DAME drill does not autonomously capture and deliver cores, nor does it autonomously assemble and disassemble drill strings. However, the DAME drill is much "smarter" when it comes to drilling. This drill system utilizes a number of below- and above-ground sensors along with an intelligent control method that enables the system autonomously to detect and recover from drilling problem situations. To date, the DAME team has enabled the drill autonomously to identify and recover from six such challenges.

While drilling, the ROP was controlled to prevent the drill from exceeding a maximum WOB and to prevent the drill from operating with more than 100 W of power. In some cases, controlling the ROP did not help reduce the operating power to less than 100 W. If this were the case, then depending on how the bit torque compared with the auger torque along with the vibration frequency of the drill and other factors, one of two problems (designated "auger binding" and "auger choking") would be autonomously detected by the drill controller and a fault recovery procedure would ensue. Other identified problems that are detectable (and recoverable) by the DAME system include "bit jamming" (identified by a high bit torque or stalled auger axis), "bit inclusion" (identified by oscillating WOB and bit torque), "drilling hard material" (identified by high WOB, low ROP, and low bit torque), and "auger corkscrewing" (identified by high negative WOB). During the 2006 field test, the DAME team penetrated to a depth of 3.2 m. At one point, during this test, the team showed their faith in the control design by issuing a "drill" command and promptly abandoning the drill to allow it to operate without human supervision. Upon returning to the drill, the team discovered that the system had autonomously detected the "hard material" fault and recovered as designed. (In this case, the recovery procedure was to run the drill head to the top of the drill column, while maintaining a slow auger rotation to prevent the drill string from freezing in the ground, and wait for the drill team to switch to a more appropriate bit.)

In addition to providing a hole or a core for chemistry, material property, and other sensors, the drill also provides useful information on the material that is being drilled. During the 2006 field test at Haughton Crater, cuttings and cores (that 6.104 periodically collected) were examined to determine what material was being drilled. 6.105 From these data, a local stratigraphy was inferred (shown in Figure 6.106 and Table 6.18). Since different materials tend to drill differently, drill telemetry can be used to distinguish various materials (shown in Figure 6.107, and Table 6.19). This means that a library could be built for any drill (if it were tested in the proper manner and across a broad range of materials) correlating drill telemetry with material type and composition. Once built, the library could be referenced while drilling to speculate on what is being drilled. This information can possibly be used to determine when to collect a core or when to send another instrument down the hole.

6.106 Although the DAME drill was built primarily to help the evolution of intelligent drill control software, there were still some limited efforts applied to drill bit design. A number of the drill bits designed and tested with the DAME drill are shown in Figure 6.108. To compare different drill bits, it is often useful to compute the specific energy required for the bit to fracture (i.e., drill) material. The data in Table 6.20 were taken during the 2006 field test in the Haughton Crater.

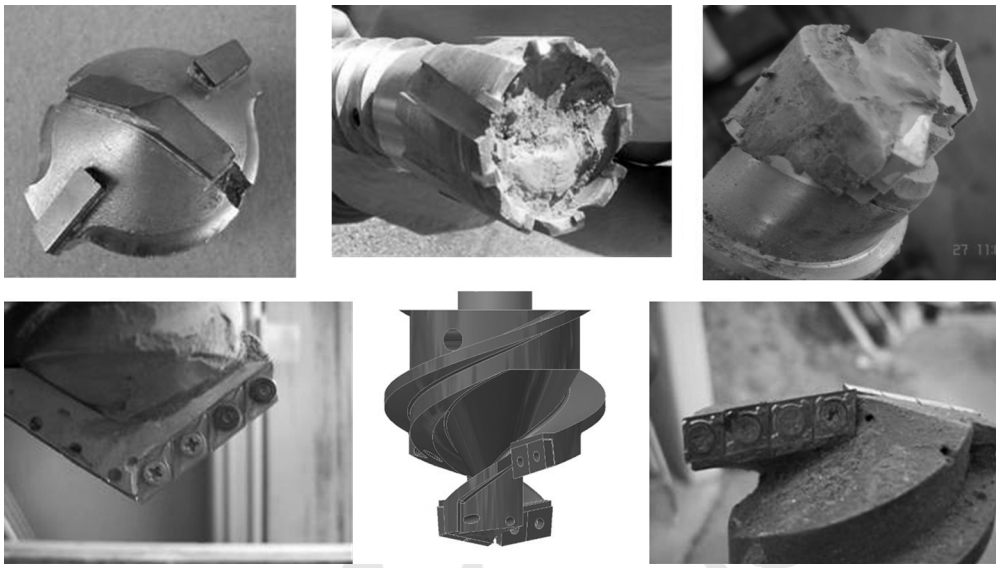

Figure 6.106 A selection of drill bits used with the DAME drill. Courtesy Honeybee Robotics.

6.9.3 NORCAT's SCaD Deep Drill

When deep drilling (depths greater than 2 m), it is necessary to utilize different techniques for sample retrieval. In addition, the NORCAT drill system requires the simultaneous removal of drill cuttings. The sample and cuttings retrieval is accomplished on a more frequent basis (approximately every 10–20 cm of hole drilled) to compensate for reduced auger length and volume of cuttings produced. The sample retrieval is accomplished by a coordinated wireline system adapted for use in planetary exploration (Figure 6.109). The system consists of a mechanism for "winching" the SCaD and cuttings bucket out of the drill string, pushing it back into position, and providing mechanical forces used to lock the SCaD into place and open and close cuttings ports in the auger (used to allow cuttings to drop into the internal cuttings bucket).

Table 6.18 Summary of stratified regions.

Stratified region	Depth range (cm)	Composition
Region 1	0–45	Active layer – reworked breccia
Region 2	45–92	Permafrost – reworked breccia and ice
Region 3	92–137	Thick ice lens with some gravel size breccia
Region 4	137–322	Permafrost (breccia, 19% >2 mm and 81% <2 mm; water content, 12 wt%) with thin ice lenses

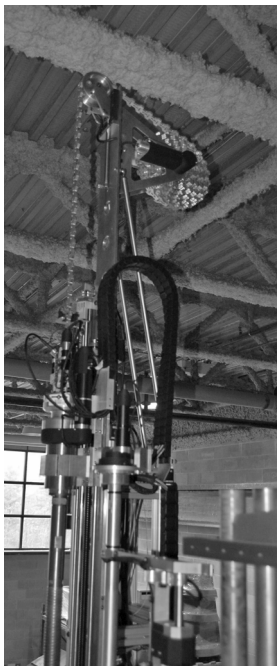

Figure 6.107 NORCAT deep drill with wireline (note wireline takeup reel at upper right). Courtesy NORCAT.

Table 6.19 DAME drill rate of penetration at different depths.

Section	Description	Start depth (cm)	End depth (cm)	Bit type	Average ROP (cm h^{-1})	Average ROP (cm min^{-1})
1	Permafrost – reworked breccia and ice	55	70	Full-faced	105	1.76
2	Ice lenses; some gravel-sized breccia	110	120	Full-faced	16	0.27
3	Ice lenses; some gravel-sized breccia	113	116	Coring	30	0.50
4	Permafrost – some dolomite	242	243	Coring	84	1.40
5	Permafrost – reworked breccia and ice	243	247	Coring	19	0.32
6	Permafrost – reworked breccia and ice	247	252	Coring	25	0.41
7	Permafrost – reworked breccia and ice	261	281	Full-faced	22	0.37

page proof © WILEY-VCH

Figure 6.108 NORCAT deep drill with rod handler at left. Courtesy NORCAT.

The wireline consists of a series of links which are maintained in tension (unlocked from one another and able to move independently of one another) when being fed into the drill string or removed from the drill string during sample retrieval and cuttings removal. The links are compressed (locked together to behave as a single rigid unit) for SCaD gate closure, dogging mechanism activation, or port control. Tension must be maintained during the drill advance and subsequent wireline feed.

There are three components involved in deploying and retrieving the wireline – the wireline take-up spool, the wireline tensioner, and the wireline feed mechanism.

The wireline take-up spool, located on the side of the backplane distal to the drill head, stores and delivers wireline. It is rotated by the wireline take-up spool motor. This motor is controlled by the position of the wireline tensioner. The wireline tensioner is a roller which is spring loaded to be capable of variable vertical positioning along a slider bracket at the top of the wireline mast. As the drill advances, wireline will be pulled off the take-up spool and fed down the drill string through the wireline feed mechanism. Compression of the spring on the tensioner will activate the spool motor to release more wireline. This ensures that the wireline is fed at a controlled rate so that the links remain in tension between the take up spool and the feed mechanism.

Table 6.20 The DAME drill full face bit versus coring bit for a cutting depth of 100–112 cm

Bit type	Average ROP (cm min^{-})	WOB (N)	Auger torque (N m)	Bit torque (N m)	Total torque (N m)	Total power (W)	Specific energy (MJ m^{-3})
Full face	0.143	2700	11.2	2.3	13.5	63.6	1544
Coring	0.152	2700	8.7	0	8.7	41.0	2510
Full face	0.172	2700	9.7	2.6	12.3	58.0	1171

Figure 6.109 Images of SPECES drill with 10 m of sample cuttings (a), SPECES drill extension segment in borehole during 10 m drill test (note these segments do not use augers therefore cuttings do not continue to pile on ground surface) (b), and custom sample core capture container with a sandstone 10 × 75 mm core sample (c). Photographs courtesy of ATK Space.

The wireline feed mechanism controls the feed of wireline into the drill string to ensure that the links remain in tension with the drill string. The wireline is sandwiched between the feed mechanism and a keeper plate. The keeper plate holds the wireline against the feed chain.

For SCaD removal, the keeper plate and feed mechanism are moved apart from one another, away from the opening in the drill spindle. With the wireline now freed from the feed mechanism, the wireline take-up spool can be activated to wind the wireline, pulling the SCaD from the drill string.

When the SCaD is reinserted into the drill string, the wireline feed mechanism must be engaged. Controlled feed of wireline into the drill string via the wireline feed mechanism then proceeds.

The rod handling system is responsible for storing drill rods not in use, supplying rods to the drill string, permitting the head to couple to newly added rods, assisting in the decoupling of the top rod from the drill head and returning decoupled rods to storage. A rod handling system is an absolute must for deep drilling (depths greater than 2 m) or drilling when multiple drill rods are required. The rod handling system is usually coordinated and integrated with a wireline sample recovery system to effect deep drilling sample recovery.

Drill rods are joined together into a drill string via a rod coupling device and technique. The rod coupling technique is key to the ability to vary the drill string

length. It is what allows the system to impart rotation and thrust to the drill bit from surface via the drill rods. An effective rod coupling must be capable of repeatedly coupling drill rods together or separating them from the drill string with a minimum of complexity. The coupling must also be capable of supporting tensile and compressive forces during various rod handling cycles, the worst case being the removal of a long drill string from the drill hole, in which case the rod coupling is under enormous tensile stress as it tries to pull the drill string up against friction and gravity.

Previous rod coupling techniques utilized 10 threads per inch acme threads for connection. This is a mining industry standard for AQ size and E size coring drill rods. Testing under dry drilling and highly autonomous conditions, however, indicated that this design was unreliable and resulted in an inordinate number of damaged coupling joints and complexity in autonomous coupling. In addition, it prevented the drill string from being rotated backwards to assist in a stuck rod recovery.

The NORCAT design utilizes a modified bayonet mount that differentiates between coupling to another drill rod and coupling to the drill stem. This allows forward and reverse rotation, stuck rod removal, and a simple and elegant method for the coupling and uncoupling of drill rods with the drill string.

Make/break cycles are those machine sequences required to add a drill rod into the drill string, thereby extending the drill string and consequent depth, or removing a drill rod from the drill string as the drill is being removed from the site; rods must then be stored (Figure 6.110). The cycle requires coordinated movements of the drill itself, the sample capture system, the rod coupling technologies, and rod storage hardware. The cycle refers to the combined hardware and control system strategies used. The system relies upon six pick-and-place robotics strategies for drill rod transfer and support during rod handling. It also relies upon existing sensors and

6.108

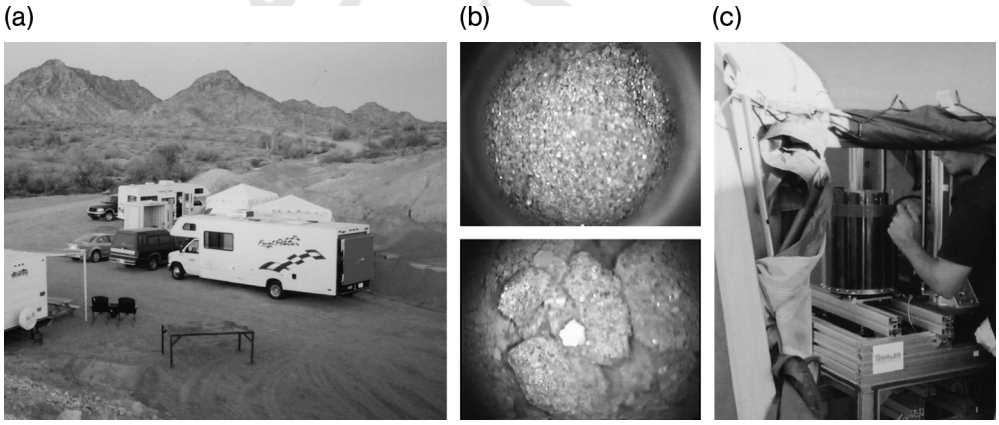

Figure 6.110 (a) Images of Arizona field test site, (b) sandstone layers through coring bit, and (c) engineer using the down-hole video camera instrument during SPECES 10 m field test. Photographs courtesy of ATK Space.

adapted control techniques in the drill subsystem for coordination of movement during rod coupling/decoupling.

Rod storage is required to facilitate reuse of drill rods from one drill hole to the next for the mission life. Appropriate storage design can also consider the potential for the storage of replaceable bits, augers, and so on.

A drill rod magazine was designed for 40 drill rods. This concept is scalable to the mass and inertia limits of the actuating system. The design utilized an *X*–*Y* table design. This allowed the rod handler swing arm (the arm used to transfer rods between the magazine and the drill string) to be reduced in complexity of motion. The moving table, with a drill storage rack unit, also allowed pseudo-random access to the storage slots.

The storage magazine consists of a rack mounted on linear *X*–*Y* tables. The rack has five upper and five lower arms that project horizontally to form four aisles or rows which can each hold ten 50 cm long rods for a total of 20 m of drill string. The system is scalable; with minor design modifications. The arm pair location corresponds to the axial distance between pairs of flats machined into each rod inset from the end. The arms of the rack fit into these flats, suspending the rods on the arms and allowing them to travel along the length of the arms. This keeps the rod ends from resting on a potentially dirty surface which could lead to deposition of debris in the coupling mechanism, thereby hindering proper coupling. Furthermore, the flats allow the rod storage system to maintain a specific rotational orientation for mating drill rods during rod coupling. To prevent the rods from slipping out of position on the arms, the upper arms each have detents over which a rod can be pushed or pulled using the gripper arm. The detents are intended to localize and retain the rods not currently in use.

The system decouple was a requirement to recover from a stuck rod condition. This condition is one within which the drill string ceases to move in an axial direction and usually also stalls in the rotary action. A stuck rod condition is triggered by a geotechnical fault, such as severe hole slump or fracture slip. It is significant as a mission killer and has been cited as a major factor in keeping deep drilling technology off mobility platforms. That is, the mission planners have stated that a stuck rod condition on day one of a multi-day rover-based mission could result in the rover being literally pinned in place. Recovery from this condition is paramount.

The design relies upon the rod coupling technique and drill control software to alleviate this condition. In addition, the design of the auger and drill rods is such that the rod which is stuck, and all rods and hardware below it, are disconnected from the drill string and the free drill string is recovered from the drill hole.

6.9.4
Subsurface Planetary Exploration Core Extracting System (SPECES) Drill

The Subsurface Planetary Exploration Core Extracting System (SPECES) was developed in 2002 by ATK Space (with funding from NASA and JPL) for the purpose of drilling 10 m deep in support future drill missions. After reviewing past SCAD tests results and lessons learned, a new approach was determined to be necessary because

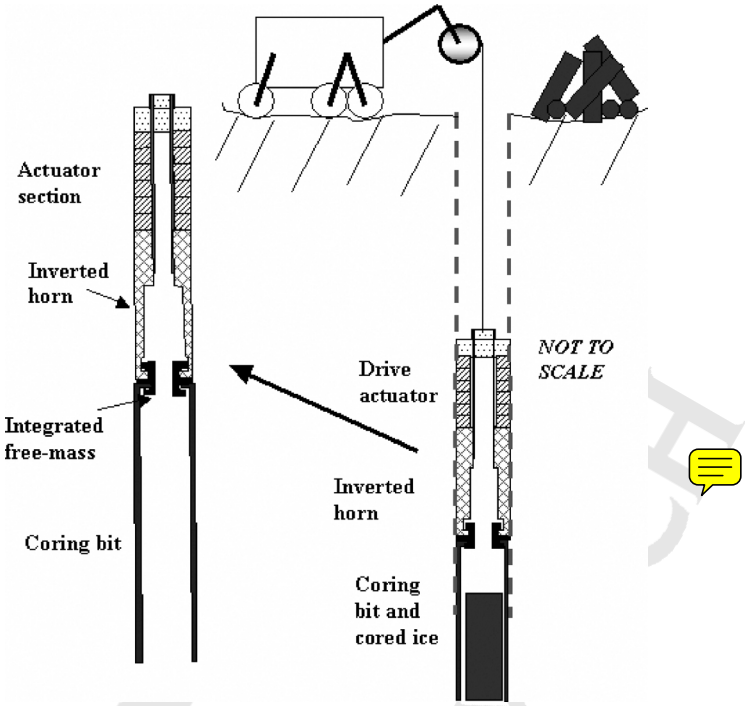

Figure 6.111 Schematic view of the ultrasonic/sonic gopher operating inside the borehole. Courtesy NASA/JPL.

a pure auger drill method was not feasible beyond 1 m using the expected flight low-power levels (Guerrero *et al.*, 2005). SPECES consists of a custom bottom hole assembly (BHA), a custom internal sample container mechanism and smooth extension drill segments to reach the target drill depth. The rotational drive, vertical drive, and segment mating approaches were not modified and therefore used the same hardware as developed for the SCAD (see Figure 6.111).

The SPECES design provides an effective approach using a dry cuttings removal system (no fluids), hole stabilization method, single deeper hole approach, and continuous sample recovery feature. The combination of a BHA and an independent coaxial sample container mechanism solved cuttings-related problems and significantly reduced friction issues. Custom dry drilling coring bits with thinner walls provided lower power consumption and solved clogging issues at the drill bit interface (Guerrero *et al.*, 2006). The novel system design stabilizes the borehole while allowing for continuous core and cuttings removal without the need for entire drill segments to be removed from the borehole to retrieve a core sample. This method saves a tremendous amount of operational time and reduces the risk of the borehole collapsing.

On 5 December 2002, the NASA-supervised 10 m field test demonstrations began site safety and hardware transport operations. The Arizona Desert Rose Sandstone mine location (near Buckeye, AZ) was selected by NASA as an ideal site to conduct

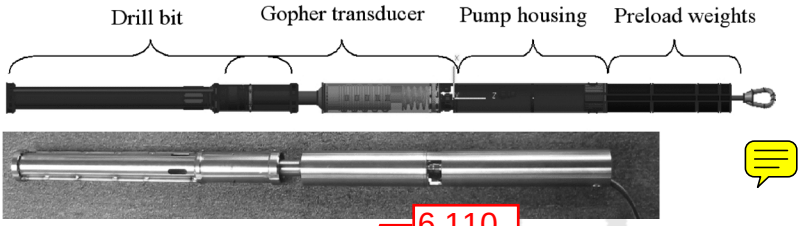

Figure 6.112 A view of the ultrasonic/sonic go[illegible]sy NASA/JPL.

this 10 m TRL 5 test (see Figure 6.112). The field test duration was limited to 10 days. The SPECES drill successfully penetrated the entire 10 m layer of sandstone using a single bit in just 7 days of drilling operations. The custom bit was evaluated by the NASA Review Board and it was concluded that there was only negligible bit wear. SPECES power levels were maintained between 80 and 100 W (standard light bulb) and provided proof that drilling to 10 m can be achieved using expected flight low-power levels. The power usage data were collected using a professional power logger. Power data showed only 82 W usage for the total system at 1 m depth and only 105 W at the 10 m target depth. These low power levels verified the effectiveness of the dry drilling method that generates only negligible heat and prolongs bit life.

The SPECES team completed several technology developments and field test demonstrations:

- Demonstrated technology to drill a 10 m borehole with all necessary automation level A1 subsystems. Demonstrated automation of drill segment coupling/decoupling and multi-stem assembly by remote control feature.
- Developed technology to solve the problem of cuttings removal for dry drilling without interruption of the drilling operations and removal of the whole drill head from the borehole.
- Developed technology to stabilize the borehole without using additional braces. Demonstrated an effective casing function by using a hollow segment approach.
- Demonstrated miniaturization of breadboard components. Drill bit, segments, and sample container mechanism were sized to meet flight power requirements. These components were used successfully during the field test.
- Demonstrated "straightness" of the borehole by manually rotating the complete drill string near the 10 m depth point.
- Demonstrated down-hole instrument capability using the hollow segment access to the bottom of the borehole with a down-hole video camera that took images through the tip of the coring bit (see Figure 6.112).

6.9.5 Ultrasonic/Sonic Gopher

The USDC mechanism was used to develop a "gopher" (wireline drill) that can acquire core samples using a bit diameter as large as 6.4 cm, which was larger than the USDC actuator (Badescu *et al.*, 2006; Bar-Cohen *et al.*, 2001). The device is shown

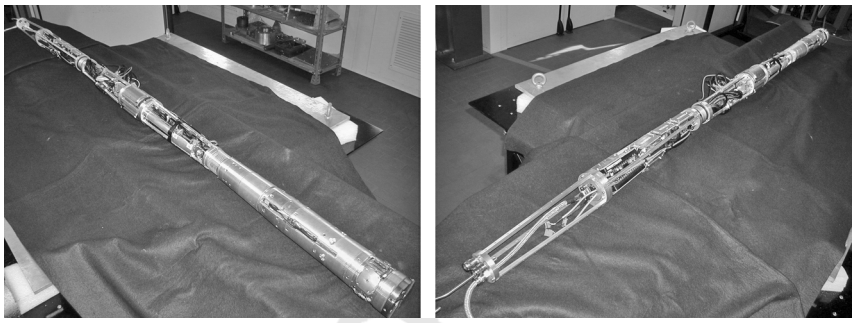

Figure 6.113 Ground Mole Demonstrator (GMD): cover shells of segments 2 and 3 are removed to show internal arrangement. Courtesy ESA, Tecnomare and CISAS G. Colombo.

6.111

schematically in Figure 6.113, where a core is formed up to the length of the internal size of the bit and it is removed from the borehole. This process is repeated until the desired depth is reached. To demonstrate the capability of the gopher, it was tested on a glacier at Mount Hood, OR, and the lessons learned were implemented into the design; the enhanced gopher was tested in Antarctica. The modified unit is shown schematically and photographically in Figure 6.114, where the various components of the gopher are identified. The field test in Antarctica was conducted at Lake Vida and it provided an important opportunity to demonstrate the feasibility of this technology while determining the associated challenges and requirements to enhance its capability for future drilling objectives. The unit successfully reached a depth of 1.76 m and it was a major milestone since it is significantly deeper than the length of the whole gopher assembly.

6.112

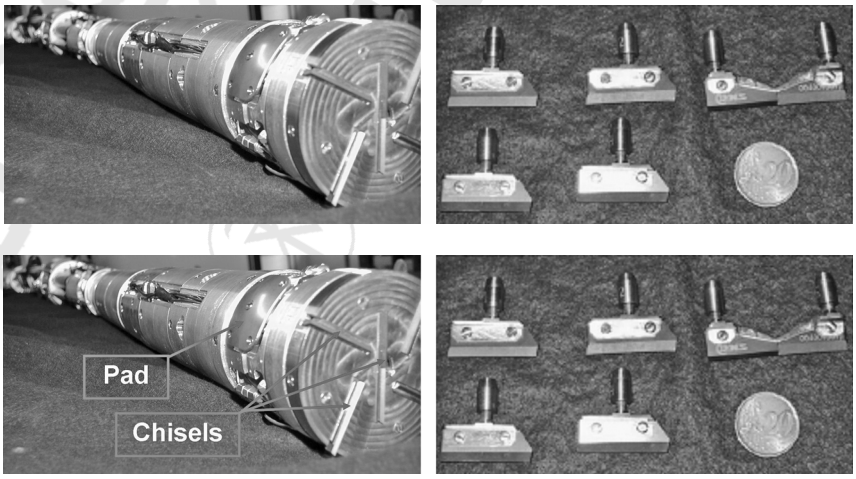

Figure 6.14 Ground Mole Demonstrator: (a) rotary percussive boring head and pads; (b) chisels. Courtesy ESA, Tecnomare and CISAS G. Colombo.

6.10
Deep Drills (>10 m)

Reaching depths of more than 10 m is required for a number of scientific investigations. For example, it is believed that the first few meters on Mars were sterilized by high-energy cosmic rays and solar particles potentially killing any form of life. Therefore, in order to reach habitable zones where living forms may have been preserved, it is necessary to go deeper, below this "dead" zone. Another good example where reaching a greater depth is necessary was shown during the heat flow experiment performed on the Moon by Apollo astronauts. The heat flow probe was inserted more than 2 m below the lunar surface. The probe was designed to determine the flow of heat that originates in the deep interior of the Moon and in turn to map the Moon's internal temperature distribution and chemical composition. However, it was determined that heat inflow into the surface associated with solar radiation affected the measurement of heat generated deep in the lunar interior. The affected depth was on the order of 1 m or less for the diurnal and annual temperature fluctuations and over 5 m for the fluctuations associated with the 18.6 year period orbital precession. Therefore, to remove the effect of solar radiation, a heat flow probe on the future lunar missions will have to be placed at the depth of around 7–10 m below the lunar surface. The following sections describe examples of various drills with a depth capability of more than 10 m.

6.10.1
Subsurface Explorer (SUBEX)

The development of a subsurface explorer (SUBEX) is one of the most challenging current European developments. In its conceptual definition, a SUBEX is a robotic mole, which, despite its minimalist volume, mass, and power consumption, is capable of penetrating hundred(s) of meters below the surface. A SUBEX is an expendable system; it carries a package of scientific instruments to perform *in situ* analysis of the subsoil. To govern its trajectory, a SUBEX is equipped with a steering system and a localization system. The first development activity to realize a SUBEX was performed for ESA by Tecnomare with CISAS "G. Colombo" (Center of Studies and Activities for Space). Due to the technology demonstration nature of this activity, the first SUBEX prototype was named the Ground Mole Demonstrator (GMD) (Campaci *et al.*, 2005), (Zaccariotto *et al.*, 2007). The GMD has the capability of boring a hole, advance within it and to remove cuttings up to a depth of 100 m. The GMD (see Figure 6.115) is articulated in three sections, having a diameter of 87 mm and a length exceeding 2 m. It may progress at up to 3 mm h^{-1} in the hardest foreseen rock (maximum compressive strength of 150 MPa); it is capable of steering with a minimum radius of 10 m. The GMD uses a hybrid rotary and percussive boring, suitable for both soft and hard soils (see Figure 6.116). The maximum drilling power is limited to 100 W. The percussion is generated by a spring-loaded plunger that follows an S-shaped head cam, which is rotated independently from the drilling motor: each time the plunger reaches the end of the S profile, it is strikes the back of

6.113 6.114

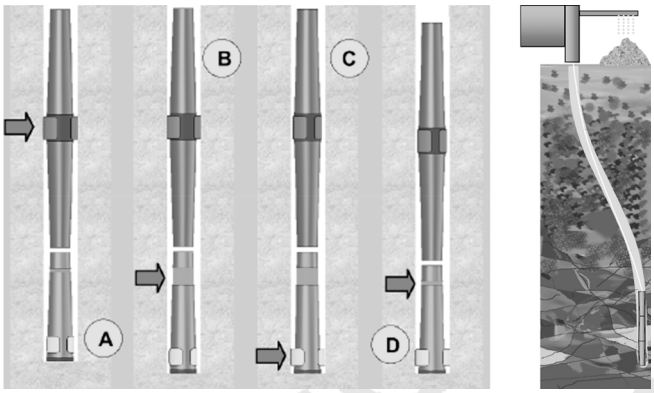

Figure 6.115 GMD propulsion. (a) The four steps of the GMD peristaltic propulsion: (A) top pads engage; (B) GMD drills and extends down; (C) bottom pads engage and top pads disengage; (D) GMD contracts. (b) Steering ability. Courtesy ESA, Tecnomare and CISAS G. Colombo.

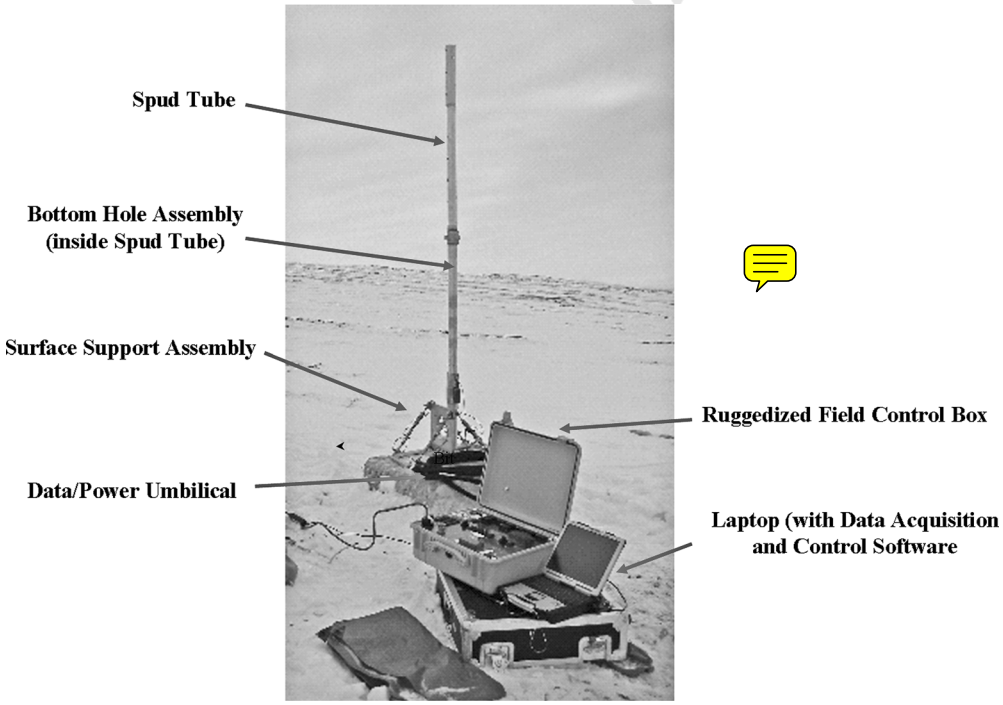

Figure 6.116 The major components of the NASA–Baker Hughes drill system in the Arctic. Courtesy NASA.

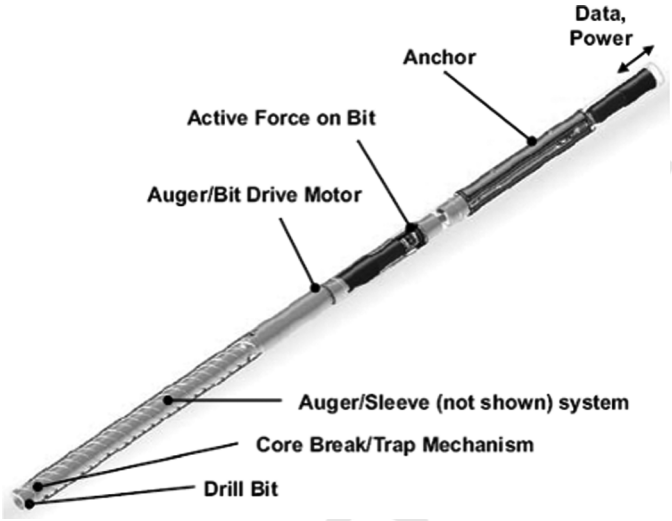

Figure 6.117 Details of the bottom 6.115 bly (BHA). Courtesy NASA.

five chisels (see Figure 6.117). ~~At the depth reached by the GMD, in order to progress downwards cuttings must be actively disposed of.~~ The GMD propulsion is peristaltic (see Figure 6.117). the two front sections are linked with a linear actuator, each section having its holding system with three expanding/retracting pads actuated by a sealed oil circuit. For steering, an actuated 2-DOF joint – a hollow wedge-disk joint – is inserted between the tw 6.115a ons. The third section is linked by a passive 2-DOF joint.

Proving the successful disposal of the cuttings was an essential goal of the GMD activity (Figure 6.117a). The cuttings management mechanism realized in the GMD is composed of a local (internal) and a long-range (external) system; the local system displaces the cuttings produced from the boring head to the rear part of the mole, while the long-range transportation brings the debris to the surface. The local part uses a hollow auger to raise the fine grains produced by the drill to a pick-up chamber of the long-range system. The latter is based on a loop of special cord stretched between a surface station and the GMD. The cord (a) revolves on a first pulley inside the mole, where it is covered with the fine-grained dust coming from the auger, (b) leaves the mole encased in a plastic conduit, (c) reaches the surface station where a set of pulleys and brushes offloads the dust, and (d) returns to the mole encased in the plastic conduit. In the final design of the GMD (not yet realized), the plastic conduit is created inside the mole during its advance: three tape films are thermally bonded, forming two parallel tubes (each having an omega-shaped section), one for the outgoing cord and one for the returning cord. An electric umbilical, embedded in the plastic conduit, links the GMD vehicle to its surface station for power and signal. The GMD prototype was tested to show the validity of the engineering solutions. The test was performed on a specifically designed test set-up about 5 m in height. The test results proved the efficacy of the boring technique against various materials. The

propulsion and steering performed according to expectations (Figure 6.117b). The cuttings management system, implemented in all its parts, showed successful transport of the cuttings to the surface. The GMD has demonstrated that the concept of a SUBEX is feasible and within reach of present-day technology. However, the GMD is only a technology demonstration and much more development is needed to realize a space-qualified SUBEX.

6.10.2 Mars/Arctic Deep Drill

Over the past several years, NASA Johnson Space Center and Baker Hughes Inc. have ~~been developing~~ a low-mass and -power planetary drilling approach based on a dry rotary-coring wireline ~~BHA~~. The 8.5 kg BHA was designed to recover a continuous record of 2.5 cm diameter by 15 cm length cores. Typical operations ~~occurred~~ at 100 W electrical power and a 20 cm h^{-1} rate of penetration in consolidated sandstone. The drill has been field tested in the United States and Canadian Arctic to depths of 2 m in sandstone and in ice. Other field tests have demonstrated mobile deployment and operation of the drill from a rover, and "virtual" commanding, monitoring and control from a remote experimental cockpit. Maturity on the NASA technology readiness scale is approximately TRL 6 (prototype demonstration in a relevant environment).

6.10.2.1 Drill Description

The drill system shown in Figure 6.118 is comprised of the following major elements:

- ~~BHA~~
- ~~surface~~ support assembly with umbilical

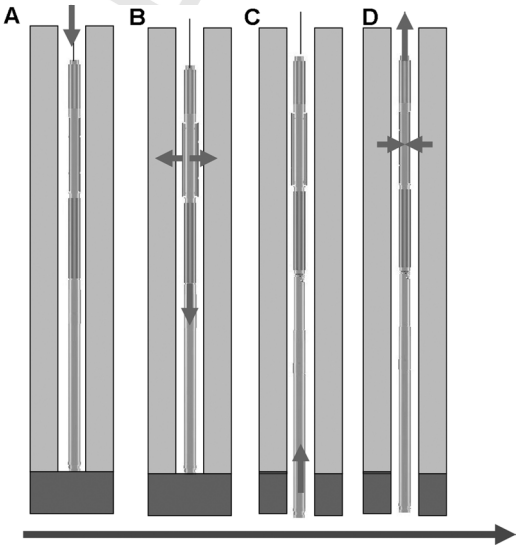

- **A – Initial Deployment, BHA is Lowered to tag the bottom of the Bore Hole**
- **B - Anchor Module is Expanded against bore; FOB activated; drilling starts**
- **C – Drilling Ends; bite is created; Core Break/Trap Activated**
- **D – Anchor Retracted: BHA extracted from hole to surface**

Figure 6.118 Drill operational sequence. Courtesy NASA.

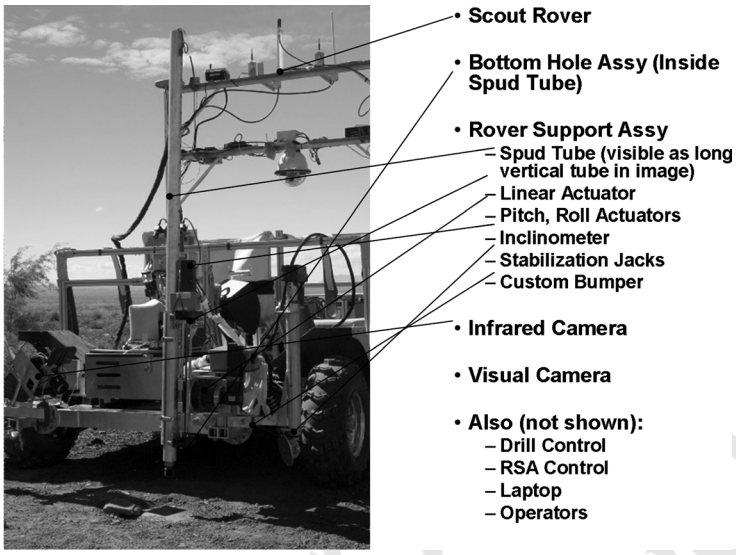

Figure 6.119 ~~Rover support assembly (shown in use during a field test)~~. Courtesy NASA.

- ~~power~~ conditioning and control/moni[illegible]ctronics (field control box)
[illegible]~~gedized~~ laptop computer with control and logging software.

The BHA, detailed in Figure 6.119, is the primary drilling actuator of the system. All subsystems required to provide mechanical actuation to facilitate drilling and core/cuttings collection are contained within this device.

The primary functions of the BHA are to provide the rotational and axial drilling forces necessary to penetrate the formation, provide reaction to those forces, and capture the core and cuttings generated during the drilling process. The force on bit (FOB) module [also referred to as weight on bit (WOB)] provides downward axial force to the drill bit, in addition to measuring its forward progress. The primary mechanism in the FOB is a lead screw/power nut apparatus, coupled with DC brushless motors. [illegible] motion is measured via a built-in linear potentiometer. The FOB drills ah[illegible]determined distance, then is retracted. After each of these cycles, the core is captured and brought to the surface. This is called a drilling "bite." Figure 6.120 details how a bite is generated, along with the general operational concept of this drilling system.

A second brushless DC motor coupled to a planetary gearhead is used to provide rotational torque to the drill bit. The output of the gearhead is attached to an auger shaft, which is also coupled to the bit. Therefore, as the auger rotates, so does the bit. It is this rotation, coupled with the downward force provided by the FOB, which allows downward penetration of the drill bit and removal of the cuttings. The drill bit is fixed to the end of a hollow auger, which is used to channel drill cuttings away from the drill bit up the height of the auger, and into a storage compartment. The drill bit itself is annular, and creates a core as it drills forward. As downward progress is made, the drill surrounds the stationary core (still attached to the formation), while also

Figure 6.120 Field testing in Arctic ice. Photo courtesy G. Briggs, NASA ARC.

capturing the cuttings. A mechanism contained in the drill bit breaks and captures the core at the conclusion of each drill bite, thus clearing the hole for the next drilling operation.

The key component to enable this drilling concept is the drill bit. The bit has two primary functions, to create a hole in a controlled and predictable manner in the formation through the use of mechanical action, and to channel the resulting cuttings away from the cutting surface. The bit and the core/cuttings management subsystems are particularly difficult to specify due to the wide range of conditions and diversity of substrate that the drill may encounter. A few examples of the diverse substrate include abrasive and non-abrasive rocks, friable and ductile materials, clay, unconsolidated sand, ice, and permafrost. There is also the possibility that various combinations may exist at a particular drilling site, even within a few centimeters apart.

Coupled with the unknowns mentioned above, there are also several other constraints that present a challenge for the drill bit, which include:

- ~~Micro~~ hole and core size
  - Bore hole diameters in the region of 45 mm (1.75 in) with a core diameter of 25 cm (1.00 in) result in very little "kerf" to position and align cutting surfaces (or cutters). This also means that the cutters must not erode at a high rate, since the BHA itself must fit within the borehole with a very small margin.

- Low mechanical power at the bit/rock interface
  - Bit and drill systems have been constructed to operate using 50–100 W of electrical power, which translates into low rotational velocity and low available torque at the bit/rock interface. This limits the method of delivering power to the bit and emphasizes high efficiency in converting from electrical to mechanical energy.

- Low FOB/WOB
  -Since the downward drilling forces are reacted via the anchor pads, the force on the drill bit is a function of the ability of the local formation to withstand the pressures/loads imparted by the anchor pads. In some formations, such as hard non-abrasive formations, low WOB is problematic coupled with an inferior bit design.

- Dry drilling
  -This concept does not require a drilling fluid ~~(preferably gas)~~, which was born out of the mass challenges associated with compressing ambient atmosphere or preloading gas and the necessity for aseptically captured cores from the subsurface. The lack of fluid presents some interesting constraints regarding bit cleaning and cuttings transport. Consolidated formations rapidly expand by volume after being liberated from the parent material. This material must be carried away from the bit/rock interface so as to maximize the transfer of energy to the formation (versus allowing some of that energy to interact with the cuttings). Given the absence of drilling fluid, mechanical means must be employed to channel the cuttings away from the bit face. Another challenge of dry drilling is bit cooling, or rejecting the heat developed from the inefficient transfer of rotational/translational energy into destroying the formation.

- Retrieval of cuttings and core
  -In addition to the functions mentioned above, the bit also has to (at least) accommodate other subsystems to trap and break the core that is created by the act of drilling, along with all of the cuttings created. This, coupled with the small borehole and large core size, presents unique packaging challenges.

Given the requirements and constraints listed above, a suite of drilling bits was developed to accommodate different drilling conditions and formations. The ultimate goal is to combine key attributes into a single or small subset of drilling bits that would handle the majority of drilling challenges presented, while working within the mission constraints (low power, mass, volume). The first generation bit used diamonds impregnated in a metallic matrix (the bit is referred to as a diamond-impregnated bit). The bit surface contacted the borehole either on the cutting surface or to the sides. The diamond-impregnated bit has the advantage of being "self-sharpening", in that fresh diamonds are exposed as the matrix is worn away at a controlled rate during drilling. The first diamond-impregnated bit did not perform well in laboratory tests since the large amount of contact area over-distributed the low available downforce and available mechanical energy at the bit/formation interface. The result was a bit that was very strong and had good wear characteristics, but could not penetrate the surface. The second-generation diamond-impregnated bit was designed to apply the diamonds (contact surfaces with the borehole) in fewer locations to maximize the amount of pressure developed at the cutting surface. Care was taken to ensure to match the wear characteristics of this bit with the layout geometry so that as the bit wore, the hole and core dimensions were maintained. This evolved bit worked well in abrasive rocks, since the formation would act to sharpen the bit (or remove old diamonds that have worn and expose fresh diamonds in the

substrate). With the smaller areas of contact, even modest amounts of downforce applied by the drill were sufficient to achieve acceptable penetration rates. This was demonstrated in several field tests. This bit, however, is not optimum for non-abrasive formations, where the formation does not "sharpen" the bit and expose new diamonds. This is because once the first layer of diamonds had worn the bit lost its effectiveness. To combat this, a third-generation bit was developed, abandoning the diamond-impregnated bit for one incorporating a polycrystalline diamond cutter. The third-generation bit showed good performance in the majority of the formations and was used in the last set of field tests.

A separate development tackled the drilling ice and permafrost. This bit and auger system, scaled from existing, commercially available ice drilling technology, performed the same functions as the bits mentioned above, but were tailored especially for ice. The difference between the rock and ice bits was the mechanism used to break away the formation. For ice, shaving versus "plowing" was employed. The drill was successfully tested in the Arctic and functioned within the constraints of the planetary drilling system (low power and low downforce). However, some challenges remained with ice/permafrost drilling due to the vulnerability of the ice cutters to fracture or chip when encountering ingrained pebbles or to excessive wear when drilling ice-cemented sands. Also, it was found that combining the ice/permafrost bit with the features required for a rock bit may present an issue. The alternative to having a single bit for all formations is to have the capability to change the drill bits whenever the formations or conditions (e.g., bit wear) change.

The final key function in the BHA is drill force reaction, which is provided via an anchor mechanism. Design of the anchor mechanism proved difficult in that the interface to the borehole may not always be well characterized, and the mechanism also has to operate in dusty and abrasive environments. The primary design parameters of the anchor system proved to be pressure exerted on the borehole wall and the coefficient of friction between the anchor device and the borehole. To provide reaction to the drilling loads, a wide concept tradespace was considered that included inflatable bladders, mechanical pads, and mechanical springs/compliant materials. The selected concept included mechanical pads that could be actuated radially from the drill to contact the borehole. The pads could then be retracted to fit within the body diameter of the drill for ease of extraction.

An umbilical (or tether) provided physical connection to surface hardware, transmitted power to the BHA, and transmitted command/monitoring signals. The unique aspect of this concept was that the BHA was lowered via tether into the formation. As greater depth was desired, only additional tether was required.

To facilitate BHA downhole drilling operations, certain hardware was required on the surface. This surface support assembly included a "starter" tube (called a spud tube), a small winch assembly to move the BHA up and down in the borehole, and additional hardware necessary to extract the core/cuttings from the BHA after each drill bite. The spud tube contained the BHA during transport and was essentially an artificial borehole that extended above the formation, such that the anchor mechanism could attach and react the initial drilling forces. After the tool had penetrated the length of the BHA into the formation, the spud tube served only

as a guide for the tool as it was being retracted or deployed out of or into the borehole.

Additional equipment included a field control box that supplied the necessary power conditioning and signal conversion/input/output electronic devices to facilitate control and monitoring of the BHA. For the laboratory and field tests, all of this equipment was packaged in a small ruggedized field control box. In addition, data logging and control of the drill (via the field control box) were performed using a ruggedized laptop computer running data acquisition and control software. This software could be run from any remote source via an Internet connection.

Finally, to support rover tests, a specialized Rover Support Assembly (RSA) was created to mount and actuate the BHA and spud tube from two NASA JSC rovers. This RSA included mechanisms to stabilize the rover (using deployable jackstands) and provided three DOF to maneuver the spud tube/BHA into and out of the borehole. All monitoring/control of this hardware was performed with a small ruggedized field control box and remotely operated using the same data acquisition and control software as mentioned above. Figure 6.121 illustrates the drill and RSA integrated with the JSC SCOUT rover during field testing at Meteor Crater, AZ, in 2005.

6.119

6.10.2.2 Drill Development and Testing

Development of the drill progressed from concept to hardware; from subsystem testing through two full system prototype cycles; from laboratory operations to remote field testing in a range of different materials; and ultimately from fixed site to mobile rover-based drilling via remote command and control. Laboratory testing occurred primarily at JSC and Baker Hughes, and was supplemented by environmental chamber work at UC-Berkeley. Field testing has been performed in Texas (Houston, Galveston, Huntsville), Arizona (Meteor Crater), New Mexico (NASA

Figure 6.121 Demonstrating remote command and control of drill during Arizona field test. Courtesy NASA.

White Sands Test Facility), and the Canadian High Arctic (Eureka Weather Station). The system has drilled rock, ice, and sand to depths of 2 m.

Initial concept exploration and analysis suggested the desirability of the wireline BHA approach for achieving goals of depth to tens of meters, power levels in the 100 W class, and mass on the order of tens of kilograms. Subsequent laboratory testing evaluated competing means for achieving critical functions such as anchoring, application of FOB, and coring. Four families of coring bit design were explored and improved through testing in various rock lithologies, sands, planetary simulants, water-ice, and ice–sand mixtures. All testing was performed under terrestrial atmosphere, temperature, and gravity, though low-temperature freezer runs were made to prepare for Arctic field testing. FOB testing explored both passive and active approaches. Anchor development included tests to characterize the anchor-to-borewall frictional interface, and also alternative mechanical approaches to exerting pressure to the borewall.

The Mk1 drill prototype was built upon these lessons learned, and demonstrated NASA TRL 4 (component and/or breadboard validation in a laboratory environment). This first system utilized two brushed DC electric motors to drive bit and anchor assemblies, and a simple spring and latching mechanism to apply FOB. The Mk1 drilled 2.2 m deep into iron-rich Mansfield sandstone in June, 2003. The 7 kg BHA operated at 50 W average electrical power and achieved an average ROP of 8.9 cm h^{-1} (3.5 in h^{-1}). The typical rotary speed was 70 rpm, with applied FOB ranging from 140 to 330 N (31–74 lbf). Twenty-three sequential cores were retrieved. In another laboratory demonstration, the drill achieved 2 m depth in unconsolidated sand with the aid of a flighted spud tube that sequentially "chased" the BHA into the medium after each bite, demonstrating the potential for a secure wellhead to be established as insurance for questionable stratigraphy.

The Mk2 drill was an imp 6.120 ldable system that demonstrated TRL 6 (prototype demonstration in a relevant environment) during Arctic field testing in 2004 and 2006 (Figure 6.122). This second system featured numerous improvements in approach, capability, and instrumentation. Depths of 2 m were demonstrated in ice and sandstone in the vicinity of the Eureka Weather Station on Canada's Ellesmere Island. The 8.5 kg BHA drilled sandstone at an average rate of 20 cm h^{-1} and recovered 24 cores. Average performance parameters for the test were 96 W of electrical power and 387 N (87 lbf) of applied FOB. Typical rotary speed was 100–120 rpm.

6.10.2.3 Drill Testing from a Rover and Tele-Drilling Operation

The original drill concept was envisioned for a Mars Scout-class lander, which implied drilling from a stationary platform. Natural questions arose as to how the approach could be applied to mobile platforms, and what imaging/remote control capability would be required to control/monitor the drill from Earth. The previously described RSA was fabricated to interface the drill and rover systems. Using the drill, RSA, and two pre-existing JSC rovers, the following objectives were demonstrated:

- ~~select~~ drill site using video/images/terrain mapping
- ~~maneuver~~ the rover to selected drill site

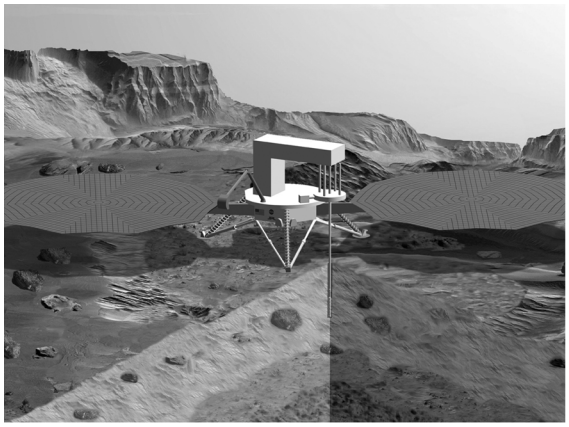

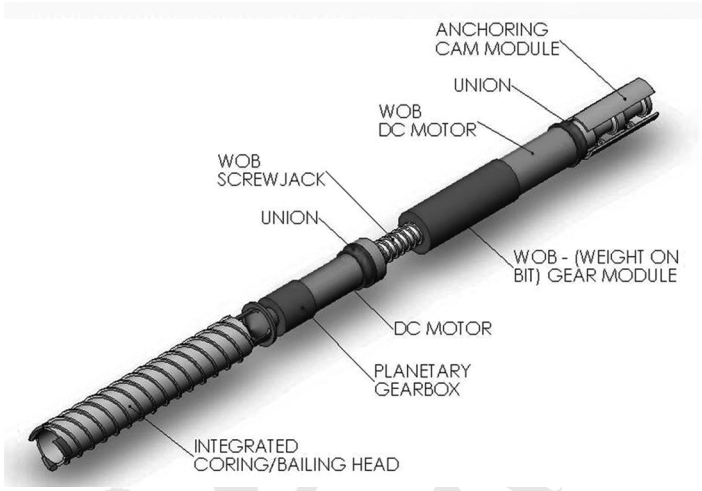

Figure 6.122 ATC system: (a) shown on a conceptual Mars lander; (b) conceptual CAD model with major subsystems called out. Courtesy M. Brennan, Raytheon UTD.

- ~~rotate~~ drill into drilling position
- ~~commanding~~ and control complete drill sequence
- ~~acquire~~ performance data from the drill
- ~~retract~~/stow drill.

This functionality was tested using an unpressurized crewed rover prototype and a smaller ~~unscrewed~~ robotic rover (roughly the size of the MERs). The rover tests were carried out at JSC and in desert field tests near Meteor Crater, AZ. In addition, the ability to command the BHA and RSA using wireless remote control was demonstrated. This was achieved using Ethernet protocols built into the control hardware and software coupled with existing remote control/monitoring/communication platforms. This configuration was fielded in the desert tests and successfully

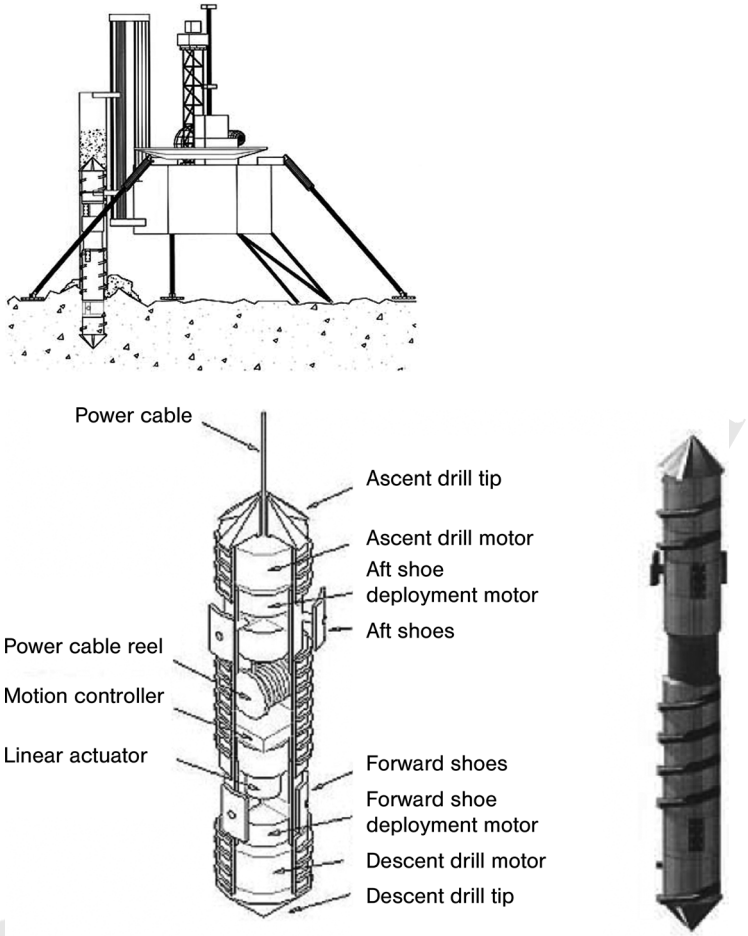

Figure 6.123 IDDS concept: (a) being deployed from a lander; (b) quarter-section and rendered views shown with major components called out. Courtesy Honeybee Robotics.

performed all of the drilling operations mentioned above, additionally providing visible and infrared camera views. A view of the cockpit and displays used in this test is shown in Figure 6.123.

6.10.2.4 Lessons Learned

This technical approach reflects early design goals for a planetary subsurface exploration tool extensible to "deep" depth (tens of meters), yet entailing only modest mass and power requirements. The wireline BHA method eliminates the mass and complexity of drilling pipe, and is therefore relatively mass insensitive with increasing depth. Each additional meter of design depth can be "bought" for only the small additional mass of another meter of wireline. Dry drilling further reduces system

mass by eliminating the need for drilling muds and infrastructure. Low system power is afforded by the coring style bit, which reduces the total volume and energy of rock comminution.

From a scientific standpoint, the drill provides a continuous series of 2.5 cm diameter by 15 cm length cores, as well as fine powdered cuttings, which record the entire explored stratigraphy. These samples are relatively uncontaminated and undisturbed, due to the aseptic dry drilling approach and modest drilling-imparted energy. Core interiors can be further subsampled if even "cleaner" material is desired. The created 4.5 cm diameter borehole is itself a valuable resource, and may be logged after or between drilling bites. Although not yet exercised, design provisions also exist in the BHA to accommodate onboard science sensors.

Challenges also exist with this drilling approach. Modest penetration rates are a direct result of the low design operating power, in addition to inherent limitations on the size of the down-hole electrical motor. The borehole wall anchoring approach invokes sensitivity to formation stability, and preference for well-consolidated stratigraphy.

6.10.3 Autonomous Tethered C

6.122a

The Autonomous Tethered Corer (ATC) is a lander- or rover-based tethered drilling system (Figure 6.124a) that was developed by Raytheon UTD to drill and sample to depths ~~that~~ greater than 200 m with little reaction force required (Brennan *et al.*, 2005). The depth and low system profile are accomplished by the elimination of an auger system that extends from the bottom of the borehole to the surface. The ATC (Figure 6.124b), by comparison, brings cuttings to the surface via a cuttings reservoir at the top of the core barrel. The cuttings reservoir and core are dropped off after every 110 mm of penetration. The mass of the system is 7 kg and it uses a power of 50–75 W, 6.122b t is capable of 4 N m maximum torque and 151 N maximum WOB. The TRL of this drill system is currently 4.

The total length of the ATC system is 2 m and its subsystems include a coring/bailing head, a WOB module, and an anchoring module. Operationally, the ATC works by an inch-worm type of motion where the anchoring module expands first to clamp against the borehole wall. The WOB module is then used to provide both WOB (445 N) and control rate of penetration, while the coring/bailing head provides rotary motion (250 rpm) and torque. The total stroke of the WOB module is 110 mm, after which the ATC must be retrieved from the borehole via a tether reel to empty the cuttings reservoir and drop the core off. The system is a continuously coring system so a 110 mm core is obtained during every cycle. The system creates a borehole that is 37 mm in diameter and a core that is 25 mm in diameter. During the initial creation of a borehole, the ATC anchoring module clamps against a fixed grounding tube held above the target location. The core is retained with a slip, tapered collar that compresses around the outer diameter of the core during retraction. During development testing, the ATC drilled 10 m in Texas limestone with average power consumption of 74 W and a ROP of 3.4 mm min^{-1}.

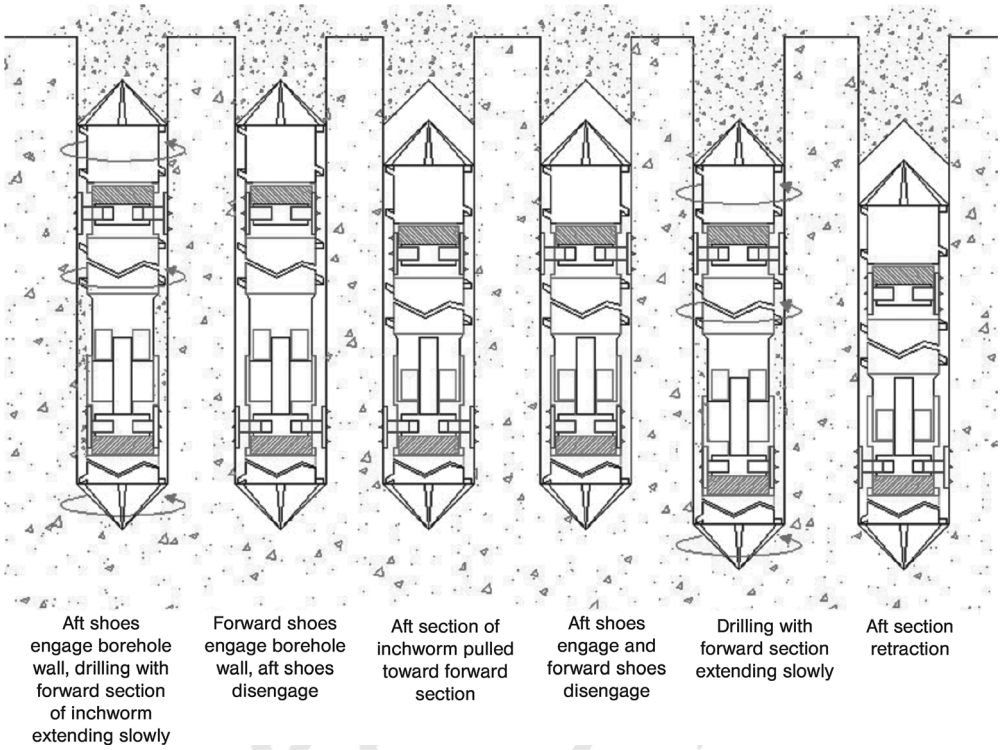

Figure 6.124 IDDS operational sequence. Courtesy Honeybee Robotics. (Please find a color version of this figure on the color plates.)

6.10.4 Inchworm Deep Drilling System

Developed by Honeybee Robotics SMC for NASA, the inchworm deep drilling system (IDDS) is a low-mass, compact, novel access technology capable of accessing regions deep below (>100 m) the surface of multiple planetary bodies. Candidate mission destinations include the ~~suspected~~ subsurface water ice deposits on Mars; the ~~suspected~~ subsurface oceans on Europa, Ganymede, and Callisto; and Lake Vostok, the largest known subsurface lake on Earth. The IDDS (Figure 6.125) is a semi-autonomous robotic device that moves like an inchworm and drills very deep through soil, ice, and rock. 6.123

The IDDS traverses drilled boreholes to perform *in situ* analyses and to transport material to the surface. By keeping one set of borehole wall shoes on either the forward or aft section firmly secured to the borehole wall, the other section is able to expand or retract; allowing the drilling system to move easily up or down the borehole (Figure 6.126). Either a sampler or an *in situ* instrument may be located at the forward end of the IDDS. The fundamental problem with moles is the need to remove the accumulating cuttings. Thus, the mole will have to climb up the hole to 6.124

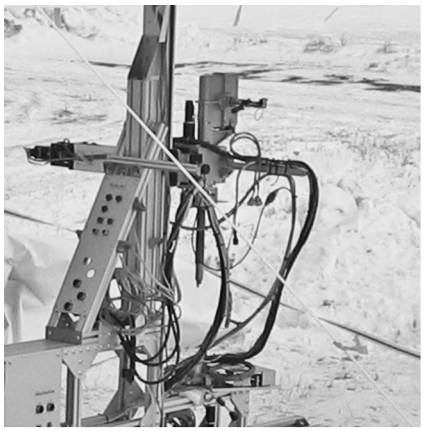

This is (b)

This is c

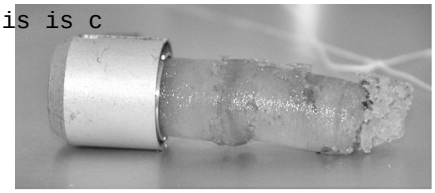

This is (a)

This is d

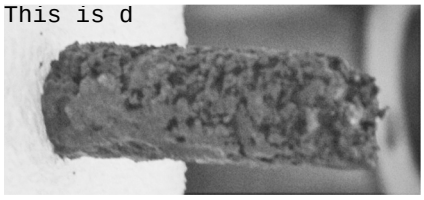

This is e

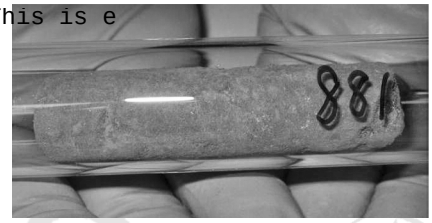

Figure 6.125 Images of(a) MPDS during laboratory limestone testing, (b) MPDS during Idaho Falls field test, (c) ice-soil core 1.5 × 10 cm captured, (d) frozen soil–pebble–rock core, and (e) solid basalt core. All core samples were created and captured during a 2 m Idaho Falls field test. Photographs courtesy of ATK Space.

dispose of the cuttings at the surface every so often. An added tether, on the other hand, could potentially speed up the trip of the mole to the surface. A prototype of the IDDS system was 90% fabricated and assembled; however, the project was put on hold due to funding cutbacks. At the time of this writing, no additional work has been planned.

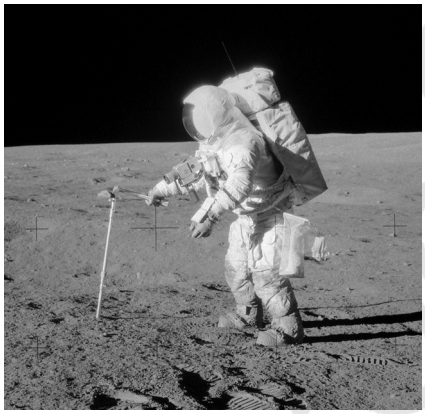

Figure 6.126 Astronaut Alan Bean hammering in a double-tube drive core near Halo Crater during the Apollo 12 mission. Courtesy NASA.

6.10.5
Modular Planetary Drill System (MPDS)

In 2004, ATK Space began a 4 year NASA-funded development of a modular planetary drill system (MPDS). The MPDS project goal was to develop a dry drilling system with a minimum depth capability of 20 m and possible maximum capability just beyond 50 m. This research faced the many challenges of planetary drilling technology development. Cuttings (fines) removal, axial preload, and borehole maintenance problems limit dry drilling. The cuttings accumulation consumes the limited energy of many drill systems. Drag friction, combined with subsurface formation layers that contain rock materials with high cuttings expansion or unstable borehole, can quickly cause the phenomenon of choking that leads to permanent segment jamming. Adding the complexity and issues of sample capture, recovery and handling to the overall drill system design were understood to be the main challenges of this research task. All of these issues were addressed to create this deep drill system.

Based on the successful SPECES design approach, the MPDS used a more advanced BHA, sample capture mechanism, and rotational and vertical drive systems capable of operating in extraterrestrial environmental conditions. The new BHA is capable of drilling through ice, frozen soil, and basalt with negligible wear. All cuttings and core samples are removed immediately after acquisition using an internal sample capture mechanism. A new custom remote-controlled wireline system operates without removing any segment from the borehole. Cores, of 1.5 cm diameter × 10 cm length, and fine cuttings are stored separately and brought to the surface to maintain a record of borehole stratigraphy for science investigation. The external surface of the drill segments act as a casing to provide borehole stabilization until the sampling process is completed and the target depth is reached. The MPDS provides an advantage over subsurface-drive drill systems due to the effective borehole maintenance and cuttings removal subsystems.

page proof WILEY-VCH

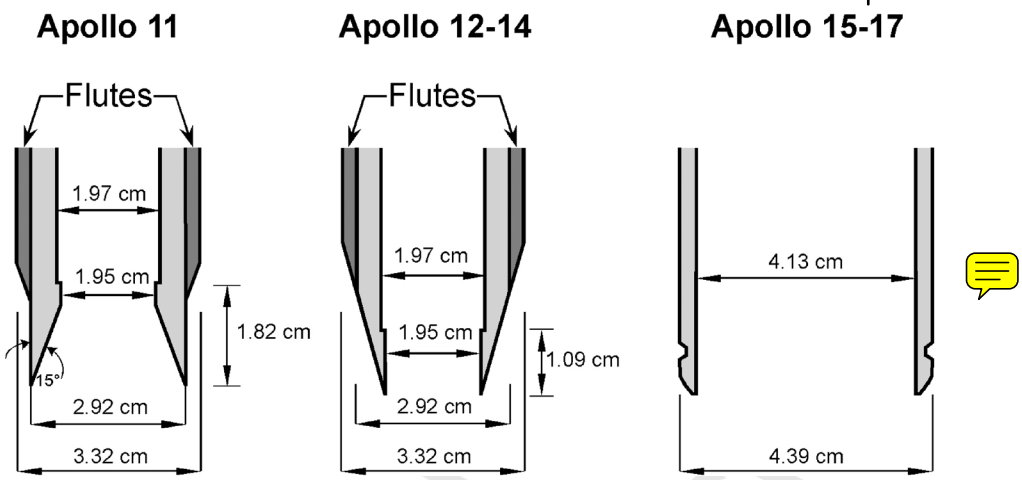

Figure 6.127 Comparison of Apollo drive tube bits. Modified from Scott *et al.* (1970) and Carrier *et al.* (1971). Courtesy NASA/MIT Press.

6.125

The design and integration phases were completed in early 2006 (see Figure 6.127). The development team tested the MPDS at Idaho National Laboratory (INL), Idaho Falls, ID, to penetrate ice–soil mixtures, frozen–soil–pebble–rock layers and hard basalt. New hybrid drill bits were developed and demonstrated to penetrate ice, permafrost, and hard basalt with negligible wear. The MPDS test results showed that drilling ice required 40–50 W, frozen soil mixture 50–70 W, and basalt about 80–100 W. The MPDS was able to drill through basalt down to 2.1 m. However, the MPDS drilling operations were affected by weather conditions (rain and melting ice) at the field site and limited the duration of the test at the INL site.

6.125

The MPDS field test, laboratory test, and demonstration were successful at penetrating ice, frozen soil, limestone rock, and hard basalt with no visible wear. Many high-quality cores samples were collected (see Figure 6.127). Critical drill subsystems were validated during the field and laboratory tests. During future stages of development, the MPDS prototype drill will be made available for collaborative field testing with other science instruments under NASA and other program efforts.

6.11 Past and Present Subsurface Access Missions

6.11.1 Apollo Drive Tubes and Drill

Drilling on the manned Apollo missions to the Moon were conducted via two methods: drive cores, which were hollow tubes hammered down manually into the regolith, and drill cores, which used a small electric motor to bore deeper into the substrate. In both cases, the drilling was conducted dry, that is, without the assistance

of drilling fluids. Retrieved core samples provide unique insight into the vertical structure and exposure history of the lunar regolith.

6.11.1.1 Drive Cores

Shallow (<1 m) regolith cores were collected throughout the Apollo program with drive cores. The design of the drive cores evolved through three iterations to improve retrieval of undisturbed lunar sediment. Drive tubes used on Apollo 11–14 were narrow aluminum tubes with an interior diameter of 1.95 cm at their narrowest point and an interior length of 31.75 cm (Allton, 1989). Each tube contained a thin inner aluminum sleeve that was divided into two lengthwise halves held together with a Teflon membrane. A detachable stainless-steel bit was affixed to the end of the core tube; once the core sample had been successfully retrieved, this was unscrewed and replaced with an aluminum cap. Inside the core tube was a spring-loaded Teflon follower. The followe 6.126 was displaced upwards as regolith entered the tube from below, forming a restraint for the upper soil boundary. An astronaut attached an extension handle to the upper end of the tube and drove it into the soil with blows from a rock hammer (Figure 6.128).

The first Apollo 11 drive tubes used bits with a 15° inward flange (Figure 6.129) that caused some distortion of the core stratigraphy during collection (Carrier *et al.*, 1971). On the Apollo 12 and 14 missions, bits with an outward taper were used so that th 6.127 walls of the sample tube remained parallel during collection (Figure 6.129). For Apollo 15–17, redesigned drive tubes with larger interior diameters of 4.13 cm, exterior diameters of 4.39 cm, and lengths of 37.5 cm were used (Mitchell *et al.*, 1972).

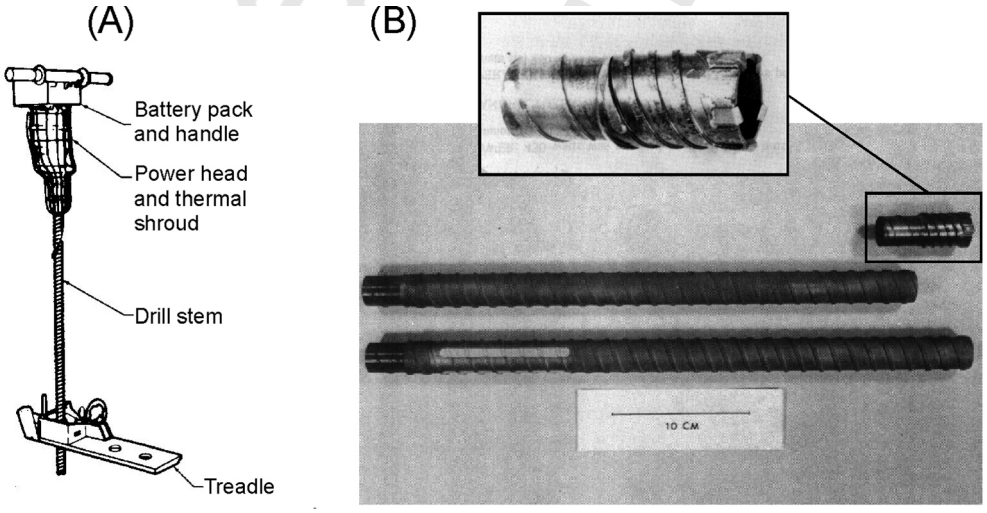

Figure 6.128 (a) Sketch of Apollo Lunar Surface Drill (ALSD) components in its assembled configuration (modified from ALSD Support Manual, 1971 and Allton, 1989). (b) ALSD drill stems and bit (NASA photograph S89-25295). Longer stem is standard-sized; shorter stem is lowermost stem to which bit attaches. Inset shows close-up of drill bit (from Allton, 1989). Images courtesy NASA/JSC.

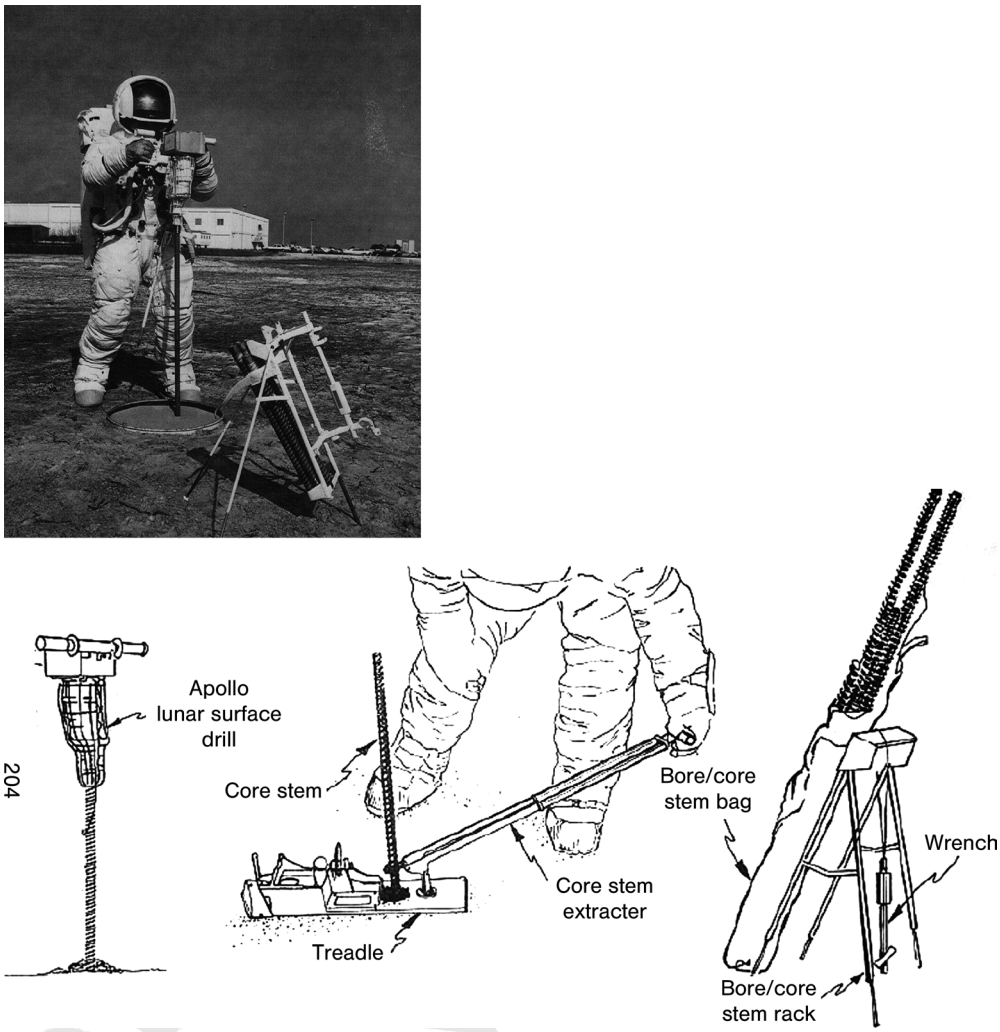

Figure 6.129 (a) Test engineer operating ALSD prototype; (b) illustration of ALSD system components. From Allton (1989). Images courtesy NASA/JSC. (Please find a color version of this figure on the color plates).

The larger diameter drive tubes reduced core self-compaction resulting from wall friction. Also, the Teflon follower was replaced with a plug that was manually loaded after the sample was in place, thus further reducing the resistance to the soil entering the tube. Drill bits were permanently affixed to the tubes, and an end cap was fitted over the bit following extraction (Allton, 1989). Tubes could be used singly or two core tubes could be screwed together to collect a deeper sample, though more forceful hammer blows were required to drive the double-tube assemblage into the regolith (e.g., Bean, Conrad and Gordon, 1970).

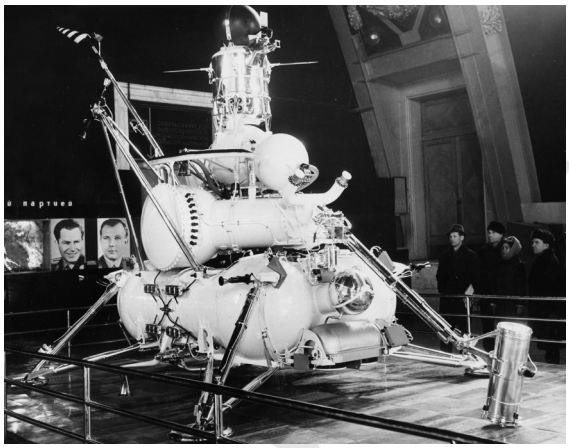

Figure 6.130 Luna 16 lunar lander on exhibit at the Cosmos Pavilion of the USSR Economic Achievements Exhibition in Moscow, November 1970. Photograph No. TASS-B-774448. Courtesy ITAR-TASS/Sovfoto.

6.11.1.2 Drill Cores

6.129 6.128

Deeper cores (up to 3 m deep) of lunar regolith were obtained using the ALSD, which was designed and built by Martin Marietta Corporation and is shown in Figures 6.130 and 6.131 (Martin Marietta Corp., 1971). The drill was battery powered and was driven by a rotary–percussive motor at approximately 2270 bpm (blows per minute) and 280 rpm (Fryxell and Heiken, 1974). It weighed a total of 13.4 kg, and was 57.7 cm tall by 24.4 × 17.8 cm (not including the drill string). As shown in Figure 6.130b, each core stem was about 40 cm in length and had an interior diameter of 2.0 cm and an

6.128b

Figure 6.131 Soviet lunar lander Luna 24 in the assembly shop prior to its mission, August 1976. In the foreground is its "soil intaker" (boring mechanism). Photograph No. TASS-B-917809. Courtesy ITAR-TASS/Sovfoto.

exterior diameter of 2.5 cm. A total of eight stems could be fitted together to attain a depth of just over 3 m. The stems were made of titanium alloy Al-4V; attached to the lower drill stem was a 6 cm drill bit that consisted of five tungsten carbide cutting tips brazed to a steel bit (Martin Marietta Corp., 1971). Helical flutes ran along the outer surface of the drill stems to clear cuttings as drilling progressed. It typically took 5–15 min to drill a hole, depending on the hardness and compaction of the substrate.

The ALSD was first deployed on the Apollo 15 mission, and significant difficulties were encountered during drilling and especially with the task of removing the core from the ground. A principal cause of these difficulties was the fact that the initial design of the drill stems did not include a continuous auger; the helical flutes on each drill segment were interrupted at the connection points between drill segments. As a result, the cuttings could not be completely cleared from the bore hole. Additionally, the resulting high torque levels on the chuck/stem interface caused the drill chuck to bind to the stem; in one case it was necessary to destroy the stem to detach it from the chuck (Scott, Worden and Irwin, 1972). Given the difficulty encountered during core extraction on Apollo 15, the treadle (stabilizing footplate) was modified to include a jack assembly. Core extraction was subsequently conducted ~~without~~ difficulty on Apollo 16 and 17.

6.11.2 Soviet Luna Drill

Developed by the Soviet Union for the Luna 16, 20, and 24 missions, the E-8-5 and E-8-5M sampling systems were designed to collect an unconsolidated sample from the lunar surface via a fully autonomous rotary–percussive drilling action (Williams, 2005). This achievement marked the first autonomous sampling of an extraterrestrial body. The Luna lander had both a descent and an ascent stage (Figures 6.132 ~~and 6.134~~). In addition to the drilling system, the ascent stage contained a hermetically sealed sample return container that was designed to return to Earth. The approximately 60 kN (Earth weight) lander was sufficiently heavy to react any loads created during the drilling process. The Luna 16 and 20 drill units were 69 cm long and 29 cm in diameter and had a mass of 13.6 kg. Operational parameters were as follows:

6.130

- maximum power: 140 W
- rate of penetration: 8–24 cm min^{-1}
- specific energy: 1.2–1.5 kJ cm^{-1}
- estimated torque: 0.2–0.3 N m.

The Luna 24 drill differed from the Luna 16 and 20 drills in that the penetration axis consisted of a pair of fixed rails that the drill head ran on. The earlier design, by comparison, utilized a robotic arm to lower the drill to the surface ~~(Figure 6.133)~~.

Q27

The Luna 24 drill was oriented at 30° with respect to the lander's vertical axis. The drills run at 500 rpm and penetrate the surface via a rotary–percussive action. It required 30 min to penetrate the lunar surface fully. Mechanisms were lubricated via an oil vapor that evaporated in the low-pressure environment on the Moon. The thin-walled drill tube had helical threads that enabled cuttings removal from the borehole. Regolith was captured in an elastic tube which was subsequently wound in a cylindrical

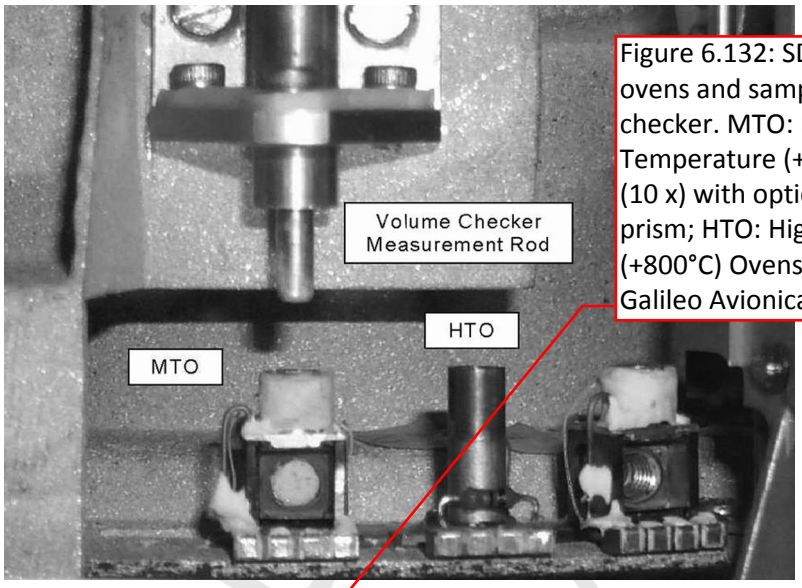

Figure 6.132: SD2-carousel with ovens and sample volume checker. MTO: Medium-Temperature (+180°C) Ovens (10 x) with optical sapphire prism; HTO: High-Temperature (+800°C) Ovens (16 x). Courtesy Galileo Avionica.

Figure 6.132 (a) The descent module of the Soviet space probe Venera 11 or 12 in the assembly and testing shop, 1978. Photograph No. TASS-B-983360. (b) A technician working on the soil drill assembly of the Venera 11 and 12 Soviet space probes, 1978. Photograph No. TASS-B-983654. Courtesy TASS/Sovfoto.

spiral inside of a hermetically sealed sample container ~~(Figure 6.135)~~. The sample
Q27 container was launched back to Earth where the sample coil was retrieved and rewound on to a helicoidal plate for analysis.

The Luna 16 lander arrived on the surface of the Moon in 1970 and penetrated to a depth of 35 cm in 7 min, when the drill tip hit hard rock that it could not drill through.

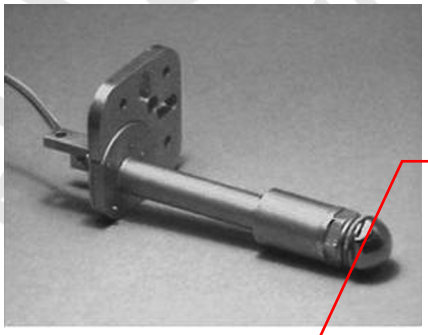

Figure 6.133: The HUYGENS penetrometer with its mast. Courtesy R. Lorenz, University of Kent & ESA.

Figure 6.133 Rosetta Philae SD^2 drill. (a) Situation on platform, drill partially extended, carousel visible at the base; (b) drill tip detail, shown with its sampler coring tube extended: the tube, retracted while drilling, remains extended for sample acquisition and is retracted during sample discharge. Courtesy Galileo Avionica.

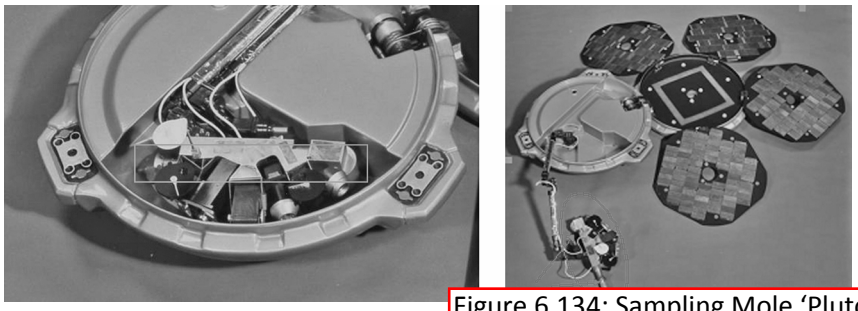

Figure 6.134 SD^2 carousel with ovens and sample checker. MTO, medium-temperature (+180 °C) ov with optical sapphire prism; HTO, high-temperatu ovens (16×). Courtesy Galileo Avionica.

Figure 6.134: Sampling Mole 'Pluto' on Mars Express – Beagle 2. Courtesy Derek Pullan, University of Leicester Beagle 2 team &DLR.

Regolith totaling 101 g was transferred to the soil sample container. Luna 20 arrived on the Moon in 1972 and penetrated to a depth of 25 cm, collecting 30 or 55 g of regolith (depending on the source documentation). The Luna 20 drill overheated multiple times during operation due to hard material in the target surface. Luna 24 landed on the Moon in 1976 and drilled to a depth of 2.25 m (2 m vertical), collecting an unconsolidated core 1.6 m long containing 170.1 g of sample (Barsukov, 1977).

A preliminary study of the Luna 24 core sample showed that once the elastic tube was filled, core stratigraphy was well maintained.

6.11.3
Venera Drill

Developed by the Soviet Union, the GZU system (Figure 6.136) was designed to drill a few centimeters into soil or rock for the Venera 13, Venera 14, Vega 1, and Vega 2 landed missions to Venus. The Venera 13 and 14 landers reached the surface of Venus in March 1982 and Vega 1 and 2 touched down in June 1985. Venera 13 and 14

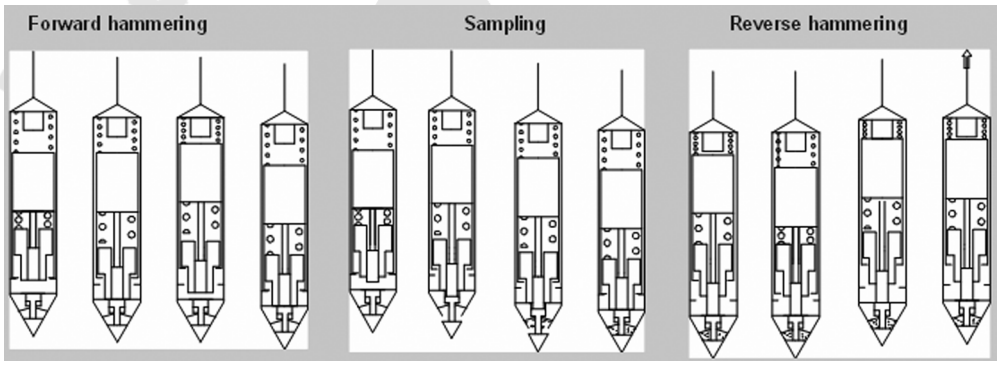

Figure 6.135 The HUYGENS penetrometer with its mast. Courtesy R. Lorenz, University of Kent and ESA.

Figure 6.135: Sampling Mole, main modes (forward/backward hammering and sampling). Courtesy ESA, DLR & VNII Transmash.

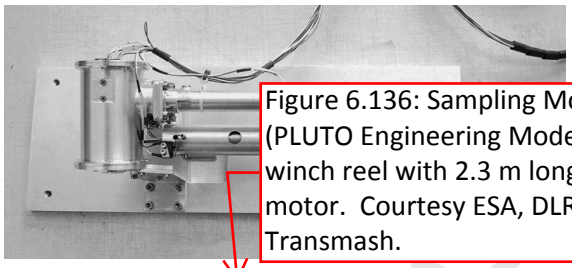

Figure 6.136: Sampling Mole in launch tube (PLUTO Engineering Model) – note the winch reel with 2.3 m long tether and its motor. Courtesy ESA, DLR & VNII Transmash.

Figure 6.136 Sampling mole PLUTO on Mars Express – Beagle 2. Courtesy Derek Pullan, University of Leicester Beagle 2 team and DLR.

were the first Venus landers to have a drill in their suite of instruments. Surface operation instruments included an XRF spectrometer, the GZU drill and surface sampler, a penetrometer, and a seismometer. The GZU assembly performed successful operations on each mission, with the exception of Vega 1 due to a malfunction during entry, descent, and landing that damaged the unit.

The GZU system was capable of drilling to depths of up to 30 mm in igneous rock. The system mass was 26.2 kg, the system height was approximately 500 mm, and the drill motor was capable of outputting 90 W. Total sampling cycle time was less than 200 s. The GZU operational sequence is as follows:

1. The drill head is lowered to the surface and the drill is turned on.
2. After 120 s of drilling, pyrotechnic charges break seals in pyrotechnic valves, allowing the Venus atmosphere (100 bar of CO_2) to flow through tubes. This acts to transfer a 1–6 cm^3 sample via a pressure differential from the drill head into soil transfer tubes and into a sample tray.
3. The sample tray is moved through an airlock, reducing the pressure, and the sample is dropped off to an XRF spectrometer via another set of pyrotechnic valves.

In addition to sample analysis, drilling telemetry was also utilized to determine soil physical properties.

During operations, the Venera 13 lander measured a temperature of 462 °C and a pressure of 88.7 bar. The Venera 14 lander measured a maximum temperature of 465 °C and a pressure of 94.7 bar.

6.11.4
The Rosetta Lander Drill, Sampler and Distribution System (SD2)

~~When the previously planned CNSR scenario had to be redefined,~~ the ESA mission Rosetta ~~was scaled back to a comet rendezvous. The spacecraft would~~ meet the comet ~~and remain "orbiting" at close distance but without landing on it. Its target is the comet~~ 67 P/Churyumov–Gerasimenko, ~~However,~~ the Rosetta spacecraft carries a lander as part of its scientific payload, known as Philae: this complex unit or "surface science package" will be ejected on to the comet. Its sampling subsystem [sampling,

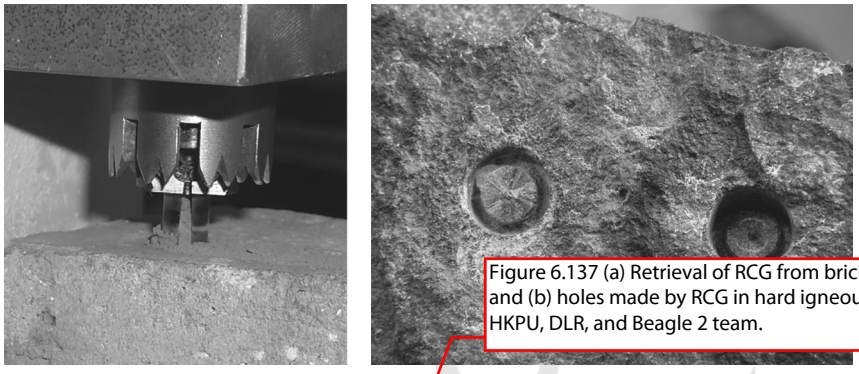

Figure 6.137 (a) Retrieval of RCG from brick after 15 min coring and (b) holes made by RCG in hard igneous rock. Courtesy HKPU, DLR, and Beagle 2 team.

Figure 6.137 Sampling mole, main modes (forward/backward hammering and sampling). Courtesy ESA, DLR, and VNII Transmash. (Please find a color version of this figure on the color plates.)

drilling and distribution (SD^2)] will acquire samples and deliver them to ovens. Subsequently, they will be analyzed by a microscope and gas chromatographs (such as CIVA, ~~CESAC~~ and Modulus) (Magnani *et al.*, 1998). SD^2 consists of the following components:

- an integrated drill/sampler having the function of drilling the soil, collecting the samples and discharging them into the ovens
- a carousel that accommodates the ovens for sample containment and moves the ovens to the different experiment locations
- a volume checker for estimating the collected sample volume
- an electronics unit for managing the system with a high degree of autonomy.

The drill, mounted on the platform "balcony", ~~is~~ lowered to the surface (30 cm maximum below), and then must penetrate the soil at least 20 cm ~~(Figure 6.137a)~~. The drill OD is 12 mm and it contains polycrystalline diamond inserts as cutting teeth. A small concentric tube of 2.5 mm ID may be extended axially up to 6.5 mm out of the tip by an electromagnet ~~(Figure 6.137b)~~.

Having reached the desired depth in the soil, the drill ~~is~~ lifted by 1 mm and the sampling tube ~~is~~ released ~~against the soil; the~~ drill ~~rotates~~ again for 20 s and ~~is~~ then retracted~~: a~~ sample of drill cuttings and soil will be collected ~~by adherence. Then, on the Philae platform,~~ by retracting the tube the sample ~~is~~ discharged into one of the 26 ovens present on the carousel (Figure 6.138). The sample volume ~~is then~~ checked. The SD^2 sampler flight envelope is approximately $0.2 \times 0.16 \times 0.76\ m^3$~~; the~~ drill may be deployed by ~~0.58 m;~~ the total mass is 5.1 kg, including 3.7 kg for the mechanical unit~~, 1 kg~~ for the electronics and 0.4 kg for the harness~~;~~ peak power is 14.5 W, average during drilling/sampling 6.0 W and~~1.5 W~~ average in standby. Drilling tests in "Gas-Beton" (porous concrete) at −150 °C ~~that was~~ used as a soil simulant ~~could be~~ performed with a torque of less than 0.2 N m and a thrust between 10 and 20 N at 100 rpm. ~~The penetration depth increased with the rotary speed and power, varying from 14 cm at 100 rpm and 1.8 W to 47 cm at 500 rpm and 6.1 W.~~

6.132

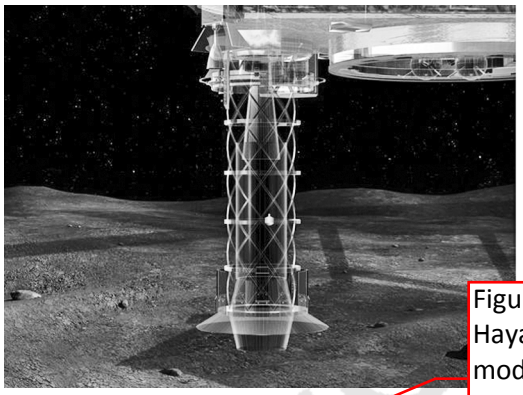

Figure 6.138: Left: Artist's rendering of the JAXA Hayabusa spacecraft (Courtesy JAXA); Right: flight model of the Hayabusa sampler horn. Courtesy JAXA.

Figure 6.138 Sampling mole in launch tube (PLUTO E Model) – note the winch reel with 2.3 m long tether and its motor. Courtesy ESA, DLR, and VNII Transmash.

SD^2 is a sampling and distribution device; it benefits from the expertise acquired during the precursor sampling studies of ESA: the design team which developed the SD^2, formed by Galileo Avionica, Tecnomare and Rodio, took part in the SAS-3m, SAS-1m and SSA/DT studies. The Italian Space Agency, Agenzia Spaziale Italiana (ASI), delivered SD^2 to the Philae team, ~~which is~~ German led with French and Italian cooperation. Rosetta was launched on 2 March 2004~~; it~~ is due to rendezvous with Comet 67 P/Churyumov–Gerasimenko in May 2014. The Philae Lander ejection and operations should start in November 2014, after completion of the global mapping of the comet.

6.11.5
The Huygens Penetrometer

6.133

In the NASA–ESA joint mission Cassini–Huygens, launched on 15 October 1997, the Huygens probe from the ESA was carried by the NASA spacecraft Cassini. Huygens was ejected towards Saturn's moon Titan and impacted its surface on 14 January 2005. The penetrometer (Figure 6.139), part of the Huygens Surface Science Package, was a short mast (approximate diameter 15 × 100 mm) with a piezoelectric washer mounted under the probe~~; it~~ measured the surface impact of the Huygens probe and transmitted nominally its data, revealing a "soft solid surface" (Zarnecki *et al.*, 2005). It was built by R. Lorenz at the University of Kent (UK) (Lorenz *et al.*, 2001). It is worth noting that this penetrometer is actually the first instrument ever aboard an ESA lander which contacted an extraterrestrial body.

6.11.6
Sampling Mole PLUTO on Mars Express – Beagle 2

6.134

The lander Beagle 2 was carried by the ESA spacecraft Mars Express as part of its scientific payload (Figure 6.140). After launch on 2 June 2003, Beagle 2 was ejected

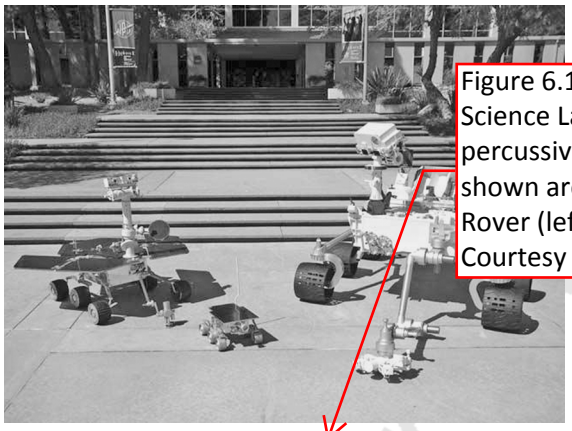

Figure 6.139: The Full scale model of NASA Mars Science Laboratory Rover (right) with a rotary percussive drill at the end of the robotic arm. Also shown are full sacle models of Mars Exploration Rover (left) and Sojourner rover (center). Image Courtesy NASA/JPL-Caltech.

Figure 6.139 (a) Retrieval of RCG from brick after 15 min coring and (b) holes made by RCG in hard igneous rock. Courtesy HKPU, DLR, and Beagle 2 team.

towards Mars on 19 December 2003. Despite a nominal ejection, Beagle 2 was unfortunately lost ~~and never retrieved.~~ Beagle 2 was to deploy a robotic arm, holding at its end a multifunctional end-effector, the ~~PAW.~~ The main sampling tools of the PAW were the RCG and the PLUTO sampling mole. The PAW contained numerous scientific instruments that were designed to be served by these sampling tools. A stereo camera, an XRS, a Mössbauer spectrometer, a microscope, and a wind sensor

Figure 6.140: The MSL drill pulverizing volcanic rock. Image Courtesy NASA/ JPL-Caltech.

Figure 6.140 (a) Artist's rendering of the JAXA Hayabusa spacecraft; (b) flight model of the Hayabusa sampler horn. Courtesy JAXA.

Figure 6.141: Artist's impression of the ExoMars rover drilling into the martian surface (Drill Box cover removed for clarity). Courtesy ESA.

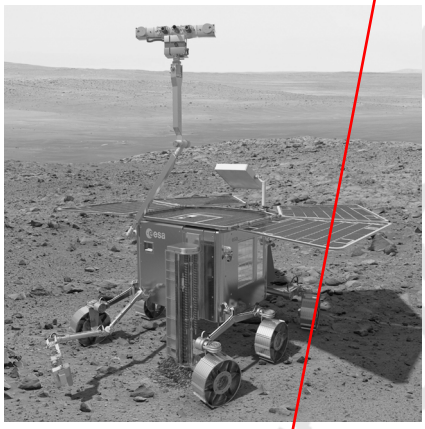

Figure 6.141 Full-scale model of the NASA Mars Science Laboratory Rover (right) with a rotary percussive drill at the end of the robotic arm. Also shown are full-scale models of Mars Exploration Rover (left) and Sojourner Rover (center). Image credit NASA/JPL.

made up the instrument suite of the PAW (Phillips, 2001). PLUTO was a flight model of the sampling mole previously developed for ESA; DLR and VNII Transmash completed the qualification of this item for the Beagle team (Richter *et al.*, 2000, 2002). Sampling was performed at the tip: a cavity in the tip could be opened axially a few millimeters; during further penetration, ~~it served to catch~~ some grains of soil inside. Retrieval to the surface was carried out by a winch pulling a tether assisted by backward hammering; this additional feature greatly helped extraction of the mole. With this sampling system, the sampling mole would then deliver its sample to a port above the surface.

PLUTO ~~was part of the "PAW" composite of instruments and tools: it had to be released from the PAW at the end of the deployed arm. Nominally~~ deployed on to the surface from a vertical position, ~~it~~ would penetrate and sample Mars soil down to a depth of 2 m; ~~it would be brought back to the surface, with backwards hammering, and then positioned by the robotic arm above the sample delivery port.~~ Figure 6.142 shows a photograph of the sampling mole in its launch tube. ~~Additional plans to let PLUTO crawl on the surface were contemplated towards moving further away from the lander and acquire a sample from beneath a nearby large rock.~~

6.136

6.11.7 The Beagle 2 Rock Corer Grinder (RCG)

6.137

This instrument flew aboard the "ill-fated" Beagle 2 mission; more details may be found in the previous section. Figure 6.143, views of a protoflight model testing, shows retrieval of a 10 mm long core and some remnant holes. The RCG was conceived and prototyped by an HKPU team, which then developed it under DLR management within the Beagle 2 team.

page proof WILEY-VCH

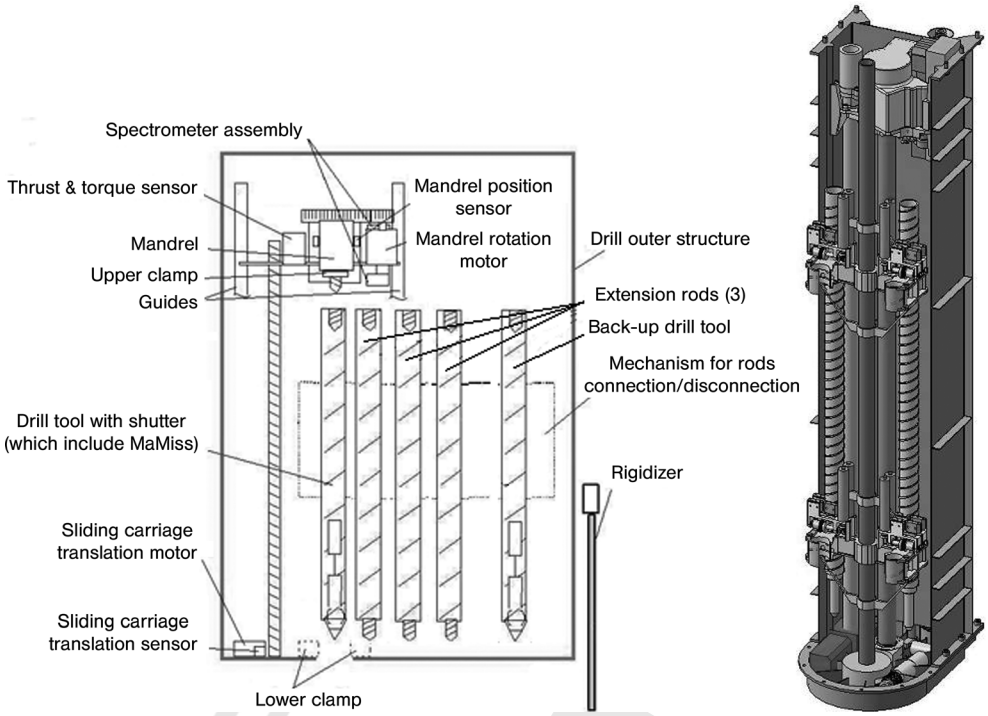

Figure 6.142 The MSL drill pulverizing volcanic rock. Image credit NASA/JPL

Figure 6.142: Drill box: schematics and configuration. Courtesy Galileo Avionica (from ExoMars activities for ESA

6.11.8
Asteroid Surface Sampling Device

Developed by JAXA, the asteroid surface sampling device (A 6.138 flown on the Hayabusa, or MUSES-C, spacecraft (Figure 6.144) to collect surface samples from the 25 143 Itokawa asteroid. The ASSD fires a 5 g projectile at the asteroid's surface at a velocity of 300 m s^{-1}. A cone and sample return chamber is used to collect the ejecta.

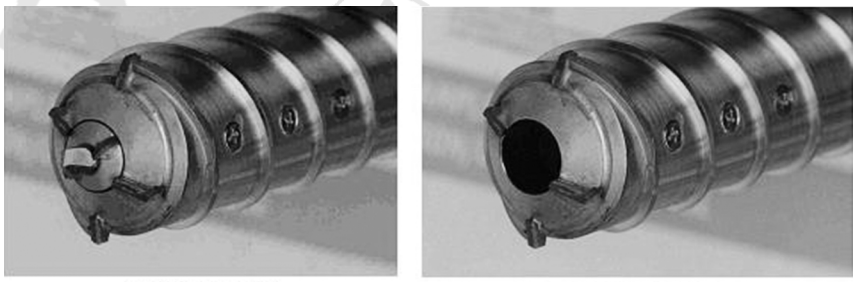

Figure 6.143 Artist's impressi
into the Martian surface (drill
Courtesy ESA.

Figure 6.143: Picture showing a drill tool prototype in drilling mode (left) and in sampling mode (right). Courtesy Galileo Avionica (from DeeDri activities for ASI)

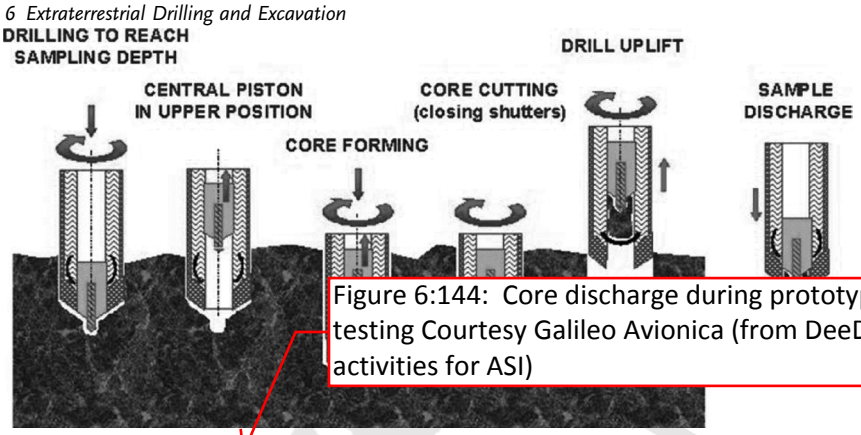

Figure 6:144: Core discharge during prototype testing Courtesy Galileo Avionica (from DeeDri activities for ASI)

Figure 6.144 Drill box: schematics and configuration. From ExoMars activities for ESA. Courtesy Galileo Avionica.

Total sample collected is expected to be on the order of 0.1–10 g with a size fraction in the sub-millimeter range.

The Hayabusa spacecraft is currently traveling back to Earth with a planned sample container re-entry in 2010. Although the spacecraft successfully approached in close proximity to the asteroid for sampling, questions have been raised as to whether the sampler was able to capture any material due to uncertainty as to whether or not the projectiles were fired during surface contact.

6.12 Future Sampling Missions

6.139

6.12.1 The Mars Science Laboratory (MSL) Rover Drill

The MSL rover is a roving mission schedule to launch in late ~~2009~~ (Figure 6.145). The rover itself weighs almost 1000 kg and is the size of a small car. The MSL rover will be

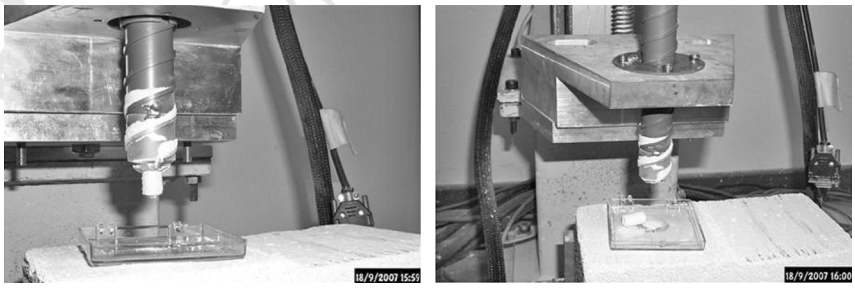

Figure 6.145 A drill tool prototype in drilling mode and in sampling mode. From DeeDri activities for ASI. Courtesy Galileo Avionica.

Figure 6:145: Sampling procedure: discharge of collected sample during. Courtesy Galileo Avionica (from ExoMars activities for ESA).

page proof WILEY-VCH

powered by a radioisotope power system that generates electricity from the heat of plutonium's radioactive decay. This power source will allow the mission to operate on the surface of Mars for a full Martian year (687 Earth days) and possibly more. In addition, it will allow some operation at night since the power is continuous (as opposed to solar-powered spacecraft that can operate only when the Sun is ~~up~~). The rover will be able to traverse close to 20 km on the surface of Mars during a single Martian year.

The scientific goal of the MSL mission is to explore and assess the surface of Mars as a potential habitat for past or present life.

The MSL rover will have 10 scientific instruments weighing a total of 80 kg. The largest ones are the Sample Analysis at Mars (SAM) and Chemistry and Mineralogy X-Ray Diffraction/X-Ray Fluorescence Instrument (Chemin). SAM consists of the chemical separation and processing laboratory: a combined gas chromatograph–mass spectrometer and a tunable laser spectrometer. It can analyze organics and gases from both atmospheric and solid samples. The Chemin is a combined X-ray diffraction–X-ray fluorescence instrument and it will quantify minerals and the mineral structure of powder samples. Thus both instruments require small, powdered samples. These powdered samples will be acquired by the MSL drill.

The MSL drill is a rotary–percussive drill able to penetrate [illegible] cm into rocks ranging from soft sedimentary to strong basalts and to acquire rock cuttings from depths ranging from 0.5 to 5 cm (Figure 6.146). The drill percussive motion is actuated by a voice coil assembly. One of the requirements for this drill system included the ability to support the entire rover in case all six wheels of the rover slip on a 20° slope. If for some reason the drill becomes stuck in a rock, the rover can hammer and rotate the drill to try to pull it back. If that fails, the rover can release the drill bit and replace it with another one (the drill will have a few spare drill bits).

6.12.2
The ExoMars Drill

ESA plans to launch the ExoMars mission in ~~2011, landing in 2013.~~ A spacecraft carrying a rover payload (Figure 6.147) will be sent to Mars to perform, among other tasks, the following:

1. land on, or traverse to, a location with high exobiology interest for past and/or present life signatures, ~~that is,~~ access to the appropriate geological environment
2. collect scientific samples from different sites using a rover carrying ~~a~~ drill capable of ~~reaching well~~ into the soil and surface rocks (Vago *et al.*, 2006).

Figure 6.146 Core discharge durin[illegible] DeeDri activities for ASI. Courtesy

Page Proof © WILEY-VCH

Figure 6.147: Positioner operations of drill box on rover: 1) launch and rover progression; 2) drilling/ coring; 3) sample discharge. Courtesy Galileo Avionica (from ExoMars activities for ESA)

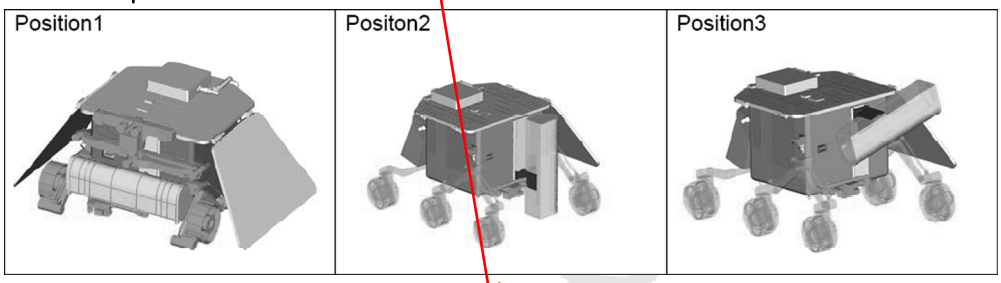

Figure 6.147 Sampling procedure; discharge of collected sample, prototype testing. From ExoMars activities for ESA. Courtesy Galileo Avionica.

6.142

The ExoMars corer/drill (Figure 6.148) may acquire core samples at selected intermediate depths down to 2 m, using up to three extension rods. The drill carries a built-in imaging instrument, the Mars Multispectral Imager for Subsurface (MaMiss), which observes the drilled hole through a lateral optical window at approximately 20 cm above the tip (Ammannito *et al.*, 2008) and provides core samples to the "Pasteur" instrument payload (Vago *et al.*, 2006). The ~~model~~ soil is a homogeneous soil matrix with embedded fractured basaltic rock material of different sizes. The matrix – a poorly consolidated dust/sand ("duricrust") – is assumed to have cohesion of 8–12 kPa, from the surface to 2 m. The unconfined compressive fracture strength of the rock material is up to approximately 100 MPa.

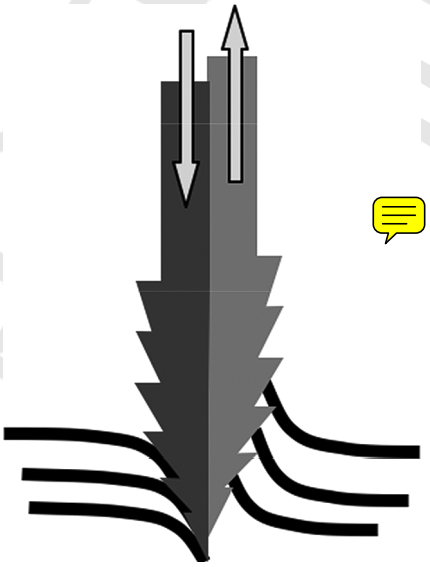

Figure 6.148 ExoMars drill tool breadboard development model: disassembled parts and detail of open shutter. From ExoMars activities for ESA. Courtesy Galileo Avionica.

Figure 6.148: Digging action of Sirex Noctilio ovipositor.

Details of the soil specifications are as follows:

- *Homogeneous soil:*
  -Poorly consolidated dust/sand or duricrust, formed by surface/atmosphere interactions leading to cementation in the presence of solutes and water (e.g., Viking-1 blocky soil).
  -Assumed bulk density: 2000 kg m^{-3} at the surface, rising to 2850 kg m^{-3} at 1 m depth, 2925 kg m^{-3} at 2 m depth, and 2950 kg m^{-3} at 3 m depth.
  -Assumed cohesion: 8 kPa at the surface, rising to 11.6 kPa at 1 m depth, 12.2 kPa at 2 m depth, and 12.4 kPa at 3 m depth.
  -Assumed angle of internal friction: 34° at the surface, rising to 48° at 1 m depth, 49° at 2 m depth, and 49.5° at 3 m depth.

- *Embedded rocks:* unconfined compressive fracture strength 6.143 150 MPa, bulk density 2700–3100 kg m^{-3}.

The tool consi 6.144 ollow tube equipped with an auger thread on its outer surface and a dri the lower end (Figure 6.149). The drill has a diameter of 25 mm and is about 0.5 m long. A nominal core sample has a diameter of 10 mm and a length of 20 mm. Figure 6.150 illustrates the sampling procedure: the corer/drill head is closed in the drilling mode; at a desired depth, the advance is stopped and the head is set up in sampling mode: the tip, linked to a motorized central

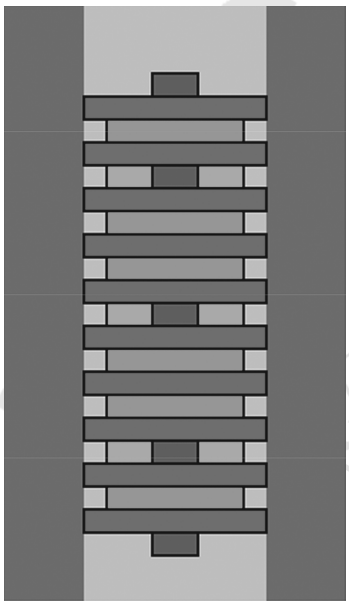

Figure 6.149 Positioner operations of drill box on rover: position 1, launch and rover progression; 2, drilling/coring; 3, sample discharge. From ExoMars activities for ESA. Courtesy Galileo Avionica. (Please find a color version of this figure on the color plates).

Figure 6.149: Descending system based on earth-worm locomotion

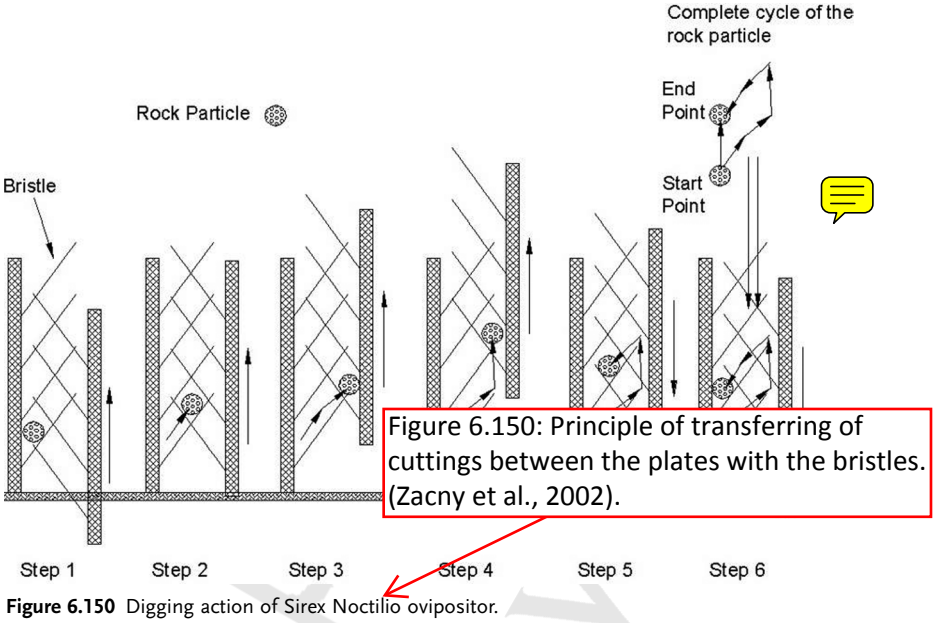

Figure 6.150: Principle of transferring of cuttings between the plates with the bristles. (Zacny et al., 2002).

Figure 6.150 Digging action of Sirex Noctilio ovipositor.

piston, is retracted, forming a corin[illegible]. The drill advance is resumed; when the cavity is full, stopping advance, [illegible] is progressively closed, cutting the base of the core and eventually closing the corer. The drill/corer is extracted from the hole to discharge its sample: the shutter is opened and the central piston pushes the core. Figure 6.151 shows also a core discharge during prototype testing. Figure 6.152 shows disassembled parts of a prototype development model of the drill tool.

6.145

6.146

The ExoMars drill/corer inherits several features developed previously for the DeeDri drill for the ASI (Magnani *et al.*, 2004), within studies which followed the SAS drill/corer for ESA. The full 2 m drill string is composed of a drill tool and three extension rods, each about 0.5 m long. The mechanical interfaces joining the extension rods together and to the drill are threads. They also provide electrical interfaces via an axial stack of electrical contacts, with an optical fiber connection for the imager. A secondary drill tool is provided as sampling back-up, without imager. The drill tools and extension rods are stored on a carousel. The mandrel is translated along a sliding carriage during drilling, core sample acquisition and retri[illegible] assembly and disassembly of the extension rods. These latter operations are assisted with upper, lower and carousel sets of clamps (Figure 6.152).

6.146

A maximum thrust of 300 N is anticipated. A drill box structure, made of carbon fiber, encloses the drill unit that is formed by the drill and its extension mechanisms. The drill box overall envelope is $180 \times 250 \times 820$ mm. The drill unit is mounted on the front part of the rover, supported by a positioner which allows it to pivot from horizontal (during cruise and rover progress) to vertical (for

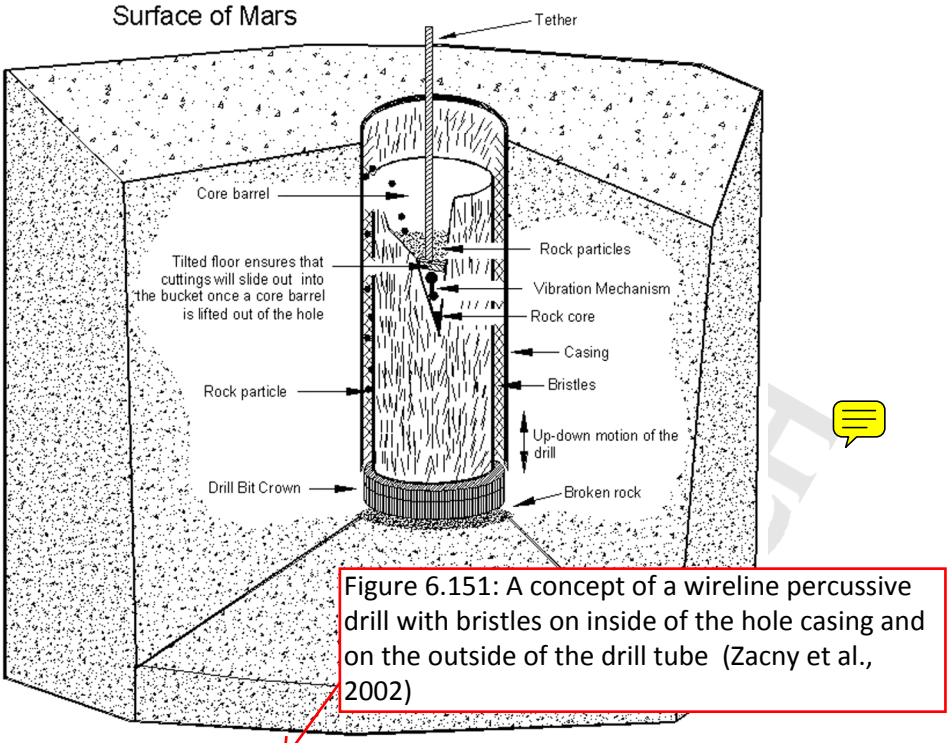

Figure 6.151: A concept of a wireline percussive drill with bristles on inside of the hole casing and on the outside of the drill tube (Zacny et al., 2002)

Figure 6.151 Descending system based on earthworm locomotion.

nominal drilling) and to translate vertically (Figure 6.153). In a worst case where the rover would be anchored by its drill, it could, as a last-resort rescue solution, detach the whole drill box and positioner with an emergency separation mechanism based on Frangibolts.

6.147

6.12.2.1 ExoMars Heat Flow and Physical Properties Instrument HP3

The heat flow and physical properties instrument HP3 is part of the ExoMars Geophysical and Environmental Package, mounted on the platform supporting the ExoMars rover until landing. ~~Within HP3,~~ an instrumented mole system ~~future sampling developments~~ will deploy sensors down to 5 m. The HP3 mole will be sized to house the flight sensors.

6.13 Future European Prospects in Science and Exploration Programs

The prospects for European future developments including extraterrestrial landings are described in two recent programs of the ESA: Aurora and Cosmic Vision.

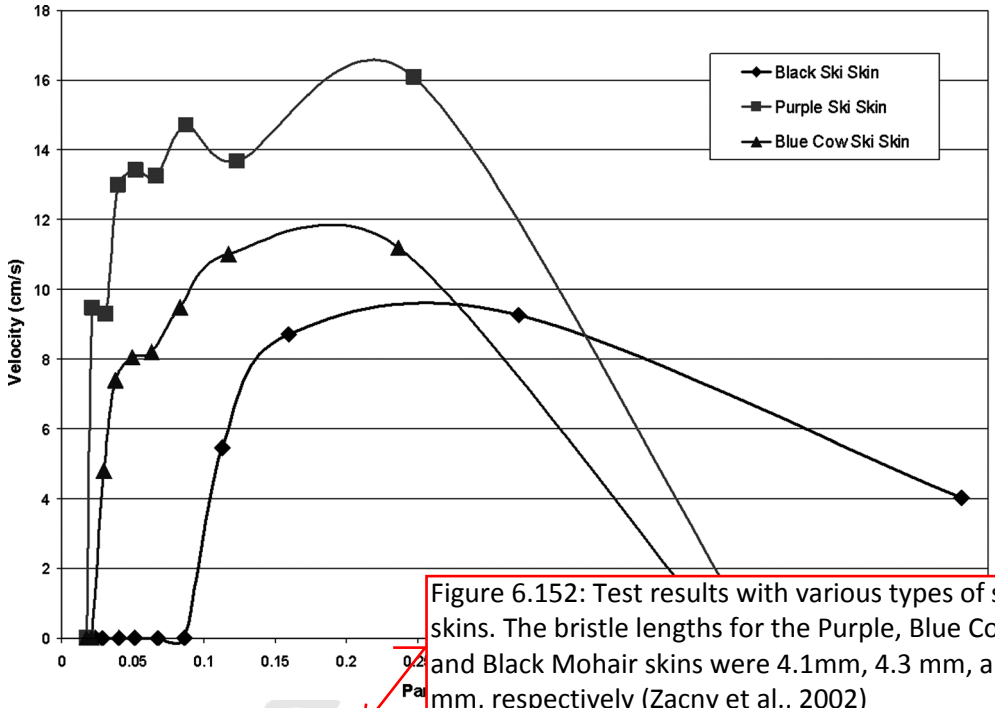

Figure 6.152: Test results with various types of ski skins. The bristle lengths for the Purple, Blue Cow and Black Mohair skins were 4.1mm, 4.3 mm, and 3.2 mm, respectively (Zacny et al., 2002)

Figure 6.152 Principle of transferring cuttings between the plates with the bristles. Courtesy Honeybee Robotics.

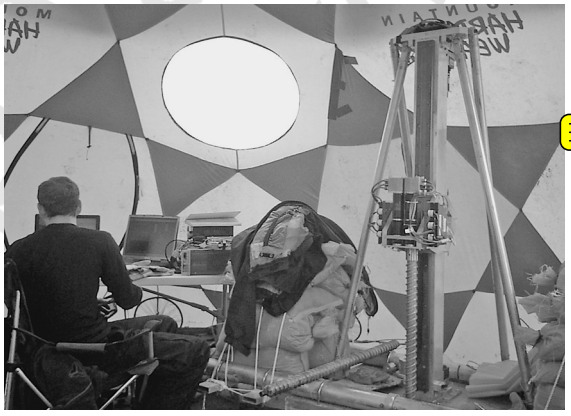

Figure 6.153 Concept of a wireline percussive drill with bristles on the inside of the hole casing and on the outside of the drill tube. Courtesy Honeybee Robotics.

Figure 6.153: The DAME drill hardware was a Mars-prototype derived from the Honeybee Robotics Advanced Deep Drill. Courtesy Honeybee Robotics.

6.13.1 Aurora

Aurora was defined in 2001 as an exploration and technology program, performed in a stepped approach that culminates in human exploration with, eventually, the establishment of an extraterrestrial human colony on Mars. The current ExoMars mission that plans to send a rover for exobiological exploration with deep drilling, and the future MSR mission that is currently being studied, were both initiated in the Aurora program. Other exobiology missions to Mars following ExoMars include an MSR mission and associated preparatory missions are expected to follow. International cooperation including NASA is anticipated. Marco Polo is a near-Earth object sample return mission studied within the Cosmic Vision program; it has been proposed by lead scientists from France, Japan and the United States. Marco Polo is currently undergoing an assessment study. Sampling missions to Europa have already been studied at the ASI and may become part of Cosmic Vision.

6.13.1.1 Aurora Program

Aurora is part of Europe's strategy for space exploration and has been endorsed by the European Union Council of Research and the ESA Council in 2001. This strategy calls for Europe to (1) explore the solar system and the universe, (2) stimulate new technology, and (3) inspire the young people of Europe to take a greater interest in science and technology.

As a result, in 2001 ESA set up the Aurora program. The primary objective of Aurora is to create, and then implement, a long-term European plan for the robotic and human exploration of the solar system, with Mars, the Moon, and the asteroids as the most likely targets. A second objective is to search for life beyond the Earth. Future missions under the program will carry sophisticated exobiology payloads to investigate the possibility of life forms existing on other worlds within the solar system. The interdependence of exploration and technology is the basis of the Aurora program. It is recognized that the desire to explore provides the stimulus to develop new technology while only through the introduction of innovative technology will that exploration be made possible.

6.13.1.2 Step-by-Step Approach

Aurora's step-by-step approach means that missions will increase in complexity over time, culminating if all goes well in a human expedition to Mars by 2030. Steps on the way to Mars will probably include exploration of the Moon and also (1) remote sensing of the Martian environment, (2) robotic exploration and surface analysis, (3) MSR missions, and (4) a robotic outpost.

Not all of these steps towards the ultimate goal of sending humans to Mars will necessarily be part of the Aurora program. As a result of international cooperation, it is expected that the various collaborating agencies will make a contribution to those missions that best meet their particular requirements and areas of expertise.

page proof © WILEY-VCH

6.13.2
Cosmic Vision

The Cosmic Vision program, defined in 2005, looks towards space science for Europe in the period 2015–2025 (Bignami *et al.*, 2005). In particular, it addresses the question: what are the conditions for planet formation and the emergence of life? Cosmic Vision is consistent with Aurora in its exobiology theme, but keeps the question of human exploration otherwise open. In 10–20 years from now, a succession of new spacecraft will make up ESA's continuing science program, now called Cosmic Vision. These missions will address the scientific questions that are high on the agenda of research across Europe (and, indeed, worldwide) concerning the Universe and our place within it:

- What are the conditions for planet formation and the emergence of life?
- How does the Solar System work?
- What are the fundamental physical laws of the Universe?
- How did the Universe originate and what is it made of?

The quest for evidence of a second, independent genesis of life in the Solar System must begin with an understanding of what makes a planet habitable and how habitable conditions change, either improving or degrading with time. For instance, the environmental conditions on the Earth today are not the same as when life first arose on this planet. The early Earth, with its oxygen-free atmosphere, high ultraviolet radiation, high temperatures, and slightly acidic waters, could not support the highly evolved life forms so familiar to us today. However, life could not have arisen on a planet with the environmental conditions that exist on Earth today.

The Cosmic Vision program has the goal of exploring *in situ* the surface and subsurface of solid bodies in the Solar System most likely to host – or have hosted – life. Important considerations include:

1. Mars is ideally suited to address key scientific questions of habitability. Europa is the other priority for studying internal structure, composition of oceans and icy crust and the radiation environment around Jupiter.

2. Environmental conditions for the appearance and evolution of life include not only geological processes, the presence of water, and favorable climatic and atmospheric conditions, but also the magnetic and radiation environments determined in part by the Sun's magnetic field.

These considerations have led to the following mission scenarios:

1. Mars exploration with landers and sample return.
2. Europa orbiter and/or lander as part of a Jupiter Exploration Programme (JEP).
3. Solar polar orbiter to chart the Sun's magnetic field in three dimensions.

page proof WILEY-VCH

6.14
Bio-Inspired Drilling Systems for Future Space Applications

6.14.1
Biomimetics

Nature's systems have been a source of inspiration for the conception of novel inventions for thousands of years. Researchers have recently shown an increasing interest in investigating biological systems through a systematic approach and *biomimetics* has thus become a well-defined scientific discipline (Bar-Cohen, 2005). Biomimetics could be defined as "the practice of reverse engineering ideas and concepts from nature and implementing them in a field of technology" (Menon, Ayre and Ellery, 2006a). Several compelling factors point towards the attractiveness of a biomimetic approach:

1. Engineers often face problems that have already been addressed and solved by Nature.
2. Nature evolved through a very stringent optimization process based on natural selection over millions of years – natural solutions are robust.
3. Numerous biological systems show features desirable for space systems, such as autonomy, adaptability, and holistic design.

Engineers should, however, be aware of some caveats while they take inspiration from Nature:

1. It is fairly rare to find engineering objectives that perfectly match natural objectives – natural organisms should not generally be simply copied.
2. Natural solutions often represent *locally* optimal solutions.
3. There exist excellent engineering solutions that are *not* bioinspired – a bioinspired approach is not always suitable.

Considering the aforementioned advantages and caveats, ~~biomimetics~~ approaches are described here suggesting designs of drilling systems that are potentially applicable for *in situ* exploration in space. Drivers for such space systems include low mass, volume, and power consumption, in addition to robustness and autonomy, areas in which many biological drilling systems excel. Earlier in this chapter, the ultrasonic/sonic gopher was described following the concept of incrementally removing material from the subsurface while advancing inwards. Further, an earthworm system was described modeling the biological creature. The concept designs of three other penetrating systems, a descent mechanism, and a material transport system are presented and discussed in the followings sections.

As mentioned in Chapter 1, Nature presents a large number of examples of digging systems. Several species belonging to both flora and fauna are capable of digging into soil, rocks, trees, and other substrates to deposit eggs, find nutrients, escape from predators, build burrows, and so on. Three natural digging systems and their corresponding engineering concept designs are described in this section.

Page proof © WILEY-VCH

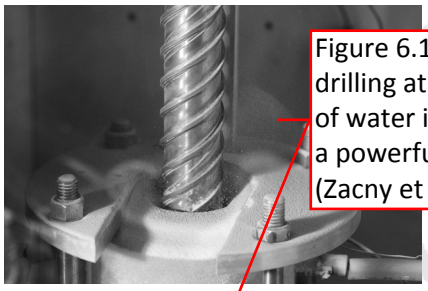

Figure 6.154: Sublimation of ice during drilling at pressures below the triple point of water in ice-bearing formations can be a powerful cuttings cleaning mechanism (Zacny et al., 2004).

Figure 6.154 Test results with various types of ski skins. The bristle lengths for the purple, blue cow and black mohair skins were 4.1, 4.3, and 3.2 mm, respectively.

6.14.2
Bio-Inspiration from Wood Wasp Digging System

6.148

Sirex noctilio, a type of wood wasp, utilizes a longitudinal cyclical motion in its two ovipositor valves to penetrate wood (Vincent and King, 1996), as shown in Figure 6.154. Directionally active teeth on each valve alternately provide a reaction force for the drilling action. These teeth become pockets on different sides that allow transport of debris away from the cutting edges and are spaced to distribute forces evenly along the valve. The behavior of the valves in stabilizing each other during alternate compression and tension phases like inner and outer components of a Bowden cable means that forces may potentially be transferred over unlimited distance. Mimicry of such a system includes the inherent potential for miniaturization, with a maximum valve dimension along its length of 10 mm.

In addition to a preliminary macro-scale engineering design, different micro-fabrication techniques were considered, in the frame of an ESA-funded study, for their potential to produce valves with features on similar scales to those of the biological system and to explore possibilities for a miniaturized system based on this concept (Menon *et al.*, 2006c; Gao *et al.*, 2007). First iterations of mimicked valve morphologies were found to be achievable using current techniques with different methods leading to differing translations of micro-scale tooth-like features on a variety of structural materials. Realization of a workable system would require the refinement of such processes along with integration with other micro-scale subsystems, particularly for actuation.

6.14.3
Plant-Inspired Space Probe

Pioneering species of plants are well known to be able to grow on uncolonized land with few nutrients. For instance, fireweed is a well-known pioneering species that grows on burnt sites after forest fires, and Buckler leaved sorrel (*Rumex scutatus*) lives on solidified lava. Harsh terrestrial environments have extraterrestrial similarities, providing us with motivation to investigate how pioneering plants manage to survive.

The growth of the ramified roots of plants follows environmental inputs such as gravity, light, touch, and humidity gradients (Eapen *et al.*, 2005;Esmon, Pedmale and Liscum, 2005). Roots are able to penetrate into a large variety of substrates, and are able to grow on rocks. Sensors embedded in the root apex permit the analysis of the environment and the finding of locally optimal paths for growth. Plants process information gathered from the environment and autonomously ~~identifies~~ optimal paths to (1) penetrate efficiently into the terrain, (2) search for and absorb nutrients, and (3) provide anchorage, albeit on a longer time scale.

By taking inspiration from Nature, a plant-inspired space probe might be designed (Dario *et al.*, 2008; Menon and Broschart, 2006; Menon and Lan, 2006). Plant roots display several characteristics that would be useful if able to be translated to an engineering system including:

1. Low power consumption. Plants are well known to grow slowly and efficiently. For many space applications time is not a strict constraint but rather resource utilization is critical.
2. Miniaturized system. Miniaturization is a driver of space systems due to the high costs associated with the launch phase. Plant root tips are ready miniaturized systems with sensors at the micrometer scale. However, these systems are also capable of digging relatively deep holes.
3. Intelligent penetration. A digging mechanism with tip sensors, capable of processing data in real time and autonomously determining optimal penetration trajectory, could increase the probability of finding desirable substances in planetary substrates and of optimizing energy resources.
4. Capability of penetration at any angle. Most conventional drilling systems are capable only of drilling in straight lines. Inspiration might be taken from Nature for a penetration system able to circumvent obstacles by changing direction, thereby relaxing other requirements on the system.

6.14.4
The Locust as a Model for Inspiring Digging System

The ovipositor mechanism of the female locust has also been studied as a potential digging system. Thy mechanism comprises two hinged valves. As the valves open, their geometry causes excavation in addition to pulling the system further into the hole and extending the locust abdomen. Cyclical opening and closing achieve an efficient digging process. Extrapolating this design to an engineering concept, it is evident that actuation of this opening motion can be achieved through pulling forces from a remote source through, for instance, wires. This could potentially allow the design of a quasi-remote digging mechanism, reducing the required system mass between digging mechanism and a remote source of actuation. Identified potential applications include the collection of small subsurface samples.

A physical prototype was implemented to demonstrate the actuation of such a system, and simulations of the digging mechanism in various substrates were carried

out (Menon *et al.*, 2006c). Again, in exploring the potential for miniaturization, a system of roughly the same dimensions as those of the natural system has been considered. Simulations have found that the system was suitable for digging through granular soils.

6.14.5
Descent Mechanism

Space systems for digging to depths of up to 100 m have been proposed by space agencies (Campaci *et al.*, 2005). There are several challenges for boring mechanisms, which could be addressed by, for instance, conventional approaches such as percussion, ultrasonic, or rotary drills. It appears that the main challenge is the development of an autonomous miniaturized descending mechanism – because for deeper holes traditional drilling methods gain mass and volume quickly. The locomotion system of the earthworm, for example, seems appropriate as an analog for this application. In 6.149 peristaltic motion is accomplished by means of waves of muscular contraction with a consequent increase and decrease in the cross-sectional area of the body. Such a behavior could be replicated on the macro-scale as shown in Figure 6.155. A modular design of circular rings (represented in red and green in Figure 6.155) capable of radially expanding and axially contracting could enable motion of the system along a tube, a principle that has similarities with inchworm actuators (Fukuda and Menz, 2001). Steering could be achieved by introducing pairs of linear actuators (depicted in cyan in Figure 6.155) along the body of the robot.

A relatively high level of abstraction (Menon and Lan, 2006) may be used in this biomimetics process, mimicking behavior but using conventional systems for actuation. Electric motors have been proposed, for example, for the design of an autonomous space digging mechanism (Campaci *et al.*, 2005). In addition, miniaturized systems capable of locomotion inside hollow tubes have recently been tested (~~Huba~~ and Keskeny, 2006; Phee *et al.*, 2002) and locomotion by peristaltic motion has been demonstrated.

6.14.6
Material Transport System

Material transport from a deep hole to the surface is a significant challenge for deep drilling. Traditional transport lines (Campaci *et al.*, 2005) are bulky, complicated, and heavy and are therefore unfeasible for practical implementation in many space applications.

In Nature, transport of material along a duct could be achieved by using distributed actuators (Menon, Carpi and de Rossi, 2006b). In Nature, motile cilia, for instance, which are macrotubules that constantly beat in one direction, are used in various systems such as in the respiratory tract to move mucus and particles, in the fallopian tubes to propel the ovum to the uterus, and in the vesicles of the brain to circulate the cerebrospinal fluid. Another example of distributed actuators is the use of distributed muscles along the human digestive tract, which use a peristaltic motion to propel food. By taking inspiration from this second natural mechanism, a material transport system for space application could be proposed.

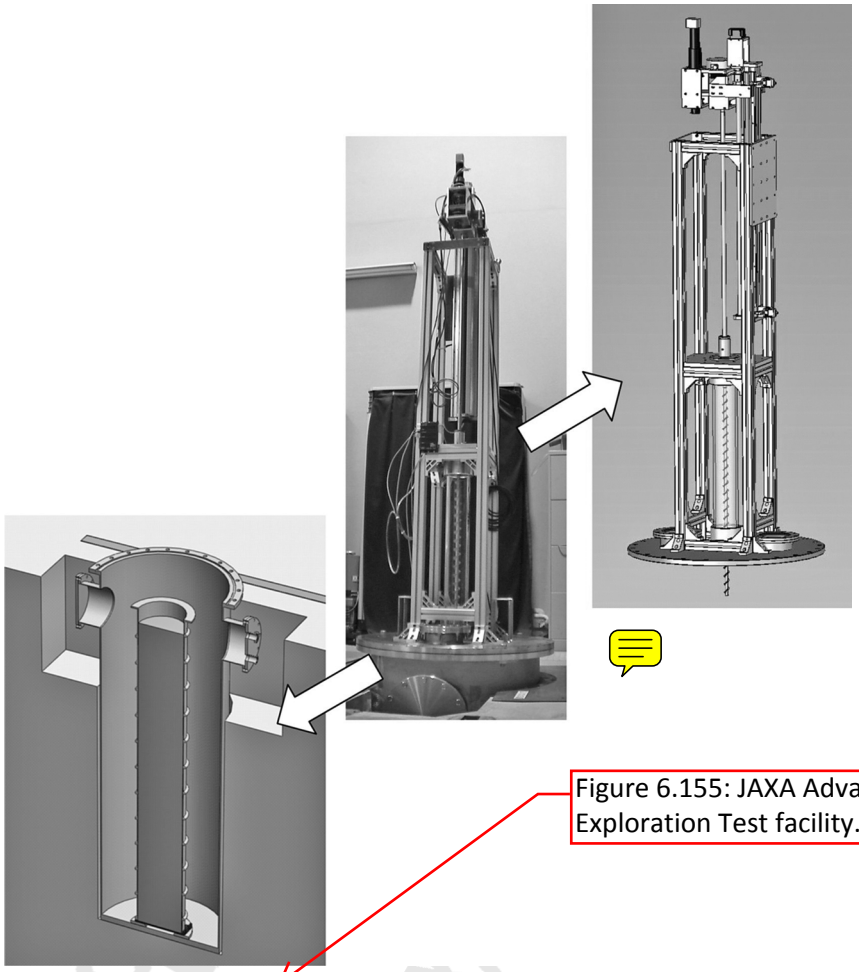

Figure 6.155: JAXA Advanced Subsurface Exploration Test facility. Courtesy of JAXA.

Figure 6.155 The DAME drill hardware was a Mars prototype derived from the Honeybee Robotics Advanced Deep Drill. Courtesy Honeybee Robotics.

6.14.7 Gecko-Inspired Cuttings Removal

The most effective ways to lift cuttings out of a hole inc 6.150 ation of fluid or air/gas. However, if for any reason air or fluid cannot be used, an auger can do the job provided that the drilling motion is rotary or rotary–percussive. In pure dry percussive drilling, where the motion is up and down, such as in the NASA–JPL ultrasonic drill, there is no mechanism to lift the cuttings out of the hole. For this reason, a novel means for conveying the drilled cuttings of a rock or soil-like material was developed (Zacny *et al.*, 2002). This system is characterized by having two opposed surfaces covered by angled hairs or bristles (Figure 6.156). Both sets of bristles point

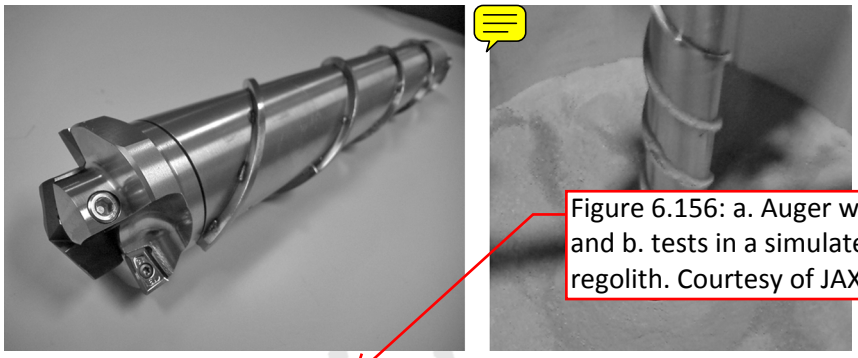

Figure 6.156: a. Auger with the drill bit and b. tests in a simulated lunar regolith. Courtesy of JAXA.

Figure 6.156 Sublimation of ice during drilling at pressures below the triple point of water in ice-bearing formations can be a powerful cuttings cleaning mechanism (Zacny, Quayle and Cooper, 2004). Photograph courtesy A. Cooper).

approximately in the direction in which it is desired to convey the cuttings, usually upwards. The two sets of bristles are placed close enough to overlap or just barely touch, depending on the diameter of particles being transported.

The principle of the invention lies in the oscillatory motion of the two plates with angled bristles attached to them. One plate can be stationary (but it does not have to be) the other moves up and down with a low amplitude and high frequency. If a particle is trapped in one of the plates, the bristles of the other plate will scoop it out and transfer it to the other plate.

6.151

This system could be used, for example, in a wireline percussive coring drill as shown in Figure 6.157. In this particular case, the hole casing can have dual roles: to support the hole from collapsing and to act as a second surface for the bristle mechanism of cuttings removal. Note that for wireline drills, casing is of paramount importance; if a hole collapses above the drill, it may trap the drill inside the hole for ever. The outside of the core drill will have a second set of matching bristles; this is also an active surface since the drill will be actuated percussively.

In order to test this theory of cuttings removal, a number of tests were conducted with an experimental apparatus simulating a casing and percussive core barrel. The heart of the experimental apparatus included two flat plates with bristles on them, one plate stationary and the other moving up and down at various frequencies. The test material included commercial ski skins (which have angled bristles). Ski skins are normally attached to the bottom of the skis to allow a skier to climb a mountain without sliding down. For this reason, they tend to be very strong and have a high fatigue life.

6.152

The test results are shown as the vertical velocity of particles leaving the top of the plates as they were being accelerated by the moving plates as a function of the ratio of particle diameters to bristle length for three different types of ski skins.

The test results showed the particles flying out at speeds exceeding $16\,\mathrm{m\,s^{-1}}$ (Figure 6.158). In addition, the purple ski skin proved best at handling most sizes of particles, from small (90 μm), to large (1015 μm). However, the purple ski skin failed

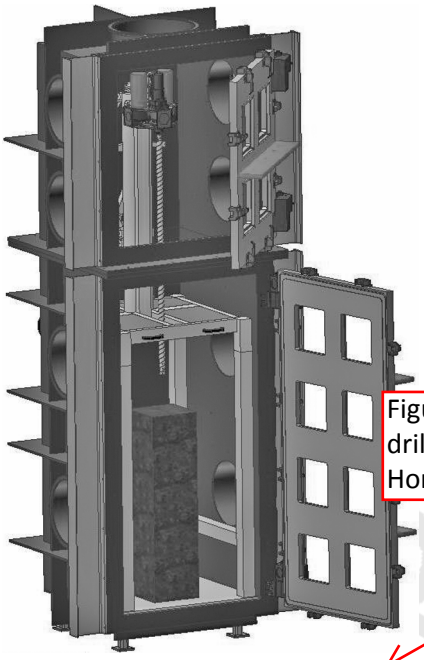

Figure 6.157: Honeybee Robotics 11 ft drill chamber. Courtesy M. Maksymuk, Honeybee Robotics.

Figure 6.157 JAXA Advanced Subsurface Exploration Test Facility. Courtesy JAXA.

Figure 6.158 (a) Auger with the drill bit and (b) test in a simulated lunar regolith Courtesy JAXA.

Figure 6.158: Images of ATK Space Subsurface Access Testing Laboratory with the 2-meter drill tower, SPECES and MPDS drill platforms (left) and low temperature stress test images (right). Photographs courtesy of ATK Space.

to convey the large 2000 μm glass beads. The "Blue Cow" ski skin transported all particles except 75, 90, and 2000 μm, the extreme ends of the range. However, across the range, it always had slower speeds than the purple ski skin. The black ski skin worked well for particles between 295 and 2000 μm, but failed to convey any particles smaller than 295 μm. Thus, each ski skin seemed to perform best with different sizes of particles. This is what we expect given the different bristle length of each ski skin.

It is believed that the angle between the bristles and the backing of the ski skin is the second most important factor after the bristle length. However, a close analysis of the results shows that this angle can also be influenced by the areal density and stiffness of the bristles. Thus, when analyzing the effects of the angle, the stiffness and areal density of the bristles should also be taken into account.

6.15 Drilling Automation

6.15.1 Background

The search for evidence of ancient climates, extinct life, and potential habitats for extant life on Mars, given the desiccated and irradiated conditions near the surface, will require drilling or some other form of subsurface access. Future lunar missions will also require some means of acquiring cores and other subsurface specimens. Whether 10 cm deep cores into exposed outcrops, or 5–10 m deep drilling in search of Martian fossils or ice lenses, the drill becomes both an instrument and a means of acquiring fresh unweathered specimens. Given light-speed time delays (tens of minutes) that are much longer than the time required (seconds) to get a drilling instrument stuck, Earth-based teleoperation is not feasible for drilling operations beyond the Moon. Drilling on Mars, Europa, or Titan must be self-contained and autonomous, unlike terrestrial commercial drilling technologies.

6.15.2 Why Space Drilling Needs Automation

Modern commercial drilling has increased the level of automation used in terrestrial applications, but it should be noted that, for space science applications, the term "automation" takes on some very different meanings. In the commercial realm, "automation" and "remote control" mean the capability to watch values and open and close valves with a mouse click in a control room, as opposed to sending out a human with a wrench – eliminating direct hand contact other than joysticks and touchscreens. In space, these definitions imply minimal or no direct human involvement, even with regard to monitoring and decision-making. Hence the hands-off automation of DAME (Figure 6.159) reflects a qualitative advance over teleoperated commercial drilling operations.

6.153

page proof © WILEY-VCH

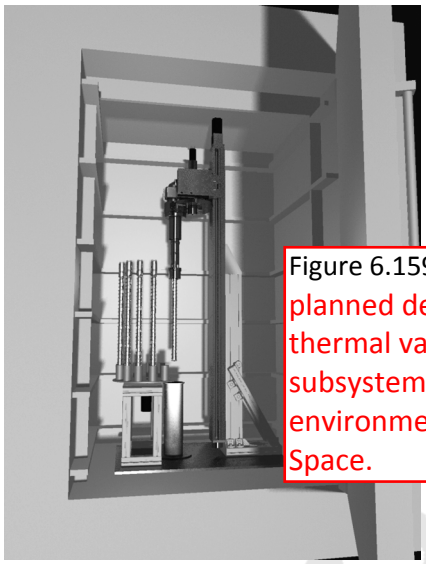

Figure 6.159: Image of modified MPDS for 2009 planned development testing in 1m x 1m x 2m thermal vacuum chamber to verify key subsystems operations in Mars and Lunar environment. Photograph courtesy of ATK Space.

Figure 6.159 Honeybee Robotics 11 ft drill chamber. Courtesy M. Maksymuk, Honeybee Robotics.

Early attempts at automation in oil and gas exploration led to the development of rule-based systems in the 1980s for interpreting well logs as a drilling advisor or monitor. These systems were successful only in narrowly defined, offline applications, because the inflexibility and brittleness of rule-based systems were not compatible with the poorly characterized, dynamic drilling environment.

6.15.3 Diagnostic Approaches

Enormous advances over the decades, however, have allowed researchers to move beyond this type of inflexibility in reasoning. The development of integrated system health management techniques for aircraft and spacecraft, for example, added model-based reasoning or hybrid approaches in parallel with faster rule- or table lookup-based approaches. Further, connectionist approaches using neural nets have been developed to identify and reconfigure aircraft flight controls. Application of these newer diagnostic and control approaches to the drilling automation problem offers a hope of achieving hands-off drilling, at least for lightweight space drills.

6.16 Testing of Subsurface Systems

This section gives an overview of motivations behind the testing of drill systems in a relevant environment and introduces a few existing systems that can be

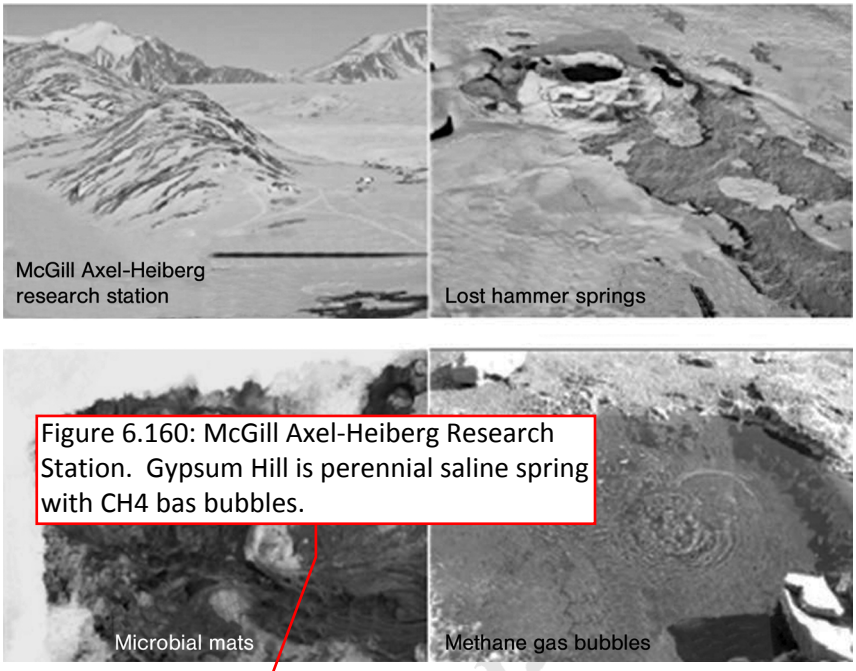

Figure 6.160: McGill Axel-Heiberg Research Station. Gypsum Hill is perennial saline spring with CH4 bas bubbles.

Figure 6.160 (a) ATK Space Subsurface Access Testing Laboratory with the 2 m drill tower, SPECES, and MPDS drill platforms and (b) low-temperature stress test images. Photographs courtesy of ATK Space. (Please find a color version of this figure on the color plates).

used for the testing of drill systems under low-pressure and low-temperature conditions.

6.16.1
Reason for Testing in a Relevant Environment

It has been found ~~by Zacny's group (Zacny, Quayle and~~ 6.154 ~~004; Zacny *et al.*, 2008b)~~ that when drilling at pressures of below the triple point of water (4.5 Torr or 6.1 mbar), water-ice in contact with a warm drill bit sublimes to vapor. The volumetric expansion of ice as it turns into vapor is of the order of ~~700-fold~~ and therefore even a small amount of water-ice can generate a substantial quantity of vapor that will effectively clean a hole from drilled chips (Figure 6.160). In effect, this is like a drilling fluid that we use on Earth but instead of pumping it down hole as we do on Earth, it is already there on Mars, below the surface. The effect of clearing of drilled cuttings from a hole has a tremendous effect ~~of~~ on the excavation efficiency. Not only does the penetration rate increase, but also the power drops and the bit wear decreases, allowing deeper holes to be drilled without the need to change the drill bits. In addition, since sublimation consumes heat generated by the drilling process, it ~~helps~~

the drill bit and the surrounding formation ~~to remain~~ cool. This helps in preserving the sampled formation at its original temperature ~~or close to its original temperature~~ for scientific investigation.

This sublimation phenomenon, of course, does not exist on Earth, where atmospheric pressure is always above the triple point. However, the Martian Southern Polar regions have an atmospheric pressure below the triple point and also formations ~~that~~ contain water-ice (Zacny and Cooper, 2006). Hence simulating this condition in the laboratory on Earth prior to deploying drills on Mars is of paramount importance.

Simulating conditions which are slightly above the triple point of water is also of importance since ~~now liquid water can exist.~~ Liquid water at a pressure close to the triple point can be very unstable and re-freeze when the temperature drops below 0 °C (if soil contains clay~~ey~~ minerals, the freezing temperature can be much lower). When water re-freezes back it can effectively trap the drill inside the hole ~~and at this point the drill will be trapped~~ for ever. This has happened to many drills penetrating Arctic permafrost.

Apart from issues related to sublimation, another phenomenon that exhibits itself at pressure below the triple point is that of coefficient of friction. In particular, the coefficient of friction can be lower, by as much as 50%, at pressures below the triple point of water. This is because below this pressure, surfaces do not have adsorbed molecular water and in turn their surface friction properties are changed (Zacny and Cooper, 2007a). Higher vacuum, on the other hand, can contribute to much higher friction coefficients. This is because when two surfaces are rubbed against each other, surface oxides are removed and never replaced because of a lack of oxygen molecules in vacuum. In turn, the oxide-free surfaces tend to weld together when put in contact with each other (Buckley, 1971).

As mentioned earlier, on Earth some drill rigs use air to clear the hole of drilled cuttings. This has initially been sidelined for planetary drilling systems due to a belief that the volumes of required gas that would need to be brought to a planet or a moon will be prohibitively large and in turn expensive. However, in more recent tests, it has been demonstrated that the efficiency of gas flushing is very high in vacuum or low-pressure environments. This is attributed to the fact that the gas does not have to work against a large back-pressure, which on Earth is 760 Torr or 1 atm (Zacny and Cooper, 2007b). A number of tests conducted in a 1 Torr environment has shown soil lifting efficiencies of 1 to 3000, that is, with 1 g of gas it was possible to lift 3000 g of soil (Zacny *et al.*, 2008a).

The low temperature has also an indirect effect on drilling performance. The drilling specific energy or energy required to drill a unit volume of rock, and also WOB or thrust on the drill bit required to penetrate the rock, are directly proportional to the rock's UCS. The UCS of any rock, on the other hand, changes depending on the water content and also temperature (Zacny and Cooper, 2007c). For example, water-saturated sandstone at −80 °C can have a UCS three times higher than ~~that~~ when it is dry at room temperature. This translates into a three times higher specific drilling energy and also three times higher WOB. The strength of basalt at −100 °C is 20% higher than at +100 °C.

6.16.2
Japan Aerospace Exploration Agency (JAXA)

Subsurface exploration on the Moon and other celestial bodies is the next step towards further understanding ~~and utilizing them, after conducting surface exploration~~. JAXA has set the exploration and possible utilization of the Moon as a key activity in the JAXA Vision (http://www.jaxa.jp/about/2025/index_e.html). Beginning with the next landing mission following "KAGUYA"~~, a~~ Japanese lunar orbiter launched in 2007~~,~~ towards the long-term goal of a human lunar base, handling techniques of lunar soil, including drilling, will be one of the key technologies to achieve these goals.

To develop reliable mission-qualified mechanisms, the ability to conduct ground tests and evaluate performance in simulated environments is a crucial factor to mission success. However, there are ~~still~~ few facilities that can simulate the lunar environment well enough to evaluate system performance. The key factors required to simulate accurately the mechanism interactions with the lunar environment include soil simulation, vacuum, temperature, and low-gravity environment. Among these four factors, low gravity is the most difficult to simulate because soil ~~particle~~ compaction needs sustained low-gravity compensation~~; however, the~~ other three factors are relatively easier to simulate.

The Advanced Subsurface Exploration Test Facility simulates soil, vacuum, and temperature of the lunar environment, enabling vertical drilling of up to 2 m (Figure ~~6.~~161). The vacuum chamber is buried below the floor and the drilling mechanism is placed on it, the base serving as the lid of the vacuum chamber. The

6.155

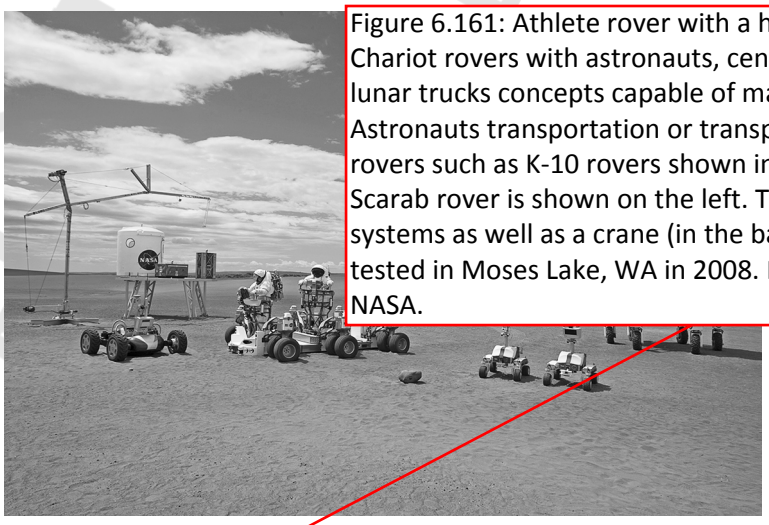

Figure 6.161: Athlete rover with a habitat (right), and Chariot rovers with astronauts, center) are mobility lunar trucks concepts capable of many tasks such as Astronauts transportation or transporting smaller rovers such as K-10 rovers shown in the center. Scarab rover is shown on the left. These mobility systems as well as a crane (in the background) were tested in Moses Lake, WA in 2008. Photo courtesy NASA.

Figure 6.161 Image of modified MPDS for 2009 planned development testing in a 1 × 1 × 2 m thermal vacuum chamber to verify key subsystems operations in Mars and lunar environments. Photograph courtesy of ATK Space.

DO NOT COPY REVIEW

Table 6.21 Specification of the advanced subsurface exploration test facility.

Item	Specification
Height	6 m (for 2 m drilling)
Drilling depth	Up to 2 m
Soil container diameter	Up to 700 mm
Vacuum condition	<10 Pa with soil
Soil container coolant	LN_2 or hydrofluoro ether
Maximum speed of rotation	600 rpm

drills are exchangeable and connected to the driving section, ~~which is~~ located ~~at~~ the outside of the vacuum chamber~~,~~ by a feed-through assembly using a stainless-steel rod ~~that is rotated by an electric motor~~. The drill and the motor are mounted on a linear motion assembly using a ball-screw that moves the drilling part vertically by another electric motor. A soil container is lowered into the vacuum chamber ~~for~~ each experiment after being packed with simulated lunar soil to appropriate density. The soil container has adapters for thermocouples and a coolant pipe to simulate a low-temperature environment. Producing the same soil condition for each experiment is essential to obtain reliable data with repeatability. The drill is controlled by a computer~~, and sensor~~ data, such as thrust force and drilling torque, are obtained along with the history of drill motion or rate of penetration. Table 6.21 gives the specification of the Advanced Subsurface Exploration Test Facility.

The simulated lunar environment of the Advanced Subsurface Exploration Test Facility can be used for ~~various~~ tests ~~other than those of long drills attached to the drilling mechanism~~. A small automatic auger has been developed for the purpose of ~~sensor~~ subsurface placement on the Moon and its deep drilling performance has been evaluated ~~using~~ this facility (Figure 6.162). The auger is about 30 cm long and 5 cm in diameter and the bit and the body rotate in opposite directions. The drilling test using simulated lunar soil was conducted and the auger was found to perform to design specifications.

6.156

6.16.3 Honeybee Robotics Drill Testing Facility

6.157

Honeybee Robotics developed a planetary drill testing facility which comprises a 3.3 m (11 ft) tall vacuum chamber and a matching drill system capable of drilling to at least 1 m depth (Figure 6.163). The chamber ~~itself~~ is almost 1 m deep and 1 m wide and can be set in a vertical or horizontal position. The latter position is particularly useful when performing mining and excavation tests requiring a long horizontal traverse of an excavator. The chamber itself consists of two chambers, the lower one being 84 in tall and the upper one 48 in tall. This split chamber allows for testing to be performed in smaller chambers if desired. It also reduces the weight of the chamber doors and in turn the size of the supporting hinges.

Page Proof

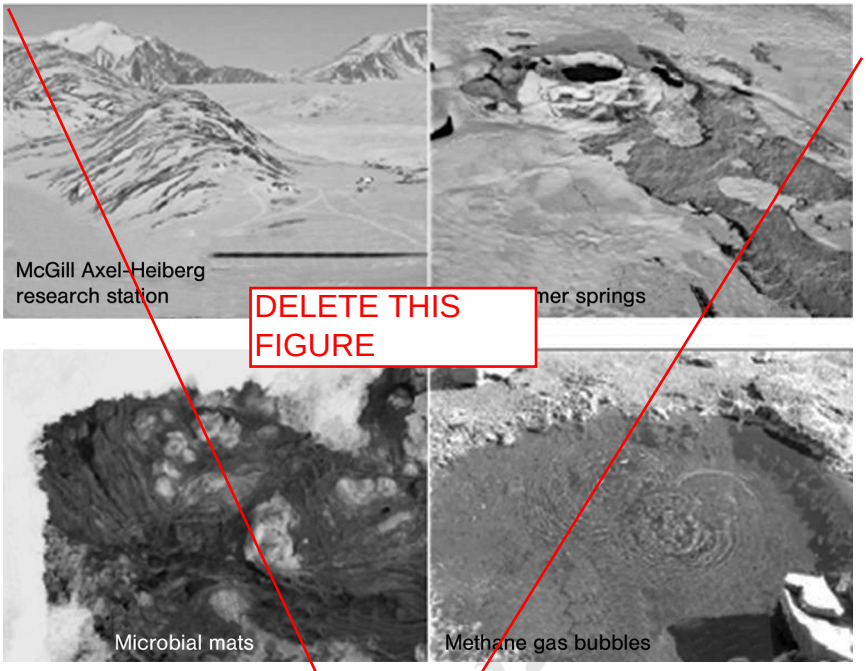

DELETE THIS FIGURE

Figure 6.162 McGill Axel–Heiberg Research Station. Gypsum Hill is a perennial saline spring with methane gas bubbles.

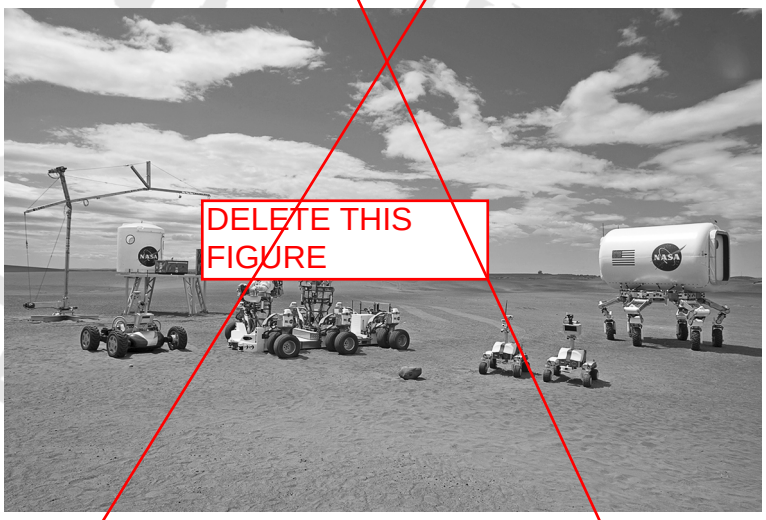

DELETE THIS FIGURE

Figure 6.163 Athlete rover with a habitat (right), and Chariot rovers with astronauts (center) are mobility lunar truck concepts capable of many tasks such as astronaut transportation or transporting smaller rovers such as K-10 rovers shown in the center. Scarab rover is shown on the left. These mobility systems and also a crane (in the background) were tested at Moses Lake, WA. Photograph courtesy NASA.

The chamber ~~has two~~ SV300 rotary vane vacuum pump~~s~~ allowing reaching a vacuum of the order of 1 Torr. Additional pumps such as a roots blower–mechanical pump combination can be used to reach low to medium vacuum of the order of 10^{-3} Torr. The reason for having a modest vacuum of 1 Torr is to speed up the pumping process and in turn to perform a higher number of tests in a day. Trying to reach a higher vacuum can take many hours and days due to continuous degassing of regolith simulants, and planetary simulant rocks, soil–ice mixtures, and ice.

In addition, medium to high vacuum is required only for simulating conditions that exist on the Moon or asteroids. For Mars, a chamber that can hold a pressure of between 1 and 11 Torr is sufficient.

It is very difficult to cool a low-pressure atmosphere. Instead, the chamber is equipped with a system for cooling a drilled sample. This can be achieved via either a closed-loop cooling system capable of extracting 150 W of power at −40 °C or liquid nitrogen that allows a sample to reach 77 K (−196 °C).

The chamber also has a gas purging capability so that it can maintain an atmosphere containing a predominantly desired gas, such as carbon dioxide (for Mars).

The inherent part of this drilling chamber facility is a drill system itself described in Section 6.8.9. Note that in contrast to other drill systems which are optimized for low power or WOB, this drill has ample power, torque, WOB, and drill pull-out capability. This is because it is a research drill, the purpose of which is to test various drilling scenarios, such as drill binding in a hole, and quantify the forces and torques required to free the drill.

6.16.4
ATK Space Subsurface Access Testing Laboratory

6.158

In August 1998, ATK Space (formerly Swales Aerospace) began developing and testing planetary research drills in the ATK Space Subsurface Access Testing Laboratory (see Figure 6.164). This facility and equipment were used to carry out the subsurface access technology development described in previous sections.

The high bay reserved section of the ATK Subsurface Access Laboratory is 6.1 × 15.8 × 4.1 m. This area is used for prototype testing and housing of rock test samples and environmental test equipment. Adjacent to the high bay, the laboratory contains three rooms with about 372 m^2 of additional total space containing a small machine shop, electronics laboratory, clean room (3.6 × 5.6 × 2 m), and low-temperature equipment used to support testing operations.

The drill tower's inner dimensions are 84 × 102 × 406 cm and enable drill tests to various depths depending on drill prototype setup location and sample target depth. As mentioned in previous sections, the SCAD and SPECES were able to drill 2.2 m using this drill tower. The high bay also stores about 1200 kg of various natural rock materials to test current hybrid drill bit designs and sample capture mechanisms.

The high bay also contains three environmental test chambers. The three thermal vacuum chambers provide the capability to test key subsystems for flight acceptance and qualification test ranges. The temperature range is from −180 °C (using liquid nitrogen) to 100 °C. Vacuum can be obtained to 10^{-3} Torr. The chambers have three different internal volumes, 30 × 30 × 49.5, 46 × 46 × 61, and 38.7 × 38 × 133 cm, that allow a variety of component sizes and subsystems to be tested.

This drill research laboratory was used to test and troubleshoot drill systems in preparation for final laboratory and field performance tests. The next step is to test key subsystems in Martian and lunar environments. A modified configuration of the MPDS drill (Figure 6.165) is currently planned to begin further development testing in a 2 m tall chamber during 2009.

6.159

6.17 Space Analogs on Earth for Field Test Simulations of *In Situ* Planetary Drilling

There are some locations on Earth that to a certain extent are similar to what can be found on some extraterrestrial bodies. For example, Arctic and Antarctic regions are cold and therefore can be good analogs for planets that have very low surface temperatures. Although analog sites are somewhat different, they offer a good and relatively inexpensive training and testing ground for various extraterrestrial drilling systems. This section will cover a number of analog sites that have been used by engineers and scientists to test drills and to conduct various experiments.

6.17.1 Arctic Sites

6.17.1.1 Devon Island (Haughton Crater)

Haughton Crater is located at approximately 75°N, 89°W on Devon Island in the Nunavut Territory of Canada. The Haughton site presents many analog aspects that have been used over the past 12 years for both science and exploration operations applications (see Lee and Osinski, 2005 for a summary). With regard to drilling analog investigations, Haughton presents the following combination of key aspects that are of both scientific and operational relevance to the Mars subsurface – and in some cases possibly lunar polar subsurface – exploration: (1) massive surface exposures of well-preserved impact-processed fragmentary materials, specifically Haughton's polymict impact (melt) breccia and associated alteration features (see Lee and Osinski, 2005 and references therein); (2) quasi-continuous ground ice in continuous permafrost below a depth of approximately 1 m; (3) patchy exposures of post-impact fluvio-glacial deposits (Osinski and Lee, 2005), (4) well-preserved and well-exposed intracrater paleolacustrine deposits (Osinski and Lee, 2005); (5) well-preserved impact-induced hydrothermal deposits (Osinski *et al.*, 2005); and (6) lack of any significant vegetation that would affect drilling operations (roots). Although by no means identical with Mars, Haughton offers a unique combination of features, processes, and operational challenges that provide an optimal terrestrial context for asking a wide range of Mars-relevant astrobiology science questions and for driving Moon/Mars-relevant drilling technology development. Haughton Crater has been the primary field target for DAME drilling automation software and 10 m-class drill tests into the frozen fallback breccia.

page proof WILEY-VCH

6.17.1.2 Ellesmere Island (Eureka)

The Eureka weather station, located at approximately 80°N latitude on Ellesmere Island, offers a site for drilling fluvio-glacial deposits and target sedimentary rocks in permafrost, with the services nearby of a machine shop and lodging and other logistics. It has been used in NASA Johnson Space Center-led tests of the MADD inchworm deeper drill prototypes in 2002–2004.

6.17.1.3 Kugluktuk (High Lake Mine)

The High Lake mining property in the Nunavut Province of northeastern Canada sits amid gossan outcrops that are 1.5×0.3 km in size and overlie an Archean-age, massive, volcanogenic sulfide deposit. (Gossan is intensely oxidized, weathered or decomposed rock, usually the upper and exposed part of an ore deposit or mineral vein.) These deposits are readily visible in satellite images and are readily accessible from the mining camp (Tullies, 2008). Although the permafrost at High Lake extends to ~440 m depth (Pfiffner *et al.*, 2008; Freifeld *et al.*, 2008), the gossan outcrops are ~1 m thick and are restricted to the seasonally frozen, active layer. These gossans are of interest because they represent a natural acid drainage site in an Arctic environment that could potentially serve as an analog to the conditions under which sulfates and iron oxides possibly formed on Mars. Rock and soil samples from three different outcrops that were analyzed using SEM, XRD and Mössbauer spectroscopy revealed the presence of Fe^{3+} oxides, oxyhydroxides, phosphates, and sulfates and gypsum. The iron oxides and phosphates that were primarily derived with altered metavolcanic rock were associated with chlorites, talc, and quartz. Hematite, goethite and jarosite were primarily observed in altered quartz/sulfide veins and were associated with mostly quartz and muscovite. Assuming thermodynamic equilibrium with seasonal snow melt, the gossan pore water should range from pH 0.5–3, $SO_4^{2-} > 3000$ mg L^{-1} for the latter assemblage to pH 3–6, $SO_4^{2-} < 1000$ mg L^{-1} for the altered metavolcanic rock (West *et al.*, 2008).

The High Lake gossan differs from acid mine drainage (AMD) sites by its lack of diverse sulfate species and smaller crystal sizes, which broaden the Mössbauer and XRD peaks and make these gossans very similar to the results reported by Opportunity at Eagle Crater (Klingelhöfer *et al.*, 2004) and to Hesperian age deposits, in general (Bibring *et al.*, 2005, 2006, 2007; Gendrin *et al.*, 2005). The smaller crystal size may reflect the slower reaction rates in the colder temperatures and the periodic water saturation (West *et al.*, 2008).

6.160

6.17.1.4 Axel Heiberg Island

MARS on Axel Heiberg Island (Figure 6.166) has been the site of recent investigations into permafrost geomorphology, hydrology, and microbiology (Omelon, Pollard and Andersen, 2006a; Perreault *et al.*, 2007; Pollard *et al.*, 2008). The cold saline springs on Axel Heiberg Island are among the only known cold springs in thick permafrost on Earth and represent unique, extreme cold environments for expanding our knowledge of terrestrial microbial life. MARS is proximal to perennial cold springs that are fed by subglacial recharge through a Permian evaporite deposit. Because of their high salinity, the springs flow year round, beneath the ice and snow

during the winter, and as such represent potential analogs of the Martian gullies (Andersen *et al.*, 2002; Malin *et al.*, 2007). Extensive, chemolithoautotrophic sulfur-oxidizing *Thiomicrospira* sp. streamers develop in the snow covered run-off channels during the winter months and appear to represent a unique microhabitat that flourishes via phototrophic-independent metabolism (Niederberger *et al.*, ~~2008~~). The 16S rDNA analyses of some of these springs indicate that anaerobic methane oxidizing communities may also be present. Permafrost cores collected during a previous ASTEP-funded field campaign to nearby Eureka contained diverse phylogenetic groups including Actinobacteria, Proteobacteria, Firmicutes, Cytophaga–-Flavobacteria–Bacteroides, Planctomyces and Gemmatimonadetes. An Archaea 16S rRNA gene clone library contained phylotypes related to both Euryarchaeota and Crenarchaeota, and the majority of sequences in the Archaea library were related to halophilic Archaea (Steven *et al.*, 2007). Culture-dependent and culture-independent methods were also used in an investigation of the microbial diversity in a permafrost/massive ground ice core from the Eureka site. Denaturing gradient gel electrophoresis and Bacteria and Archaea 16S rRNA gene clone libraries showed differences in the composition of the microbial communities in the distinct core horizons. Microbial diversity was similar in the active layer (surface) soil, permafrost table, and permafrost horizons while the ground ice microbial community showed low diversity. Mineralization was detected at near-ambient permafrost temperatures (−15 °C), indicating that permafrost harbors an active microbial population, while the low microbial diversity, abundance, and activity in ground ice suggest a less hospitable microbial habitat (Steven *et al.*, 2008) and indicate that such relatively ice-rich permafrost environments may be poor astrobiology targets for detecting potential microbial life or biosignatures. Most recently, MARS has been developing methods for detecting and characterizing the gas emanating from the springs and permafrost in order to determine the rates of *in situ* metabolism (Perreault *et al.*, 2008). Such processes are particularly relevant if the Martian atmospheric does contain trace amounts of potentially biogenic methane that is being released from the subsurface (Krasnopolsky, Maillard and Owen, 2004) and if these trace gases are to be utilized to locate drilling sites for extraterrestrial drilling campaigns.

6.17.2
Rio Tinto, Spain

The Rio Tinto analog site is located in the Iberian pyrite belt at a location that was mined for the past 3000 years, the mining operations continuing until post-World War II. It lacks paved access roads into the site, and also any local broadband communications. The nearest support facilities are in the towns of Rio Tinto and Nerva, 7–10 km distant. The microbiological uniqueness of this site and its relevance as a possible biological Mars analog have been discussed (Stoker, Gonzales and Zavaleta, 2007; Fernández-Remolara and Knoll, 2008), as anaerobic microbial populations survive well below the surface, drawing energy from subsurface sulfite deposits. Drilling is the only practical way to reach these, as was demonstrated in part of the MARTE project.

6.17.3
Atacama Desert, Chile

Salt basins and lava flows in a desiccated plateau have made the Atacama Desert a preferred analog test site for lunar and Mars rover prototypes. The andesitic flows are a possible drilling target, as is the duracrust found in the salt basins, but the Atacama is more advantageous as a host target for systems-level mobile coring and drilling tests, including rover navigation and sample handling.

6.17.4
Lonar Crater, India

Lonar Crater, located 550 km east of Mumbai, India, is a simple impact crater approximately 45 000–55 000 years old, with a diameter of about 2 km. It is unique in being the only known impact crater on Earth that occurs in basaltic target material (the Deccan Traps). Samples from the fallback breccia layer on the rim and ejecta blanket (a lake occupies the center) were used as benchmarks in the 1970s for comparison with Apollo lunar samples. It offers impact-shocked and altered soil and rocks, impact crater morphology, and natural chemical similarity to lunar materials. This could be highly advantageous as an analog site for testing lunar drilling prototype equipment and for ISRU prospecting tests, and has been proposed as such.

6.17.5
Southwest United States

6.17.5.1 Barringer Crater, Arizona

The ejecta flanks of Barringer Crater in central Arizona have been used by NASA for astronaut training and equipment tests since Project Apollo in the 1960s. Given the sedimentary target material for this simple impact crater, local vegetative cover, and lack of permafrost or periglacial features, it has been better suited to exploration systems-level simulations and tests which include sampling and drilling. Apollo hand-held tools, including the coring drill, have been tested here in the past.

6.17.5.2 Black Point, Arizona

Early MER prototype tests were conducted in 2002 on the Black Point lava flow north of Flagstaff, AZ. Lack of vegetative cover and basaltic target rocks contribute to this site as a good potential lunar drilling simulation.

6.161

6.17.5.3 Moses Lake, Washington

Reshaped dunes of volcanic source material have made the Moses Lake, WA, area attractive as a lunar traverse simulation and training area, leading to NASA-led tests in June 2008 (Figure 6.167). Although not a high-fidelity drilling-specific analog site, drilling and sampling tests are often part of NASA's larger lunar exploration simulations.

page proof © WILEY-VCH

6.17.6
Antarctic Dry Valleys

The Antarctic Dry Valleys have mean annual air temperatures from −18 to −30 °C and mean annual water equivalent precipitation ranges from 10 to 100 mm (Doran *et al.*, 2002). Older soil profiles (e.g., Dickinson and Rosen, 2003; Mahaney *et al.*, 2001) have been undergoing a variety of small-scale processes for around 10–15 Ma. Differences in soil water and salt properties are very localized and may reflect small variations in the environment and history of each sampling site.

Prospect Mesa soils in the Wright Valley (one of the Dry Valleys) is about 250 m in elevation, implying that during the most recent ice ages, about 8000 years ago (Hall and Denton, 2006), this soil was below the surface of ancient Lake Wright, and probably saturated with water. First, within only 78 cm depth it includes (1) an aeolian zone recording the effect of winds, temperature oscillations, and evaporation/sublimation processes; (2) duricrust within regolith (salt zone); (3) an active zone with thawing and freezing cycles, potential transient liquid water, and where the maximum rate of weathering/secondary mineral formation is observed; and (4) a permanently frozen zone at ∼40 cm depth, where some weathering still occurs (Gibson, Wentworth and McKay, 1983).

6.18
Drill Evaluation Criteria

The first step in creating an evaluation matrix of existing sampling technologies is the definition of evaluation metrics against which existing architectures can be weighed. These metrics can be broken down into three main categories: primary capabilities, sampling characteristics, and system requirements.

Primary capabilities capture information about the sampling system's operational functions. These are the functions that mission planners may desire for a lander or rover sampling mechanism. These include:

1. *Solid core capture:* The system can break and capture a core sample from a solid rock target. This includes the capability to produce a core, break the core from the target rock, and positively capture the core for hand-off to an analysis instrument.
2. *Unconsolidated core capture:* The system can break and capture a core sample from an unconsolidated rock target. This includes the capability to produce a core, break the core from the rock, and positively capture the core for hand-off to an analysis instrument. An unconsolidated core can contain horizontal fractures so that the core sample consists of many chips or rock "coins" stacked together.
3. *Loose regolith capture:* The system can retain a sample from a target containing loose regolith. This includes the capability to capture a regolith sample, and positively capture the regolith sample for hand-off to an analysis instrument. Loose regolith is defined as particulate larger than 50 μm in diameter.

page proof WILEY-VCH

4. *Powder sample capture:* The system can create and retain a powder sample from a solid rock target. This includes the capability to pulverize a solid rock target and capture the powder created in a positive manner, allowing for subsequent hand-off to an analysis instrument. Powder is defined as particulate less than 50 μm in diameter.
5. *Icy soil capture:* The system can retain a sample from a target containing icy soil. This includes the use of design features specific to sampling icy soil. Design considerations might include reducing heat input during the coring process and/or bit design specific to icy conditions.
6. *Solid core ejection:* The system can actively eject a captured solid core sample.
7. *Unconsolidated core/loose regolith ejection:* The system can actively eject a captured unconsolidated core or regolith sample. This includes design features that mitigate jamming issues inherent with either sample type.
8. *Powder sample ejection:* The system can actively eject a captured powder sample. This includes design features that mitigate jamming issues inherent with powder samples and features that allow for the undisturbed (e.g., wind shield) transfer of powder from the sampling mechanism to an analysis instrument.
9. *Icy soil ejection:* The system can actively eject an icy soil sample. This includes the use of design features specific to releasing an icy soil core. Design considerations might include dealing with the issue of refreezing.
10. *Solid core stratigraphy:* The system preserves stratigraphy in a captured and ejected solid core sample.
11. *Loose regolith stratigraphy:* The system preserves stratigraphy in a captured and ejected regolith sample.
12. *Autonomous operation:* The as-built system does not require human intervention during operation. An existing universal rating system is utilized to compare between different levels of system autonomy (see Table 6.22).

Sampling characteristics capture information about the interface between the sampling system and the target surface. They can give mission planners insight into

Table 6.22 Autonomy rating system (Mukherjee *et al.*, 2006).

Category	Description
A0: automated	Open-loop control for drilling, sample acquisition and delivery
A1: semi-autonomous	Some closed-loop control: closed-loop drilling control with respect to drill rate and platform reaction forces
A2: semi-autonomous	Primarily closed-loop control: closed-loop drilling, sample acquisition and delivery
A3: autonomous	Primarily closed-loop control: failure diagnosis and recovery for drilling and sampling
A4: fully autonomous	Closed-loop control: failure diagnosis, failure recovery/avoidance, and performance optimization for drilling and sampling

page proof WILEY-VCH

the types of potential target surfaces accessible, and also system-level issues such as power usage and dynamic interface loads. These include:

1. *Use with rotary drills:* The system utilizes rotary drills for penetration.
2. *Use with rotary–percussive or percussive drills:* The system utilizes rotary–percussive or percussive drills for penetration.
3. *Use with pneumatic drills:* The system utilizes pneumatic drills for penetration.
4. *Use with ultrasonic actuator:* The system utilizes ultrasonic actuators for penetration.

System requirements capture information about the functional and environmental requirements that the sampling system may be required to meet. They will give mission planners insight into the requirements that a particular system has been designed for and subjected to. These include:

1. *Operation in a Martian-relevant environment:* The system has been *demonstrated* in 2–1250 μm Torr CO_2 at temperatures ranging from −135 to 70 °C.
2. *Operation in a lunar-relevant environment:* The system has been *demonstrated* in a high vacuum ($<10^{-6}$50 μm Torr) at temperatures ranging from −196 to 125 °C.
3. *Operation in a Venus-relevant environment:* The system has been *demonstrated* in 9050 μm bar CO_2 at temperatures up to 460 °C.
4. *System robustness:* The system tolerates the presence of or mitigates the effects of dust (particulates smaller than 20 μm). The system is tolerant to inadvertent contact with surrounding obstacles. Specific features and/or test data have been published to show the system robustness.
5. *Reliability of operations:* The system mechanisms are resistant to operational failures and methods of recovery exist for potential failure scenarios. This is primarily software development and testing, but may include mechanical features.
6. *Sample preservation:* The system mitigates cross-contamination, minimizes forward contamination, reduces heating of the core, and does not alter sample mechanical properties (i.e., density, UCS, etc.). Specific features and/or test data have been published to show sample preservation.
7. *System profile:* The instruments' mass, volume, and power signatures are on the same order as likely flight systems requirements.
8. *Depth class:* There are four depth classes: surface drilling (centimeters); shallow drilling (tens of centimeters to a few meters), 10 m-class drilling (up to 10 m) and very deep drilling (>10 m).
9. *Core properties:* The coring instrument can capture target material(s) with an appropriate diameter and length at required depths.

Some of the existing architectures were rated based on how they perform in terms of the above metrics. The results are given in Tables 6.23–6.26 (these tables do not include all of the drilling systems described in this chapter). The symbols in these tables are as follows:

page proof © WILEY-VCH

Table 6.23 Drill matrix for surface drills (centimeters).

System architecture	Mission/ program (if applicable)	Company	TRL	Sample size	Sampling depth capability	Stowed volume	Power (w)	WOB (preload) (N)	Mass	Primary capabilities	Solid core capture	Unconsolidated core capture	Loose regolith capture	Power sample capture	Icy soil capture	Solid core ejection	Unconsolidated core / loose regolith ejection	Powder sample ejection	Icy soil ejection	Solid core stratigraphy	Loose regolith stratigraphy	Autonomy rating	Sampling characteristics	Use with rotary drills	Use with rotary-percussive or percussive drills	Use with pnuematic drills	Use with ultrasonic actuator	System requirements	Operation in Martian relevant environment	Operation in lunar relevant environment	Operation in Venus relevant environment	System robustness	Reliability of operations	Sample preservation	System profile	Core properties
Low Force Sample Acquisition System (LSAS)		Alliance Spacesystems	6	1.5 cc powder	19 mm	D 33 x L 229 mm	15–20	(35)	440 g				✓	✓	✓		✓	✓							✓				✓			0			2	✓
Min-Corer (MC)	MSR Athena	Honeybee Robotics SMC	6	8 x 25 mm core	50 mm	29.8 x 14.51 x 9.64 cm	25–100	(135–175)	2.63 kg		✓		•			✓	•			✓				✓				•			•	✓		2	
Coring and Abrading Tool (CAT)	MSL	Honeybee Robotics SMC	6	8 x 100 mm core	100 mm	29.8 x 14.51 x 9.64 cm	< 80	(135–175)	4 kg		✓					✓				✓				✓				•						2	
Asteroid Surface Sampling Device (ASSD)	Hayabusa	JAXA	8	01–10 g	mm						0	0	0	0	0	0	0	0	0	0	0					✓									
Touch and Go Surface Sampler (TAGSS)		Honeybee Robotics SMC	4-5	50 cm^3		50 x 75 x 150 mm	20–30		0.5–1 kg			✓	✓																						
Sampling Drilling and Distribution System (SD^2)	Rosetta	Galileo Avionica	8	3 mg of 0.02 cm^3	23 cm	D 150 x L 760 mm	8–14.5	10–20	< 3.7 kg		✓	✓	✓	✓	✓	✓				✓		3		✓				•	•			•		2	✓
Ultrasonic Sonic Driller Corer (USDC)		JPL / Cybersonics	5	10 x 25 mm core; tbd cm^3 powder	25 mm		10–25	(<10)	< 0.5 kg		✓	✓		•	✓	✓				✓							✓								
MSL powder drill	Mars Science Laboratory	Jet Propulsion Laboratory		tbd cm^3 powder	5 cm									✓										✓				0	0	0	0	0	0	2	0
Mars Integrated Drilling and Sampling System (MIDAS)	MEPAT	Alliance Spacesystems	5-6		50 cm		2	20	6 kg		✓	0	✓	0	0	✓	✓	0	0					✓		✓						✓	1	
Subsurface sampler (rotary hammer / USDC)		Honeybee Robotics / JPL	6	9 x 51 mm or 0.25 cm^3	20 cm				9 kg		✓		✓	✓		✓	✓	✓						✓		✓		✓			0	0			
Icy-Soil Acquisition Device (ISAD)	Phoenix	Honeybee Robotics SMC	8	1–4 cm^3 powder, tbd cm^3 regolith	mm	85.8 x 157.3 x 169.5 mm	38	(~6)	888.3 g				✓		✓									✓				✓						2	
Viking Lander Surface Sampler Acquisition Assembly	Viking 1 & 2	NASA?	9	tbd cm^3 regolith		614.8 x 233.7 x 342.9 mm	30		11.3 kg				✓	✓	✓													✓						3	
Soil Mechanics Surface Sampler (SMSS)	Surveyor 3 & 7	NASA?	9	30 mm rock or 100 cm^3 regolith	180 mm								✓																	✓					
GZU drill and surface sampler	Venera 13 & 14; Vega 1 & 2	Soviet Union	9	1–6 cm^3 powder	30 mm	500 mm	90		26.2 kg					✓										0	0					✓			2	

Table 6.24 Drill matrix for shallow drilling (tens of centimeters to a few meters).

System architecture	Mission/ program (if applicable)	Company	TRL	Sample size	Sampling depth capability (m)	Stowed volume	Power (w)	WOB (preload) (N)	Mass	Primary capabilities	Solid core capture	Unconsolidated core capture	Loose regolith capture	Power sample capture	Icy soil capture	Solid core ejection	Unconsolidated core / loose regolith ejection	Powder sample ejection	Icy soil ejection	Solid core stratigraphy	Loose regolith stratigraphy	Autonomy rating	Sampling characteristics	Use with rotary drills	Use with rotary-percussive or percussive drills	Use with pnuematic drills	Use with ultrasonic actuator	System requirements	Operation in Martian relevant environment	Operation in lunar relevant environment	Operation in Venus relevant environment	System robustness	Reliability of operations	Sample preservation	System profile	Core properties
Apollo Lunar Surface Drill(ALSD)	Apollo 15–17	Martin Marietta Co	9	19.1 mm core; powder	3.5	55.9 x 24.4 x 17.8 cm	500	67–89	11.8 kg		✓					✓								✓					✓					3	
MRoSA2 Drilling and Sampling Subsystem		Helsinki Univ. of Technology	4	10 x 20 mm	2	11x11 x 35 cm	6	30	< 5 kg		•	•								✓				0	0								•	2	
LUNA E drills	LUNA 24	Soviet Union	9	1.6 m, 170.1 g	2.25 (2 vert)		140		13.6 kg			✓		✓							✓	4			✓				✓					3	
Sample Acquisition and Transfer Mechanism Drill (SATM)	Champollion	Honeybee Robotics SMC	4	0.1–1.0 cm^3 powder	1.2	60 x 60 x 138 cm		55.6	9 kg		•	•						✓				2		✓						•			✓	3	
Sample Acquisition System Corer	CSNR	Galileo Avionica	5	100 x 1000 mm		100	100			✓			✓	✓									✓					•	•						
Construction and Resource Utilization Explorer Drill(CRUX)		Honeybee Robotics SMC	4–5	25 mm	2		< 40	1000			•	•	•	•	•									✓	✓				✓						
Drill-Integrated Package for Borehole Sciences (DIBS)	ExoMars	Galileo Avionica	4	10 x 20 mm	2		60	300	17.3 kg			✓					0							0	0				0					3	
DeeDri	Mars Exploration Program	Galileo Avionica	3	14 x 25 mm core; tbd cm^3 powder	1–2.5	12.51 x 2.20 x 1.55 cm	< 30	3–196	7–8.3 kg		✓		✓			✓	✓							✓										1	
Small Sample Acquistion and Distribution Tool (SSA/DT)		Galileo Avionica	4–5	0.2 cm^3	2		5		1.7 kg		0	0	0	0	0	0	0	0	0	0	0			0	0				•	•					
Subsurface Corer Sampling System (SCSS)		Honeybee Robotics SMC	4	0.8 x 4 cm; 50 cm^3	1	56 x 46 x 175 cm	70	150 lb	122 x lb		✓	✓				✓	✓							✓								✓			3	
Segmented Coring Auger Drill(SCAD)	1998 Tech Dev	ATK Space	3	10 x 75 mm core	2.5	90 x 100 x 125 cm					✓					✓								0	0										
Planetary Underground Tool (PLUTO)	Mars Express	German Aerospace Center	8	0.2 cm^3	1.5	3.8 x 9 x 8 cm	3		0.89 kg				✓				✓								✓				✓					1	
Instrumented Mole System(IMS)	Mars Express	Galileo Avionica	6		5						0	0	0	0	0	0	0	0	0	0	0			0	0				0	0	0	0	0	0		0
Moon/Mars Underground Mole (MUM)		Amesh Research Center	4–5	5 cm^3	2		10		5 kg				✓				✓								✓				0	0	0	0	0	0		0
Compact Drilling and Sample System		Jet Propulsion Laboratory	4	0.4 cm^3	1.5		25		2 kg				✓				✓					2			✓				✓	•				✓		✓
USDC Penetrator		Jet Propulsion Laboratory	4		1		14		0.5–1.5 kg																											

Table 6.25 Drill matrix for 10 m class drills (<10 m).

System architecture	Mission/ program (if applicable)	Company	TRL	Sample size	Sampling depth capability (m)	Stowed volume	Power (w)	WOB (preload) (N)	Mass (kg)
Mars Analog Research & Technology Experiment (MARTE)		Honeybee Robotics SMC	5–6	27 x 25 cm core, tbd cm³ powder	10		150		
Drilling Automation for Mars Exploration (DAME)		Honeybee Robotics SMC	4–5			150 x 50 x 50 cm	200	400	20
Subsurface sampling unit	HESOLVE	NOHCAT/EVC	4	10 mm dia core	1–20				
Subsurface Telescoping Sampling System (STSS)		Honeybee Robotics SMC			2				
Subsurface Planetary Exploration Core Extracting System (SPECES)	2002 TechDev	ATK Space	5	10–15 mm x 100 mm core	10	100 x 100 x 90 cm	90–100	100–350	
Primary capabilities									
Solid core capture			✓						
Unconsolidated core capture									
Loose regolith capture									
Power sample capture									
Icy soil capture									
Solid core ejection			✓						
Unconsolidated core / loose regolith ejection									
Power sample ejection									
Icy soil ejection									
Subcore stratigraphy			✓						
Loose regolith stratigraphy									
Autonomy rating			2		3				
Sampling characteristics									
Use with rotary drills			✓						
Use with rotary-percussive or percussive drills									
Use with pnuematic drills									
Use with ultrasonic actuator									
System requirements									
Operation in Martian relevant environment									
Operation in lunar relevant environment									
Operation in Venus relevant environment									
System robustness									
Reliability of operations									
Sample preservation									
System profile									
Core properties									

pass

Table 6.26 Drill matrix for deep drills (> 10 m).

System architecture	Mission/ program (if applicable)	Company	TRL	Sample size	Sampling depth capability (m)	Stowed volume	Power (w)	WOB (preload) (N)	Mass (kg)	Primary capabilities	Solid core capture	Unconsolidated core capture	Loose regolith capture	Power sample capture	Icy soil capture	Solid core ejection	Unconsolidated core / loose regolith ejection	Powder sample ejection	Icy soil ejection	Solid core stratigraphy	Loose regolith stratigraphy	Autonomy rating	Sampling characteristics	Use with rotary drills	Use with rotary-percussive or percussive drills	Use with pnuematic drills	Use with ultrasonic actuator	System requirements	Operation in Martian relevant environment	Operation in lunar relevant environment	System robustness	Reliability of operations	Sample preservation	System profile	Core properties
Autonomous Tethered Corer (ATC)		Raytheon-UTD	4	25 × 110 mm core	200		50–75	151	7		✓					✓								✓											
Ultrasonic gopher		Jet Propulsion Laboratory	5	45 × tbd mm core	20–100										✓				✓					✓			✓		•	○	○				
Mars/Arctic Deep Drill (MADD)		JSC / Baker-Hughes	5	25 × 150 mm core	>100		100		8.5															✓											
Inchwork Deep Drilling System (IDDS)		Honeybee Robotics SMC			>100						✓			✓	✓									✓											
Modular Planetary Drill System (MPDS)	2004 MEPAT	ATK Space	4–5	1.5 × 10 cm	20–50	90 × 100 × 125 cm	40–100	100–400	100		✓				✓		✓		✓			1		✓											

6.19 Conclusions

Planetary geology science can provide a great deal of information regarding the history and current state of a body. Of particular interest today is the characterization of both the lunar and Martian surfaces toward constructing a historical view of significant events (i.e., meteor impacts, volcanism, and evidence of water flow). Such characterization also serves to identify materials for ~~ISRU. Such characterization is~~ a critical step to further human presence into the universe. Fundamental to this is the need to carry out robotic planetary exploration missions capable of performing *in situ* analyses of rock and/or regolith core samples that deliver the stratigraphy of the target formation ~~intact~~ to the analysis suite. Autonomously obtaining and delivering a core, be it consolidated or unconsolidated material, is a much more complex engineering problem than simply drilling a hole; it requires additional mechanisms to break-off, capture, eject, and hand-off of the core to the sample processing and analysis chain. To support future missions, these sample handling technologies must be developed to meet a broad range of potential requirements, including a variety of rock or subsurface materials, rigorous sample preservation, and the general problem of autonomous operation ~~in~~ the presence of dust and ~~with~~ limited resources.

To date, coring tool development has focused on integration and far-horizon proof of concepts, resulting in complete systems designed around general technology goals and NASA-directed contractual requirements. For example, many systems were designed assuming that the material being sampled was consolidated and homogeneous. Evolving the design of the certain systems to accommodate a variety of rock and regolith characteristics would have meant months in redesign ~~and reintegration~~ exceeding the scope of the projects. Although lessons have been learned from these efforts, these research drill technologies may or may not support sampling tool requirements for future missions. To reduce overall mission schedule and budget risk, concerted technology development to meet these requirements must begin early. The path forward in sampling tool development lies in maturing specific aspects of designs quickly. This will allow for the development of a complete system based on various subsystems that have been matured to a TRL of 5 or 6.

The purpose of this chapter was to survey existing sampling systems that have been developed for robotic planetary missions. This information was compiled to allow for fast comparisons to aid future mission planners to identify areas where existing technology is lacking. This survey can be used as a starting point from which to add information as current systems are matured and additional systems are developed.

Appendix A: Glossary

A **Bailer** is a small bucket suspended by a tether that is used to remove drilled formation from the bottom of a hole.

Bit chatter is a strong vibration of the drill bit during drilling.

Page Proof © WILEY-VCH

Breadboard engineering proof of concept – basic working model.

Choking is a phenomenon that occurs when cuttings fail to move up the auger flutes or flights; the torque increases dramatically, and the drill jams.

A **Core** is a cylindrical piece of subsurface formation (e.g., solid rock, ice, or compacted regolith) that is formed by a coring bit after making a borehole.

A **Coring bit** is a drill bit that excavates an annular part of a hole, leaving a central, solid core of a subsurface formation.

The **Cut per revolution** is the amount of penetration that a drill bit achieves in a single revolution. The overall rate of penetration is equal to the cut per revolution multiplied by the rpm of the bit.

Cuttings, also known as **chips** and **fines**, are the pulverized remains of the formation that the bit has excavated from the formation.

Diamond-impregnated cutters consist of randomly placed, very small diamonds embedded in a softer matrix. If designed correctly, the matrix wears away just when the exposed layer of diamonds becomes dull, thus exposing a new layer of sharp diamonds.

Drilling power, measured in watts, is the sum of the power consumed by the bit as it breaks down the formation and the power used by the cuttings removal system. It represents some fraction of the energy consumed by the drill system, and is calculated by subtracting the total system power while drilling into air from the total system power while drilling into a subsurface formation.

Total drilling power, measured in watts, is the total power consumed by the drill system while drilling. It includes the power to break down the formation, move the cuttings to the surface and any mechanical losses (e.g., drill motor) associated with the drilling system.

The **Drill string** consists of the bit and cuttings removal structures (usually an auger) in subsurface drills. In drills longer than about 1 m, the drill string is usually made of more than one segment.

Dry drilling is drilling without the benefit of the injection of a fluid into the hole (strictly, a liquid, since gases are fluids, and dry drilling could include drilling with gas flushing). It is more challenging than wet drilling, because of less efficient cooling and cuttings removal.

Flutes (or **flights**) are the spiraling surfaces on an auger that convey cuttings from the bottom of the borehole region (just above the bit) towards the surface.

The **Formation** (short for geological formation) is the volume of material in which a drill makes a hole.

A solid front or **Full-faced bit** is a drill bit that excavates the entire area of the hole (as opposed to a coring bit that excavates an annular region or solid segment).

Polycrystalline diamond compact cutters consist of a thin layer of polycrystalline synthetic diamonds lying on a thicker layer of cemented tungsten carbide.

A **Rotary drill** uses simple rotation, combined with weight-on-bit, to excavate a hole.

A **Rotary–percussive drill** combines rotation of the bit with high-frequency (perhaps 50 Hz) downward hammering. The hammering results in much higher peak forces than can be achieved with a rotary drill, and is most suitable for brittle

page proof WILEY-VCH

materials. Rotary–percussive drill bits have to be designed so that they themselves do not fracture or deform due to the hammering.

A **Slipring assembly** is a device that allows electrical signals to pass between stationary and rotating structures in a drill, including, for example, a sensor or sampling actuator that is located inside the rotating drill string.

The **Unconfined compressive strength (UCS)** of a material is the stress needed to cause fracture when a sample of the material is subjected to a compressive force with no support on the lateral surfaces.

Drill **Wandering** refers to the parasitic, uncontrolled motion of a drill bit attacking a surface and poorly supported laterally: when its edge meets a hard inclusion, the drill pivots around the contact point until it returns under elastic forces of its support. This effect is particularly marked with corers (it is equivalent to low-frequency, high-amplitude drill chatter).

Weight, in this chapter, is quoted in units of force (newtons) and **Mass** in kilograms.

The **Weight on bit(WOB)**, measured in newtons or pounds, is the downward force applied to the drill string, and hence to the bit.

A **Wireline drill** is a drill that is suspended from a tether. The tether cannot exert any downward force, so WOB is provided by reaction against structures that press against the hole walls. Cuttings are stored in the drill until the drill penetrates to its maximum stroke, whereupon the entire drill is pulled up to the surface to remove the cuttings.

Appendix B: List of abbreviations

ALSD	Apollo Lunar Surface Drill
AMD	Acid mine drainage
ASI	Agenzia Spaziale Italiana (Italian Space Agency)
ASSD	Asteroid surface sampling device
ATC	Autonomous Tethered Corer
BHA	Bottom hole assembly
CAT	Coring and Abrading Tool
CFRP	Carbon fiber-reinforced polymer
CNSR	Comet nucleus sample return
CRUX	Construction and Resource Utilization Explorer
DAME	Drilling Automation for Mars Exploration
DLR	Deutsches Zentrum für Luft- und Raumfahrt (German Aerospace Center)
DOF	Degrees of freedom
ESA	European Space Agency
FOB	Force on bit
GC/MS	Gas chromatograph–mass spectrometer
GFRP	Glass fiber-reinforced polymer
GMD	Ground Mole Demonstrator

Page Proof WILEY-VCH

HKPU	Hong Kong Polytechnic University
HUT	Helsinki University of Technology
IDDS	Inchworm deep drilling system
INL	Idaho National Laboratory
ISAD	Icy Soil Acquisition Device
ISRU	*In situ* resource utilization
JAXA	Japan Aerospace Exploration Agency
JPL	Jet Propulsion Laboratory
JSC	Johnson Space Center
LSAS	Low Force Sample Acquisition System
MARTE	Mars Astrobiology Research and Technology Experiment
MC	Mini-Corer
MEE	Micro End-Effector
MER	Mars Exploration Rover
MIDAS	Mars Integrated Drilling and Sampling
MMC	Metal matrix composite
MMUM	Moon/Mars Underground Mole
MPDS	Modular planetary drill system
MSL	Mars Science Laboratory
MSR	Mars Sample Return
NASA	National Aeronautics and Space Administration
NEA	Near-Earth asteroid
NORCAT	Northern Centre for Advanced Technology
PLUTO	Planetary Underground Tool
PCD	Polycrystalline diamond
PDA	Processing and distribution assembly
RAT	Rock abrasion tool
RCG	Rock corer grinder
ROP	Rate of penetration
RSA	Rover Support Assembly
RSCT	Robotic Sampling and Containerization Technology
SAS	Sample acquisition system
SATM	Sample Acquisition and Transfer Mechanism
SBIR	Small Business Innovation Research
SCaD	Sample capture device
SCAD	Segmented coring auger drill
SCSS	Subsurface Corer Sampling System
SD^2	Sampling, drilling, and distribution
SMC	Spacecraft Mechanisms Corporation
SPECES	Subsurface Planetary Exploration Core Extracting System
SSA/DT	Small Sample Acquisition and Distribution Tool
STSS	Subsurface Telescoping Sampling System
SUBEX	Subsurface explorer
TRL	Technology readiness level
UAD	Ultrasonically assisted drilling

page proof WILEY-VCH

UCS	Unconfined compressive strength
UDT	Ultrasonic drill tool
URAT	Ultrasonic/sonic rock abrasion tool
USDC	Ultrasonic/Sonic Driller/Corer
WOB	Weight on bit
XRS	X-ray spectrometer

Acknowledgments

Research reported in this chapter was conducted at the Jet Propulsion Laboratory (JPL), California Institute of Technology, and Honeybee Robotics under various contracts with NASA.

The authors would like to thank Geoffrey A. Briggs, NASA Ames, George Cooper, University of California at Berkeley, and Edward Tunstel, JHU Applied Physics Laboratory.

~~The authors acknowledge the contributions from the following Honeybee Robotics employees: Arthur Ashley, Philip Chu, Jack Craft, Larry Parrington, Patrick Fink, Jason Herman, Magnus Hedlund, Jerri Ji, Alastair Kusack, Nishant Kumar, Mike Maksymuk, Erik Mumm, Mike Passaretti, Dustyn Roberts, Mike Rutberg, Chris Santoro, Sase Singh, Serge Stroescu, Jack Wilson, and Irene Yachbes. In addition, the authors would like to thank Paul Bartlett, Logical Expression LLC.~~

Q8

References

Agnolon, D. (May 31, 2007) *Study Overview of the Near-Earth Asteroid Sample Return*. ESA SCI-A/2007/DA, European Space Agency, Noordwijk.

Aldrich, J., Sherrit, S., Badescu, M., Bar-Cohen, Y., Bao, X. and Chang, Z. (2006) Controller Using Extremum-Seeking to Drive Heavily Perturbed Electroactive Actuators at Resonance. NASA New Technology Report (NTR), Docket 43519, NASA.

Allton, J.H. (1989) Catalog of Apollo Lunar Surface Geological Sampling Tools and Containers. Document JSC-23454, NASA Johnson Space Center.

Ammannito, E., Coradini, A., De Sanctis, M.C. and Piccioni, G. (2008) Imaging spectroscopy in lab: a tool supporting the interpretation of remotely sensed data by dawn mission. Asteroids, Comets, Meteors, Paper 8295.

~~Andersen, D.T., Pollard, W.H., McKay, C.P. and Heldmann, J. (2002) Cold springs in permafrost on Earth and Mars. *Journal of Geophysics Research*, DOI:107:10.1029/2000JE001436.~~ Q9

Anttila, M. (2005) Concept Evaluation of Mars Drilling and Sampling Instrument. PhD dissertation, University of Technology, Laboratory of Space Technology, Helsinki.

Aoki, S. and Nishimura, T. (2004) Prevention of delamination during drilling of composite material using vibration. *Key Engineering Materials*, **261/263** (1), 381–386.

Astashev, V.K. and Babitsky, V.I. (2007) *Ultrasonic Processes and Machines – Dynamics, Control and Applications*, Springer, Berlin.

Atzei, A., Hechler, M. and Coste, P. (1989) ESA preparatory programme for the Rosetta/CNSR Mission. In: *Proceedings of the 40th International Astronautical Congress, Malaga, Spain (7–13*

page proof WILEY-VCH

October 1989), IAF-89-023, vol. 1/8, International Astronautical Federation, Paris.

Babitsky, V.I. (1998) *Theory of Vibro-Impact Systems and Applications*, Springer, Berlin.

Babitsky, V.I., Meadows, A.,*et al.* (2007) Vibration excitation and energy transfer during ultrasonically assisted drilling. *Journal of Sound and Vibration*, **308** (Special Issue "Vibro-Impact Systems"), 805–814.

Badescu, M., Sherrit, S., Olorunsola, A., Aldrich, J., Bao, X., Bar-Cohen, Y., Chang, Z., Doran, P.T., Fritsen, C.H., Kenig, F., McKay, C.P., Murray, A., Du, S., Peterson, T. and Song, T. (2006) Ultrasonic/sonic gopher for subsurface ice and brine sampling: analysis and fabrication challenges, and testing results. Proceedings of the SPIE Smart Structures and Materials Symposium, San Diego, CA, 27 February–2 March 2006, Paper 6171-07.

Badescu, M., Sherrit, S., Bar-Cohen, Y., Bao, X. and Kassab, S. (2007) Ultrasonic/Sonic Rotary–Hammer Drill (USRoHD). NTR Docket No. 44765, 19 December 2006. Patent application submitted 17 August 2007.

Bao, X., Bar-Cohen, Y., Chang, Z., Dolgin, B.P., Sherrit, S., Pal, D.S., Du, S. and Peterson, T. (2003) Modeling and computer simulation of ultrasonic/sonic driller/corer (USDC). *IEEE Transactions on Ultrasonics, Ferroelectrics and Frequency, Control (UFFC)*, **50** (9), 1147–1160.

Bar-Cohen, Y. (2005) *Biomimetics – Biologically Inspired Technologies*, CRC Press, Boca Raton, FL, pp. 1–527.

Bar-Cohen, Y. and Sherrit, S. (2003) Self-Mountable and Extractable Ultrasonic/Sonic Anchor (U/S-Anchor). NASA New Technology Report (NTR), 9 December 2003, Docket No. 40827, NASA.

Bar-Cohen, Y., Sherrit, S., *et al.* (2001) Ultrasonic/sonic drilling/coring (USDC) for planetary applications. SPIE Smart Structures, Newport Beach, CA, 5–8 March 2001, Paper 4327-55.

Bar-Cohen, Y., Randolph, J., Ritz, C., Cook, G., Bao, X. and Sherrit, S. (2002) Sample Preparation, Acquisition, Handling and Delivery (SPAHD) System using the Ultrasonic/Sonic Driller/Corer (USDC) with Interchangeable Bits. NASA New Technology Report (NTR), 1 May 2002, Docket No. 30640, NASA.

Bar-Cohen, Y., Sherrit, S. and Herz, J.L. (2003) Ultrasonic/Sonic Jackhammer (USJ). NASA New Technology Report (NTR), 31 October 2003, Docket No. 40771, NASA.

Bao, X., Bar-Cohen, Y., Chang, Z., Sherrit, S. and Stark, R. (2004) Ultrasonic/Sonic Impacting Penetrator (USIP). NASA New Technology Report (NTR), 22 December 2004, Docket No. 41666, NASA.

Bar-Cohen, Y., Sherrit, S., Dolgin, B., Peterson, T., Pal, D. and Kroh, J. (2005) Smart-Ultrasonic/Sonic Driller/Corer. NASA New Technology Report (NTR), 30 August 1999, Docket No. 20856; US Patent 6,863,136, 8 March 2005

Bar-Cohen, Y., Sherrit, S., Bao, X., Badescu, M., Aldrich, J. and Chang, Z. (2007) Ultrasonic/sonic driller/corer (USDC) as a subsurface sampler and sensors platform for planetary exploration applications. Proceedings of the NASA Science and Technology Conference (NSTC-07), University of Maryland Conference Center, 19–21 June 2007.

Barmin, I.V. and Shevchenko, A.A. (1983) Soil-scooping mechanism for the Venera 13 and Venera 14 unmanned interplanetary spacecraft. *Kosmicheskie Issledovanie*, **21**, 171–175.

Barsukov, V.L. (1977) Preliminary data for the regolith core brought to Earth by the automatic lunar station Luna 24. 8th Lunar Planetary Science Conference, pp. 3303–3318.

Batako, A.D., Babitsky, V.I. and Halliwell, N.A. (2003) A self-excited system for percussive–rotary drilling. *Journal of Sound and Vibration*, **259** (1), 97–118.

Batako, A.D., Babitsky, V.I. and Halliwell, N.A. (2004) Modeling of vibro-impact penetration of self-exciting percussive–rotary drill bit. *Journal of Sound and Vibration*, **271**, 209–225.

Bean, A.L., Conrad, C. Jr, and Gordon, R.F. (1970) Crew observations. In: Apollo 12 Preliminary Science Report (ed. A.J. Calio *et al.*), pp. 29–38.

Bibring, J.-P., Langevin, Y., Mustard, J.F., Poulet, F., Arvidson, R., Gendrin, A., Gondet, B., Mangold, N., Pinet, P. and Forget, F. (2006) Global mineralogical and aqueous Mars history derived from OMEGA/Mars Express data. *Science*, **312**, 400–404.

Bibring, J.P., Langevin, Y., Gendrin, A., Gondet, B., Poulet, F. and Berthé, M. (2005) Mars surface diversity as revealed by the OMEGA/Mars Express observations. *Science*, **307**, 1576–1579.

Bibring, J.P., Arvidson, R.E., Gendrin, A., Gondet, B., Langevin, Y., Le Mouellic, S., Mongold, N., Morris, R.V., Mustard, J.F., Poulet, F., Quantin, C. and Sotin, C. (2007) Coupled ferric oxides and sulfates on the Martian surface. *Science*, **317**, 1206–1210.

Bignami, G., Cargil, P., Schutz, B. and Turon, C. (2005) *Cosmic Vision: Space Science for Europe 2015–2025, BR-247*, ESA Publications Division, ESTEC, Noordwijk, pp. 1–111. Available at http://www.esa.int/esapub/br/br247/br247.pdf (accessed 31 May 2005).

Blake, D.F., Sarrazin, P., Chipera, S.J., Bish, D.L., Vaniman, D.T., Bar-Cohen, Y., Sherrit, S., Collins, S., Boyer, B., Bryson, C. and King, J. (2003) Definitive mineralogical analysis of Martian rocks and soil using the CHEMIN XRD/XRF instrument and the USDC sampler. Proceedings of the Sixth International Conference on Mars, Caltech, Pasadena, CA, 20–25 July 2003.

Brennan, M., Cotten, S., Dolgin, B., Goldstein, B., Hill, J., Roberts, D. and Shenhar, J. (2005) Mars lander based 1000m class drill. European Geosciences Union General Assembly, Vienna, 24–29 April 2005, GI5-1FR5O-001.

Briggs, G. and Gross, A. (2002) Technical challenges of drilling on Mars. AIAA Aerospace Sciences Meeting and Exhibit, 40th, Reno, NV, 14–17 January 2002, 2002, AIAA-2002-469, American Institute of Aeronautics and Astronautics.

Buckley, D. (1971) Friction, Wear and Lubrication in Vacuum. NASA Special Publication SP-277.

Campaci, R., Debei, S., Finotello, R., Parzianello, G., Bettanini, C., Giacometti, M., Rossi, G., Visentin, G. and Zaccariotto, M. (2005) Design and optimization of a terrestrial guided mole for deep subsoil exploration – boring performance experimental analyses. i-SAIRAS 2005, 8th International Symposium on Artificial Intelligence, Robotics, and Automation in Space, 5–8 September 2005, Munich.

Carrier, W.D. (2005) *The Four Things You Need to Know about the Geotechnical Properties of Lunar Soil*, Lunar Geotechnical Institute, Lakeland, FL.

Carrier, W.D., Johnson, S.W., Werner, R.A. and Schmidt, R. (1971) Disturbance in samples recovered with the Apollo core tubes. In: Proceedings of the Second Lunar Science Conference, pp. 2959–2972.

Carrier, W.D., Olhoeft, G.R. and Mendell, W. (1991) Physical properties of the lunar surface. In: *Lunar Sourcebook* (eds G. Heiken, D. Vaniman and B.M. French), Cambridge University Press, Cambridge, pp. 475–594.

Chang, S.S.F. and Bone, G.M. (2005) Burr size reduction in drilling by ultrasonic assistance. *Robotics and Computer-Integrated Manufacturing*, **211** (4–5), 442–450.

Chang, Z., Sherrit, S., Bao, X. and Bar-Cohen, Y. (2004) Design and analysis of ultrasonic horn for USDC (ultrasonic/sonic driller/corer). SPIE Smart Structures and Materials Symposium, San Diego, CA, 15–18 March 2004, Paper 5387-58.

Chipera, S.J., Bish, D.L., Vaniman, D.T., Sherrit, S., Bar-Cohen, Y. and Blake, D.F. (2003) Use of an ultrasonic/sonic driller/corer to obtain sample powder for CHEMIN - a combined XRD/XRF instrument. 34th Lunar and Planetary Science Conference, League City, TX, 17–21 March 2003, Poster Paper 1603.

Chu, P., Wilson, J., Davis, K., Shiraishi, L. and Burke, K. (2008) Icy soil acquisition device for the 2007 Phoenix Mars Lander. 39th Aerospace Mechanisms Symposium, Huntsville, AL, May 2008.

Coste, P. (1998) Mobile penetrometer ground tests. In: *Proceedings of the Fifth Workshop on Advanced Space Technologies for Robotics and Automation (ASTRA'98), 1–3 December 1998*

(ed. M. Van Winnendael), WPP-154, ESTEC, European Space Agency, Noordwijk, p. E-3.

Coste, P., Fenzi, M. and Eiden, M. (1993) Collecting cometary soil samples – development of the ROSETTA sample acquisition system. In: *Proceedings of the 27th Aerospace Mechanisms Symposium, 12–14 May 1993* (ed. R. Mancini), NASA Conference Publication 3205, NASA, Moffet Field, CA, pp. 1–19.

Coste, P., Richter, L., Kochan, H. and Gromov, V. (2001) Sampling mole, development and application on the Beagle 2 Mars Lander. XXVIth General Assembly of the European Geophysical Society, Nice, 20–25 March 2001.

Dario, P., Laschi, C., Mazzolai, B., Corradi, P., Mattoli, V., Mondini, A., Mancuso, S., Mugnai, S., Masi, E., Azzarello, E., Hlavacka, A. and Pandolci, C. (2008) Bio-Inspiration from Plants' Roots, European Space Agency, the Advanced Concepts Team. Ariadna Final Report, 06/6301.

Devine, J. (1985) Ultrasonically assisted metal removal. In: *Fabrication of Composite Materials: Source Book*, American Society for Metals, Materials Park, OH, pp. 329–334.

Dickinson, W. and Rosen, M.R. (2003) Antarctic permafrost: an analogue for water and diagenetic minerals on Mars. *Geology*, **31** (3), 199–202.

Dolgin, B., Sherrit, S., Bar-Cohen, Y., Rainen, R., Askins, S., Sigel, D., Bickler, D., Carson, J., Dawson, S., Bao, X., Chang, Z. and Peterson, T. (2001a) Ultrasonic Rock Abrasion Tool (URAT). NASA New Technology Report (NTR), 12 October 2001, Docket No. 30403.

Dolgin, B., Sherrit, S., Bar-Cohen, Y., Askins, S., Sigel, D., Bao, X. and Chang, Z. (2001b) Ultrasonic/Sonic Vibrating/Rotating Tool. NASA New Technology Report (NTR), 5 September 2001, Docket No. 30370.

Doran, P.T., Priscu, J.C., Lyons, W.B., Walsh, J.E., Fountain, A.G., McKnight, D.M., Moorhead, D.L., Virginia, R.A., Wall, D.H., Clow, G.D., Fritsen, C.H., McKay, C.P. and Parsons, A.N. (2002) Antarctic climate cooling and terrestrial ecosystem response. *Nature*, **415**, 517–520.

Eapen, D., Barroso, M.L., Ponce, G., Campos, M.E. and Cassab, G.I. (2005) Hydrotropism: root growth responses to water. *Trends in Plant Science*, 44–50. Q10 10(1):44-50

Egashira, K., Mizutani, K. *et al.* (2002) Ultrasonic vibration drilling of microholes in glass. *CIRP Annals*, **51** (1), 339–342.

Eiden, M. and Coste, P. (1991) The Challenge of Sample Acquisition in a Commentary Environment. *ESA Journal*, **15**, 199–211.

Eitel, R.E., Randall, C.A., Shrout, T.R. and Park, S.E. (2002) Preparation, characterization of high temperature perovskite ferroelectrics in the solid solution $(1 - x)BiScO_3$–$xPbTiO_3$. *Japanese Journal of Applied Physics*, **41**, 1–6.

Esmon, C.A., Pedmale, U.V. and Liscum, E. (2005) Plant tropisms: providing the power of movement to a sessile organism. *International Journal of Development Biology*, **49**, 665–674.

Feldman, W.C., Boynton, W.V., Tokar, R.L., Prettyman, T.H., Gasnault, O., Squyres, S.W., Elphic, R.C., Lawrence, D.J., Lawson, S.L., Maurice, S., McKinney, G.W., Moore, K.R. and Reedy, R.C. (2002) Global distribution of neutrons from Mars: results from Mars Odyssey. *Science*, **297**, 75–78.

Fenzi, M., Pozzi, E. and Coste, P. (1993) A system for the challenging task of collecting samples from a comet surface. In: *Fifth European Space Mechanisms and Tribology Symposium – Proceedings of an International Symposium Organized by the European Space Agency (5th ESMATS), 28–30 October 1992* (ed. W.R. Burke), ESA SP-334, ESTEC, European Space Agency, Noordwijk, pp. 137–142.

Fernández-Remolara, D. and Knoll, A. (2008) Fossilization potential of iron-bearing minerals in acidic environments of Rio Tinto, Spain: implications for Mars exploration. *Icarus*, **194** (1), 72–85.

~~Freifeld, B.M., Finsterle, S., Onstott, T.C., Toole, T., Rickard, J. and Pratt, L., (2008) Ground surface temperature reconstructions: using *in situ* estimates for thermal conductivity acquired with a fiber-optic distributed thermal perturbation sensor. *Geophysics Research Letters*,~~ Q11

Fryxell, R. and Heiken, G. (1974) Preservation of lunar core samples: preparation and interpretation of three dimensional stratigraphic sections. In: Proceedings of the 5th Lunar Science Conference, pp. 935–966.

Q12 Fukuda, T. and Menz, W. (2001) *Micro Mecha Systems – Principles and Technology*, p. 211.

Q13 Gao, Y., Ellery, A., Jaddou, M., Vincent, J. and Eckersley, S. (2007) Planetary micro-penetrator concept study with biomimetic drill and sampler. *IEEE Transactions on Aerospace and Electronic Systems*, **43** (3).

Gelmi, R., Mirko, I., Magnani, P.G., Re, E., Grzesik, A., Richter, L., Nadalini, R. and Coste, P. (2007) Mole-carried sensor package. In: *12th European Space Mechanisms and Tribology Symposium (ESMATS), Liverpool, 19–21 September 2007* (ed. A. Wilson), ESA SP-653, ESTEC, European Space Agency, Noordwijk.

Gendrin, A., Mangold, N., Bibring, J.P., Langevin, Y., Gondet, B., Poulet, F., Bonello, G., Quantin, C., Mustard, J., Arvidson, R. and LeMouélic, S. (2005) Sulfates in Martian layered terrains: the OMEGA/Mars Express View. *Science*, **307**, 1587–1591.

Gibson, E.K., Wentworth, S.J. and McKay, D.S. (1983) Chemical weathering and diagenesis of a cold desert soil from Wright Valley, Antarctica: an analog of Martian weathering processes. In: Proceedings of the Lunar Science Conference, 13, pp. 912–928.

Glass, B., Cannon, H., Branson, M., Hanagud, S. and Paulsen, G. (2008) DAME: planetary-prototype drilling automation. *Astrobiology*, **8** (3), 653–664.

Q14 Gorevan, S.P., Myrick, T., Davis, K., Chau, J.J., Bartlett, P., Mukherjee, S., Anderson, R., Bares, S.W., Arvidson, R.E., Madsen, M.B., Bertelsen, P., Goetz, W., Binau, C.S., Richter, L. and Hoehe, L. (2003) Rock abrasion tool: Mars Exploration Rover Mission. *Journal of Geophysical Research*, **108**, DIO :10.1029/2003JE002061.

Graff, K.F. (1975) Macrosonics in industry 5: ultrasonic machining. *Ultrasonics*, **13** (3), 103–109.

Gromov, V.V., Misckevich, A.V., Yudkin, E.N., Kochan, H., Coste, P. and Re, E. (1997) The mobile penetrometer, a mole for sub-surface soil investigation. In: *Proceedings of the 7th European Space Mechanisms and Tribology Symposium (7th ESMATS), ESTEC, Noordwijk, 1–3 October 1997* (ed. B.H. Kaldeich-Schürmann), ESA SP-410, ESTEC, European Space Agency, Noordwijk.

Guerrero, J.L., Craig, J., Meyers, M., Reiter, J.W., Wang, G.Y. and Wu, D. (2005) Planetary drill technology and applications to future space missions. Proceeding Space Resources Roundtable VII: LEAG Conference on Lunar Exploration, Lunar and Planetary Institute, Houston, TX.

Guerrero, J.L., Beegle, L., Craig, J., Meyers, M., Wang, G.Y., Rumann, A., Abbay, W., Reiter, J.W. and Wu, D. (2006) Robotic drilling technology and applications to future space missions. *Proceedings of the 2006 American Geophysical Union Conference*, American Geophysical Union, Washington, DC.

Haberle, R.M., McKay, C.P., Schaeffer, J., Cabrol, N.A., Grin, E.A., Zent, A.P. and Quinn, R. (2001) On the possibility of liquid water on present-day Mars. *Journal of Geophysical Research*, **106**, 23317–23326.

Hall, B.L. and Denton, G.H. (2006) Surficial geology and geomorphology of eastern and central Wright Valley, Antarctica. *Geomorphology*, **64** (1–2), 25–65.

Hashimoto, T., Hoshino, T., Tanaka, S., Matsumoto, K. and Kawaguchi, J. (2008) Japanese Moon landing mission SELENE-2. 26th International Symposium on Space Technology and Science, 2008-k-55.

Holmberg, N.A., Faust, R.P. and Holt, H.M. (November, 1980) *Viking '75 Spacecraft Design and Test Summary: Volume 1 – Lander Design. NASA Reference Publication 1027.* NASA Langley Research Center, Hampton, VA

Huba, A. and Keskeny, J. (2006) Design of a flexible tube robot. *Facta Universitatis Series: Mechanical Engineering*, **4** (1), 45–51.

Huekelom, W. and Klomp, A. (1962) Dynamic testing as a means of controlling pavements during and after construction. In: International Conference on the Structural Design of Asphalt Pavements, pp. 667–685.

Juck, D.F., Whissell, G., Steven, B., Pollard, W., McKay, C.P., Greer, C.W. and Whyte, L.G. (2005) Utilization of fluorescent microspheres and a green fluorescent protein-marked strain for assessment of microbiological contamination of permafrost and ground ice core samples from the Canadian High Arctic. *Applied and Environmental Microbiology*, **71**, 1035–1041.

Kennedy, B., Okon, A., Aghazarian, H., Badescu, M., Bao, X., Bar-Cohen, Y., Chang, Z., Dabiri, B., Garrett, M., Magnone, L. and Sherrit, S. (2006) Lemur IIb: a robotic system for steep terrain access. Proceedings of the 8th International Conference on Climbing and Walking Robots (CLAWAR 2005), 12–15 September 2005, *Industrial Robot – An International Journal*, **33** (4), 265–269.

Q15 Kessler, F. and Leitner, J., (2000) Investigations into the material flow at the intake of vertical screw conveyors. *International Journal of Storing, Handling and Transporting Bulk*, **20** (4).

Klingelhöfer, G., Morris, R.V., Bernhardt, B., Schröder, C., Rodionov, D.S., de Souza, P.A. Jr, Yen, A., Gellert, R., Evlanov, E.N., Zubkov, B., Foh, J., Bonnes, U., Kankeleit, E., Gütlich, P., Ming, D.W., Renz, F., Wdowiak, T., Squyres, S.W. and Arvidson, R.E. (2004) Jarosite and hematite at Meridiani Planum from Opportunity's Mössbauer spectrometer. *Science*, **306**, 1740–1745.

Krasnopolsky, V.A., Maillard, J.P. and Owen, T.C. (2004) Detection of methane in the Martian atmosphere: evidence for life? *Icarus*, **172**, 537–547.

Kubota, T., Nakatani, I., Watanabe, K. and Shimoda, S. (2005) Study on mole-type deep driller robot for subsurface exploration. In: IEEE International Conference on Robotics and Automation, pp. 1309–1314.

Laskar, J., Levrard, B. and Mustard, J. (2002) Orbital forcing of the Martian polar deposits. *Nature*, **419**, 375–377.

Lee, P. and Osinski, G.R. (2005) The Haughton-Mars Project: overiew of science investigations at the Haughton impact structure and surrounding terrains, and relevance to planetary studies. *Meteoritics and Planetary Science*, **40** (HMP Special Issue), 1755–1758.

Liu, C.S., Zhao, B., Gao, G.F. and Zhang, X.H. (2005) Study on ultrasonic vibration drilling of particulate reinforced aluminum matrix composites. *Key Engineering Materials*, **291/292**, 447–452.

Lobitz, B., Wood, B.L., Averner, M.A. and McKay, C.P. (2001) Use of spacecraft data to derive regions on Mars where liquid water would be stable. *Proceedings of the National Academy of Sciences of the United States of America*, **98**, 2132–2137.

Lorenz, R.D., Hathi, B., Leese, M.R., Garry, J.R.C. and Zarnecki, J.C. (2001) The Huygens SSP penetrometer: an update. In: *Penetrometry in the Solar System* (eds N.I. Kömle G. Kargl A.J. Ball and R.D. Lorenz), Austrian Academy of Sciences Press, Vienna, pp. 99–108.

Magnani, P.G., Re, E., Mugnuolo, R. and Olivieri, A. (1998) Robotics and technology aspects of the Rosetta drill, sample and distribution system. In: *Proceedings of the Fifth Workshop on Advanced Space Technologies for Robotics and Automation (ASTRA'98), 1–3 December 1998* (ed. M. Van Winnendael), WPP-154, ESTEC, European Space Agency, Noordwijk, pp. 1.4–1.5.

Magnani, P.G., Re, E., Ylikorpi, T., Cherubini, G. and Olivieri, A. (2004) Deep drill (DeeDri) for Mars application. *Planetary and Space Science*, **52** (Special Issue 1–3), 79–82.

Mahaney, W.C., Dohm, J.M., Baker, V.R., Malloch, D., Hancock, R.G.V., Campbell, I., Sheppard, D. and Milner, M.W. (2001) Morphogenesis of Antarctic paleosols: Martian analogue. *Icarus*, **154**, 113–130.

Malin, M.C., Edgett, K.S., Posiolova, L.V., McColley, S.M. and Noe Dobrea, E.Z. (2007) Present-day impact cratering rate and contemporary gully activity on Mars. *Science*, **314**, 1573–1575.

Martin Marietta Corp. (1971) Familiarization and Support Manual for Apollo Lunar Surface Drill. MCR-71-35. Martin Marietta Corp., Bethesda, MD, p. 270.

Maurer, W.C. (1968) *Novel Drilling Techniques*, Pergamon Press, New York.

Q16 McKay, C.P., (2001) The search for a second genesis of life in our Solar System. In: *First Steps in the Origin of Life in the Universe* (ed. J. Chela-Flores), pp. 269–277.

McKay, C.P. (2004) What is life and how do we search for it on other worlds? *PLoS Biology*, **2**, 1260–1263.

Menon, C. and Broschart, M. (2006) Advanced space concepts bio-inspired by spider attaching mechanisms and plant roots. In: Proceedings of Patente aus der Natur, Bremen, pp. 22–30.

Menon, C. and Lan, N. (2006) Methodical approach to implement biomimetic paradigms in the design of novel engineering and space systems. 57th International Astronautical Congress, Valencia, Spain.

Q17 Menon, C., Ayre, M. and Ellery, A. (2006a) Biomimetics, a new approach for space systems design. *ESA Bulletin*, (125), 20–26.

Menon, C., Carpi, F. and de Rossi, D. (2006b) Concept design of novel bio-inspired distributed actuators for space applications. 57th International Astronautical Congress, Valencia, Spain.

Menon, C., Vincent, J., Lan, N., Bilhaut, L., Ellery, A., Gao, Y., Zangani, D., Carosio, S., Manning, C., Jaddou, M. and Eckersley, S. (2006c) Bio-inspired micro drillers for future planetary exploration. CANEUS2006-11022, CANEUS Micro-Nano-technology for Aerospace Applications, Toulouse.

~~Mitchell, D.P. Soviet Moon Images. Mental Landcape, http://www.mentallandscape.com/C_CatalogMoon.htm (accessed 9 June 2008).~~

Mitchell, J.K., Bromwell, L.G., Carrier, W.D. III, Costes, N.C., Houston, W.N. and Scott, R.F. (1972) Soil-mechanics experiment. In: Apollo 15 Preliminary Science Report (ed. J.P. Allen et al.), NASA SP-289, NASA, pp. 7-1–7-28.

Mukherjee, S., Bartlett, P., Glass, B., Guerrero, J. and Stanley, S. (2006) Technologies for exploring the Martian subsurface. Proceedings of the IEEE Aerospace Conference, March 2006, Big Sky, MT.

Nakamura, T., Kato, T., Iwanaga, T. and Muranaka, Y. (2006) Development of a peristalic crawling robot using servo motors based on the locomotion mechanism of earthworms. In: Proceedings of 2006 IEEE International Conference on Robotics and Automation, pp. 4342–4344.

Nathan, M., Barnes, F., Ko, H. and Sture, S. (1992) Mass and energy tradeoffs of axial penetration devices on lunar soil simulant. In: *Proceedings of Space '92*, American Society of Civil Engineers, Reston, VA, pp. 441–457.

Neugebauer, R. and Stoll, A. (2004) Ultrasonic application in drilling. *Journal of Materials Processing Technology*, **149** (1–3), 633–639.

Ng, T.C., Yung, K.L., Yu, C.H. and Chan, C.C. (2002) Planetary Sampling Tools – Micro End-Effectors (MEE) for Planetary Geological Samplings, http://www.ise.polyu.edu.hk/general_info/general_information.html (last accessed 19 September 2008).

~~Niederberger, T.D., Perreault, N., Nadeau, J.L., Greer, C.W., Andersen, D.T. and Whyte, L.G. (2008) Characterization of the filamentous community inhabiting cold saline springs situated at Gypsum Hill, Axel Heiberg Island in the Canadian High Arctic. Environmental Microbiology, in press.~~ Q18

Omelon, C.R., Pollard, W.H. and Marion, G.M. (2001) Seasonal formation of ikaite ($CaCO_3 \cdot 6H_2O$) in saline spring discharge at Expedition Fiord, Canadian High Arctic: assessing conditional constraints for natural crystal growth. *Geochimica et Cosmochimica Acta*, **65**, 1429–1437.

Omelon, C.R., Pollard, W.H. and Andersen, D.T. (2006a) A geochemical evaluation of perennial spring activity and associated mineral precipitates at Expedition Fiord, Axel Heiberg Island, Canadian High Arctic. *Applied Geochemistry*, **21**, 1–15.

Omelon, C.R., Pollard, W.H. and Ferris, F.G. (2006b) Environmental controls on microbial colonization of high Arctic cryptoendolithic habitats. *Polar Biology*, **30**, 19–29.

~~Omelon, C.R., Pollard, W.H. and Ferris, F.G. (2006c) Chemical and ultrastructural characterization of High Arctic cryptoendolithic habitats. *Geomicrobiology Journal*, **23**, 189–200.~~

Q19 Osinski, G.R. and Lee, P., (2005) Intra-crater sedimentary deposits at the Haughton impact structure, Devon Island, High Arctic. *Meteoritics and Planetary Science* (HMP Special Issue).

Osinski, G.R., Lee, P., Parnell, J., Spray, J.G. and Baron, M. (2005) A case study of impact induced hydrothermal activity: The Haughton impact structure, Devon Island, Canadian High Arctic. *Meteoritics and Planetary Science*, **40** (HMP Special Issue), 1859–1877.

Paulsen, G., Zacny, K., Cannon, H., Glass, B., Chu, P., Mumm, E., Davis, K., Frader-Thompson, S., Petrich, K., Bartlett, P. and Glaser, D. (2006) Robotic drill systems for planetary exploration. Proceedings of AIAA Space, San Jose, CA.

Perreault, N.N., Andersen, D.T., Pollard, W.H., Greer, C.W. and Whyte, L.G. (2007) Characterization of the prokaryotic diversity in cold saline perennial springs of the Canadian High Arctic. *Applied and Environmental Microbiology*, **73**, 1532–1543.

Q20 Perreault, N., Greer, C.W., Andersen, D.T., Tille, S., Lacrampe-Couloume, G., Sherwood-Lollar, B. and Whyte, L.G., (2008) Heterotrophic and autotrophic microbial populations in cold perennial springs of the High Arctic. ~~Applied and Environmental Microbiology, in press.~~

Peters, G.H., Mungas, G.S., Bearman, G.H., Beegle, L.W. and Smith, J.A. (2007) RASP sample acquisition on the Phoenix Mars Scout Mission. Lunar and Planetary Science Conference, LPSC XXXVIII, Abstract 2008.

Q21 ~~Pfiffner, S.M., Onstott, T.C., Ruskeeniemi, T., Talikka, M., Bakermans, C., McGown, D., Chan, E., Johnson, A., Phelps, T.J., Le Puil, M., Difurio, S.A., Pratt, L.M., Stotler, R., Frape, S., Telling, J., Sherwood-Lollar, B., Neill, I. and Zerbin, B., (2008) Challenges for CORING DEEP PERMAFROST ON Earth and Mars. Astrobiology Journal, in press.~~

Q22 Phee, L., Accoto, D., Menciassi, A., Stefanini, C., Carrozza, M.C. and Dario, P. (2002) Analysis and development of locomotion devices for the gastrointestinal tract. *IEEE Transactions on Biomedical Engineering*, **49** (6).

Phillips, N. (2001) Mechanisms for the Beagle2 Lander. In: *Proceedings of the 9th European Space Mechanisms and Tribology Symposium, 19–21 September 2001, Liège, Belgium. 9th ESMATS Proceedings* (ed. R.A. Harris), ESA SP-480, ESTEC, European Space Agency, Noordwijk, pp. 25–32.

Pollard, W.H., Whyte, L.G., Andersen, D.T., Niederberger, T.D., Nadeau, J.L., Eccelstone, M. and Haltigin, T., (2008) Overview of the analogue science activities at the McGill High Arctic Research Station, Axel Heiberg Island, Canadian High Arctic. Planetary and Space Science, (Special Issue, Mars Analogues), submitted. Q23

Re, E., Ylikorpi, T., Brighenti, A., Nista, A., Kochan, H. and Coste, P. (Oct., 1997) Small sample acquisition/distribution tool. In: *Proceedings of the 7th European Space Mechanisms and Tribology Symposium (7th ESMATS), 1–3 October 1997* (ed. B.H. Kaldeich-Schürmann), ESA SP-410, ESTEC, European Space Agency, Noordwijk, pp. 271–275.

~~Reston, V.A. and Buckley, D. (1971) Friction, Wear and Lubrication in Vacuum. NASA Special Publication SP-277.~~

Richter, L., Kochan, H., Gromov, V. and Coste, P. (2000) The development of the "mole with sampling mechanism" subsurface sampler. Proceedings, 6th ESA Workshop on Advanced Space Technologies for Robotics and Automation (ASTRA 2000), Noordwijk, 5–7 December 2000.

Richter, L., Coste, P., Gromov, V.V., Kochan, H., Pinna, S. and Richter, H.-E. (2001) Development of the "Planetary Underground Tool," subsurface soil sampler for the Mars Express "Beagle 2" lander. *Advances in Space Research*, **28** (8), 1225–1230.

Richter, L., Coste, P., Gromov, V.V., Kochan, H., Nadalini, R., Ng, T.C., Pinna, S., Richter, H.-E. and Yung, K.L. (2002) Development and testing of subsurface sampling devices for the Beagle 2 lander. *Planetary and Space Science*, **50**, 903–913.

Rivkina, E.M., Friedmann, E.I., McKay, C.P. and Gilichinsky, D.A. (2000) Metabolic activity of permafrost bacteria below the

PROOF WILEY-VCH

freezing point. *Applied and Environmental Microbiology*, **66**, 3230–3233.

Roberts, A.W. (1999) The influence of granular vortex motion on the volumetric performance of enclosed screw conveyors. *Powder Technology*, **104**, 56–67.

Roberts, A.W. and Willis, A.H. (1962) Performance of grain augers. *Proceedings of the Institution of Mechanical Engineers*, **176**, 165.

Scott, D.R., Worden, A.F. and Irwin, J.B. (1972) Crew observations. In: Apollo 15 Preliminary Science Report (eds J.P. Allen *et al.*), NASA SP-289, pp. 4-1–4-4.

Q24 Scott, R.F. and Roberson, F.I. (1968) Soil mechanics surface sampler: lunar surface results, and analyses. *Journal of Geophysical Research*, **73** (12).

Scott, R.F. and Roberson, F.I. (1969) Soil mechanics surface sampler. *Journal of Geophysical Research*, **74**, 25.

Scott, R.F., Carrier, W.D., Costes, N.C. and Mitchell, J.K. (1970) Preliminary geologic investigation of the Apollo 12 landing site. Part C. Mechanical properties of the lunar regolith. In: Apollo 12 Preliminary Science Report (ed. A.J. Calio *et al.*), pp. 161–182.

Sherrit, S. (2005) Mars Sample Return – Rover Clean Sampling Tool, Jet Propulsion Laboratory Internal Report, 24 June 2005, Jet Propulsion Laboratory, Pasadena, CA.

Sherrit, S., Askins, S.A., Gradziel, M., Dolgin, B.P., Bar-Cohen, Y., Bao, X. and Cheng, Z. (2001) Novel ultrasonic horns for power ultrasonics. NASA New Technology Report (NTR), Docket No. 30489 (6 December 2001). *NASA Technical Briefs*, **27** (4), 54–55

Sherrit, S., Bar-Cohen, Y., Dolgin, B., Bao, X. and Chang, Z. (2002) Ultrasonic crusher for crushing, milling, and powdering. NASA New Technology Report (NTR), Docket No. 30682 (21 June 2002).

Sherrit, S., Bar-Cohen, Y., Bao, X., Chang, Z., Blake, D. and Bryson, C. (2003) Ultrasonic/sonic rock powdering sampler and delivery tool. NASA New Technology Report (NTR), Docket No. 40564 (13 August 2003).

Sherrit, S., Bar-Cohen, Y., Badescu, M., Bao, X., Chang, Z., Jones, C. and Aldrich, J. (2006) Compact non-pneumatic powder sampler (NPPS). NASA New Technology Report (NTR), Docket No. 43614 (23 February 2006).

Shrout, T.R., Zhang, S.J., Eitel, R., Stringer, C. and Randall, C.A. (2004) High performance, high temperature perovskite piezoelectrics. In: Applications of Ferroelectrics, 2004. ISAF-04, August 2004. 14th IEEE International Symposium, pp. 23–27, 126–129.

Sims, M.R., Sykes, J., Stevenson, T., Wiercigroch, M., Parnell, J. and Hole, M. (2002) Design of an ultrasonic rock corer for use in planetary missions. Final Report, December 2002. Final report of contract No. 16222/02/NL/PA. ESTEC, European Space Agency, Noordwijk.

Smith, H.D. and McKay, C.P. (2005) Drilling in ancient permafrost on Mars for evidence of a second genesis of life. *Planetary and Space Science*, **53**, 1302–1308.

Squyres, S.W., Wilhelms, D.E. and Moosman, A.C. (1987) Large-scale volcano–ground ice interactions on Mars. *Icarus*, **70**, 385–408.

Stanley, S., Dougherty, S. and Laramee, J. (2007) The Low-force Sample Acquisition System. Proceedings of the NASA Science Technology Conference, University of Maryland, Adelphi, MD, June 2007.

Steele, A. and Beaty, D. (2006) The Astrobiology Field Laboratory – Final Report of the MEPAG Astrobiology Field Laboratory Science Steering Group (AFL-SSG), Version 3, 26 September 2006, Mars Exploration Program Analysis Group (MEPAG).

Steven, B., Leveille, R., Pollard, W.H. and Whyte, L.G. (2006) Microbial ecology and biodiversity of permafrost. *Extremophiles*, **10**, 259–267.

Steven, B., Briggs, G., McKay, C.P., Pollard, W.H., Greer, C.W. and Whyte, L.G. (2007) Characterization of the microbial diversity in a permafrost sample from the Canadian High Arctic using culture-dependent and culture-independent methods. *FEMS Microbiology Ecology*, **59**, 513–523.

Steven, B., Pollard, W.H., Greer, C.W. and Whyte, L.G., (2008) Microbial diversity and activity through a permafrost/grounded ice Q25

core profile from the Canadian High Arctic. *Environmental Microbiology*, in press.

Stoker, C.R. (2008) Mars Underground Mole. Final Report to Mars Technology Program, January 2008, NASA Ames Research Center, Moffett Field, CA.

Stoker, C.R., Gonzales, A. and Zavaleta, J.R. (June, 2007) The Mars and Moon Underground Mole. Proceedings of the NASA Science Technology Conference, University of Maryland, Adelphi, MD.

Takeyama, H. and Kato, S. (1991) Burrless drilling by means of ultrasonic vibration. *CIRP Annals*, **40** (1), 83–86.

Thomas, P.N.H. (2008) Modeling of an Ultrasonically Assisted Drill Bit. PhD thesis, Loughborough University of Technology.

Thomas, P.N.H. and Babitsky, V.I. (2007) Experiments and simulations on ultrasonically assisted drilling. *Journal of Sound and Vibration*, **308**, 815–830.

Tullies, T.C. http://geoweb.princeton.edu/people/faculty/onstott/index.html (last accessed 1 November 2008).

Vago, J., Gardini, B., Baglioni, P., Kminek, G. and Gianfiglio, D. (2006) ExoMars: ESA's mission to search for signs of life on the red planet. Lunar and Planetary Science XXXVII, Paper No. 1871, http://www.cosis.net/abstracts/EGU06/10407/EGU06-A-10407.pdf.

Vincent, J.F.V. and King, M.J. (1996) The mechanism of drilling by wood wasp ovipositors. *Biomimetics*, **3**, 187–201.

Watanabe, K., Shimoda, S., Kubota, T. and Nakatani, I. (2003) A mole-type drilling robot for lunar subsurface exploration. Proceeding of the 7th International Symposium on Artificial Intelligence and Robotics and Automation in Space.

Q26 West, L., McGown, D.J., Onstott, T.C., Morris, R.V., Suchecki, P. and Pratt, L.M., (2008) Lake Gossan Deposit: an Arctic analogue for ancient Martian surficial processes? *Planetary and Space Science*, submitted.

Williams, D.R. Soviet Missions to the Moon. National Space Science Data Center. Updated 27 September 2005. National Aeronautics and Space Administration, http://nssdc.gsfc.nasa.gov/planetary/lunar/lunarussr.html (Accessed 9 June 2008).

Ylikorpi, T., Visentin, G. and Suomela, J. (2001) A robotic rover-based deep driller for Mars exploration. In: *Proceedings of the 35th Aerospace Mechanisms Symposium; Sunnyvale, CA. Springfield, VA, 9–11 May 2001* (ed. E.A. Boesiger), NASA/CP-2001-209626, NASA, pp. 185–196.

Yokoyama, T. and Higuchi, K. (2002) Drilling on the lunar surface by torsion vibration. Proceedings of the 46th Space Science and Technology Conference (in Japanese).

Yoshida, K., Mizuno, N., Yokoyama, T., Kanamori, H., Sonoyama, M. and Watabe, T. (2002) Development of a mole-type robot for lunar/planetary sub-surface exploration and its performance evaluation. Proceeding of the 20th Annual Conference of the Robotics Society of Japan (in Japanese).

Yu, Y. and Arnold, P. (1997) Theoretical modeling of torque requirements for single screw feeders. *Powder Technology*, **93** (2), 151–162.

Yung, K.L., Ng, T.C., Chan, C.C. and Yu, C.H. (1997) Passive self adapting end-effectors for blind grappling on Mars soil. In: *Proceedings of the 7th European Space Mechanisms and Tribology Symposium (7th ESMATS), ESTEC, Noordwijk, 1–3 October 1997* (ed. B.H. Kaldeich-Schürmann), ESA SP-410, ESTEC, European Space Agency, Noordwijk, pp. 145–150.

Zaccariotto, M., Debei, S., Bettanini, C., Parzianello, G., Giacometti, M., Finotello, R., Campaci, R., Rossi, G. and Visentin, G. (2007) Autonomous robot for subsoil exploration: GMD system development and integration. Proceedings of the 2nd International Workshop on Exploring Mars and its Earth Analogues, 18–22 June 2007, Trento, Italy.

Zacny, K. and Cooper, G. (2006) Considerations, constraints and strategies for drilling on Mars. *Planetary and Space Science Journal*, **54** (4), 345–356, DOI:10.1016/j.pss.2005.12.003.

Zacny, K.A. and Cooper, G.A. (2007a) Friction of drill bits under Martian pressure. *Journal*

page proof WILEY-VCH

of Geophysical Research, **112**, E03003, DIO:10.1029/2005JE002538.

Zacny, K. and Cooper, G. (2007b) methods for cuttings removal from holes drilled on Mars. *Mars Journal*, **3**, 42–56, DOI:10.1555/mars.2007.0004.

Zacny, K. and Cooper, G. (2007c) Coring basalt rock under simulated Martian atmospheric conditions. *Mars Journal*, **3**, 1–11, DOI:10.1555/mars.2007.0001.

Zacny, K. and Mungas, G. (2009) Novel method of regolith sample return from extraterrestrial body using a puff of gas. Proceedings of the IEEE Aerospace Conference, 7–14 March 2009, Big Sky, MT.

Zacny, K., Huang, K., McFaden, M., Neugebauer, A., Quayle, M. and Cooper, G. (2002) Novel methods of cuttings removal from holes during percussive drilling on Mars. Proceedings of Revolutionary Aerospace Systems Concepts – Academic Linkage (RASC-AL) Conference, 6–8 November 2002, Cocoa Beach, FL.

Zacny, K.A., Quayle, M.C. and Cooper, G.A. (2004) Laboratory drilling under Martian conditions yields unexpected results. *Journal of Geophysical Research*, **109**, E07S16, DOI:10.1029/2003JE002203.

Zacny, K., Mungas, G., Parrington, L., Mungas, C. and Fisher, D. (2007) Pneumatic lunar regolith excavator. Space Resources Roundtable, 25–27 October 2007, Golden, CO.

Zacny, K., Mungas, G., Mungas, C., Fisher, D. and Hedlund, M. (2008a) Pneumatic excavator and regolith transport system for lunar ISRU and construction. Paper No. AIAA-2008-7824 and Presentation, AIAA SPACE 2008 Conference and Exposition, 9–11 September 2008, San Diego Convention Center, San Diego, CA.

Zacny, K., Bar-Cohen, Y., Boucher, D., Brennan, M., Briggs, G., Cooper, G., Davis, K., Dolgin, B., Glaser, D., Glass, B., Gorevan, S., Guerrero, J., Paulsen, G., Stanley, S. and Stoker, C. (2008b) Drilling systems for extraterrestrial subsurface exploration. *Astrobiology*, **8** (3), 665–706, DOI:10.1089/ast.2007.0179.

Zacny, K., Fong, T., Wilson, J., Lee, S., Kobayashi, K., Deans, M., Ashley, A. and Santoro, C. (2008c) Percussive dynamic cone penetrometer for geotechnical surface assessment with a planetary rover. NLSI Lunar Science Conference, p. 2138.

Zarnecki, J.C., Leese, M.R., Hathi, B., Ball, A.J., Hagermann, A., Towner, M.C., Lorenz, R.D., McDonnell, J.A.M., Green, S.F., Patel, M.R., Ringrose, T.J., Rosenberg, P.D., Atkinson, K.R., Paton, M.D., Banaszkiewicz, M., Clark, B.C., Ferri, F., Fulchignoni, M., Ghafoor, N.A.L., Kargl, G., Svedhem, H., Delderfield, J., Grande, M., Parker, D.J., Challenor, P. and Geake, J.E. (2005) A soft solid surface on Titan as revealed by the Huygens Surface Science Package. *Nature*, **438**, 792–795, DOI:10.1038/nature04211.

Zhang, D.-Y., Feng, X.-j., Wang, L. and Chen, D.C. (1994) Study on the drill skidding motion in ultrasonic vibration microdrilling. *International Journal of Machine Tools and Manufacture*, **34** (6), 847–857.

Internet Links

http://antti.la/space/phd_thesis/ (accessed 28 May 2008).

http://robotics.estec.esa.int/i-SAIRAS/isairas2005/session_04a/1_finotella-4a.pdf (accessed 30 May 2008).

http://www.cosis.net/abstracts/EGU2007/06259/ EGU2007-J-06259.pdf?PHPSESSID=e (accessed 28 May 2008).

http://www.hkmars.net/ (accessed 28 May 2008).

page proof WILEY

Keywords/Abstract

Dear Author,

Please check and/or supply keywords and an abstract. These will not be included in the print version of your chapter but in the online version.

If you do not supply an abstract, the section heading will be used instead.

Keywords: Drilling, coring, sampling, planetary exploration, sample acquisition,

Abstract

Extraterrestrial drilling and coring is increasingly becoming part of the tasks that are conducted in planetary exploration missions. The key objective is to acquire samples for in-situ analysis or for sample return to earth for extensive tests. The capability of deployed systems has been limited due to the great challenges that are involved with their use in such missions. However, the scientific motivation to study the subsurface of planetary bodies is very strong and driving the exploration community to overcome the engineering challenges to performing autonomous, robotic drilling. Drilling consists of 2 separate, but equally important, processes: breaking the formation with a bit and removing cuttings and cores to the surface. The bit is designed with cutting teeth, and it is made of a material that is both suitable for breaking the formation and wearing as slowly as possible. Generally, extraterrestrial drilling imposes 2 categories of constraints on a planetary drilling system: the extreme environmental conditions and mission-driven constraints. The depth to which a drill system can penetrate is one of its most salient capabilities for extraterrestrial exploration, as different depths offer distinct science benefits. A useful classification of drill systems is to divide them into the following categories: surface drills, 1-meter class drills, 10-meter class drills, and deep drills. Over the years, the various drilling methods and the related designs were enhanced in technology readiness levels to the point that some are being used or are about to be used for *in situ* planetary missions. Recently, there has been a growing recognition of the importance of the capability of the percussive and rotary-percussive drilling techniques, and greater attention is now being given to this technology, including the use in the Mars Science Laboratory that is scheduled to be launched in 2011. In the more distant future, most likely in the era of human exploration, sufficient mass and real-time supervision should be available to carry out truly deep penetration of the subsurface of extraterrestrial bodies.

This is a reference to a publication in a website that is dated 2002 but we accessed it in 2008. See correction on page 356.

Author Query

1. The reference Ng et al., 2008 is cited in the text but not listed among the references. Please supply full reference, or the citation will be deleted from the text.
2. Section 6.1.2.1, 3rd paragraph: is 77°51.891 163°45.062′, elevation 1693 m expressed correctly?
3. Section 6.6.2, end of subsection Operation in Extreme Environments: please define BST. Delete BSTpe3
4. Section 6.6.6: the last 3 sentences do not make sense: (a) what does "(right)" refer to?; (b) you say a "pentagonal shape is visible": where? (c) you have "as shown in,": this is incomplete – shown where? None of this is in Figure 45. Has a Figure been deleted? Please clarify.
5. Section 6.6.7, discussion of Table 4: in the text you defined resilient modulus as MR, but this is not used in the equations in Table 4: we have changed it to k – is that correct? Also, in Table 4 you give k in units of M/m3: what is M? Further, Table 4 has two different equations for E with no explanation: please clarify.
6. Section 6.7.3: you have "For lack of a better candidate, Honeybee used this rock during CAT development testing and received direction from the JPL CTM to use this rock for CAT V&V testing." Please define CTM and V&V.
7. Section 6.8.2, subsection "Drill Bit Design", equation in 3rd paragraph: Please define z and x. Please ensure it is set in the correct maths format.
8. The following references (Barmin and Shevchenko, 1983; Kennedy et al., 2006; Mitchell, 2008; Omelon et al., 2006b; Omelon et al., 2006c; Omelon et al., 2001; Reston and Buckley, 1971) are not cited in the text. Please cite them in the text or remove them form the reference list.
9. Please provide the Volume and page in Ref. (Andersen et al., 2002).
10. Please provide the Volume number in Ref. (Eapen et al., 2005).
11. Please provide volume and page range in Ref. (Freifeld et al., 2008).
12. Please provide publisher + location, and any Editors, in Ref. (Fukuda and Menz, 2001).
13. Please provide page range in Ref. (Gao et al., 2007).
14. Please provide the Page range in Ref. (Gorevan et al., 2003).
15. Please provide page range in Ref. (Kessler and Leitner, 2000)
16. Please provide publisher +location in Ref. (McKay, 2001).

Page proof NEVER

17. Please provide the Volume in Ref. (Menon et al., 2006a).
18. Please update Ref. (Niederberger et al., 2008).
19. Please provide volume and page range in Ref. (Osinski and Lee, 2005).
20. Please update Ref. (Perreault et al., 2008).
21. Please update Ref. (Pfiffner et al., 2008).
22. Please provide page range in Ref. (Phee et al., 2002).
23. Please update Ref. (Pollard et al., 2008).
24. Please provide the page range in Ref. (Scott and Roberson, 1968).
25. Please update Ref. (Steven et al., 2008).
26. Please update Ref. (West et al., 2008).
27. Your original figures 6.10, 6.11, 6.133 and 6.135 have been removed. All other figures have been renumbered accordingly. We removed the cross-ref in text as well. Please check for correctness.

page proof
WILEY-VCH